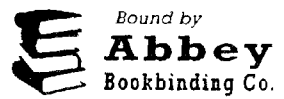


University of South Wales



2059450



105 Cathays Terrace, Cardiff CF24 4PU, U.K.

Tel: +44 (0)29 2039 5882

Email: [info@bookbindersuk.com](mailto:info@bookbindersuk.com)

[www.bookbindersuk.com](http://www.bookbindersuk.com)

# NEURAL NETWORK MODELLING AND CONTROL OF COAL FIRED BOILER PLANT

**SHEE MENG THAI**

A thesis presented in partial fulfilment of the requirements of the University of  
Glamorgan/Prifysgol Morgannwg for the award of the degree of Doctor of  
Philosophy

This research programme was carried out in collaboration with the European  
Coal and Steel Community (ECSC), the British Coal Utilisation Research  
Association (BCURA) and James Proctor Limited

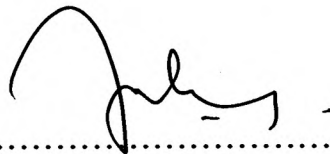
**August 2005**

**The University of Glamorgan**

***Certificate of Research***

*This is to certify that, except where specific reference is made, the work described in this thesis is the result of the candidate. Neither this thesis, nor any part of it, has been presented, or is currently submitted, in candidature for any degree at any other University.*

*Signed*



.....  
*Candidate*

*Signed*



.....  
*Director of Studies*

*Date*

.....*13th October 2005*.....

*~Thai Family~*



# Abstract

This thesis presents the development of a Neural Network Based Controller (NNBC) for chain grate stoker fired boilers. The objective of the controller was to increase combustion efficiency and maintain pollutant emissions below future medium term stringent legislation. Artificial Neural Networks (ANNs) were used to estimate future emissions from and control the combustion process. Initial tests at Casella CRE Ltd demonstrated the ability of ANNs to characterise the complex functional relationships which subsisted in the data set, and utilised previously gained knowledge to deliver predictions up to three minutes into the future. This technique was then built into a carefully designed control strategy that fundamentally mimicked the actions of an expert boiler operator, to control an industrial chain grate stoker at HM Prison Garth, Lancashire. Test results demonstrated that the developed novel NNBC was able to control the industrial stoker boiler plant to deliver the load demand whilst keeping the excess air level to a minimum. As a result the NNBC also managed to maintain the pollutant emissions within probable future limits for this size of boiler. This prototype controller would thus offer the industrial coal user with a means to improve the combustion efficiency on chain grate stokers as well as meeting medium term legislation limits on pollutant emissions that could be imposed by the European Commission.

# Acknowledgements

First of all, I would like to express my sincere gratitude to my Director of Studies, Professor Steven Wilcox for his encouragement and continuous supervision. The completion of this PhD research would not have been possible without his patience and constant support over the last five years. Heartfelt thanks also to my second supervisor, Professor John Ward for his inspirational ideas and guidance throughout the course of my PhD program. My special thanks to Dr. Alex Chong and Dr. C.K. Tan for their constructive help especially in understanding the software development aspect of the research project. Thanks are also due to Dr. O.H. Tan for his companionship and fruitful discussion of relevant research topics over the past few years.

My sincere appreciation to Professor William G. Kaye of BCURA for his enthusiasm and commitment to the project. His “tough” questions have made a number of project meetings over the last few years a memorable experience. Thanks also to Managing Director of James Proctor Limited, Mr. Andrew Proctor for his association in this project. Many thanks also to former Proctor’s senior commissioning engineer, Mr. Wayne Jessop for his passionate assistance in setting up the interface communication between the control instrument and the plant control panel at the industrial chain grate. Much of the commissioning tests on the industrial boiler would not have been possible without his experience on efficient chain grate stoker operation. Thanks are also due to the staff of Casella CRE Ltd, Mr. Nigel Black for carrying out the tests at the test facility.

Many thanks are also to Mr. Gareth Betteney, Senior Technical Officer in the School of Technology for his kind help and guidance during the construction of the data logging and control instrument for work on the industrial stoker boiler. Thanks also to Mr. Wayne Byrne, Senior Service Engineer of Testo Ltd, for his number of “free” guidance to diagnose and rectify the flue gas analyser. The important emission readings for the control experiments would not have been possible to obtain without his invaluable help.

Finally, I would like to thanks my family, especially my parents for their love, support and encouragement throughout my study life. Thanks also to friends, in particular Molly, Alex, Lai, Teck Hin, Jacky, Eric, Priscilla and Khuan, for their warm friendship and support.

# Table of Contents

<b>ABSTRACT</b>	<b>i</b>
<b>ACKNOWLEDGEMENTS</b>	<b>ii</b>
<b>TABLE OF CONTENTS</b>	<b>iii</b>
<b>LIST OF FIGURES</b>	<b>vii</b>
<b>LIST OF TABLES</b>	<b>xiv</b>
<b>NOMENCLATURE</b>	<b>xv</b>
CHAPTER 1 INTRODUCTION	1
CHAPTER 2 LITERATURE REVIEW	6
2.1 The Importance of Coal	6
2.1.1 Influence of Coal Combustion on Environmental Aspects	7
2.1.2 Current Legislation Limits for Coal Fired Boilers	8
2.1.3 Summary	9
2.2 Industrial Coal Firing Appliances	9
2.2.1 Chain and Travelling Grate Stokers	11
2.2.2 The Combustion Process on a Chain Grate Stoker	13
2.2.3 Requisites for Efficient Coal Combustion on Chain Grates	17
2.2.4 Summary	18
2.3 Lump Coal Combustion	19
2.3.1 Previous Research in Lump Coal Combustion	19
2.3.2 Summary	23
2.4 Artificial Intelligence (AI) Using Artificial Neural Networks (ANNs)	24
2.4.1 Artificial Neural Networks (ANNs)	24
2.4.2 Feed Forward Multi-Layered Perceptron Network Training with Error Back-Propagation Learning Algorithm	28
2.5 Neural Network Based System Identification and Black Box Modelling	31
2.5.1 System Identification	32
2.5.2 Non-linear Neural Network ARX Model with Multi-Step-Ahead Prediction	36
2.6 Literature on Related Artificial Neural Networks Applications	39
2.6.1 Summary	44

CHAPTER 3	PLANT DESCRIPTION OF PILOT SCALE CHAIN GRATE	
	STOKER BOILER & EXPERIMENTAL RESULTS	45
3.1	Plant Description	45
3.2	The Plant Control System and Instrumentation	49
3.3	Experimental Procedures	52
3.3.1	Experiments with Gradual Load Changes	53
3.3.2	Experiments with Large Load Changes	53
3.4	Experimental Results & Discussion	55
3.4.1	Gradual Load Changes at Optimal and Sub-Optimal Operating Conditions for Dawmill Smalls	55
3.4.2	Gradual Load Changes at Optimal and Sub-Optimal Operating Conditions for Dawmill Singles	57
3.4.3	Gradual Load Changes at Optimal and Sub-Optimal Operating Conditions for Columbian Smalls	59
3.4.4	Large Load Changes at Optimal and Sub-Optimal Operating Conditions for Dawmill Smalls	61
3.4.5	Large Load Changes at Optimal and Sub-Optimal Operating Conditions for Dawmill Singles	63
3.4.6	Large Load Changes at Optimal and Sub-Optimal Operating Conditions for Columbian Smalls	65
3.4.7	Summary of Section 3.4	67
CHAPTER 4	BLACK BOX MODELS OF PILOT SCALE CHAIN	
	GRATE STOKER BOILER	68
4.1	Training and Testing of Neural Network ARX Model	68
4.1.1	Neural Network ARX Model for Oxygen Concentration in the Flue Gas	70
4.1.2	Neural Network ARX Model for Nitrogen Oxides Emissions	77
4.1.3	Neural Network ARX Model for Carbon Monoxide Emissions	83
4.2	Summary of Chapter 4	89
CHAPTER 5	PLANT DESCRIPTION OF INDUSTRIAL SCALE CHAIN	
	GRATE STOKER BOILER & COMMISSIONING TEST	
	RESULTS	90
5.1	Plant Description of 3.7MW Industrial Scale Chain Grate Stoker & Plant Instrumentation	90

5.2 Commissioning Tests on the 3.7MW Chain Grate Stoker Fired Shell Boiler	93
5.2.1 Preliminary Commissioning Test	95
5.2.2 Detailed Commissioning Tests	98
5.2.3 Final Commissioning Tests	103
5.3 Summary	106
CHAPTER 6 DEVELOPMENT OF THE NEURAL NETWORK BASED CONTROLLER (NNBC)	107
6.1 The Basic Concept of the Control Strategy	107
6.1.1 Background	108
6.1.2 Target Areas where Heat Losses can be Minimised	108
6.1.3 The Control Strategy	109
6.2 The Development of the Neural Network Based Controller (NNBC)	111
6.2.1 The Overall Controller Approach	112
6.2.2 NNBC Signal Interface Configuration	114
6.2.3 Calibration of the Coal Feed, Airflow and K-Type Thermocouple	116
6.2.4 Selection of Training Data	119
6.3 Conclusion	123
CHAPTER 7 COMMISSIONING & TESTING OF THE NEURAL NETWORK BASED CONTROLLER (NNBC)	124
7.1 Commissioning of the Neural Network Based Controller (NNBC)	125
7.1.1 Stoker Control Using the NNBC with Inappropriate Settings	127
7.2 Testing of the Neural Network Based Controller (NNBC)	129
7.2.1 Combustion Optimisation with the NNBC	130
7.2.2 Hot Water Temperature Control Experiments with the NNBC	144
7.3 Summary of Chapter 7	156
CHAPTER 8 CONCLUSIONS & FURTHER RECOMMENDATION	157
8.1 Identification of Combustion Derivatives Using Black Box Models	157
8.2 Application of the Neural Network Based Controller to an Industrial Stoker Boiler	158
8.3 Recommendation for Further Work	160

<b>REFERENCES</b>	164
<b>APPENDIX A FUEL SPECIFICATION FOR EXPERIMENTS ON THE STOKER TEST FACILITY</b>	173
<b>APPENDIX B FUEL SPECIFICATION FOR EXPERIMENTS ON THE INDUSTRIAL STOKER</b>	175
<b>APPENDIX C GRATE ASH ANALYSIS FOR EXPERIMENTS ON THE STOKER TEST FACILITY</b>	176
<b>APPENDIX D THE NNBC PROGRAMME IN MATLAB™ FILE FOR THE INDUSTRIAL STOKER PLANT – COMBUSTION OPTIMISATION TEST</b>	177
<b>APPENDIX E THE NNBC PROGRAMME IN MATLAB™ FILE FOR THE INDUSTRIAL STOKER PLANT – HOT WATER TEMPERATURE CONTROL TEST</b>	187

# List of Figures

Figure 2.1	Sequence of Combustion on a Chain Grate Stoker [Good Practice Guide 88, 2000]	16
Figure 2.2	A Three-Layer Feed Forward MLP Network Architecture	31
Figure 2.3	The System Identification Procedure [Noorgard, 2000]	33
Figure 2.4	The Feed Forward MLP Network Architecture with ARX Model Structure	38
Figure 3.1	Guillotine & Firebreak Assemblies [Good Practice Guide 88, 2000]	47
Figure 3.2	The 0.7MW Chain Grate Stoker Test Facility & Sensors Location at Casella CRE Ltd	51
Figure 3.3	Coal Feed & Airflow Staging Sequence Following Large Load Changes	54
Figure 3.4	NO <sub>x</sub> & CO Emissions and Percentage of CO <sub>2</sub> in Exhaust Duct following Gradual Load Changes at Near Optimum Air Setting for Dawmill Smalls – <i>Test 1</i>	56
Figure 3.5	NO <sub>x</sub> & CO Emissions and Oxygen Concentration in Exhaust Duct following Gradual Load Changes at Near Optimum Air Setting for Dawmill Singles – <i>Test 4</i>	58
Figure 3.6	NO <sub>x</sub> & CO Emissions and Oxygen Concentration in Exhaust Duct following Gradual Load Changes at Near Optimum Air Setting for Columbian Smalls – <i>Test 7</i>	60
Figure 3.7	NO <sub>x</sub> & CO Emissions and Oxygen Concentration in Exhaust Duct following Large Load Changes at Optimal and Sub-Optimal Air Settings for Dawmill Smalls – <i>Test 10</i>	62
Figure 3.8	NO <sub>x</sub> & CO Emissions and Oxygen Concentration in Exhaust Duct following Large Load Changes at Optimum and Sub-Optimal Air Settings for Dawmill Singles – <i>Test 11</i>	64
Figure 3.9	NO <sub>x</sub> & CO Emissions and Oxygen Concentration in Exhaust Duct following Large Load Changes at Optimal and Sub-Optimal Air Settings for Columbian Smalls – <i>Test 12</i>	66
Figure 4.1	Network Structure of ARX Model for Oxygen in the Flue Gas	71

Figure 4.2	Three Step Ahead Predictions by the Pruned Neural Network ARX Model (nnarx) for Oxygen in the Flue Gas following Gradual Load Changes at Near Optimum Air for Dawmill Singles - BCURA B35 Data ( <i>Training Model 1</i> )	73
Figure 4.3	Three Step Ahead Simulations of Oxygen in the Flue Gas by <i>Training Model 1</i> following Large Load Changes with Staging Profile 1 for Dawmill Singles - BCURA B35 Data ( <i>Validation</i> )	73
Figure 4.4	Six Step Ahead Predictions by the Pruned Neural Network ARX Model (nnarx) for Oxygen in the Flue Gas following Gradual Load Changes at Near Optimum Air for Dawmill Singles – <i>Test 4</i> ( <i>Training Model 2</i> )	74
Figure 4.5	Six Step Ahead Simulations of Oxygen in the Flue Gas by <i>Training Model 2</i> following Gradual Load Changes at Near Optimum Air for Columbian Smalls – <i>Test 7</i> ( <i>Validation</i> )	74
Figure 4.6	Three Step Ahead Predictions by the Pruned Neural Network ARX Model (nnarx) for Oxygen in the Flue Gas following Gradual Load Changes at Near Optimum Air for Columbian Smalls – <i>Test 7</i> ( <i>Training Model 3</i> )	75
Figure 4.7	Three Step Ahead Simulations of Oxygen in the Flue Gas by <i>Training Model 3</i> following Large Load Changes at Optimal and Sub-Optimal Air Settings for Columbian Smalls – <i>Test 12</i> ( <i>Validation</i> )	75
Figure 4.8	Network Structure of ARX Model for Nitrogen Oxides Emission	78
Figure 4.9	Three Step Ahead Predictions by the Pruned Neural Network ARX Model (nnarx) for Nitrogen Oxides Emission following Gradual Load Changes at Near Optimum Air for Dawmill Singles - BCURA B35 Data ( <i>Training Model 4</i> )	80
Figure 4.10	Three Step Ahead Simulations of Nitrogen Oxides Emission by <i>Training Model 4</i> following Large Load Changes with Staging Profile 1 for Dawmill Singles - BCURA B35 Data ( <i>Validation</i> )	80
Figure 4.11	Three Step Ahead Predictions by the Pruned Neural Network ARX Model (nnarx) for Nitrogen Oxides Emission following Gradual Load Changes at Near Optimum Air for Dawmill Singles – <i>Test 4</i> ( <i>Training Model 5</i> )	81



Figure 4.12	Three Step Ahead Simulations of Nitrogen Oxides Emission by <i>Training Model 5</i> following Gradual Load Changes at Near Optimum Air for Columbian Smalls – <i>Test 7 (Validation)</i>	81
Figure 4.13	Three Step Ahead Predictions by the Pruned Neural Network ARX Model (nnarx) for Nitrogen Oxides Emissions following Gradual Load Changes at Near Optimum Air for Columbian Smalls – <i>Test 7</i> ( <i>Training Model 6</i> )	82
Figure 4.14	Three Step Ahead Simulations of Nitrogen Oxides Emissions by <i>Training Model 6</i> following Large Load Changes at Optimal and Sub-Optimal Air Settings for Columbian Smalls – <i>Test 12 (Validation)</i>	82
Figure 4.15	Network Structure of ARX Model for Carbon Monoxide Emission	84
Figure 4.16	Three Step Ahead Prediction by the Pruned Neural Network ARX Model (nnarx) for Carbon Monoxide Emission following Gradual Load Changes at Near Optimum Air for Dawmill Singles - BCURA B35 Data ( <i>Training Model 7</i> )	86
Figure 4.17	Three Step Ahead Simulations of Carbon Monoxide Emission by <i>Training Model 7</i> following Large Load Changes with Staging Profile 2 for Dawmill Singles - BCURA B35 Data ( <i>Validation</i> )	86
Figure 4.18	Three Step Ahead Predictions by the Pruned Neural Network ARX Model (nnarx) for Carbon Monoxide Emission following Gradual Load Changes at Near Optimum Air for Dawmill Singles – <i>Test 4</i> ( <i>Training Model 8</i> )	87
Figure 4.19	Three Step Ahead Simulations of Carbon Monoxide Emission by <i>Training Model 8</i> following Gradual Load Changes at Near Optimum Air for Columbian Smalls – <i>Test 7 (Validation)</i>	87
Figure 4.20	Three Step Ahead Predictions by the Pruned Neural Network ARX Model (nnarx) for Carbon Monoxide Emissions following Gradual Load Changes at Near Optimum Air for Columbian Smalls – <i>Test 7</i> ( <i>Training Model 9</i> )	88
Figure 4.21	Three Step Ahead Simulations of Carbon Monoxide Emissions by <i>Training Model 9</i> following Large Load Changes at Optimal and Sub-Optimal Air Settings for Columbian Smalls – <i>Test 12 (Validation)</i>	88
Figure 5.1	The 3.7MW <sub>th</sub> Industrial Scale Stoker located at HMP Garth (Boiler No. 2)	94

Figure 5.2	NO <sub>x</sub> & CO Emissions and Oxygen Concentration in Exhaust Duct following Gradual Load Changes under Operator's Best Practise for Columbian Smalls on the Industrial Stoker – <i>Test 13</i>	97
Figure 5.3	Flue Gas & Hot Water Temperature following Gradual Load Changes under Operator's Best Practise for Columbian Smalls on the Industrial Stoker – <i>Test 13</i>	97
Figure 5.4	CO Emission and Oxygen in Exhaust Duct Whilst Manually Altering the Airflow at Different Load Levels – <i>Test 14</i>	99
Figure 5.5	CO Emission and Oxygen in Exhaust Duct Whilst Manually Altering the Airflow at Different Load Levels – <i>Test 15</i>	100
Figure 5.6	CO Emission and Oxygen in Exhaust Duct Whilst Manually Altering the Airflow at Different Load Levels – <i>Test 16</i>	101
Figure 5.7	CO Emission and Oxygen in Exhaust Duct Whilst Manually Altering the Airflow at 30%, 60% and 90% of MCR – <i>Test 17</i>	104
Figure 5.8	CO Emission and Oxygen in Exhaust Duct Whilst Manually Altering the Airflow at 40% and 70% of MCR – <i>Test 18</i>	104
Figure 5.9	CO Emission and Oxygen in Exhaust Duct Whilst Manually Altering the Airflow at 40% and 70% of MCR – <i>Test 19</i>	105
Figure 6.1	Schematic of the Overall NNBC for the Chain Grate Stoker Fired Shell Boiler	112
Figure 6.2	Schematic of the Overall Signal Interface Configuration for Part of the NNBC Development	115
Figure 6.3	Calibration Setting between the Coal Feed Rate (in terms of Percentage of MCR) and the Signal in Voltage for the Boiler Plant in Garth	117
Figure 6.4	Calibration Setting between the FD Fan Speed (in terms of Percentage of MCR) and the Signal in Voltage for the Boiler Plant in Garth	117
Figure 6.5	Calibration Setting between the Signal Voltage generated by the K-Type Thermocouple and the Temperature Reading in term of Degree Celsius	118
Figure 6.6	Six Steps Ahead Prediction by the ARX Model (nnarx) for O <sub>2</sub> at Constant Load of 40% of MCR Using <i>Test 18</i> Data (Odd No. Data Set for Training & Even No. Data Set for Validation - <i>Training Model 10</i> )	120
Figure 6.7	Six Steps Ahead Prediction by the ARX Model for CO at Constant Load of 40% of MCR Using <i>Test 18</i> Data (1 <sup>st</sup> & 3 <sup>rd</sup> Quarter Data Set for Training & 2 <sup>nd</sup> & 4 <sup>th</sup> Quarter Data Set for Validation - <i>Training Model 11</i> )	120

Figure 6.8	Six Steps Ahead Prediction by the ARX Model (nnarx) for O <sub>2</sub> at Constant Load of 70% of MCR Using <i>Test 18</i> Data (Odd No. Data Set for Training & Even No. Data Set for Validation - <i>Training Model 12</i> )	121
Figure 6.9	Six Steps Ahead Prediction by the ARX Model (nnarx) for O <sub>2</sub> at Constant Load of 70% of MCR Using <i>Test 18</i> Data (1 <sup>st</sup> & 3 <sup>rd</sup> Quarter Data Set for Training & 2 <sup>nd</sup> & 4 <sup>th</sup> Quarter Data Set for Validation - <i>Training Model 13</i> )	121
Figure 6.10	Six Steps Ahead Prediction by the ARX Model (nnarx) for CO at Constant Load of 70% of MCR Using <i>Test 18</i> Data (Odd No. Data Set for Training & Even No. Data Set for Validation - <i>Training Model 14</i> )	122
Figure 6.11	Six Steps Ahead Prediction by the ARX Model (nnarx) for CO at Constant Load of 70% of MCR Using <i>Test 18</i> Data (1 <sup>st</sup> & 3 <sup>rd</sup> Quarter Data Set for Training & 2 <sup>nd</sup> & 4 <sup>th</sup> Quarter Data Set for Validation - <i>Training Model 15</i> )	122
Figure 7.1	Predicted & Actual Oxygen Response to Unsuitable Controller Gain for Combustion Optimisation Test at Constant Load of 40% of MCR – <i>Test 20</i>	128
Figure 7.2	Predicted & Actual CO & NO <sub>x</sub> Emissions to Unsuitable Controller Gain for Combustion Optimisation Test at Constant Load of 40% of MCR – <i>Test 20</i>	129
Figure 7.3	Predicted & Actual Oxygen Response following Combustion Optimisation Test at Constant Load of 40% of MCR with O <sub>2</sub> Neural Model Using <i>Training Model 10</i> – <i>Test 21</i>	131
Figure 7.4	Actual Oxygen Response following Combustion Optimisation Test at Constant Load of 40% of MCR without O <sub>2</sub> Neural Model – <i>Test 22</i>	131
Figure 7.5	Predicted & Actual CO & NO <sub>x</sub> Emissions following Combustion Optimisation Test at Constant Load of 40% of MCR with CO Neural Model Using <i>Training Model 11</i> – <i>Test 21</i>	133
Figure 7.6	Actual CO Emission following Combustion Optimisation Test at Constant Load of 40% of MCR without CO Neural Model – <i>Test 22</i>	133
Figure 7.7	Predicted & Actual Oxygen Response following Combustion Optimisation Test at Constant Load of 70% of MCR with O <sub>2</sub> Neural Model Using <i>Training Model 12</i> (Test Profile 1) – <i>Test 23</i>	135

Figure 7.8	Actual Oxygen Response following Combustion Optimisation Test at Constant Load of 70% of MCR without O <sub>2</sub> Neural Model (Test Profile 1) – <i>Test 24</i>	135
Figure 7.9	Predicted & Actual CO & NO <sub>x</sub> Emissions following Combustion Optimisation Test at Constant Load of 70% of MCR with CO Neural Model Using <i>Training Model 15</i> (Test Profile 1) – <i>Test 23</i>	137
Figure 7.10	Actual CO & NO <sub>x</sub> Emission following Combustion Optimisation Test at Constant Load of 70% of MCR without CO Neural Model (Test Profile 1) – <i>Test 24</i>	137
Figure 7.11	Predicted & Actual Oxygen Response following Combustion Optimisation Test at Constant Load of 70% of MCR with O <sub>2</sub> Neural Model Using <i>Training Model 12</i> (Test Profile 2) – <i>Test 25</i>	139
Figure 7.12	Actual Oxygen Response following Combustion Optimisation Test at Constant Load of 70% of MCR without O <sub>2</sub> Neural Model (Test Profile 2) – <i>Test 26</i>	139
Figure 7.13	Predicted & Actual CO & NO <sub>x</sub> Emissions following Combustion Optimisation Test at Constant Load of 70% of MCR with CO Neural Model Using <i>Training Model 14</i> (Test Profile 2) – <i>Test 25</i>	141
Figure 7.14	Actual CO Emission following Combustion Optimisation Test at Constant Load of 70% of MCR without CO Neural Model (Test Profile 2) – <i>Test 26</i>	141
Figure 7.15	Predicted & Actual Oxygen Response following Combustion Optimisation Test with Unseen Data at Constant Load of 60% of MCR with O <sub>2</sub> Neural Model Using <i>Training Model 13</i> – <i>Test 27</i>	143
Figure 7.16	Predicted & Actual CO & NO <sub>x</sub> Emissions following Combustion Optimisation Test with Unseen Data at Constant Load of 60% of MCR with CO Neural Model Using <i>Training Model 15</i> – <i>Test 27</i>	143
Figure 7.17	Water Temperature & Oxygen Concentration under NNBC Mode following A Step Change in the Hot Water Temperature from 105°C to 120°C – <i>Test 28</i>	146
Figure 7.18	Pollutant Emissions under NNBC Mode following A Step Change in the Hot Water Temperature from 105°C to 120°C – <i>Test 28</i>	146

Figure 7.19	Water Temperature & Oxygen Concentration under NNBC Mode following A Step Change in the Hot Water Temperature from 120°C to 105°C – <i>Test 29</i>	148
Figure 7.20	Pollutant Emissions under NNBC Mode following A Step Change in the Hot Water Temperature from 120°C to 105°C – <i>Test 29</i>	148
Figure 7.21	Water Temperature & Oxygen Concentration under NNBC Mode While Tracking Hot Water Temperature Set Point at 120°C – <i>Test 30</i>	150
Figure 7.22	Pollutant Emissions under NNBC Mode While Tracking Hot Water Temperature Set Point at 120°C – <i>Test 30</i>	150
Figure 7.23	Six Steps Ahead Prediction by the ARX Model (nnarx) for Oxygen in the Flue Gas While Tracking Hot Water Temperature at 120°C Using <i>Test 30</i> Data (1 <sup>st</sup> & 3 <sup>rd</sup> Quarter Data Set for Training & 2 <sup>nd</sup> & 4 <sup>th</sup> Quarter Data Set for Validation - <i>Training Model 16</i> )	151
Figure 7.24	Six Steps Ahead Prediction by the ARX Model (nnarx) for CO Emission While Tracking Hot Water Temperature at 120°C Using <i>Test 30</i> Data (1 <sup>st</sup> & 3 <sup>rd</sup> Quarter Data Set for Training & 2 <sup>nd</sup> & 4 <sup>th</sup> Quarter Data Set for Validation – <i>Training Model 17</i> )	151
Figure 7.25	Water Temperature & Oxygen Concentration under NNBC Integrated with O <sub>2</sub> Neural Model Mode While Tracking Hot Water Temperature Set Point at 120°C – <i>Test 31</i>	153
Figure 7.26	Pollutant Emissions under NNBC Integrated with CO Neural Model Mode While Tracking Hot Water Temperature Set Point at 120°C – <i>Test 31</i>	153
Figure 7.27	Water Temperature & Oxygen Concentration under Plant PID Controller While Tracking Hot Water Temperature Set Point at 120°C – <i>Test 32</i>	155
Figure 7.28	Pollutant Emissions under Plant PID Controller While Tracking Hot Water Temperature Set Point at 120°C – <i>Test 32</i>	155
Figure 8.1	Propose Setting Network Architecture	161
Figure 8.2	The Inclusion of Coal Properties as Input Parameters to the Setting Network Encoding into the Overall NNBC System Strategy	162

# List of Tables

Table 3.1	Experiments Conducted on the 0.7MW Chain Grate Stoker Boiler Test Facility	52
Table 3.2	Summary of Results for NO <sub>x</sub> & CO Emissions in Exhaust Duct & Oxygen Concentrations in the End of Smoke Tube following Gradual Load Changes at Lower & Higher Excess Air Levels for Dawmill Smalls – <i>Tests 2 &amp; 3</i>	57
Table 3.3	Summary of Results for NO <sub>x</sub> & CO Emissions in Exhaust Duct & Oxygen Concentrations in the End of Smoke Tube following Gradual Load Changes at Lower & Higher Excess Air Levels for Dawmill Singles – <i>Tests 5 &amp; 6</i>	59
Table 3.4	Summary of Results for NO <sub>x</sub> & CO Emissions in Exhaust Duct & Oxygen Concentrations in the End of Smoke Tube following Gradual Load Changes at Lower & Higher Excess Air Levels for Columbian Smalls – <i>Tests 8 &amp; 9</i>	61
Table 4.1	ARX Regressor Structure Configuration for Oxygen Concentration	71
Table 4.2	ARX Regressor Structure Configuration for Nitrogen Oxides Emission	78
Table 4.3	ARX Regressor Structure Configuration for Carbon Monoxide Emission	85
Table 5.1	Commissioning Tests Conducted on the 3.7MW <sub>th</sub> Chain Grate Stoker Fired Shell Boiler	94
Table 5.2	Target Oxygen Band at Different Range of Firing Rate in Percentage of MCR	98
Table 5.3	Final Target Optimum Oxygen Band from Full Turn Down to Maximum Load in Percentage of MCR	105
Table 7.1	Control Experiments Conducted on a 3.7MW <sub>th</sub> Industrial Stoker Boiler under the Influence of the NNBC & the PID Controller	125
Table 7.2	Relationship between the Ranges of Oxygen Readings with respect to the Ranges of Airflow Alterations Required	126
Table 7.3	Oxygen Target Band at Different Range of Firing Rate in Percentage of MCR	144

# Nomenclature

MW	Thermal output from a boiler in Mega Watt
MCR	Maximum continuous rating of boiler output
MLP	Multi-Layered Perceptron
$t$	Current time
BP	Back-propagation
TRAINBR	Training function of Bayesian regularisation
ARX	Auto Regressive with eXogenous inputs regressor structure
$\varphi(t)$	Regressor vector function of the ARX structure
$\theta$	Weight vector of a neural network architecture
$g$	Function realised by the neural network predictor
$n_a$	Number of past outputs used for determining the prediction
$n_b$	Number of past inputs
$n_k$	Time delay associated with an input
ASSE	Average sum squared error
$Y_i$	Actual plant response
$y_i$	Model prediction
$N$	Number of samples in the data set
$d$	Time in multi-step into future
$rv$	Rotary valve speed
$gs$	Grate speed
$af1$	Airflow from air chamber 1
$af2$	Airflow from air chamber 2
$af3$	Airflow from air chamber 3
$af4$	Airflow from air chamber 4
$O_2$	Oxygen concentration
$NO_x$	Nitrogen Oxides
$CO$	Carbon Monoxide
ppm	Part per million
PRESTD	Normalising the input and target data set to mean of 0 and standard deviation of 1
OBS	Prune feed forward networks with optimal brain Surgeon

# Chapter 1 Introduction

Coal has been and still is an important source of fuel to meet the demand for energy from various industries to provide steam/hot water for a wide range of heating and other process applications [DTI Capability Brochures CB001, 2002]. Currently, coal continues to be one of the major sources of energy in the world and provides about 25.5% of total global energy usage and generating around 38.7% of the world's electricity. [PowerClean, 2003].

Over the last decade the Clean Coal Technology (CCT) Programme of the Department of Trade and Industry (DTI) has supported UK coal R&D activities in industrial boilers to improve efficiency, reduce environmental impact and improve operational aspects of such boilers. As a result, the UK retains extensive, comprehensive technical knowledge, skill and expertise in all areas of coal-fired industrial boilers, such as design, manufacture, operation, control, safety, maintenance and pollution abatement. In fact, this high level of expertise are needed in many developing countries like China, India, Indonesia, Poland and Romania where energy demand is on the increase and coal is a cheap and readily available primary fuel source for industrial use [DTI Capability Brochures CB001, 2002].

More stringent environmental legislation on the emission of pollutants such as sulphur dioxide ( $\text{SO}_2$ ), oxides of nitrogen ( $\text{NO}_x$ ) and particulates from industrial coal-fired plant and competition from other fuels (e.g. gas and oil) have significantly reduced the quantity of coal used in the UK. These factors have, however, focused attention on efficiency and environmental improvements through changes in operating practices, upgrading of equipment and cleaner ways in which coal can be utilised [DTI Capability Brochures CB001, 2002]. Although there are no emission restrictions for a boiler below 20MW, it is likely that the emission limit will be imposed in the future to be in line with those of the 20 to 50MW range coal fired boilers [IEA Statistics, 1998].

The range of equipment available for coal firing in industrial boilers is wide-ranging. However, in many industries and countries the burning of coal in small to medium sized boilers continues to occur with the relatively simple technology of the chain grate stoker



[Neuffer *et al.*, 1998]. Despite the simplicities of design, it is enormously complicated to optimise the combustion and thermal efficiency of this boiler plant whilst simultaneously minimising pollutant emissions and other particulates under fluctuating load following conditions. Although boiler modifications can minimise pollutant emissions in particular NO<sub>x</sub> emissions, the cost of retrofits can be very expensive. However, it is possible that many boilers could meet attainment limits and improve efficiency by appropriate boiler control settings, without expensive hardware retrofits. This could perhaps be achieved by the careful setting of all control parameters. However, those settings are no longer optimal if the boiler conditions or the fuel characteristics change over time [Reinschmidt and Ling, 1994]. The resultant reduction in operating conditions may be accompanied by enhanced rates of boiler fouling and as a result, the overall thermal efficiency of the boiler can fall by 10% or more from an initial typical value of approximately 80% at full load. In some cases carbon monoxide can be substantial and similarly, NO<sub>x</sub> emissions can rise to a higher level during an operating campaign [Grainger and Gibson, 1981; Chong, 1999].

Conventional methods of control have limited application since mathematical models based on the fundamentals of combustion and heat transfer do not adequately describe the operation of the boiler and thus cannot be used to predict the effects of load changes on efficiency and pollutant emissions. Even if an adequate mathematical model could be formulated there would still be severe control limitations since the system would be unable to cope with unexpected changes because boiler combustion profiles changes continuously due to coal quality, boiler load, changes in slag/soot deposits, ambient conditions, and the condition of plant equipment over extended periods of operation. Moreover, using the mathematical model to quantify the combination effects between input parameters (coal feed and airflow) on the process variables (water temperature and excess air level) is enormously complicated thus making the task of delivering the appropriate control decision even harder.

Artificial Neural Networks (ANNs), with their massively parallel approach, are capable to learn complex patterns between input and output data. The attractive feature of an ANN is that it makes a framework for non-linear modelling, identification and control of industrial plant based on an ability to learn complex non-linear functional mappings and adaptive

capabilities [Saha *et al.*, 1998]. Moreover, the network can be taught particular responses to patterns of presented data, such that it can subsequently not only recognise such patterns when they occur again, but also recognise similar patterns by generalisation. As a result, ANNs are capable of empirically modelling the combustion process in a utility boiler as a function of parameters, such as the coal feed and air flow rates and to continually learn in an on-line mode and to modify set-points and bias adjustments to keep the unit tuned to the desired emission and performance levels [Booth and Roland, 1998]. In this case, a non-linear 'black box' model is a promising method to symbolise the expert operator's knowledge based on ANNs. Besides, as it is known that neural networks are very useful for non-linear system modelling, the use of neural networks to construct non-linear predictors may be promising for non-linear process control [Tan and Cauwenberghe, 1999]. This is evident from some earlier literature which asserted that neural networks have been proved to be very useful for non-linear system modelling and control [Narendra and Pathsarathy, 1990; Chen and Billings, 1990]. In the case of the stoker boiler, it is necessary to model the relation between the NO<sub>x</sub> emissions, carbon monoxide (CO), oxygen concentration (O<sub>2</sub>) with the coal feed and airflow rates, and to develop a controller that determines the parameter settings to minimize pollutant emissions and maximise efficiency over a wide range of operating conditions. Thus the neural model should be capable of analysing data from various sensors and once trained should be able to recognise if the combustion process is sub-optimal.

Training of the network plays an important role in designing the ANN based controller. The performance of the controller depends on how the ANN was trained and training must cover the working conditions of the plant in order to get the best performance. Backpropagation for the training of the feed-forward Multi-Layered Perceptron (MLP) network is the most widely used learning algorithm and the most-often considered member of the neural network family, was implemented in this research work and has been proven through a large number of other practical applications [Demuth & Beale, 1998]. Backpropagation is a recursive gradient descent algorithm designed to minimise the mean squared error between the actual computed output and the desired output. In addition, this method can obtain fast convergence during training.

The main objective of this project was to control a chain grate stoker fired boiler by the development of a neural network based controller (NNBC) with the aim of increasing the overall thermal efficiency and maintaining pollutant emissions below future medium term stringent legislation. At present it is usual industrial practise for the efficiency to be sacrificed by allowing the stoker to operate at a higher excess air to ensure complete burn out of the coal hence minimising any operating difficulties throughout the entire firing range. Therefore, one way to help maximise boiler efficiency and minimise pollutant emissions is to maintain the amount of excess air to an acceptable level consistent with satisfactory carbon burn out for the entire firing range. As a result, a series of experiments have been conducted to cover a wide range of boiler conditions and the gathered data were used to train the neural network components of the controller. Data gathered from these experiments included pollutant emissions ( $\text{NO}_x$  and  $\text{CO}$ ), the oxygen in the flue gas and the load condition (coal feed and air flow rate).

The remainder of the thesis is organised in the following way. Chapter 2 reviews the environmental impact from coal combustion and current legislation limits before progressing to describe the combustion principles of the chain grate stoker. The final Section of this Chapter reviews the justification of using ANNs as a modern tool to enhance the performance of the chain grate stoker before laying out the relevant literature in the application of ANNs to related processes. The main features and the range of plant instrumentation of the 0.7MW pilot scale stoker test facility located at Casella CRE Ltd are described in Chapter 3 and the detail of the preliminary experimental results obtained under various test conditions for three different types of coal are discussed. Chapter 4 describes the implementation of an ANN non-linear ARX model as a black box modelling tool to identify the combustion process (oxygen concentration in the flue gas) and pollutant formation (nitrogen oxides and carbon monoxide emissions) to predict into the future using data obtained and discussed in Chapter 3 and also from a previous research project (BCURA B35) on the same test facility.

A description of the 3.7MW industrial stoker boiler located at HMP Garth is provided in Chapter 5 together with a discussion of commissioning test results obtained while manually

varying the excess air level at a given firing rate before progressing to present a detailed description of the neural network based controller (NNBC) development in Chapter 6. This development includes the use of information presented in Chapter 5 to determine the optimal boiler setting and also for use in the training of the individual neural network components and their integration within a carefully designed control strategy that basically imitated the decision making process of an expert human operator. This allowed the controller to recognize boiler behaviour if it was sub-optimal and to decide on the necessary remedial actions. Chapter 7 provides a detailed discussion of the on-line implementation of the developed NNBC on the 3.7MW industrial stoker boiler and its performance is compared with the existing plant PID controller. The overall conclusions from the work with respect to the model predictions of the combustion derivatives using data gathered from the stoker test facility and the performance of the overall NNBC on the industrial stoker boiler are drawn in Chapter 8 together with recommendations for further work that are laid out in the last Section of this Chapter.

## Chapter 2 Literature Review

This chapter starts by introducing the importance of coal, followed by the environmental impact of coal combustion and the current legislative limits for coal fired boilers. Next the principle of operation and development of chain grate stokers is discussed before a thorough review of the implementation of Artificial Neural Networks (ANNs) as a tool to enhance the performance of combustion processes through monitoring and control.

### 2.1 The Importance of Coal

This first Section introduces the reader to the importance of coal as a primary source of energy with large reserves. This is followed by the review of the environmental impact from coal combustion and finally the current legislation limits for coal fired boilers will be discussed.

A growing world population and economic development is resulting in an ever-increasing global energy demand. Coal is one of the major sources of energy with large reserves in the world and currently meets 25.5% of global energy demand. Over 1450 millions tons of the coal produced worldwide is burnt in large combustion plant, mainly power stations, generating around 38.7% of the world's total electricity [CARNOT On-line Case Study, 2000; PowerClean, 2003]. A further 18% of the coal produced is burnt in industrial appliances to generate steam/hot water for use in industrial processes and space heating. Whilst this fraction has dropped over recent years globally, it is likely to continue to rise for the foreseeable future. It is predicted that global primary energy demand will increase by between 150% and 250% by 2050 and by between 200% and 500% by 2100 [CARNOT On-line Case Study, 2000]. According to Hobbs *et al.* (1993), world coal production increased from 4.2 billion tons in 1980 to 5.2 billion tons in 1988. At this level of production the recoverable world coal reserves would last for over 200 years [Hobbs *et al.*, 1993].

Although coal is the most plentiful and cheapest form of fossil fuel, natural oil and gas are currently supplying the majority of the world's energy needs [IEA Statistics, 1998].

Nevertheless, in order to meet demand the energy supply market would have to be supplemented by an energy source that is abundant and can easily be extracted and utilised. Coal fulfils these requirements especially with the aid of new coal combustion technology [PowerClean, 2003]. With the introduction of increasingly stringent legislation on the emissions of various pollutants from large combustion plants in the European Union (EU) during the last decade, development activities have concentrated on cleaner coal technologies (CCT) to burn coal with greater efficiency and reduced emissions. Furthermore, the competition from other fuels such as oil and gas has also given an impetus to the development and application of cost-effective CCT, taking advantage of the latest technological developments in areas such as monitoring, instrumentation and control systems [CARNOT On-line Case Study, 2000].

### 2.1.1 Influence of Coal Combustion on Environmental Aspects

As mentioned earlier, around 40% of the world's total electricity is generated by burning coal in large combustion plant located at power stations. Unfortunately, the combustion of coal in this appliance is also a major source of environmental pollution. The major emissions associated with the combustion of coal are particulates, oxides of sulphur ( $\text{SO}_x$ ), oxides of nitrogen ( $\text{NO}_x$ ) and carbon dioxide ( $\text{CO}_2$ ), which arise respectively from ash, sulphur, nitrogen and carbon in the coal. With respect to stationary combustion plant, carbon dioxide and nitrous oxide are the principle Greenhouse Gas Emissions (GHGs) with the emission of  $\text{NO}_x$  generating 5% of the total nitrogen oxides in the atmosphere. It is a constituent 'greenhouse gas' which is thought to be responsible for the global warming of the earth's surface and also the formation of nitric acid in rain. This results in increased acidity of soil and water, thus causing long term environmental damage which affects plants and animals [CARNOT On-line Case Study, 2000]. In addition, other products of combustion have also been recognised to have an adverse effect on the environment on a global scale and this has led to many countries enforcing 'green policies' to address this issue.

### 2.1.2 Current Legislation Limits for Coal Fired Boilers

The short and long-term effects of air pollution on the environment are varied and profound. Acid rain, global warming, smog and the depletion of the ozone layer are just a few of the most alarming results of pollution. Currently the 1990 Environmental Protection Act (EPA 1990) only sets limits for coal fired boiler plants of 20 to 50MW net thermal input. However, the European Union is planning to include small coal fired boiler plants of 1 to 50MW thermal input, with a large percentage of conventional stokers falling within this range, but this legislation has yet to be implemented.

The current legislative limits of sulphur oxides and nitrogen oxides for coal fired boiler plant of net thermal input between 20 to 50MW (the closest range to conventional stoker firing appliances) is 2000mg/Nm<sup>3</sup> and 500mg/Nm<sup>3</sup> (milligram per Normal meter cube) or 700ppm and 245ppm (normalised to 6% oxygen in the flue gas) respectively [IEA Statistics, 1998]. Nevertheless, NO<sub>x</sub> emission does not pose so much of an immediate threat as compared to SO<sub>x</sub>. However, it will be worth mentioning here that NO<sub>x</sub> emissions do not raise much concern in chain grate (the most popular form of stoker) due to its natural form of air staging along the fire bed. [Clarke and Williams, 1992; Livingston *et al.*, 1995].

Carbon dioxide is not a pollutant, however worry has been expressed that further increases of the CO<sub>2</sub> content in the atmosphere, resulting from additional fossil fuel combustion, might inflict significant threats on the climate due to the 'greenhouse' effect. There is no current legislative limit on CO<sub>2</sub> but the current approach is to improve the overall thermal efficiency by burning less fuel for the same output thereby reducing the total CO<sub>2</sub> produced [Good Practice Guide 30, 1999]. As asserted by Kay (1994), the emission level for carbon monoxide (CO) might well not be particularly regulated, but good practice will dictate its measurements anyway. The current legislative limit of particulate matter for stoker fired plant with an individual net thermal input of between 20 to 50MW is 300mg/Nm<sup>3</sup> (milligram per Normal meter cube) normalised to 6% oxygen in the flue gas [IEA Statistics, 1998]. However, particulate matter (grit and dust) is not so much of a problem with conventional stoker firing owing to the bigger particles which can be retained by the use of a high efficiency cyclone and also to the lower combustion intensity.

### 2.1.3 Summary

Coal combustion remains a significant contributor to the production of power globally and at current production levels, coal reserves are estimated to last over 200 years. However, changes in environmental legislation on the emissions of pollutants from coal fired plant and competition from other fuels (i.e. gas and oil) have significantly reduced the quantity of coal used over recent years. These factors have, however, focused coal users' attention on efficiency and environmental improvements through changes in operating practices and upgrading of equipment for example, in order to make coal competitive in the energy market place.

## 2.2 Industrial Coal Firing Appliances

The range of equipment available for coal firing is extremely varied. This Section describes the development of chain or travelling grate stokers as they are the most popular form of coal firing appliances for stoking devices and are of interest to the current research work. The remaining two Sub-Sections describe the combustion process on the grate and the requirements for efficient coal combustion on chain grate.

Basically, stokers are mechanical devices that burn solid fuel in a bed at the bottom of a furnace. They convert chemical energy in the fuel to thermal energy which is absorbed by the boiler surfaces to generate steam or produce high-temperature water. It is designed to ignite the fuel in the presence of an adequate supply of air, and dispose of the gaseous products and non-combustible materials. Historically, the greatest impetus for the development of stokers came from two sources; objections to smoke emission resulting from hand firing and imperfect combustion and limitations on steam output of boilers inherent in manual stoking. James Watt made the first documented attempt to fire coal by means of a mechanical stoker. In 1785 his patent described a device combining a coal hopper, a grate for fuel burning and provision for refuse [Singer and Owens, 1966].



Over the years many improvements in the design and construction of stokers has been made to increase the combustion, eliminate smoke production and automatically handle ash and coal as simply as possible. The introduction of mechanical stokers during the latter half of the nineteenth century overcame many of these problems, and provided the first opportunity for semi-automatic, smoke-free operation over extended periods and led to significant improvements in efficiency [Good Practice Guide 88, 2000].

Factors such as coal rank, size, moisture content and ash properties are important criteria for good stoker design, however, the design of stokers differs mainly in the way fresh coal is supplied to the bed. Essentially there are two main principles of combustion associated with conventional coal firing devices, and almost all of the stokers that are still in use today can be classified as being either of the overfeed or underfeed type. Overfeed stokers are designed so that the fuel enters the active combustion zone from above, in opposition to the primary airflow. A major class of this stoker design are spreader stokers which deliver the fuel so that a portion burns in suspension while the remainder burns on either a stationary or moving grate. Overfeed combustion systems are only suitable for graded fuels such as 'Singles' and are not suitable for high rank coals. In an underfeed stoker the fuel and air travel in the same relative direction - both entering the active burning zone from beneath the bed. Underfeed stokers are normally built in a single or multi-retort design and included in the underfeed category is the chain grate stoker. The underfeed combustion system is well suited to ungraded fuels, such as 'Smalls', but the coal used must be properly selected. In addition, underfeed combustion systems can provide better carbon burnout than the overfeed designs. Nevertheless, most of the principles of both underfeed and overfeed mechanical stoking were understood and applied before 1860 and improvements to the stoker design have made it possible to burn almost every conceivable solid fuel.

The advantages of mechanical stokers are that they are robust and simple as compared to pulverised fuel firing which requires grinding or gasification of solid or liquid fuel to become fuel gas. Besides, particulate emissions from mechanical stokers are relatively simple to control and modern stokers can offer high turn down ratios. Despite their long history, mechanical stokers are still widely used throughout the UK mainly for the production of

process heat (below 20MW) and a few in larger water tube boilers for steam production (between 20 to 50MW) in the process and utility sectors. Although the relative importance of stokers as a means of firing coal has decreased over the years, particularly in power-generating stations where the boiler and turbine-generator size has far exceeded the output capabilities of stokers, they remain an important type of commercial firing equipment for industrial power plant.

### 2.2.1 Chain and Travelling Grate Stokers

Chain and travelling grate stokers are the most widely applied appliance for the combustion of solid fuel for both water tube and fire tube boilers. In principle, both stokers consist of a moving grate of the endless mat type with the only distinctive difference between them being that the travelling grate has individual cast iron flap type louvres that are mounted freely on a rod to form the endless mat instead of small links. Unlike chain grates, the louvre links are never under any imposed tension or compression with the air spacing between the assembled links of the mat being regular and narrow, providing a high air-velocity for cooling and avoiding fine particles of coal falling through the grate. The chain and travelling grate systems can operate on different coal types, however an ash content of 5% or greater is one of the most important coal characteristics with these systems, as the ash layer on the grate provides protection from the potentially damaging heat in the fire bed. In general, the operation and maintenance of chain and travelling grates is very similar.

Chain grate stokers are used for the small-scale production of steam and hot water for industrial processes and have proved to be a very reliable and efficient method of burning coal. Historically, the invention of the chain grate principle is credited to Juckes in 1841, one of the oldest known forms of mechanical stoker for firing coal [Good Practice Guide 88, 2000]. With the aid of pneumatic coal and ash handling devices, the use of Proctor's fire break unit of a high-level rotary feeder, a motorised undergrate damper and also the availability of long term oxygen sensors have made them very suitable for full automation [Proctor, 2000; CARNOT On-line Case Study, 2000].

The range of output available using these systems typically is between 1.5MW and 80MW and they offer an extremely versatile coal-firing system. There have been many variations on the same theme but all consist of a partially flexible, looped 'mat' made up of metallic links connected to a drive system. The top surface of the mat remains under tension and acts as a continuously moving grate and coal is fed from a hopper which is located at the front of the boiler, from where it is conveyed into the combustion zone. As this is a continuous process, ignition of the coal is effected by radiation from a refractory arch [DTI Case Study 004, 1998]. Volatile matter in the coal is released following the radiation by the refractory arch releasing volatile matter and subsequently to combust the char. The fuel bed depth is set by regulating the speed of a rotary feeder and the grate to yield a uniform bed height required for any particular fuel or firing condition. The correct fuel bed height for burning Smalls grade bituminous coal is around 100mm [Good Practice Guide 88, 2000].

The primary air is provided by a forced draught (FD) fan and is fed from beneath the grate. The FD fan provides sufficient air for combustion and overcomes the resistance of the grate and of the fuel bed and also cools the chain mat. In addition, an induced draught (ID) fan located at the boiler exit is also needed on a chain grate stoker to ensure a slight suction within the furnace to prevent smoke and combustion gases entering the boiler house, and also prevents the stoker front from overheating. By introducing a high level rotary feeder and a variable speed motor drive, the grate speed becomes infinitely variable allowing an extensive turndown ratio to be achieved, i.e. 8:1 and the response to load changes is acceptable although this is often a problem with this type of firing system.

## 2.2.2 The Combustion Process on a Chain Grate Stoker

The process of combustion of coal on moving grates is an enormously complex one. There are hundreds of reactions occurring simultaneously involving a large number of chemical species. Most reactions take place within the gas phase in the fuel bed or above the fuel bed in the furnace. The remaining reactions occur at the surface of within the pores of the coal particles [Neuffer *et al.*, 1996]. Therefore, it is vital to initiate and maintain stable combustion conditions on the bed in order to achieve high efficiency. In addition, adequate time must be allowed for a high degree of carbon burn out and also to ensure near complete combustion of the volatile matter. The latter requirement is usually met by providing extra air and turbulence at the appropriate point and by maintaining an adequate temperature. Although the boundaries between each combustion zone are not clear and difficult to define as combustion takes place gradually along the grate, a bed of burning coal, with an adequate supply of air for complete combustion, may be broadly divided into three zones for illustrative purpose (Figure 2.1). However, it is important to note that different types of coal will have a different bed profile on the grate.

Zone 1 – The moisture content is firstly driven off as vapour as the freshly supplied coal is passed beneath the ignition arch by the radiant heat of the arch. Volatile gases such as hydrogen, methane, other hydrocarbon gases, carbon monoxide and carbon dioxide are then distilled off when the bed temperature reaches 350°C or higher [Good Practice Guide 88, 2000]. These volatiles provide a certain amount of over-bed combustion and smoke will be produced if the volatiles are not completely burnt. As this volatile matter burns ignition occurs on the top surface of the ‘green’ coal and travels downwards to the grate. This is one of the most important facets of the combustion process as the efficient combustion of coal moving at a specific feed rate is heavily reliant on this stage.

Zone 2 – Combustion of both volatiles and fixed carbon takes place as the bed of coal travels further into the furnace tube. It will be worth mentioning here that when burning low volatile coals, it is necessary to fit relatively long ignition arches that extend into the furnace in order to initiate and maintain ignition. But when using free burning high volatile coals, ignition is easily achieved by relatively short arches [Good Practice Guide 88, 2000]. The combustion

then becomes self-supporting if the conditions on the fire bed are properly maintained, i.e. the rate at which fresh coal is fed into the stoker does not exceed the rate at which it can be ignited and sufficient air is provided [Chong, 1999].

Zone 3 – Combustion of the char proceeds at a rate determined by the intrinsic kinetic rate of the residual char and the physical rate at which oxygen can diffuse to the surface of the char particle [Dudek and Wessel, 1999]. However, the remaining char should have been burnt off before the end of the grate leaving the inert ash to be dropped off the end of the grate as the chain mat travels round the roller.

The combustion rate in the furnace is controlled by regulating the flow rates of the fuel and air. The fuel supplies the combustible material which releases its total heating value when burned to completion. A more in depth explanation is that the actual combustion rate is controlled by the rate of oxygen diffusion through the outer boundary layer around the coal particle and this boundary layer thickness is directly proportional to the particle size and particle burnout time is inversely proportional to the square of the particle diameter. Optimum particle size is a fuel-dependent consideration for which bed depth, appropriate grate speed (retention time), and combustion air feed to the various grate zones can be adjusted within the limits of the equipment capability. Therefore, the optimised performance would be controlled by the ability to burn the char, with only small amounts of unburned carbon leaving the grate [Bauer *et al.*, 1991].

It is also important to maintain the operative temperatures inside the furnace within a temperature range of 200°C to 280°C in order to minimise slagging and fouling of the furnace and smoke tubes thus increasing the availability of the plant. However, different coal types have a different operating temperature range that is determined by the melting temperature of the ash in the coal. Besides, the ash content of the fuel burnt is also an important factor to protect the grate from the intense heat in the furnace tube as the ash forms an insulating layer that helps to protect the grate from overheating. In fact, the ash content of the coal to be used is a crucial factor to be considered when choosing the material for the links of the chain grate stoker [Good Practice Guide 88, 2000].

Finally, the ignition factor must also be taken into consideration to ensure stable and efficient combustion. As mentioned earlier, it is necessary to fit relatively long ignition arches that extend into the furnace when burning low volatile coal in order to initiate and maintain ignition and vice versa when using free burning high volatile coals. Therefore, the design of the ignition arch also plays an important role in deciding which types of coal that can be burned on a particular chain grate. This is the reason why there may be an additional rear refractory arch at the end of the grate in large travelling grate stokers to assist the combustion process due to the mass of coal on the grate [Gunn and Horton, 1989].

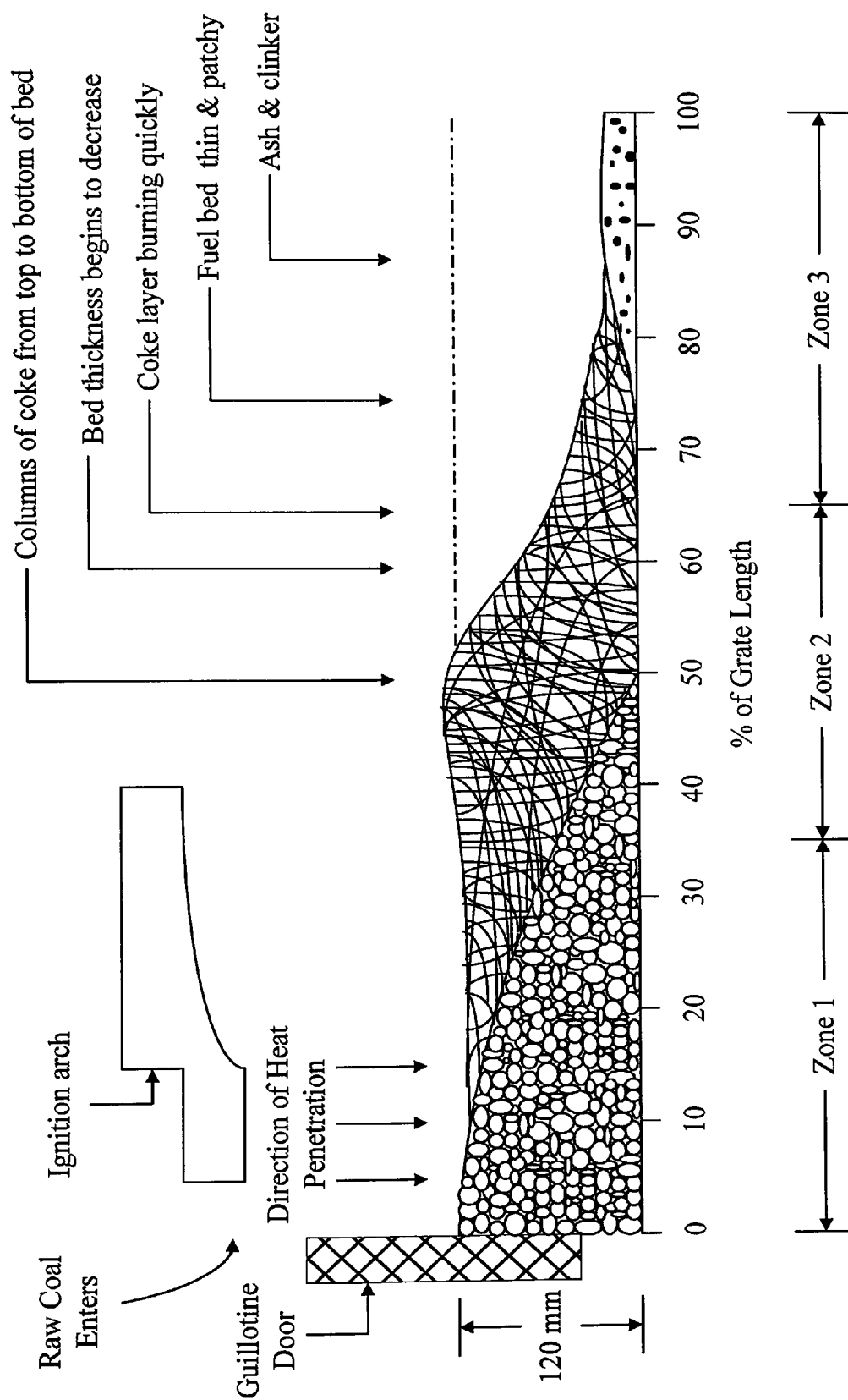


Figure 2.1: Sequence of Combustion on a Chain Grate Stoker [Good Practice Guide 88, 2000]

### 2.2.3 Requisites for Efficient Coal Combustion on Chain Grates

In order to operate a chain grate stoker efficiently, there are several conditions that must be met. The correct regulation of the coal and air feed in order to meet the load demand is the most important criteria assuming that the stoker is in good working condition and that the correct type of coal is being used in terms of the size distribution, rank and the appropriate moisture content. As asserted by Neuffer *et al.* (1998), the efficient combustion of coal moving at a specific feed rate on a chain grate stoker is dependent upon two components; sufficient heat to ignite the 'green' coal and sufficient oxygen to allow complete combustion. It is worth mentioning that the coal properties such as calorific value, volatile content, moisture content, particle size and distribution and most of these parameters are not known exactly and will vary greatly. Moreover, these parameters might be different in different parts of the bed [Neuffer *et al.* 1996]. It is important to ensure that the rate at which the coal is being fed into the furnace chamber matches the rate at which it can be ignited for an optimum bed profile. This consequently will ensure good carbon burnout and a stable self-supporting combustion process. The optimum excess air must then be provided to ensure the minimum sensible heat loss in the flue gas whilst maintaining satisfactory combustion, as the sensible heat loss in the flue gas increases with the excess air and the efficiency reduces in proportion to increasing excess air.

Careful attention must also be given to the primary air distribution along the length of the bed to ensure proper cooling of the chain mat in addition to providing good combustion. Besides, for boilers running with a good burn-off on the grate, there must be only ash at the end of the grate, i.e. the coal must be completely burnt out 100-150 mm before the end of the grate at maximum output [Good Practice Guide 88, 2000]. In addition to the forced draught supply, sufficient suction must also be provided via the use of an induced draught fan to ensure clean boiler operation. Gunn and Horton (1989) & Chong (1999) asserted that changing the air flow first over a period of at least 2 minutes before increasing the coal feed rate shortly (1 minute) after on load increase and vice versa on load decrease ensured better transient operation. In situations where large load changes are frequent, it is important to alter the coal and air feed in such a way that the ignition plane movement and also the transient CO emission is minimised.



For bituminous coal firing on a chain or travelling grate, satisfactory performance would be smoke free operation with the oxygen concentration in the flue gas falling between 7 to 9% at high fire, 9 to 11% at medium fire and 11 to 13% at low fire with corresponding excess air level of 45% to 65%, 65 to 100% and 100 to 150% respectively. In order to ensure a shorter fire bed and avoid live fire being dropped off the end of the grate during frequent large load changes, the usual practice for the vast majority of stokers is to set a high excess air level. This in turn will have little carbon in ash losses, but the penalty in dry flue gas losses can be much larger, hence reducing the overall thermal efficiency. Thus, an adequate compromise must be made to ensure optimum combustion on the grate.

#### 2.2.4 Summary

Chain and travelling grate stoker systems are still particularly important for the larger end of the industrial boiler market nowadays. They are still the preferred firing system for steam/hot water for use in industrial processes and space heating in many countries and with the aid of pneumatic coal and ash handling devices, the use of Proctor's fire break unit consisting of a high-level rotary feeder, a motorised undergrate damper and also the availability of long term oxygen sensors have made them very suitable for full automation. However, the proper control of a chain grate stoker requires scrupulous set up of the plant followed by careful manipulation of the many input variables to ensure that combustion continues under all operational modes i.e. protection of the arch condition must be ensured, in addition to lowering pollutant emissions and maximising the boiler efficiency while the load demand is met. It will be worth mentioning that improvements in instrumentation, control systems, and mechanical conditions would gain a few percent in overall thermal efficiency with corresponding reductions in pollution which would generate economic savings and carbon dioxide emission reductions.

## 2.3 Lump Coal Combustion

For many years, the combustion of coal on chain and travelling grate stokers has received little attention so the potential benefits of modern control methods have not been fully assessed. Therefore, this Section focuses on previous lump coal combustion research with an emphasis on chain and travelling grate stokers and to use this review to highlight areas where further improvements could be accomplished.

### 2.3.1 Previous Research in Lump Coal Combustion

During the 1950's and 1960's, most of the work involving the control of chain grate stokers was conducted by the British Coal Utilisation Research Association (BCURA) and the National Coal Board (NCB) who concentrated on building automatic coal and ash handling systems. Water-cooled side cheeks, which removed the requirement for manual slicing, were also included as a major design feature during this period [Thurlow, 1962; Harris *et al.*, 1962]. The even distribution of primary air over the length of the grate was felt to be the main improvement in the control of the combustion process on the grate and a good example of such work was reported by Rolfe (1961) of BCURA, who invented the use of baffles in the windbox under the grate for the uniform distribution of primary air, thereby improving the boiler efficiency by stopping excess air escaping through the back of the grate [Rolfe, 1961]. According to Good Practice Guide 88 (2000), most grates in operation today still use fixed baffles to supply the correct proportion of air to each zone along the grate.

During the 1960's, due to the availability of cheap oil and gas and the increasing demand to use pulverised fuel (pf) burners in power station boilers, the research effort into coal combustion was mainly concentrated with pf firing. This induced noticeable reduction of research work on stoker firing during that time. However, the oil embargo imposed by OPEC in the 1970's resumed interest in lump coal combustion. The revival of interest in coal combustion in the late 1970's and the increasing pressure from environmental groups for reducing pollutant emissions inevitably gave more incentive to the research work on lump coal combustion, with the main objective of minimising pollutant emissions whilst

optimising thermal efficiency. An early example of such work was published by Giammar *et al.* (1979), where the authors used a pilot scale underfeed stoker to burn a range of coals to study the emission of the oxides of nitrogen. The fuel nitrogen conversion to NO for a travelling grate stoker found through the experimental results to be low compared to spreader stokers and pf firing, under excess air firing conditions [Giammar *et al.*, 1979].

According to Smoot and Hill (1983), pollutant formation from fossil fuel combustion, in particular, NO<sub>x</sub> emissions from coal combustion sources was identified as one of the key areas for future research. With respect to underfeed mass burn stokers, the key area that can still be improved is the primary air distribution along the grate, as this is the main parameter that controls the rate of combustion, and hence the pollutant formation. One piece of work in this area was by Starley *et al.* (1985), where empirical studies were conducted on a pot furnace test facility. In this work, the amount of combustion air was varied from fuel rich to fuel lean conditions and it was found that the bed region stoichiometry was the governing parameter influencing exhaust NO emissions. It was also found that by decreasing the bed region stoichiometry to 44% below that required for stoichiometry, a 67% reduction in NO emissions was achieved.

Another effort to minimise pollutant emissions was reported by Prizzi (1985) on large chain grate stoker fired boilers. This work highlighted the importance of understanding the fundamental requirements of a stoker before considering optimisation or improving the performance of such burners. These included size distribution of the coal used with the correct bed height, good working condition of the stoker, regulation for the correct coal feed rate with near optimum excess air levels and uniform air distribution on the bed. A similar opinion was also expressed by Hadvig (1989) with a view to optimising the combustion process by regulating the amount of air flow to the various zones along the bed length with a customised gas sampling system fitted on a travelling grate stoker. In this work, the primary airflow was regulated in order to maintain a desired level of oxygen and carbon monoxide and simultaneously measuring the oxygen and carbon monoxide level in each zone of the bed. Hadvig (1989) claimed that the idea would certainly improve the combustion efficiency without jeopardising the pollutant emissions if the excess air level could be regulated in each

zone of the bed to meet the combustion needs. In practice, this idea would incur high maintenance costs as the measuring probes need to withstand high temperature since they need to be located close to the firing zone to sample the gaseous species and withstand contamination and also there would be expensive costs in installing such a long term CO sensor.

McHale (1988) asserted that in addition to the task of achieving good control over the combustion process, the aspect of complete automaton of the stoker plant is also vital to ensure competitiveness of these devices in the market with oil and gas burners. This was also recognised by Robson *et al.* (1988) who highlighted the growing effort by manufacturers to automate such devices. The main criteria quoted by the authors for automation were automatic ignition, burnback control, self-cleaning and an ignition plane control system. However, self-cleaning features, robustness and relatively higher flexibility to burn different coal types were just a few of the virtues of the chain grate stoker that attracted the authors attention.

In terms of burnback control, a better solution now available would perhaps be the Proctor firebreak unit which consists of a high-level rotary feeder which provides a permanent barrier of approximately 500mm between the fire bed and the fuel hopper. This barrier would help the chain grate stoker to operate safely especially at low loads to ensure that no possible burnback can occur. Reducing maintenance costs and improving viewing conditions along the length of the grate are also advantages of the Proctor's firebreak unit [CARNOT On-line Case Study, 2000]. Whilst for self-cleaning of slag formation, the use of water cooled sections (water cooled side cheeks) is now commercially available to overcome the problem of clinker slicing on chain grate stokers, ensuring a more consistent and efficient burning regime.

During the 1980's, much work was concentrated on modelling the combustion and these modelling studies resulted in a deeper understanding of the coal combustion process. However, more work is still required before it can be used in a practical application despite all the effort placed on modelling of this coal combustion process. According to Smoot

(1984), the entire foundation of complex process modelling relies heavily on repeated comparison with experimental observations. Smooth (1984) also claimed that many studies have emphasised fundamental aspects of this problem such as coal-pore diffusion, radiative properties of coals and chars, coal structure and its relationship to reactions and particle changes during devolatilisation. Still, the development of these coal-process models requires a large number of specific assumptions. Frequently, these assumptions are not strongly supported by experimental data [Smoot, 1984].

During the 1990's, work concentrated on the reduction of pollutant emissions and improving the thermal efficiency of the chain grate stoker combustion process. This was mainly due to the new legislation on pollutant emissions imposed by the Environmental Protection Act 1990 (EPA 1990). According to EPA 1990, one of the most stringent sections of the Act deals with single or multiple boilers and furnaces with a total net thermal input greater than the 50MW limit. However, the European Union is planning to include small coal fired boiler plants of 1 to 50MW thermal input in its directive, which would cover a large percentage of conventional stokers and this has prompted more attention and work on improving these conventional coal firing devices.

One relevant work to reduce pollutant emissions in particular nitrogen oxide emissions was suggested by Livingston *et al.* (1995) in which an air supply regime that gives relatively lower nitrogen oxides emissions was considered for chain and travelling grate stokers. According to Livingston *et al.* (1995), better air distribution along the grate bed resulted in a significant reduction of nitrogen oxides. However, sulphur dioxide emission may pose more problems than nitrogen oxides in stoker firing. This is because almost 90% of the sulphur content is emitted to the atmosphere as sulphur dioxide during the combustion process, with the rest being retained in the ash [Cooke and Pragnell, 1989].

Since the sulphur content of the fuel is the main source of sulphur dioxide emission, it was not the intention of the current research to investigate sulphur dioxide emissions. But rather to investigate better control of the firing rate to meet a specified load demand in the face of feed disturbances and uncertainties, without increasing carbon monoxide emissions and

carbon in ash losses, and in so doing improve the combustion efficiency whilst maintaining nitrogen oxides as low as possible.

In the middle of 1990's, with respect to further research and development into the control of industrial coal fired boilers, work has concentrated on implementation of artificial intelligence techniques to the on-line condition monitoring and control of chain and travelling grate stokers fired boilers. The most recent application of such work was carried out by Chong *et al.* (2001) in which the authors applied artificial neural networks of ARX structure as a simplistic means to model the gaseous emissions emitted from the combustion of lump coal on a chain grate stoker fired boiler. The resultant 'black box' models of the flue gas concentration and gaseous emissions were able to represent the dynamic behaviour of the process and modelling results showed that one-step-ahead predictions over a wide range of unseen data was accurately presented. The authors also claimed that the accuracy of the model was not only demonstrated with data sets that were obtained from the same experiments (which also demonstrated the repeatability of the model performance) but also for data with a large temporal separation of almost eight months from the training data set. According to Chong *et al.* (2001), a large training set was required for the model to cover most of the operating conditions to ensure the model accuracy [Chong *et al.*, 2001].

### 2.3.2 Summary

Chain and travelling grate stokers have been proved to be a very reliable and efficient method of burning coal and over the years, many improvements in design and construction have been implemented. Since the reduction of pollutant emissions while improving boiler efficiency has been identified as one of the prime areas for future research, the implementation of artificial neural network possesses a great potential to comply with the future requirements of the new legislation on pollutant emissions and to compete with other firing appliances in the market place.

## 2.4 Artificial Intelligence (AI) Using Artificial Neural Networks (ANNs)

The purpose of this Section is to introduce to the reader the implementation of the Artificial Intelligence (AI) techniques using Artificial Neural Networks (ANNs) on the lump coal combustion process for the current research work. The use of AI techniques in this work can be justified from the complex non-linear lump coal combustion process on the grate, in addition to the practical difficulties involved in manipulating various parameters involved in controlling such a process. The first Sub-Sections that follow explain the general view of ANNs. This is followed by an introduction to the feed forward Multi-Layered Perceptron (MLP) network with a back propagation learning algorithm before progressing to describe the neural network based system identification and black box modelling to identify the combustion process as well as pollutant formation of the chain grate stoker boiler. The remaining Sub-Section deals with the literature on related ANN's applications, which serves as an overview of the current status of ANN design and utilisation focusing on the subject of coal combustion.

### 2.4.1 Artificial Neural Networks (ANNs)

The Industrial Revolution, which started in Britain around 1760, has replaced human muscle power with the machine. In the 20th century, Artificial Intelligence aimed to supplement human intelligence with the machine [Munakata, 1998]. AI as a field has undergone rapid growth and diversification. From around the mid-1980s, the repertoire of AI techniques has evolved and expanded. In recent years the control community has witnessed a great number of AI based techniques applied to the modelling and control of processes. One of the main reasons for such interest is due to the restrictions of conventional methods of modelling and control, which can only be applied to linear systems whereas in reality most physical systems are non-linear in nature [Evans *et al.*, 1994]. In comparison to conventional techniques, AI techniques possess advantages of having faster system response, transient recovery from arbitrary initial conditions and robustness with respect to incomplete and noisy data [Bakal *et al.*, 1995].

The field of AI has experienced three stages of extensive activities in the 20<sup>th</sup> century. Earlier stages of AI development can be found in McCulloch and Pitts (1943) followed by Hebb (1949). The work on the second phase was mainly contributed by Rosenblatt (1962) and Minsky and Papert (1969), whereas a good guide to more recent events can be selected in Rumelhart and McClelland (1986) and Pao (1989) [Warwick *et al.*, 1992]. Classes of problems requiring intelligence include inference based on knowledge, reasoning with uncertain or incomplete information, various forms of perception and learning, and application to problems such as control, prediction, classification, and optimisation [Munakata, 1998; Zhou *et al.*, 2004; Yao *et al.*, 2005].

Essentially ANNs are a ‘bottom up’ approach to AI, in that a network of processing elements is designed, these elements being based on the physiology of individual processing elements of the human brain. An ANN as indicated by its name, loosely resembles the structure of a human brain, although there are more than 100 billion neurons in the human brain. An ANN is very powerful due to its robust processing and adaptive capability. It consists of a set of nodes, and is referred to as *parallel distributed processing*. The pattern of connectivity between nodes, known as *weights*, is adjusted according to the selected learning rule. The knowledge of the networks is stored in its interconnections, and the functionality is determined by changing the individual strength of the connections during the learning process [Rumelhart and McClelland, 1986]. Like biological nervous systems, they can be trained to find their own solutions once trained with the selection of data presented to the network and they are useful in applications where formal analysis would be enormously difficult or impossible.

Much of the recent drive has, however, arisen because of numerous successes achieved in demonstrating the ability of ANNs to deliver simple and powerful solutions. As assertion by Billings *et al.* (1992), is that neural networks have in recent times become an enormously fashionable area of research and have been applied in many areas such as speech processing, pattern recognition and non-linear model fitting; all of these have proved to be difficult areas for conventional computing. Other relevant research has also demonstrated the potential of employing AI techniques in the form of ANNs for control of multi-variable nonlinear



dynamical processes, including emissions from coal-fired boilers [Reinschmidt and Ling, 1994; Reifman and Feldman, 1997; Reifman and Feldman, 1998; Jensen *et al.*, 2004].

ANNs can be used where a system is too complex to model using physical laws but there are data available for which there is a lack of knowledge of the relationships between the various parameters. A neural network model is much easier to apply to a complex process where physical principles are not fully understood and thus it can be used as a universal model for many processes [Lu, 1997]. However, any neural network attempting to model a dynamic system must have dynamic properties itself. In other words, it must be able to represent time internally or have memory in a systems sense [Narendra and Parthasarathy, 1990].

An ANN is a powerful modelling tool except where there is a lack of or training data are not sufficiently rich in information about the system dynamics across the operating range of interest. One important property of an ANN is its potential to infer and induce from what might be incomplete or non-specific information. This is, however, also coupled with an improvement in performance due to the network learning appropriate modes of behaviour in response to problems presented, particularly where real-world data is concerned. The network can, therefore, be taught particular responses to patterns of presented data, such that it can subsequently not only recognise such patterns when they occur again, but also recognise similar patterns by generalisation. It is these special appealing characteristics of learning and generalisation that make ANNs distinctly different from conventional algorithm processing computers, along with their potential property of faster operational speeds realised through a computational overhead.

ANNs are prime candidates for modelling complex dynamical processes due to their ability to approximate large classes of nonlinear functions with sufficient accuracy. In particular, ANNs provide an attractive alternative for process modelling when the process is known in terms of its inputs and outputs and general physics-based models are unavailable or difficult to develop [Reifman *et al.*, 2000]. As assertion by Kasparian and Batur (1998) was that, ANNs have been successfully used to model linear and nonlinear systems and also to model the inverse dynamics of systems. Another similar view was also reported by Tan and

Cauwenberghe (1999), in which the authors claimed that ANNs are very useful for nonlinear system modelling, the use of neural networks to construct nonlinear predictors may be promising for nonlinear process control. Therefore, ANNs offer the advantage of being able to handle a large class of nonlinear control problem, which, through minor code modifications, can be customised to specific applications. In addition, unlike most traditional control approaches, neural controllers do not require linear approximations of the system behaviour, which often distorts and does not truly represent the real problem [Reifman *et al.*, 2000].

ANNs can be grouped into two categories based on the network connection architecture, namely feed-forward networks and recurrent networks. A feedforward neural network is made up of layers of neurons between the input to and output from the network, called hidden layers, with connections between neurons of intermediate layers. Information is passed from the input to the final output layer in a unidirectional manner whereas in recurrent networks, feedback connections occur within the network either between layers and/or between neurons (Jain *et al.* 1996). Basically, feed-forward networks are static, they are capable of mapping the given set of inputs to the corresponding outputs i.e. the output is independent of the previous input and output of the network. On the other hand, recurrent networks are dynamic, meaning the output at time instant  $t^1$ , is dependent on the previous output or state of the neurons within the network as a result of the feed-back paths.

The learning process in an ANN involves updating the network weights and/or architecture in order to efficiently perform a particular function. The method used to adjust the weights in the process of training the network is called the learning rule. The aim of the training task is to update the weights to obtain the best mapping from the input to the output. In other words, the data that have been collected from the system (inputs) are introduced to the neural network and the weights are iteratively updated so as to minimise the error between the output of the network and the desired response. Training is terminated when the error decreases to a pre-determined threshold value or reaches a minimum [Bakal *et al.*, 1995].

---

<sup>1</sup> Current time

ANN learning can be supervised or unsupervised. Supervised learning requires a teacher to pair each input vector to the network with a target vector representing the desired output. In most supervised neural network training algorithms, the network gradient has to be evaluated at each iteration. The network gradient is defined as the partial derivatives of the network output error with respect to the network's weights. The process model network is trained by updating the network weights such that the difference between the neural network output and the plant output is minimised [Kasparian and Batur, 1998]. While for unsupervised training, the network requires no target vector for the training input vectors presented to the network, hence, no comparisons are made to predetermine the ideal responses. The most widely used supervised learning neural network is the feed-forward Multi-Layered Perceptron network, which can be trained with the popular error back-propagation (BP) learning rule and can be applied to most real-life problems due to its virtues of robustness and a fast computational speed [Demuth and Beale, 1998].

#### 2.4.2 Feed Forward Multi-Layered Perceptron Network Training with Error Back-Propagation Learning Algorithm

This Sub-Section deals with the type of ANNs used in this research work, namely the feed forward Multi-Layered Perceptron (MLP) network trained with the error back-propagation learning algorithm. According to Rumelhart and McClelland (1986), the MLP network is probably the most-often used member of the neural network family and the famous feed-forward MLP network is usually trained with the error back-propagation learning rule [Rumelhart and McClelland, 1986]. The main reason being its capability to model a wide range of relationships, which has been proven through a large number of practical applications [Demuth and Beale, 1998].

The back-propagation algorithm was first proposed by Werbos (1974) in his Ph.D. thesis and further development of this algorithm was carried out by Rumelhart and McClelland (1986) [Billings *et al.*, 1992]. Basically, back propagation is a recursive gradient descent algorithm designed to minimise the mean squared error between the actual computed output and the

desired output and training is continued until the sum of squared error measured at the output layer for the whole training set decreases to an acceptable value. This is done by iteratively changing the values of the network weights and biases in the direction of steepest descent with respect to error. According to Tan and Cauwenberghe (1999), the back propagation method can get a rather fast convergent speed in the beginning of the training as compared to Gauss-Newton and Levenberg-Marquardt algorithms.

Parameters to be considered and selected for training a neural network by back propagation include the learning rate, momentum factor, number of hidden layers and number of neurons in each hidden layer. The learning rate is used to control the amount of weight adjustment at each training step to improve the overall network performance so as to achieve the desired target. While the momentum factor allows the network to make a rationally large weight amendment as long as the adjustments are in the same common direction for several inputs while using a small value of learning rate to prevent a large response to the error from any training input. It also reduces the likelihood that the network will settle to a set of weights that corresponds to a local minimum, not a global one. Thus the implementation of a momentum factor, along with the learning rate makes the network achieve a faster convergence [Saha *et al.*, 1998].

Properly trained MLP networks are likely to give rational answers when presented with data not seen during training. Usually, a new input will lead to an output comparable to the correct output for input vectors used in training that are similar to the new input being presented. As the network is able to generalise, it is possible to train a network on a representative set of input/target pairs and obtain results with certain accuracy without training the network on all possible input/output pairs [Demuth and Beale, 1998].

During network learning overfitting can occur when either too many neurons are used or the network is trained for too long. On testing, large errors occur when the trained network is subject to an unseen data set. In other words, the network has not learned to generalise but rather memorise the training examples. Therefore, the use of a network that is just large enough to provide a satisfactory fit is the way to improve the network generalisation ability.

One approach to this is through the use of Bayesian regularisation, in which the weights and biases of the network are assumed to be random variables with specified distributions and the regularisation parameters are then selected to the unknown variances associated with these distributions. Furthermore, Bayesian regularisation can automatically set the optimal performance function to achieve the best generalisation capability [Demuth and Beale, 1998; Teruel *et al.*, 2005]. As a result, Bayesian regularisation was adopted in this study for error back-propagation learning algorithm to train the feed forward MLP network. With this training function, which updates the weight and bias values according to Levenberg-Marquardt optimisation, a “stop training” function can be utilised to early stop the training if the network performance on the testing vectors fails to improve or remain unchanged.

The used of a feed forward MLP network with error back propagation for modelling and control has attracted the most interest in control engineering, undoubtedly because of their ability to represent arbitrary nonlinear mappings, a powerful property for nonlinear modelling and nonlinear control [Hunt *et al.*, 1992]. Eki *et al.* (1999) also claimed that the back-propagation learning algorithm does not impose any constraint on the number of learning iterations, which is extremely convenient in the case of thermal power plant applications. Figure 2.2 shows a simple example of a feed forward MLP network structure, which comprises of an input layer, a hidden layer and an output layer.

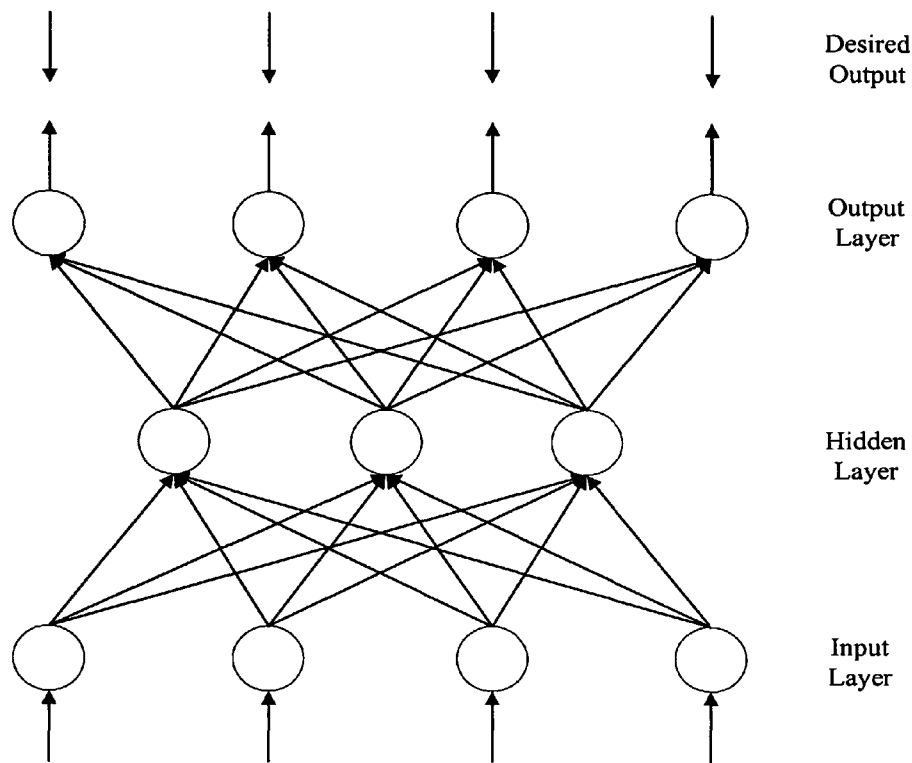


Figure 2.2: A Three-Layer Feed Forward MLP Network Architecture

## 2.5 Neural Network Based System Identification and Black Box Modelling

This Section describes the general approach used for neural network based system identification and black box modelling of the combustion process and pollutant formation on a chain grate stoker using the feed forward Multi-Layered Perceptron (MLP) network. Most of the system identification tasks implemented in this work were referred to a toolbox developed by Noorgard (2000) namely 'Neural Network Based System Identification Toolbox' for use with MATLAB<sup>TM</sup>. However, most of the basic understanding of neural network programming was gained from the 'Neural Network Toolbox', also for use with MATLAB<sup>TM</sup>, which was developed by Demuth and Beale (1998).

### 2.5.1 System Identification

System identification provides tools for creating mathematical models of dynamic systems based on measured data. As asserted by Chong *et al.* (2000), the system identification approach is in many ways an unsophisticated approach to that of the more elegant route of mathematically modelling the physical processes. It is an exceptionally useful tool which can be applied to model a process without having to take into consideration the many complex physical laws that govern a process, which are common in real life situations. According to Neuffer *et al.* (1998), essential features of the process to be modelled must be captured in order to get a useful model, namely the input-output behaviour of the process must be dynamically described; the relevant operating points must be covered; allow simulation of the relevant process variables and avoid excessive computation times since control design is an iterative process. Therefore, the authors believed that a so-called 'Black Box' model would satisfy the above criteria [Neuffer *et al.*, 1998].

In the case of system identification using feed-forward neural networks, care must be taken to ensure the hidden layer would have enough neurons to model the complex relationships of the input-output data being fitted and the usual practice to resolve this query is through trial and error. Generally, the system identification problem coupled with artificial neural networks fundamentally involves finding a suitable model structure followed by good numerical values for its parameters (weights and biases of the network).

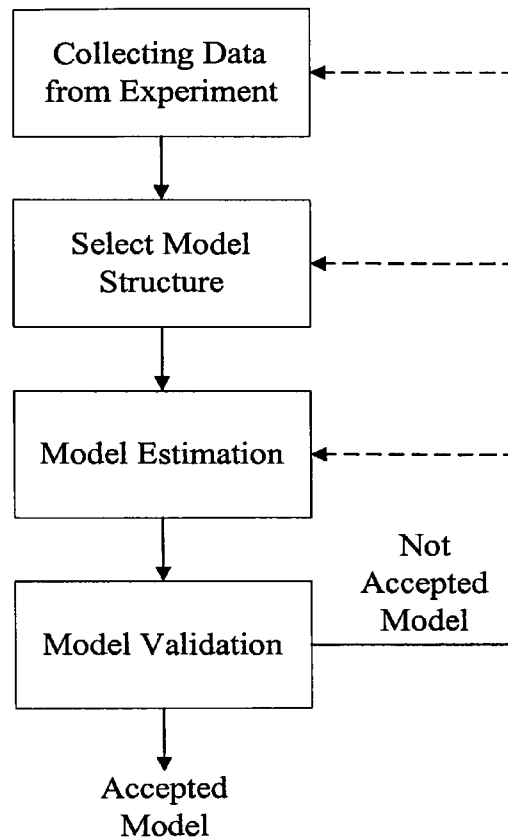


Figure 2.3: The System Identification Procedure [Noorgard, 2000]

There are four basic steps which must be executed when attempting to identify a dynamical system as summarised in Figure 2.3 above, which comprise experimental data collection, selection of the model structure, model estimation and validation with unseen data. However, it is important to note that for the first step, the training data describes the underlying system in its entire operating region with a proper choice of sampling frequency [Ljung, 2000; Noorgard, 2000]. As asserted by Tan and Cauwenberghe (1999), in order to estimate the parameters of a dynamic process model successfully, the input data must be adequately exciting. Therefore, for nonlinear system identification, it is required that the process input effectively excites the process over the entire nonlinear region to be identified [Tan and Cauwenberghe, 1999].



The next step is to select a model structure. A MLP network architecture was implemented in this work together with an appropriate set of regressor vectors, since the process to be identified was non-linear in nature. The ARX (Auto Regressive with eXogenous inputs) regressor structure in conjunction with the function NNARX in the Neural Network System Identification Toolbox was selected. The corresponding regression vector in the toolbox is expressed as:

$$\varphi(t) = [y(t-1) \quad \dots \quad y(t-n_a) \quad u(t-n_k) \quad \dots \quad u(t-n_b-n_k+1)]^T$$

while the predictor can be defined as:

$$\hat{y}(t|\theta) = \hat{y}(t|t-1, \theta) = g(\varphi(t), \theta)$$

where  $\varphi(t)$  = vector containing regressor;

$\theta$  = vector containing weights;

$g$  = function realised by the neural network;

$n_a$  = number of past outputs used for determining the prediction;

$n_b$  = number of past inputs and

$n_k$  = time delay

Basically, the construction of the ARX regressor uses previous inputs and outputs in order to deliver a prediction of the current output at one or more sample periods into the future [Premier *et al.*, 1997; Ljung, 2000]. In order to achieve a more stable network operating range, the function NNARX employs a static predictor (feed-forward only with no feedback), rather than other model types i.e. recurrent, in which future network inputs will depend on present and past network outputs [Noorgard, 2000]. However, the task of choosing the appropriate model order (number of past inputs and outputs) and also the delay of the system is fairly difficult for a non-linear process, and process knowledge will enable the designer to intuitively suggest the orders and delays of the system [Noorgard, 2000; Ljung, 2000]. In the

case of this research work, the decision was made based on experience. It will be worth adding here that more complicated regressor forms could well reduce the sum square error during neural network training but the added complexity of the model was not justified by the possible improvement in forecasting [Premier *et al.*, 1997].

After the generated model has been trained, the next step or the final step is to evaluate the model. The most common practice of validation is to examine the prediction errors by cross-validation on a test set, in other words, this can be achieved by passing unseen data to the model followed by visual inspection of the plot to compare the model predictions to actual measurements. The typical method to calculate the difference between the actual plant response with the model prediction is to use the average sum of squares of the network errors as defined below:

$$ASSE = \frac{1}{N} \sum_{i=1}^N (Y_i - y_i)^2$$

where:  $Y_i$  is the actual plant response;

$y_i$  is the model prediction and

$N$  is the number of samples.

The capability of the model to generalise relies on this validation process, thus it is of paramount importance in the procedure of system identification. If the model predictions have been found to be unacceptable, then the identification procedure will have to refer back from validation to the previous blocks, as showed by the feed back paths illustrated in Figure 2.3. When referring back to the previous blocks, different regressor structures can be tried, in which the time delay, number of past outputs and inputs can be changed to suit the dynamics of the process to be modelled. In addition, different network architectures can also be selected by altering the number of neurons in the hidden layer. However, the regressor structure normally has to be chosen on a trial and error basis until the model gives a satisfactory result [Noorgard, 2000].

## 2.5.2 Non-linear Neural Network ARX Model with Multi-Step-Ahead Prediction

Over the last decade, predictor design based on non-linear model structures has been given great attention. These include the generalisation of the traditional ARX and ARMAX models to the nonlinear domain, and the successful application of the polynomial NARX in many applications [Parlos *et al.*, 1999]. In industrial practice, it is a usual trend that many processes contain time-delays. Normally, if there is a time-delay in a process, any outcome of a control action would not be seen until the time-delay has elapsed. Consequently, the difficulty of controlling a process with a large time-delay can be enormous. This is relatively obvious especially when the time-delay is larger than or equal to the overall system time-constant, and the effect on the performance of the control system can become very significant [Tan and Cauwenberghe, 1999]. Therefore, the use of predictions in the control system is a constructive method to overcome the effect of a time-delay. The terminology of prediction is concerned with estimating the process output over a certain horizon into the future, based on a model describing the process based on available information.

For some complex or time-varying systems (i.e. coal combustion on chain grate stoker), the prediction horizon has to be expanded so that the essential dynamics of the process can be covered. Long-range or multi-step-ahead prediction satisfies the above criteria and possesses an attractive method for model-predictive control. In this scheme, the predictor uses past measurements of the process outputs and inputs to predict the future output of the process over a rather long horizon, which is usually similar or larger than the time-delay of the process, so that the controller has the potential for making a control decision to improve the performance of the control system and the process.

For non-linear prediction, it is always an important issue to determine the architecture of the neural network based predictors, which is considered to be a combination of system modelling, optimisation and prediction. As non-linear processes are usually very complex, the design route for a neural network often depends upon some empirical knowledge about the process [i.e. the time-delay, the outputs and inputs]. Therefore, it is essential for the

design of the neural predictor to rely on the empirical knowledge about the process to be predicted.

There are two different types of neural network based multi-step-ahead prediction strategies for non-linear processes, namely recursive and non-recursive multi-step-ahead neural predictors. The recursive multi-step-ahead neural predictor depends on the predictions at the previous steps within the prediction horizon. On the other hand, the non-recursive multi-step-ahead predictor predicts  $t^2 + d^3$  steps of the future values of the process, based on the available information until time  $t$ . In comparison with the recursive multi-step-ahead predictor, the non-recursive version is easy to apply for multi-step-ahead prediction since it does not need the recursive procedure that may need a lot of computational effort. Besides, in the iteration procedure of long-range prediction with a recursive predictor, any errors in the neural network output are fed back into the network, causing an accumulation of errors that can significantly degrade the network's prediction accuracy [Tan and Cauwenberghe, 1999]. Figure 2.4 below shows the architecture of the MLP network used for the modelling work.

---

<sup>2</sup> current time  
<sup>3</sup> multiple step

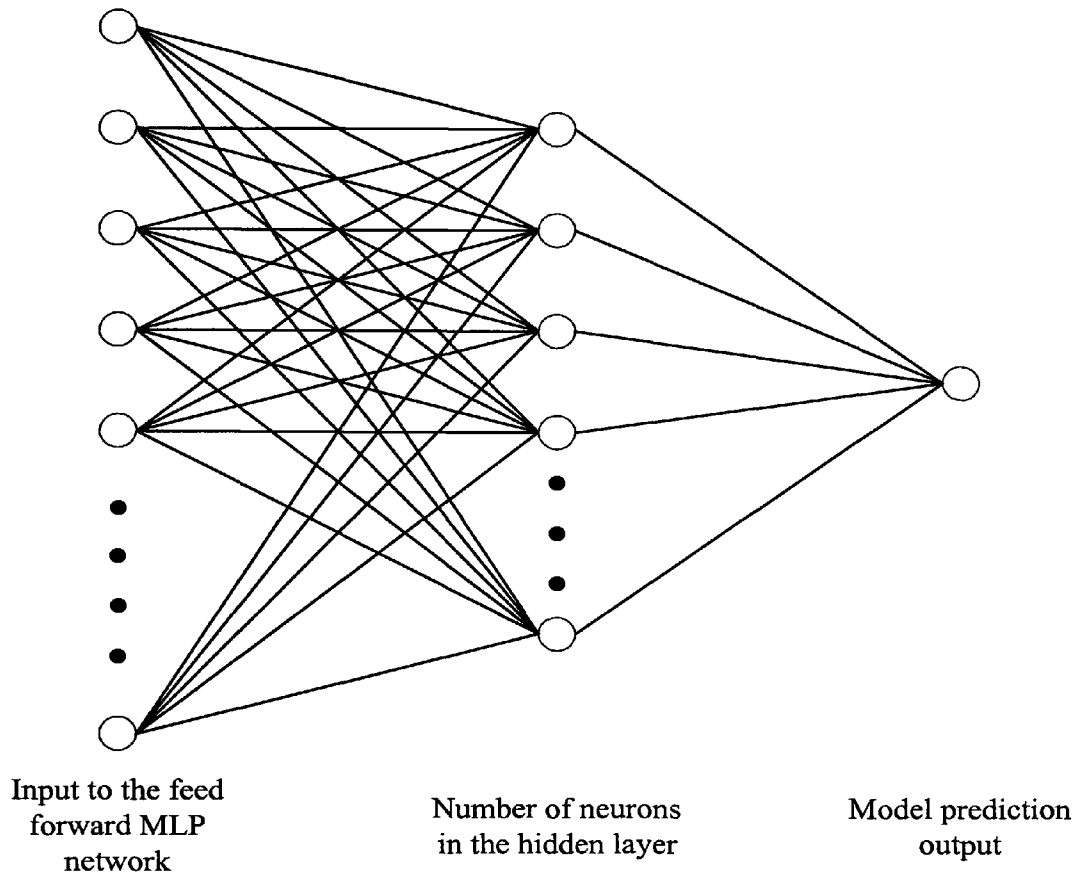


Figure 2.4: The Feed Forward MLP Network Architecture with ARX Model Structure

Previous research in the application of non-linear neural network ARX models to chain grate stokers was conducted by Chong *et al.* (2000). The authors claimed that the potential for making predictions further into the future would be great although the predictions of combustion process and gaseous emissions at that time were only 30 seconds. It was suggested that a prediction of just 2 minutes would enable a control system to act on future problems before they occurred, thereby ensuring more stable operation of the boiler, particularly during load following conditions [Chong *et al.*, 2001]. As a result in this work, in order to enable the final neural network based control system (Chapter 7) to be able to take account of future problems (combustion process) and control them before they occur, the non-linear neural network ARX model with a non-recursive multi-step-ahead predictor was implemented to predict the combustion process and gaseous products and thereby allow time for the controller to take action in advance of demand and process requirements.

## 2.6 Literature on Related Artificial Neural Networks Applications

This Section describes the literature associated with the application of ANNs. As the field in which ANNs have been applied to is broad and various, the description of this literature will be concentrated on to areas more closely related to the research aims of this work, including; lump coal combustion on chain grate stokers, the combustion of other fossil fuels (gas and oil) and other types of complex industrial processes.

One of the early industrial applications of ANNs was reported by Venkatasubramanian and Chan (1989) in pattern recognition. The classification ability of ANNs was implemented for multiple process fault diagnosis (as the traditional fault-tree diagnosis had difficulty to deal with) for a chemical process in a petroleum refinery plant. The authors found that the standard feed-forward MLP network with more than one hidden layer did not significantly increase the predictive abilities but did significantly increase the training time. They have also found that ANNs performed reasonably well in generalising unseen data that are similar to the training set. Another early application of ANNs was also reported by Gutmark *et al.* (1990), who described the use of a feed-forward MLP network to model the behaviour of a propane gas burner in an effort to derive a control strategy for the closed-loop control of the burner by investigating the chemiluminescent emission of CH as an indicator of good combustion and black-body emission from soot particles as the reverse. The authors claimed that in order to obtain a satisfactory representation of the actual system, a sufficiently large envelope of accurate training data must be made available for network training.

For the ANN simulation process, Ribeiro *et al.* (1993) investigated a computer simulation using two feed-forward MLP networks for the modelling of an industrial gas fired kiln. The authors proposed a control strategy by utilising the inverse model of the plant in a simulation environment which was claimed to be successful. The successful use of the 'inverse' model (feeding the output of the process to the network as an input and vice versa) of the simulated kiln to function as the forward loop controller hinged on the controller being trained with data (for both training and testing purposes) gathered from a heavily simplified mathematical

model of the actual plant. The need to train the ANN modules over a wide enough span of the system's operating conditions gathered using an appropriate sampling time in order to enhance the generalisation capability of the ANNs was also emphasised.

The need to gather a sufficiently large and accurate data-base regarding the process to be modelled in order to ensure a better representation was also stressed by Berger *et al.* (1996) on his report of using ANNs to dynamically model a non-linear process. The authors used a standard 3-layer MLP network to model the hydrodesulphurisation process of atmospheric gas oil as a function of the variables associated with the bench-reactor that they used. Due to the complexity of the process and lack of experimental data, they addressed the need for more robust models of such processes [Berger *et al.*, 1996]. Hobbs *et al.* (1992, 1993) expressed a similar opinion and asserted a similar fate with modelling of coal combustion on grates particularly in the gasification aspects where mathematical modelling of the process is hindered by the complex kinetics of the combustion process.

In the pulverised fuel (pf) combustion system, Reinschmidt and Ling (1994) reported a simulation study with a feed-forward MLP network where the authors constructed a steady-state NO<sub>x</sub> emission model and a feed-forward controller for the 'near optimum' setting of the input variables using real data gathered from power plant boilers. The authors claimed that the cascaded ANN models used could be employed as an on-line advisor to more inexperienced plant personnel as the computer simulation results demonstrated that they were able to represent the underlying relationship between the input and output data.

Booth and Roland (1998) presented the benefits of applying an on-line, real-time neural network to several commercially operating bituminous coal fired utility boilers. Through on-line retraining, the neural network-based system optimised the boiler operation by accommodating equipment performance changes due to wear and maintenance activities, adjusting to fluctuations in fuel quality, and improving operating flexibility. The authors claimed that the key feature of the neural network-based system was its ability to empirically model non-linear data, to continually learn in an on-line mode and to modify setpoints and bias adjustments to keep the unit tuned to the desired emission and performance level.

Saha *et al.* (1998) described the use of a feed-forward MLP network to model the ‘inverse’ dynamics of a gas fired boiler for steam production. The neural network was used as a simple feed-forward controller (taking the plant response and delivering the appropriate input settings). Test results showed that the neural network was able to represent the underlying relationship between the input and output data when simulated with unseen data (also from the plant) off-line. Eki *et al.* (1997) used an ANN to control a computer simulation of a fossil-fuel fired power plant in which the simulation results indicated that the boiler temperature fluctuation was minimised to less than  $\pm 5^{\circ}\text{C}$  with the derived neural network controller which in turn would help to maintain better steam production for the turbine generator.

Tan and Keyser (1994) described a novel approach of an adaptive PID control with a neural network based  $d^4$ -step ahead predictor to deal with the control problem for a nonlinear process with a time-delay. In their approach, two kinds of neural network based  $d$ -step ahead predictors were utilised which were respectively recursive and non-recursive predictors for predicting the output of the controlled process in the future in order to compensate for the time-delay. Simulation experiments on a heat exchanger demonstrated that the proposed control scheme could handle some nonlinearity and the time-delay effectively and temperature control result proved that the proposed strategy can be available for real-time control [Tan and Keyser, 1994].

In modelling a non-linear process using the Multi-Layered Perceptron (MLP) network with multiple-step-ahead predictions, Evans *et al.* (1994) reported an investigation of the ability of a network to model and control the height of liquid on a pilot scale dual tank non interacting liquid level system. A method of spread encoding the process data presented to the neural network was described which improved the prediction accuracy of the neural network model when operating recursively. The final conclusion of the authors was that the structure of the neural network model used to predict the process output multiple time steps ahead has the advantage of producing a smoother control action since the controller is able to forecast future process changes [Evans *et al.*, 1994].

---

<sup>4</sup> Time-delay of a system



Prasad *et al.* (1996) reviewed a model-based multivariable predictive optimal control strategy with real-time constrained optimisation to control steam temperature and pressure at an economic optimum during load-cycling operation of a 200 MW oil-fired drum-boiler power plant. The authors used Multilayer Perceptrons (MLPs), in a nonlinear autoregressive format with exogenous (NARX) input to build the model, in which the procedures used a number of past plant inputs and outputs to predict the future process outputs. The analysis of operational dynamics of the boiler along with economics and constraints of the operation indicated that the application of a model based multivariable predictive optimal control strategy can result in more economical operation of the power plant boiler and using a long range predictive control technique, such a controller can carry out real-time constrained optimisation [Prasad *et al.*, 1996].

A more recent study using the neural network based predictors was reported by Tan and Cauwenberghe (1999) who described the use of this technique to estimate the manifold pressure in an automotive engine. The authors claimed that neural predictors can be effectively applied to nonlinear process prediction and were very useful for time-delay compensation of nonlinear processes, and to design nonlinear predictive control strategies. The predictive results showed that the neural network based prediction methods obtained better performance in prediction when compared to other methods, such as modelling from first principles. They finally concluded that neural networks are very useful in handling the modelling, prediction, and control problems for nonlinear systems [Tan and Cauwenberghe, 1999].

Baines (1999) compared two different techniques for measuring emissions. The first consisted of continuous emissions monitoring systems (CEMS) based on hardware analysers and the second predictive emissions monitoring systems (PEMS) based on neural networks. For the PEMS approach, different types of neural network technologies were initially tested as prototype models for predictive emissions sensors, but multi-layer feedforward networks proved to be the most successful, because of their inherent capability as nonlinear function approximators. The author also claimed that this type of model could also be easily trained to learn the combustion process by using historical process data, which is readily available from

the distributed control systems usually installed in any boiler plant. However, the conclusion drawn by the author was that the PEMS approach based on neural networks offers a different approach to modelling, and are probably the most promising method for predicting the behaviour of boilers and their emissions, which offering accurate and reliable monitoring with potentially lower purchase, installation and maintenance costs [Baines, 1999].

Another similar technique was reported by Chong (1999) whose explained the used of the feed-forward Multi-Layered Perceptron (MLP) network to model the combustion process and pollutant formation of the chain grate stoker boiler. The author stressed that although ANNs can be successfully applied to model complex non-linear processes, the parameters of the developed model have no physical meaning and hence makes the 'black-box' model very application specific. Chong (1999) also asserted that in many industrial cases the required databases are not so readily available due to cost and the difficulty of making long term measurements. These two factors being the major inhibitions to the ANNs approach, which needs to be strongly emphasised, as the success or failure of a neural network application essentially hinges on them [Chong, 1999].

Other relevant literature includes Reifman and Feldman (1997) who proposed the combined use of two classes of neural networks, multilayer feedforward networks and fully-connected recurrent networks, in the development of a closed-loop nonlinear controller for discrete-time dynamical systems that were applied to control  $\text{NO}_x$  emissions for a simplified representation of the furnace in a coal-fired boiler. In their proposal, a feedforward network was used to represent the nonlinear controller and a recurrent network was used to represent the dynamical system in the training of the controller. Simulation results indicated that timely control maneuvers were provided by the neural controller such that for arbitrarily changing values of target  $\text{NO}_x$  and the power demanded within specified regions of operation, the predicted  $\text{NO}_x$  tracked the target  $\text{NO}_x$  with a high degree of accuracy.

### 2.6.1 Summary

The application of AI techniques, in particular the use of ANNs has been widely used for the identification (modelling) and control of nonlinear dynamical systems. The main reason being that ANNs provide a powerful and robust means for modelling if significant data exists and the network can therefore be taught particular responses to patterns of presented data. Therefore, ANNs are distinctly different from conventional processing algorithms in that it possesses special appealing characteristics of not only being able to recognise such patterns when they occur again, but also recognise similar patterns by generalisation, along with their potential property of faster operational speeds realised through inherent parallel distributed processing operation. Finally, it can be concluded that the complex non-linear lump coal combustion process on chain grate stokers justifies the use of ANN techniques.

## Chapter 3 Plant Description of Pilot Scale Chain Grate Stoker Boiler & Experimental Results

This Chapter presents the main features of the stoker test facility and the range of plant instrumentation together with the existing plant control system used for the experimental programme. This is followed by the description of all the experimental procedures carried out on the test facility to collect information about the behaviour and response of the boiler under various test conditions for three different coal types, namely Dawmill Smalls, Dawmill Singles and Columbian Smalls. The load change was simulated by manually adjusting the coal and air feed from the front-end controllers. The results obtained from the experiments are presented from three distinct areas, namely gradual and large load changes at near optimum (50%), lower (30%) and higher (80%) excess air levels. However, it should be noted here that the data used for the training and testing of the neural networks (Chapter 4) was supplemented with data from a previous research project (BCURA B35) on the same test facility (Dawmill Singles). The objective of this Chapter is to provide an understanding of the chain grate stoker operation and to allow formulation of the controller for the industrial scale stoker boiler.

### 3.1 Plant Description

The pilot-scale 0.7MW chain grate stoker fired shell boiler which was located at Casella CRE Ltd., Stoke Orchard, Cheltenham was designed as a scaled down version of an industrial scale chain grate stoker with combustion intensities of up to 1.4 MW/m<sup>2</sup>. Some of the modern features added to this test facility in order to achieve fully automatic operation of the plant were:

1. Rotary coal feeder – also known as a firebreak unit, which regulated the speed of a rotary valve and the grate. The rotary coal feeder eliminated the need for a guillotine door to maintain the fuel bed height;

2. Water cooled sections – also known as ‘water cooled side cheeks’ which were fitted at the base of the stoker refractory arch to prevent slag formation, and to ensure more consistent and efficient burning on the fire bed;
3. Automatic ash handling system – In order to prevent any unburned carbon in the ash from being further combusted, automatic de-ashing was implemented. The ash dropped off the rear end of the grate was mixed with water to form a wet ash prior to disposal by a screw feeder to an ash collection bin located outside the boiler house. For the purpose of determining the actual loss in combustion efficiency in terms of unburned combustibles in the ash at steady state, ash samples were collected during experiments.

Fresh coal was carried into a small hopper from a storage bunker located outside the boiler house via a screw feeder. Inside the boiler house, coal was gravity fed onto the grate by adjusting the rotary valve speed, whilst the fuel bed height was controlled by an appropriate grate speed. A dual loop industrial digital controller controlled the motor drive shaft and monitored the speed of the two motors with an electronic tachometer. Such a coal feeding system is also known as the Proctor ‘firebreak unit’ and can be found in modern chain grate stokers [Proctor, 2000]. This firebreak unit provides a permanent barrier of approximately 500mm between the fire bed and the fuel hopper to eliminate the risk of ‘burn back’ which can occur in conventional stokers that use a guillotine door to maintain the fuel bed height. Burn back occurs when the ignition plane moves toward the stoker front and consequently ignites the fresh coal stored in the coal hopper. Figure 3.1 below shows both the usage of a guillotine door and firebreak unit on conventional and modern stokers.

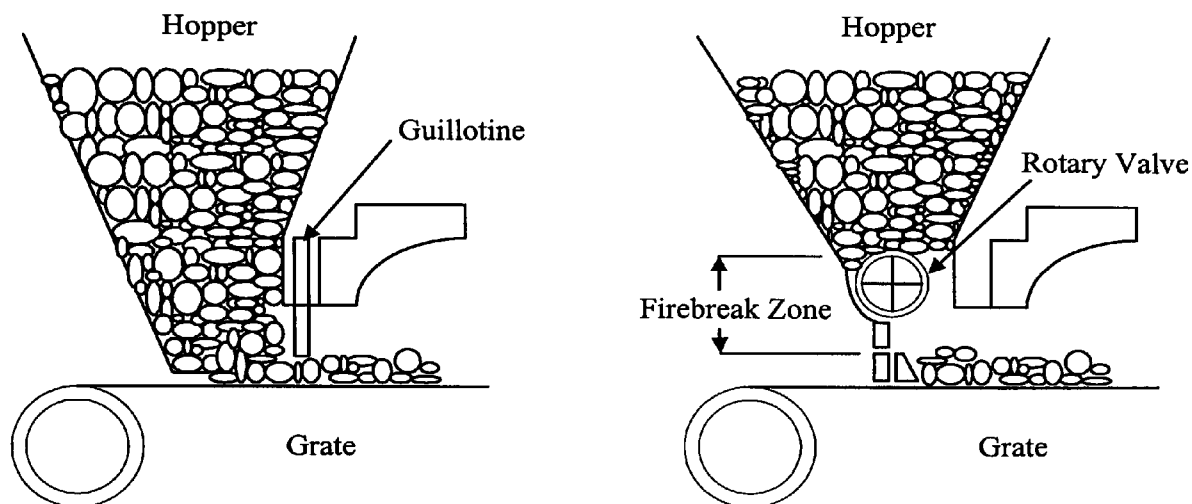


Figure 3.1 Guillotine & Firebreak Assemblies [Good Practice Guide 88, 2000]

In order to allow the plant operator to be able to check that ignition was taking place at the correct location on the grate, a 60mm diameter inspection porthole at the front part of the stoker with a view fuel bed, just before the refractory arch was utilised. For a particular boiler operating load, the location of the 'flame front' in-line with the porthole was one of the key operating parameters that needed to be satisfied [Chong, 1999]. Hence, for every coal feed rate, the grate speed was regulated in order to make sure that both the required bed height and the desired location of the flame front were achieved. This was vital to ensure that ignition occurred at the right location on the grate in order to obtain satisfactory coal burnout. It is worth mentioning that not all grades of coal react in the same way. Coals with low volatile matter and high fixed carbon, such as anthracite (high rank coals), take longer to ignite than higher volatile coals [Good Practice Guide 88, 2000]. Because of their high fixed carbon content they also liberate most of their heat directly from the firebed, and this can lead to overheating of the chain mat. However, the higher volatile bituminous coals (low rank), the most common fuels for chain grate stokers, ignite relatively easily.

The primary combustion air for the test facility stoker was supplied via a variable speed forced draught fan motor. The air supplied from the main air duct was split into four separate streams, which provided individual air chambers underneath the grate and the air flow rate in each duct was continuously monitored and controlled by a single closed loop controller. This

enabled the air distribution to be adjusted along the length of the grate so as to be able to cope with the requirements of different coal types to ensure adequate cooling of the grate and to completely combust the volatile matter and fixed carbon. The airflow distribution profile in the four air sections of the grate was typically arranged so that the front and rear sections comprised about 20% of the total primary air supply with the remaining 80% being targeted at the two middle sections where the major combustion zone was located. An induced draught fan, controlled by a closed loop set point controller, was also used to maintain a slight suction in the furnace chamber in order to maintain a suitable pressure drop across the boiler corresponding to the load required. This feature ensured clean operation of the boiler plant and also prevented the stoker front from overheating. Adequate combustion air must be provided (oxygen concentration in the flue gas of between 5 to 7%) to ensure satisfactory burnout of all combustible matter and fixed carbon without providing too much excess air, as the efficiency reduces in proportion to the excess air level [Good Practice Guide 88, 2000].

Before the hot flue gases produced during combustion were discharged into the atmosphere via a stack, they were cooled by passage through the water-cooled furnace tube, reversal chamber and the smoke tube heat exchanger and subsequently cleaned by passage through a high efficiency cyclone. In order to prevent stack corrosion caused by deposition of sulphuric acid, the exhaust flue gas temperature in the stack inlet was kept above 140°C. With the two pass test facility, most of the heat transfer was by radiation to the combustion chamber walls with the rest being transferred in the reversal chamber and the smoke tube by convection.

As green coal entered the furnace tube, it was ignited from the top by means of the heat stored in the ignition arch by radiation only. The plant operator ensured that the flame could be observed through the inspection porthole in order to make sure that the fresh coal under the refractory arch was being ignited. The coal once it had started to burn radiated heat back into the arch hence retaining the arch temperature. As the coal burnt the ignition plane travelled along with the grate, adequate excess air was supplied by the primary air. At the end of the grate, the remaining ash and unburnt coal was dropped onto the ash chute to be mixed with water prior to disposal. The wet ash was then carried from the ash chute to the ash collection bin located outside the boiler house via a screw feeder.

## 3.2 The Plant Control System and Instrumentation

The stoker test facility was fitted with a supervisory computer hosting seven front-end PID industrial controllers which could be configured to work manually (i.e. coal feed, forced draught fan and induced fan suction can be adjusted to increase or decrease to meet the desired set point via the front panel push buttons) or in automatic mode. It was also used to log measurements acquired from various plant sensors (i.e. Servonex probe for oxygen concentration in the flue gas measurement and K-type thermocouples for temperature measurement). Those measurements were logged every 30 seconds through an internal communication interface to the host computer running a "Tactician" software package. In order to provide a straightforward indication of the process and control variables for the plant operator, the software provided an on-line visual display of all the variables on the computer screen.

In order to allow the plant operator to adjust the primary air based on the correct level of excess air for a particular coal feed rate, a good reference was to measure the oxygen concentration in the flue gas. Therefore, a Servonex probe based oxygen analyser was installed at the end of the smoke tube for this purpose. According to Gunn and Horton (1989), 'oxygen trimming' techniques which monitor the oxygen concentration in the flue gas and adjust the combustion air to maintain the minimum excess air without negatively affecting the pollutant emissions has been practically applied on oil and gas fired burners [Gunn and Horton, 1989]. However, this is more difficult for lump coal firing on grates due to factors such as longer ignition time, incomplete mixing between the air and fuel and hysteresis of the system. These factors according to Gunn and Horton (1989), even when excess oxygen was present could result in incompletely burned coal being discharged from the grate and under such conditions, a signal to reduce the air (oxygen trimming) would only further exacerbate the situation. Therefore, the authors suggested the use of instrumentation to measure the unburned coal but this instrument has yet to be developed commercially [Gunn and Horton, 1989]. However, it is believed by the author that the oxygen reading allied with AI techniques and other complimentary information, such as the CO reading, could form a control system, which could probably enhance the control of lump coal combustion on chain grates. The details of which are discussed in Chapter 4.



In addition to the Servonex oxygen analyser, carbon monoxide (CO) and nitrogen oxide (NO<sub>x</sub>) emissions were also measured by a portable flue gas analyser, 'Testo 350', which was fitted at the exhaust duct before the cyclone. The gas measurements were recorded every 30 seconds with the 'Testo ComLight' that came with the analyser and ran inside Windows<sup>TM</sup>. As with the oxygen reading, the CO reading is also a very good indicator of the combustion process, and in most large coal fired plants, (i.e. the electricity generation sector), in order to ensure a good combustion efficiency and to comply with legislation, long term CO sensors have been widely installed along with flue gas oxygen measurements. For an inclusive investigation of the test facility performance under different test conditions, both CO and NO<sub>x</sub> measurements have been presented along with other sensor measurements and control variables.

As for flue gas temperatures, temperature measurements were taken at the base of the reversal chamber opposite the furnace tube and also at the stack inlet with the use of K-type thermocouples. As with the oxygen measurement, temperature measurements were also logged and stored into the control computer running the 'Tactician' software. The thermocouple located at the reversal chamber was the most sensitive to load changes or any perturbation to the system, such as moisture content and changes in the coal quality or coal distribution as it was closest to the fire bed. Several K-type thermocouples were also installed in the refractory arch to enable a temperature distribution profile to be depicted so that the combustion stability or the rate of the ignition plane movement could be inferred by the arch temperature measurements during a load change. In general, the arch temperature during coal firing on the grate is dependant on grate speed and coal properties (i.e. moisture content and volatile matter). In addition to the measurements described above, enough cooling air needed to be provided to prevent the mat from overheating as well as eliminating problems resulting from the use of high fixed carbon content coals, grate surface temperature was recorded manually by the use of a portable digital thermocouple. For the chrome alloy links, the upper limit of the grate surface temperature was 80°C. Figure 3.2 presents a block diagram of the 0.7MW chain grate stoker boiler test facility and the location of all the sensors described above.

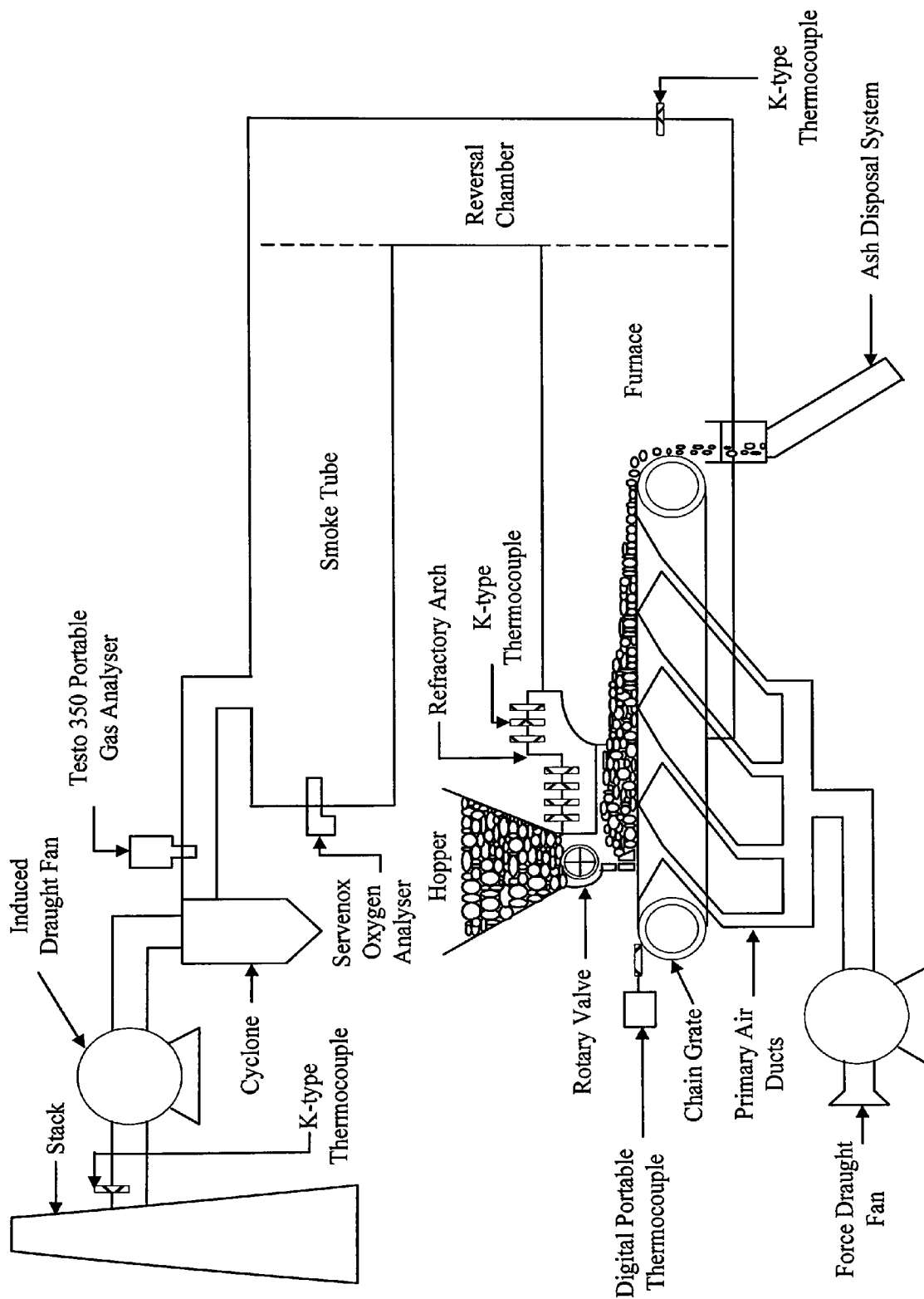


Figure 3.2 The 0.7MW Chain Grate Stoker Test Facility & Sensors Location at Casella

CRE Ltd

### 3.3 Experimental Procedures

This Section describes all the experimental procedures carried out on the test facility to collect information about the behaviour and response of the boiler under various test conditions for three different coal types, Dawmill Smalls, Dawmill Singles and Columbian Smalls. As mentioned in the previous Section, the load change in all the experiments was simulated by manually adjusting the coal and air feed via the front-end controllers. This series of manual experiments were intended to investigate the test facility stoker's response to gradual and large load changes at optimal and sub-optimal operating conditions. It essentially involved experiments carried out in three distinct areas, gradual and large load changes at near optimum (50%), lower (30%) and higher (80%) excess air levels. Table 3.1 outlines all the experiments conducted on the 0.7MW chain grate stoker boiler test facility.

Table 3.1 Experiments Conducted on the 0.7MW Chain Grate Stoker Boiler Test Facility

Test No.	Description	Oxygen Level	Coal Type
1	Gradual load changes with near optimum excess air	5 to 7%	Dawmill Smalls
2	Gradual load changes with lower excess air	3 to 5%	Dawmill Smalls
3	Gradual load changes with higher excess air	7 to 9%	Dawmill Smalls
4	Gradual load changes with near optimum excess air	5 to 7%	Dawmill Singles
5	Gradual load changes with lower excess air	3 to 5%	Dawmill Singles
6	Gradual load changes with higher excess air	7 to 9%	Dawmill Singles
7	Gradual load changes with near optimum excess air	5 to 7%	Columbian Smalls
8	Gradual load changes with lower excess air	3 to 5%	Columbian Smalls
9	Gradual load changes with higher excess air	7 to 9%	Columbian Smalls
10	Large load changes with near optimum, lower & higher excess air	5 to 7%; 3 to 5%; 7 to 9%	Dawmill Smalls
11	Large load changes with near optimum, lower & higher excess air	5 to 7%; 3 to 5%; 7 to 9%	Dawmill Singles
12	Large load changes with near optimum, lower & higher excess air	5 to 7%; 3 to 5%; 7 to 9%	Columbian Smalls

The maximum load achievable for all the tests on the stoker test facility was 0.6MW (due to plate heat exchanger fouling) although the Maximum Continuous Rating (MCR) of test facility was 0.7MW. The minimum load attainable was 0.3MW, thus the range of the operating load for the experiments was between 0.3MW to 0.6MW.

### 3.3.1 Experiments with Gradual Load Changes

The objective of these experiments was to gather information about the plant response to gradual changes at both optimal and sub-optimal operating conditions for use in training the neural networks. Preferably the process to be modelled should be constantly excited so that all the dynamic modes of response are captured in the data collected which will then be used to teach the neural network. The results presented served as a benchmark for what the plant operator would call optimum operation of the test facility stoker. The benchmark for near optimum operation included an oxygen concentration in the flue gas of 5 to 7% (50% excess air), an acceptable level of CO emissions (i.e. less than 500ppm) and an adequate and stable flame front location. The sub-optimal operating conditions on the other hand were an oxygen concentration of 3 to 5% (30% excess air) and an oxygen concentration of 7 to 9% (80% excess air). In parallel to the method of changing the load level, the primary air was also manually adjusted in order to create this envelop of sub-optimal data through the front-end controller. Due to the limitation of the operating range mentioned above, the gradual load change was varied from 0.3MW to 0.6MW in 0.1MW step increments and back to 0.3MW in the same step decrements in nine operating conditions, resulting for three different coal types (Table 3.1).

### 3.3.2 Experiments with Large Load Changes

These experiments aimed to determine the plant response to run the boiler in a single large step change from turn down (0.3MW) to full load (0.6MW) and vice versa whilst keeping stable combustion on the bed and satisfactory transient CO emissions. The time taken for the stoker test facility to move from one steady state condition to another was empirically

measured as 20 minutes. Therefore, in order to compensate for the step change in boiler load from 0.3MW to 0.6MW and vice versa and also to ensure a more stable combustion of the coal on the fire bed, the airflow change was staged. According to Chong (1999), changes in the air must lead the coal on load increase and vice versa on load decrease as a means to reduce smoke formation and to provide better transient combustion. Figure 3.3 shows the boiler load changed from 0.3 to 0.6MW and back down to 0.3MW with the staging sequence. Three sets of test were carried out for large load changes with near optimum, lower and higher excess, resulting for three different types of coal (Table 3.1).

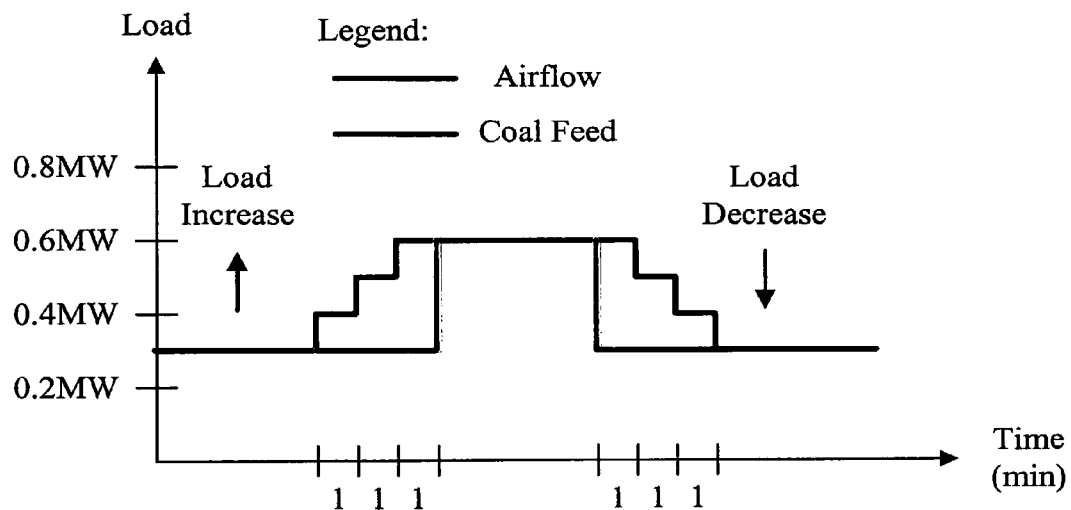


Figure 3.3 Coal Feed & Airflow Staging Sequence Following Large Load Changes

## 3.4 Experimental Results & Discussion

This Section presents the data collected from the series of experiments described in Section 3.3 which is discussed with reference to the oxygen concentration in the flue gas, nitrogen oxides and carbon monoxide emissions for the load range of 0.3MW to 0.6MW. In the interest of brevity, only the results obtained from gradual load changes at near optimum air settings will be shown here. The results for gradual load changes at lower and higher excess air will be summarised at the end of each Sub-Section. As for the large load changes, the results obtained from three different excess air levels will be shown in the same graph (as these experiments were carried out continuously) for three different types of coal.

### 3.4.1 Gradual Load Changes at Optimal and Sub-Optimal Operating Conditions for Dawmill Smalls

Figure 3.4 shows the experimental results obtained from gradual load changes at an excess air level of 50%, for which the oxygen level was between 5 to 7% in the stack at plant operator's best practice for Dawmill Smalls coal type (*Test 1*). Unfortunately due to the failure of the Servonex oxygen analyser during the first day, the oxygen reading is not available to be presented on the graph. However, the CO<sub>2</sub> trend as shown in Figure 3.4 which normally shares an inverse relationship with the oxygen trend, can be used to assess the actual oxygen concentration for what the operator would call optimum operation of this test. As expected with a near optimum excess air distributed along the grate, most of the oxygen level stayed within the 5 to 7% optimal band (equivalent to 11 to 13.5% of CO<sub>2</sub> as shown in Figure 3.4). As for CO emissions, the average level was 106ppm, which is highly acceptable with only a few peaks at lower loads on load increase and load decrease. The NO<sub>x</sub> emissions also show little that would cause concern with an average of 133ppm for the entire range of operating loads, and a maximum of 158ppm being recorded at higher load, which can be considered low although stoker fired boilers intrinsically produces low NO<sub>x</sub> emissions. The NO<sub>x</sub> emission trend possesses a similar profile to the oxygen (which is opposite to the CO<sub>2</sub> in this case) due to the fact that the fuel and thermal NO<sub>x</sub> are both greatly manipulated by the amount of combustion air available [Clarke and Williams, 1992]. Data gathered from this

experiment represents the stoker plant response at a near optimum air setting for Dawmill Smalls.

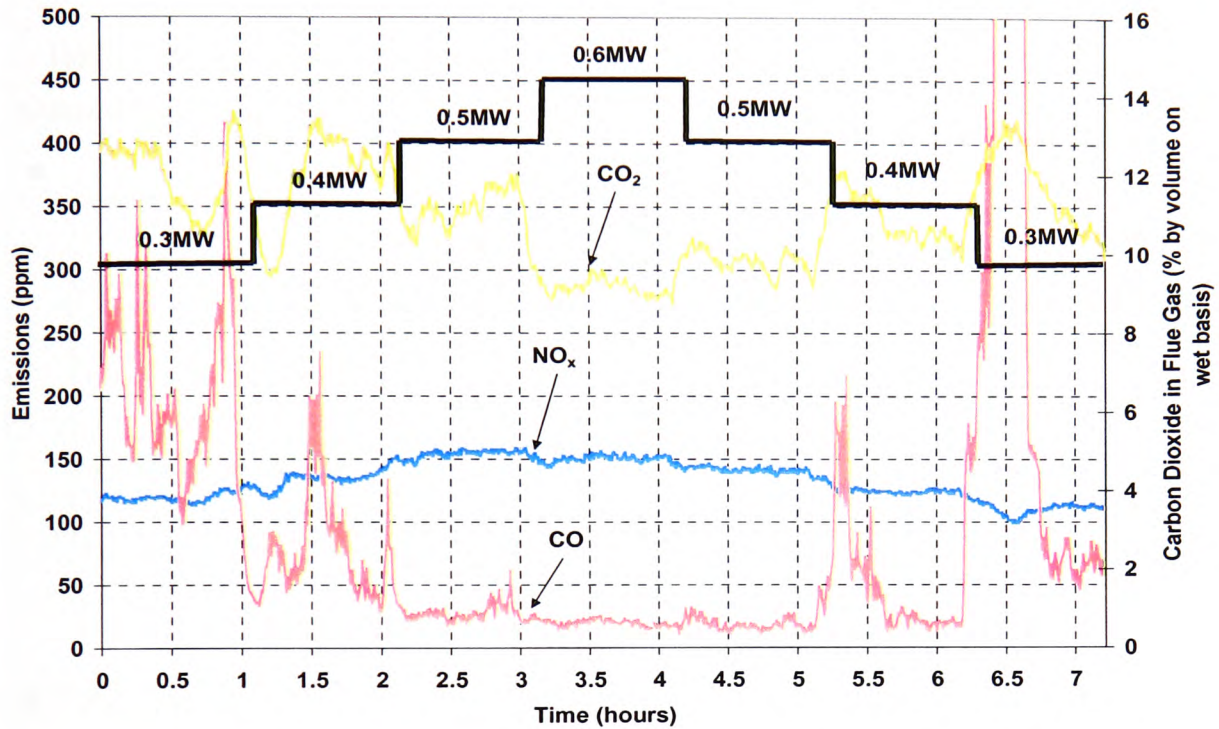


Figure 3.4 NO<sub>x</sub> & CO Emissions and Percentage of CO<sub>2</sub> in Exhaust Duct following Gradual Load Changes at Near Optimum Air Setting for Dawmill Smalls – *Test 1*

Table 3.2 below shows the summary of results obtained from the tests carried out for gradual load changes at lower and higher excess air for Dawmill Smalls (*Tests 2 & 3*). At lower excess air, a mean oxygen concentration in the flue gas of 4% was recorded. However, the reduction of the total airflow resulted in a fluctuation of the CO emissions with a peak of more than 1000ppm being recorded at lower load. Nevertheless, this did not seem to have a significant effect on the NO<sub>x</sub> production with an average emission of 125ppm throughout the test. As at higher excess air, the average oxygen level of 7% hits the targeted band of 7 to 9% with a corresponding low CO emission. This was probably mainly due to the higher combustion intensity on the bed which produced more turbulence and better combustion of the volatiles and char. As for NO<sub>x</sub> emission, it again shows no real cause of concern with a maximum emission of less than 160ppm being recorded for the entire experiment. However,

the elevated combustion air on the bed effectively cooled the flue gas thus reducing the overall thermal efficiency, so that data gathered from these experiments represents the non-optimal response of the stoker plant to lower and higher excess air levels for Dawmill Smalls.

Table 3.2 Summary of Results for NO<sub>x</sub> & CO Emissions in Exhaust Duct & Oxygen Concentrations in the End of Smoke Tube following Gradual Load Changes at Lower & Higher Excess Air Levels for Dawmill Smalls – *Tests 2 & 3*

Gas Emissions	Dawmill Smalls	
	Lower Excess Air	Higher Excess Air
O <sub>2</sub>	Mean of 4%, fluctuating between 2 and 6%	Mean of 7%, fluctuating between 5 and 9%
CO	Large fluctuation with peaks of more than 1000ppm	Stable with peaks of less than 300ppm
NO <sub>x</sub>	Maximum at 170ppm with average of 125ppm	Maximum at 153ppm with average of 116ppm

### 3.4.2 Gradual Load Changes at Optimal and Sub-Optimal Operating Conditions for Dawmill Singles

Figure 3.5 below shows the experimental results obtained from gradual load changes at an excess air level of 50% for Dawmill Singles (*Test 4*). As can be seen in this Figure, the oxygen concentration oscillated within the target band of 5 to 7% following gradual load changes from 0.3MW to 0.6MW. As for pollutant emissions, a few peaks at lower load can be observed but very little at higher load with an overall average of 197ppm being recorded for the CO emission. The very low CO emission at higher load suggests that enough air was available for the combustion of the volatile matter, but the higher CO emission at lower load implies a lack of excess air to compensate for the lower combustion intensity on the bed. On the other hand, the average NO<sub>x</sub> emission for the entire test was 161ppm with a maximum of 205ppm at higher load being recorded. The Dawmill Singles possesses a higher NO<sub>x</sub> emission when compared to Dawmill Smalls and from an ultimate analysis of these coals, the ‘as received’ nitrogen content for Dawmill Smalls and Dawmill Singles were 1.1% and 1.23% respectively, which would appear to demonstrate a correlation between the nitrogen



content of the coal and the tests conducted. However, the relationship is a complex one and other factors such as the stoker operating conditions (the amount of excess air available) will also have a large impact on the NO<sub>x</sub> emissions. Data gathered from this experiment represents the stoker plant response to a near optimum air setting for Dawmill Singles.

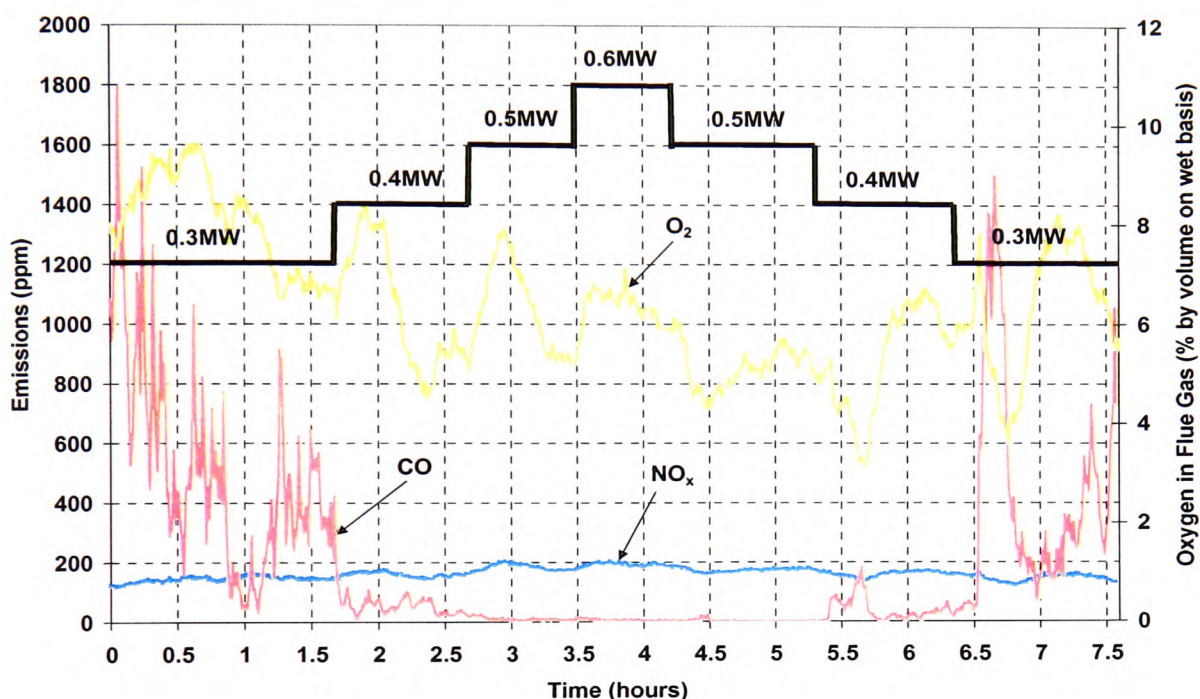


Figure 3.5 NO<sub>x</sub> & CO Emissions and Oxygen Concentration in Exhaust Duct following Gradual Load Changes at Near Optimum Air Setting for Dawmill Singles – Test 4

Table 3.3 below shows the summary of the results obtained from the tests carried out for gradual load changes at lower and higher excess air for Dawmill Singles (*Tests 5 & 6*). At lower excess air, a mean oxygen level of 4% was recorded, which satisfied the criteria of the test for the lower excess air setting. The reduction of excess air from the near optimum level increased the CO emission with a recorded peak greater than 2000ppm at low fire. As for NO<sub>x</sub> emission, the maximum emission of less than 200ppm and the mean of 135ppm were recorded for Dawmill Singles. For an average oxygen concentration of 7% at the higher excess air level, a lower CO with a mean of 117ppm was recorded for the entire test, even though one or two peaks of just below 700ppm could be observed at low load. For NO<sub>x</sub>

emissions, it again causes little concern with an average of 146ppm for the entire range of operating loads. However, the average NO<sub>x</sub> emission for Dawmill Singles at both lower and higher excess air was observably higher than that attainable by Dawmill Smalls, which would appear to be in-line with the statement mentioned above.

Table 3.3 Summary of Results for NO<sub>x</sub> & CO Emissions in Exhaust Duct & Oxygen Concentrations in the End of Smoke Tube following Gradual Load Changes at Lower & Higher Excess Air Levels for Dawmill Singles – *Tests 5 & 6*

Gas Emissions	Dawmill Singles	
	Lower Excess Air	Higher Excess Air
O <sub>2</sub>	Mean of 4%, fluctuating between 2 and 5%	Mean of 7%, fluctuating between 6 and 9%
CO	Large fluctuation at low load with peaks of more than 2000ppm	Very little at higher load with average of 117ppm
NO <sub>x</sub>	Maximum at 185ppm with average of 135ppm	Maximum at 197ppm with average of 146ppm

### 3.4.3 Gradual Load Changes at Optimal and Sub-Optimal Operating Conditions for Columbian Smalls

Figure 3.6 shows the experimental results obtained from gradual load changes at a near optimum excess air level of 50% for Columbian Smalls (*Test 7*). As can be seen in the Figure, although the average oxygen concentration in the stack was 6.5%, there were some large fluctuations especially at lower loads, demonstrating the difficulty of controlling the oxygen level within the optimum band of 5 to 7% for this coal. With the fluctuations of oxygen at lower loads, a few peaks of more than 1000ppm were observed in the CO emission. However, with the CO being low at higher loads, the overall average CO emission was 136ppm. As for NO<sub>x</sub> emission, a maximum of more than 300ppm can be seen with an overall average of 210ppm. The nitrogen content of this coal was 1.36%, which is higher than the previous two coals, which is in-line with NO<sub>x</sub> emissions recorded from this test.

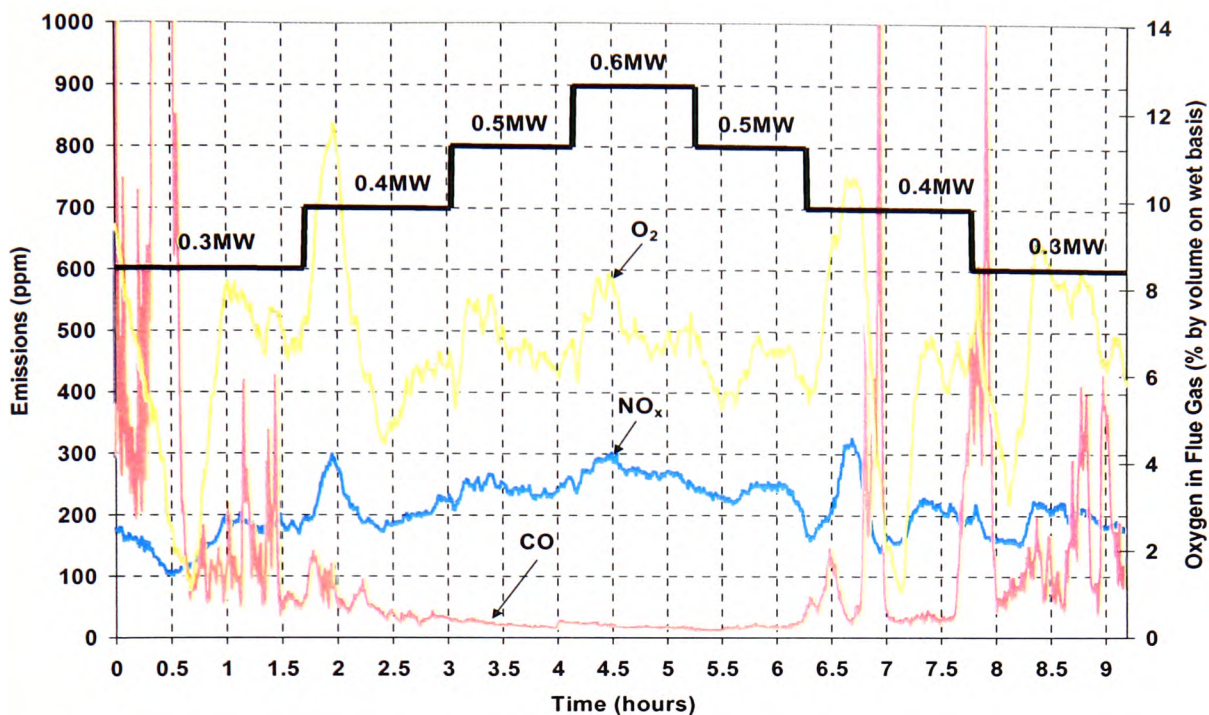


Figure 3.6 NO<sub>x</sub> & CO Emissions and Oxygen Concentration in Exhaust Duct following Gradual Load Changes at Near Optimum Air Setting for Columbian Smalls – *Test 7*

Table 3.4 below shows the summary of results obtained from the tests carried out for gradual load changes at lower and higher excess air levels for Columbian Smalls (*Test 8 & 9*). At lower excess air levels, a slightly higher mean of 5% was recorded for the oxygen concentration, but it still stayed between the target band of 3-5%. However, this resulted in a lower mean CO emission of 72ppm and only two peaks of CO emission at 900ppm at low load. Due to the inherent higher nitrogen content of this coal, a higher mean of 183ppm and maximum of 243ppm were recorded for NO<sub>x</sub> emissions. For the higher excess air, the average oxygen concentration of 8% lay in the centre of the target band of 7 to 9%. As for CO emission, the average level was 45ppm, suggesting that there was more than sufficient air available for the entire range of operating loads for the satisfactory combustion of the volatile matter. The highest average NO<sub>x</sub> emission of 251ppm was calculated from this test again partly at least resulting from the higher nitrogen content of Columbian coal with a maximum of 321ppm being recorded.

Table 3.4 Summary of Results for NO<sub>x</sub> & CO Emissions in Exhaust Duct & Oxygen Concentrations in the End of Smoke Tube following Gradual Load Changes at Lower & Higher Excess Air Levels for Columbian Smalls – *Tests 8 & 9*

Gas Emissions	Columbian Smalls	
	Lower Excess Air	Higher Excess Air
O <sub>2</sub>	Mean of 5%, fluctuating between 3 and 8%	Mean of 8%, fluctuating between 6 and 10%
CO	Peak of 900ppm but generally less than 200ppm	Very stable with the average of less than 50ppm
NO <sub>x</sub>	Maximum of 243ppm with mean of 183ppm	Maximum of more than 300ppm with the average of 251ppm

#### 3.4.4 Large Load Changes at Optimal and Sub-Optimal Operating Conditions for Dawmill Smalls

This test was carried out for large load changes, in which the load was changed from 0.3MW to 0.6MW and back to 0.3MW at three different excess air levels for Dawmill Smalls (*Test 10*). The aim was to determine the plant response to this large step change whilst maintaining stable combustion on the bed and satisfactory CO emission under the transient state. As can be seen in Figure 3.7, the experiment was carried out continuously starting from near optimum excess air setting (solid line) followed by lower excess air (small dotted line) and finally at higher excess air (dash line). The staging sequence of coal feed and airflow in-line with assertion mentioned in Section 3.3.2 in which the air should lead the coal feed on load increase and vice versa on load decrease as a means to reduce CO formation and to provide better transient combustion.



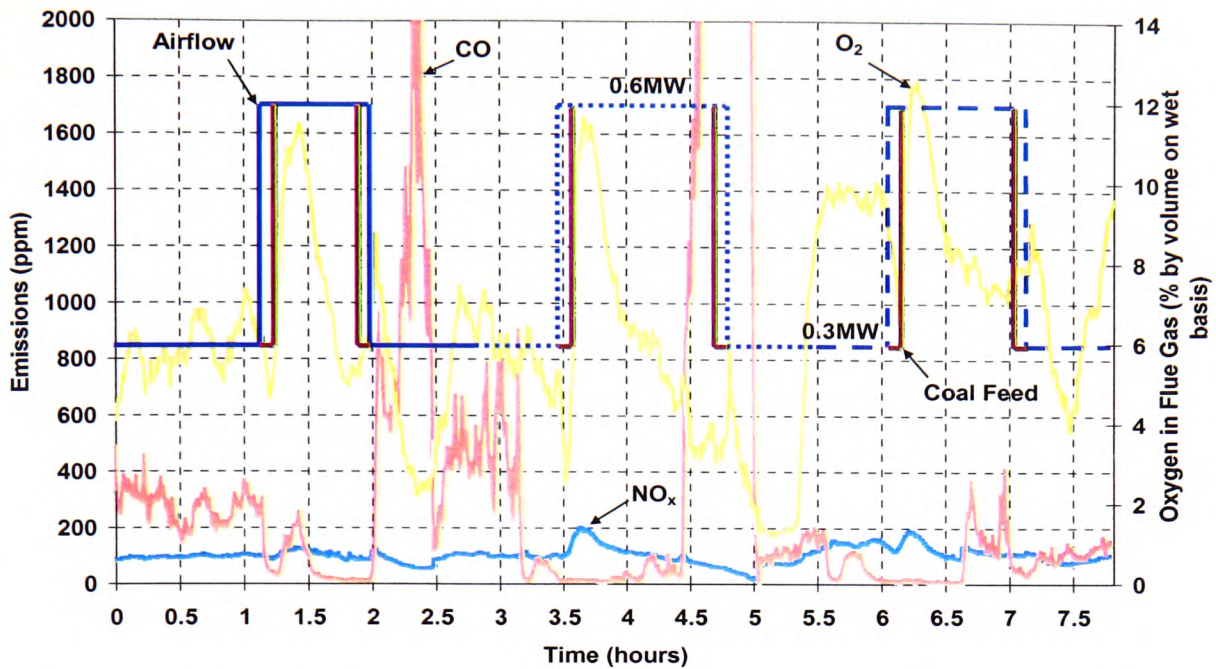


Figure 3.7 NO<sub>x</sub> & CO Emissions and Oxygen Concentration in Exhaust Duct following Large Load Changes at Optimal and Sub-Optimal Air Settings for Dawmill Smalls – Test 10

On load increase, the oxygen trends at these three different excess air levels possess a similar trend, so that increasing the air first results in an overshoot of the oxygen concentration to 12% (Figure 3.7). This was due to the changes in the coal feed requiring a much longer time (15 to 20 minutes) for the boiler to respond and to reach steady state as compared to the response of the airflow (usually 20 seconds). The large overshoot of oxygen resulted in the low CO emissions for the three excess air levels. However, the oxygen concentration at steady state for near optimum, lower and higher excess air levels were 6%, 4% and 8% respectively, which confirms the appropriate ranges of excess air setting for this test. As for NO<sub>x</sub> emission, it shows no cause for concern although there are two big increments from 98ppm to 198ppm and 115ppm to 188ppm respectively at lower and higher excess air during the transient from low to high, which was mainly due to the sudden air increment and higher bed temperature.

On load decrease, the oxygen trends at these three different excess air levels again possess a similar trend where suddenly decreasing the air caused a big drop in oxygen concentration

(Figure 3.7). This can be attributed to the fact that there was a sudden deficit in combustion air whilst the combustion intensity was still high. The lower oxygen concentration caused two overshoots of transient CO emissions at near optimum and lower excess air. It will be worth stating here that the transient CO emissions on load decrease were higher than that on load increase and can be explained by the same fact that there was combustion air starvation from the high combustion intensity on the fire bed. Nevertheless, the steady state oxygen concentration at optimum, lower and higher excess air were 6.5%, 1.5% and 9.5% respectively. The oxygen level at lower excess air dropped by 1.5% below the lower limit of the band (3 to 5%) due to the difficulty to control boiler at low fire. While the CO emissions on the other hand on the steady state condition were within an acceptable level. However, NO<sub>x</sub> emission was found to be stable during both transient and steady state conditions on load decrease. The corresponding NO<sub>x</sub> level dropped from a high of 198ppm to a low of 17ppm before settling at about 100ppm.

### 3.4.5 Large Load Changes at Optimal and Sub-Optimal Operating Conditions for Dawmill Singles

This experiment was carried out in exactly the same way to the previous test discussed in Section 3.4.4 where the objective was to determine the plant response to this large step change in load whilst keeping a steady combustion on the bed and adequate transient CO emission for Dawmill Singles (*Test 11*). The line definition in Figure 3.8 and staging sequence were both the same as in Figure 3.7.

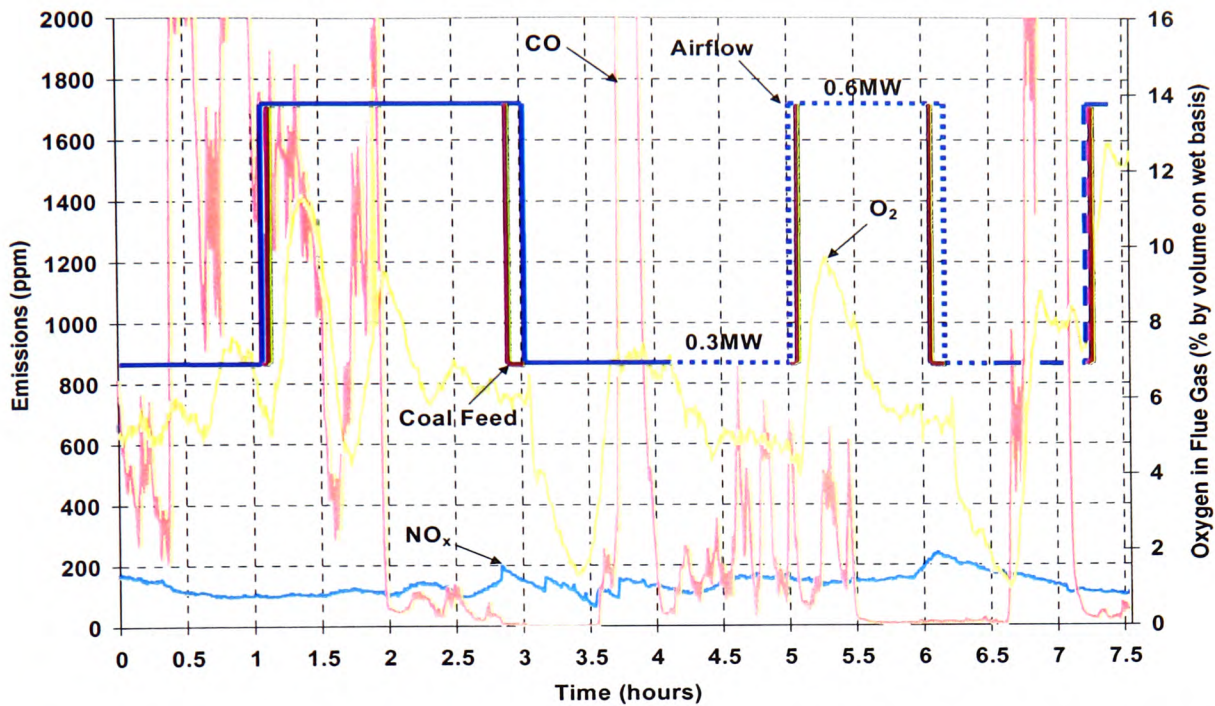


Figure 3.8 NO<sub>x</sub> & CO Emissions and Oxygen Concentration in Exhaust Duct following Large Load Changes at Optimal and Sub-Optimal Air Settings for Dawmill Singles – *Test 11*

On load increase, the time taken for the combustion to reach steady state for the near optimum air setting was longer than it usually takes. A corresponding large fluctuation in the oxygen concentration (at transient state of 0.6MW for near optimum air) can also be seen in Figure 3.8. The test at higher excess air was not completed due to the disintegration of the primary forced draught fan at the test facility plant. However, the oxygen trends at these three different excess air levels have a similar profile of overshooting following the rapid increment of the combustion air. This is probably due to the speed of adding coal being larger than the combustion air enabled to be burnt. However, the oxygen concentration at steady state for near optimum and lower excess air levels were 6.5% and 5.5% respectively, where the former was within the target oxygen band of 5 to 7% but the latter was slightly higher than the target band of 3 to 5%. The unstable combustion condition particularly at near optimum air resulted in higher transient CO emissions, whilst the overshoot of oxygen at lower excess air only caused a small fluctuation of CO. At higher excess air, the transient oxygen concentration seems to not have much effect on the CO emission (Figure 3.8). As for



the NO<sub>x</sub> emission, it shows no cause for concern on load increase at the three different excess air levels.

On load decrease, the discussion can only concentrate on the tests at near optimum and lower excess air as the test at higher excess air was terminated in the middle due to the fan problem. However, the oxygen trends at these two excess air levels again demonstrate a similar pattern where the fast decrement of combustion air resulted in a significant drop in the oxygen concentration. The transient oxygen concentrations were both reduced to about 1.5%, but the transient CO emissions seem to be negligible here which is opposed to the previous findings while burning Dawmill Smalls, in which a sudden drop in oxygen concentration caused an overshoot of the CO emission during the transient state. Instead, the peaks of CO emission can be seen at steady state and also when the combustion air was changed from lower to higher excess air (Figure 3.8). The latter may be due to the combustion intensity on the bed which was starting to get back to “normal” from the sudden deficit of combustion air on load decrease, where the combustion air was used more effectively than it was at the lower excess air setting. Nevertheless, the time allowance for the combustion to reach steady state at lower excess air was insufficient, thus the level of both the oxygen concentration and CO emission at this stage were difficult to justify. As for NO<sub>x</sub> emissions, there went back down from a high of 238ppm to an average of 170ppm following the change in load and again posed little concern.

### 3.4.6 Large Load Changes at Optimal and Sub-Optimal Operating Conditions for Columbian Smalls

Figure 3.9 shows the experimental results obtained from large load changes at optimal and sub-optimal operating conditions for the Columbian Smalls coal (*Test 12*). In parallel to the previous two experiments, the test was started from near optimum air setting (solid line) followed by lower excess air level (small dotted line) and then higher excess air level (dash line).



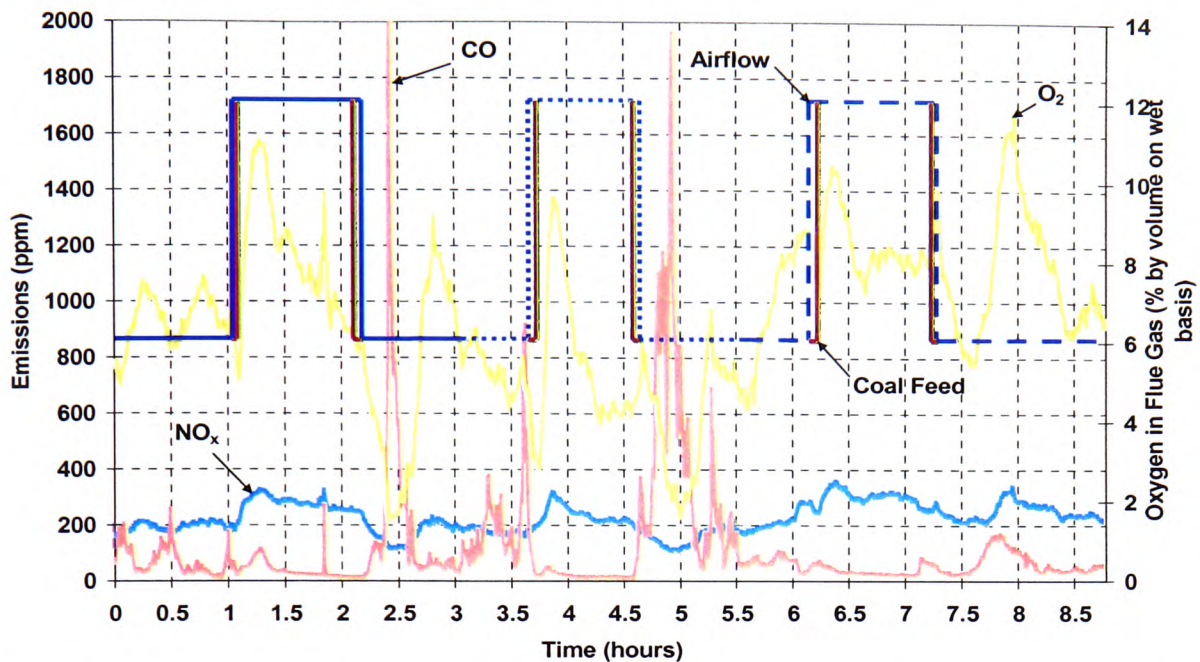


Figure 3.9 NO<sub>x</sub> & CO Emissions and Oxygen Concentration in Exhaust Duct following Large Load Changes at Optimal and Sub-Optimal Air Settings for Columbian Smalls – *Test 12*

On load increase, the overall oxygen trends seem to have a similar profile to the tests carried out for Dawmill Smalls in Section 3.4.4, where the sudden air increment resulted in a few oxygen peaks (Figure 3.9). The corresponding lower transient CO emissions can be explained by the higher excess air on the bed following a large increment in the combustion air. At steady state, the oxygen concentration at near optimum air, lower and higher excess air were 6%, 4% and 8% respectively (which were within their relevant target bands). NO<sub>x</sub> emissions at the three different excess air levels demonstrated a similar increment where they rose from about 200ppm to a high of 358ppm (at higher excess air due to the higher air supply and bed temperature). The overall NO<sub>x</sub> emission for Columbian Smalls at these three different excess air levels was perceptibly higher than that attainable by Dawmill Smalls and Dawmill Singles, justified again partly by the higher nitrogen content of Columbian coal.

On load decrease, similar trends of the oxygen concentration were observed at these three excess air levels (Figure 3.9), where a big drop in oxygen can be seen following the large decrement of combustion air on the bed. This is followed by two peaks of transient CO at

near optimum and lower excess air settings, but the transient CO emission at the higher excess air was within an acceptable limit, which can be explained by the fact that the higher combustion intensity on the bed helped to increase more turbulence and better promoted the combustion of the volatiles and char. The steady state oxygen concentration at these excess air levels were 6%, 4.5% and 7%, which were in the middle of their target bands respectively. There was an overshoot of the oxygen just before it reached steady state at the higher excess air setting (Figure 3.9) and this may be caused by a bed disturbance such as a hole in the fire bed or less coal being fed due to a non uniform coal distribution by the feeder. On the other hand, there was a significant drop in the NO<sub>x</sub> emission from a high of 358ppm to a low of 113ppm at these three excess air levels. The higher NO<sub>x</sub> emission can be attributed to the fact that the fuel and thermal NO<sub>x</sub> were both greatly influenced by the amount of combustion air available.

### 3.4.7 Summary of Section 3.4

This series of manual experiments were intended to study the test facility stoker response to gradual and large load changes at optimal and sub-optimal operating conditions in order to generate training data for neural network modelling. It also provided an initial understanding of the operation of a chain grate stoker and the knowledge obtained from the tests carried out for optimal operating conditions were important to allow the neural network based controller to efficiently operate the stoker boiler to meet the demand required (i.e. supplying hot water for industrial stoker).

## Chapter 4      Black Box Models of Pilot Scale Chain Grate Stoker Boiler

This Chapter presents the use of a feed-forward Multi-Layered Perceptron (MLP) network with an error Back Propagation (BP) learning algorithm for the identification of the combustion process (oxygen concentration in the flue gas) and pollutant formation (nitrogen oxides and carbon monoxide emissions) of the chain grate stoker test facility located at Casella CRE Ltd. Most of the system identification tasks implemented in this work were based on the toolbox developed by Noorgard (2000) namely 'Neural Network Based System Identification Toolbox' for use with MATLAB<sup>TM</sup>, whilst most of the basic understanding of the neural network programming was gained from the 'Neural Network Toolbox', also for use with MATLAB<sup>TM</sup>, developed by Demuth and Beale (1998). Details of the system identification procedure have already been discussed in Section 2.5.1 and the architecture of the non-linear neural network ARX model was also illustrated in Section 2.5.2. Therefore the sections that follow will concentrate on the training and validation of the neural model with data obtained from the series of experiments under various operating conditions for multiple-step-ahead predictions. The data sets used for this exercise were extracted from experimental results discussed in Section 3.4 and also supplemented with data from a previous research project (BCURA B35). Summary will be drawn at the end of this Chapter and the model architecture for use during the final stage of neural network based controller development will be discussed.

### 4.1 Training and Testing of a Neural Network ARX Model

This Section presents the training and testing of a neural network ARX model for the modelling of lump coal combustion on the chain grate stoker boiler located at Casella CRE Ltd. In order to enable the neural network based control system to be able to take account of future problems and control them before they occur (which should improve the load following capabilities of the boiler), training and testing of a comprehensive neural network ARX model to predict the gaseous products between 1½ to 5 minutes into the future was

considered. As mentioned in the literature review, a useful method to overcome the effect of a time-delay is by the use of a prediction approach. Long-range prediction is an attractive method for model-predictive control. In this scheme, the predictor uses past measurements of the process outputs and inputs to forecast the future output of the process over a rather long horizon, which is usually similar or larger than the time-delay of the process, so that the controller has the potential for making a control decision to improve the performance of the control system. In neural modelling, the results presented will serve as a benchmark for what the plant operator would call optimum operation of the stoker boiler and would therefore be used to simulate with unseen data sets and also with different types of coal under various operating conditions at multiple steps into the future. In this case the optimum operation of the stoker boiler was undertaken with gradual load changes at a near optimum air profile.

In the neural network modelling process considered here, the input variables for training were the chain grate and rotary valve speed (which determined the coal feed rate), four independent air ducts for primary airflow, oxygen concentration and different predicted variable readings in the flue gas. In this exercise, the predicted variables were the oxygen concentration in the flue gas ( $O_2$ ), nitrogen oxides ( $NO_x$ ) and carbon monoxide (CO) at multiple steps into the future. As mentioned above, the structure of the ARX regressor used previous inputs and outputs in order to deliver a prediction at one or more sample periods into the future. However, the task of choosing the appropriate model order (number of past inputs and outputs) and also the delay of the system is relatively difficult for any non-linear process and in this work the network was designed based on experience.

In order to obtain a more comprehensive model, several regressor vectors with different numbers of past inputs and outputs were considered and the optimal regressor structure normally has to be chosen on a trial-and-error basis. However, it was found that larger numbers of past inputs and outputs did not significantly increase the predictive abilities but did significantly increase the training time [Premier et al., 1997]. Therefore, in order to automate the network architecture selection, the Optimal Brain Surgeon (OBS) algorithm also from the 'Neural Network Based System Identification Toolbox' was employed to 'prune' the network in order to optimise the neural model performance [Norgaard, 2000].

This method involves re-training the network for a number of iterations (50 in this case) with respect to both the training data set and the testing set, after some weights of the network are removed (5%). The network weights that delivered the best performance were adopted when the algorithm ran and reached the global minimum. It should be noted however that unpredictable factors of any time varying features due to influences such as boiler fouling or corrosion are assumed to be negligible. Once the neural models were trained and validated, the neural models were tested on an unseen data set to test the capability of the neural network at modelling the combustion process of the stoker test facility. Finally, in the interest of brevity, only the optimum results (in this case the optimum prediction the neural network can predict) for each of the output variables will be shown in the following Sub-Sections.

#### 4.1.1 Neural Network ARX Model for Oxygen Concentration in the Flue Gas

This section presents a description of the neural network ARX structure used to predict the oxygen concentration in the flue gas multiple steps into the future. The input parameters for this model were selected to be the rotary valve and grate speeds and the four airflows that constituted the primary airflow. The MLP network structure consisted of ten neurons of hyperbolic tangent sigmoid transfer function in the hidden layer, whilst the output layer had one neuron of linear activation function. The number of neurons in input layer for this oxygen model was fourteen. This structure was chosen from trials and has been found to generate satisfactory results. To generate the ARX regressor structure a delay of four sample periods and two previous values was chosen for the rotary valve and grate speeds ( $rv(t-4)$ ,  $rv(t-5)$  and  $gs(t-4)$ ,  $gs(t-5)$  in Figure 4.1) whilst for the primary airflow a delay of one sample period and two previous values was chosen. Table 4.1 outlines the ARX structure configuration whilst Figure 4.1 shows the MLP network structure with the associated regressor vectors for predicting oxygen in the flue gas.



Table 4.1 ARX Regressor Structure Configuration for Oxygen Concentration

Variable	Number of Hidden Neurons	Number of Sample Period Delay	Number of Past Inputs	Number of Past Outputs
Rotary Valve Speed (rv)	10	4	2	-
Grate Speed (gs)		4	2	-
Airflows (af) 1,2 ,3 & 4		1	2	-
O <sub>2</sub>		-	-	2

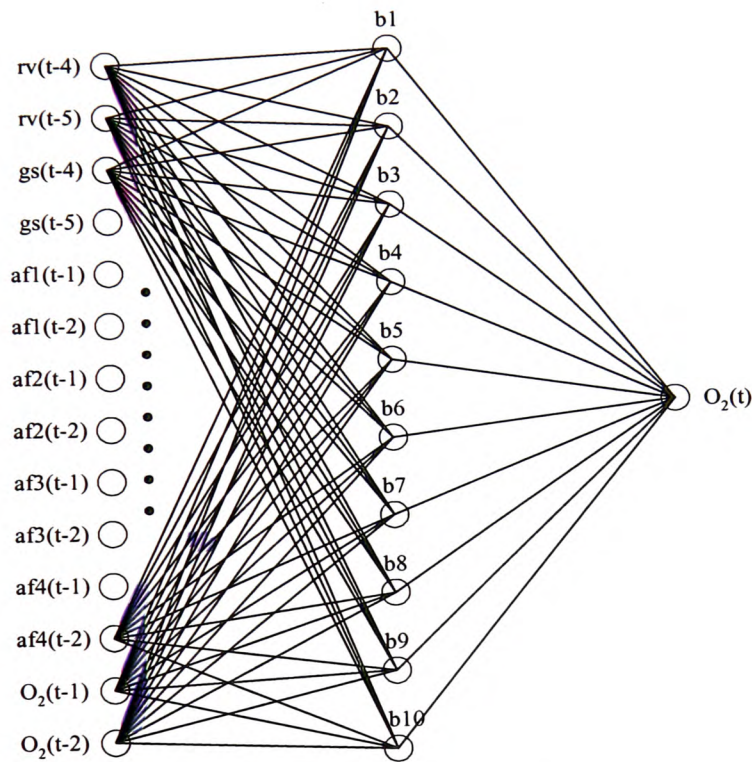


Figure 4.1 Network Structure of ARX Model for Oxygen in the Flue Gas

As mentioned earlier, the training and validation data sets were both obtained from the experimental results presented in Section 3.4 and also supplemented with data from BCURA B35 project. As for the training data set, the experimental results gathered following gradual load changes at a near optimum air setting for Dawmill Singles (*Test 4*) and Columbian Smalls (*Test 7*) were used and will serve as a benchmark for what the plant operator would

call optimum operation of the stoker boiler. The validation data set came from different operating conditions, namely large load changes under various excess air levels (*Test 12*) and gradual load changes at near optimum air settings but with a different coal type (Columbian Smalls – *Test 7*) were selected for the purpose of examining the model's prediction capability. Figures 4.2 to 4.7 show the training and validation results multiple steps into the future for oxygen concentration in the flue gas.

*Training* – During this process, the training data set was first pre-processed by normalising the inputs and targets so that they had means of zero and standard deviations of one using the MATLAB<sup>TM</sup> toolbox function PRESTD. In order to improve the dynamic performance of the neural model, odd number datum points from the data set were used for training and even numbers were used for testing. The training process stopped when the predefined performance goal was achieved. Finally, the OBS algorithm was employed to prune the network to optimise its performance. The training process with the best future predictions will be presented, corresponding to Figures 4.2, 4.4 and 4.6.

*Validation* – In order to test the capability of this neural network at modelling the combustion process of a stoker-fired boiler, the neural network model was tested with unseen data at different operating scenarios and also with a different coal type. Figures 4.3, 4.5 and 4.7 present the simulation result for oxygen concentration in the flue gas.

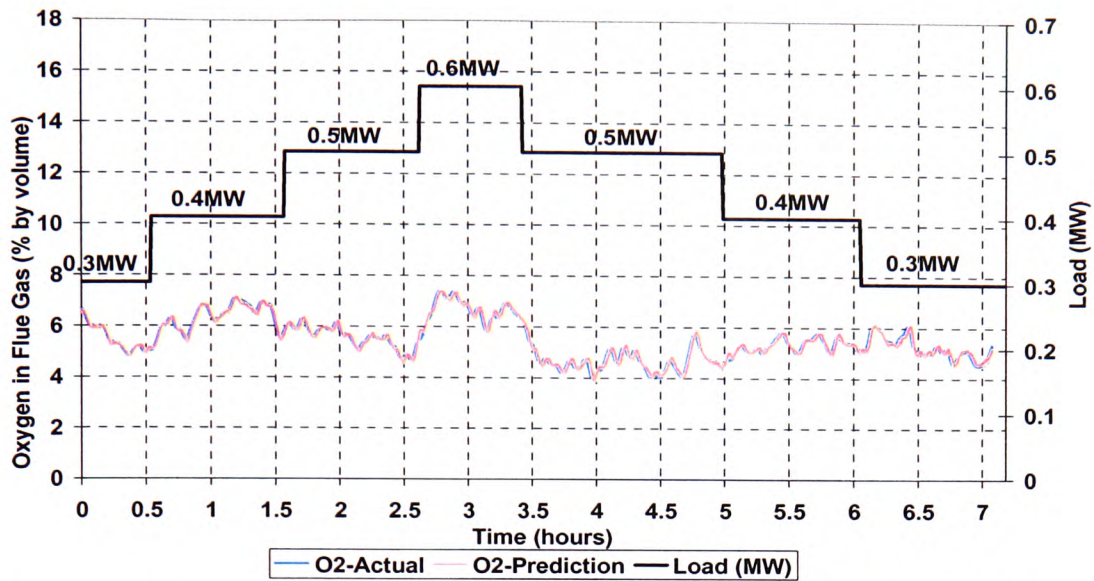


Figure 4.2 Three Step Ahead Predictions by the Pruned Neural Network ARX Model (nnarx) for Oxygen in the Flue Gas following Gradual Load Changes at Near Optimum Air for Dawmill Singles - BCURA B35 Data (*Training Model 1*)

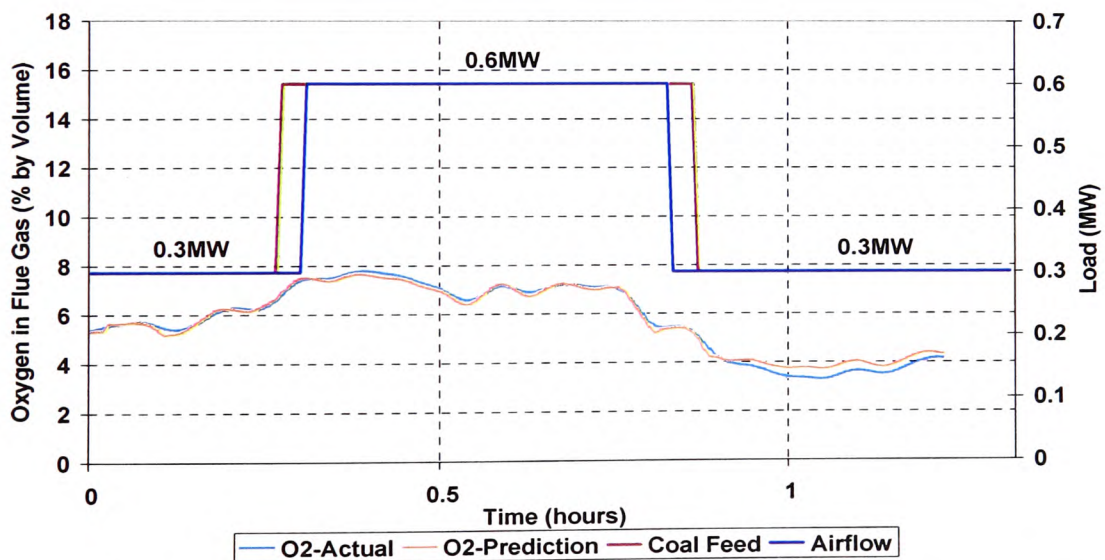


Figure 4.3 Three Step Ahead Simulations of Oxygen in the Flue Gas by *Training Model 1* following Large Load Changes with Staging Profile 1<sup>1</sup> for Dawmill Singles - BCURA B35 Data (*Validation*)

<sup>1</sup> Coal leads air on load increase, air leads coal on load decrease



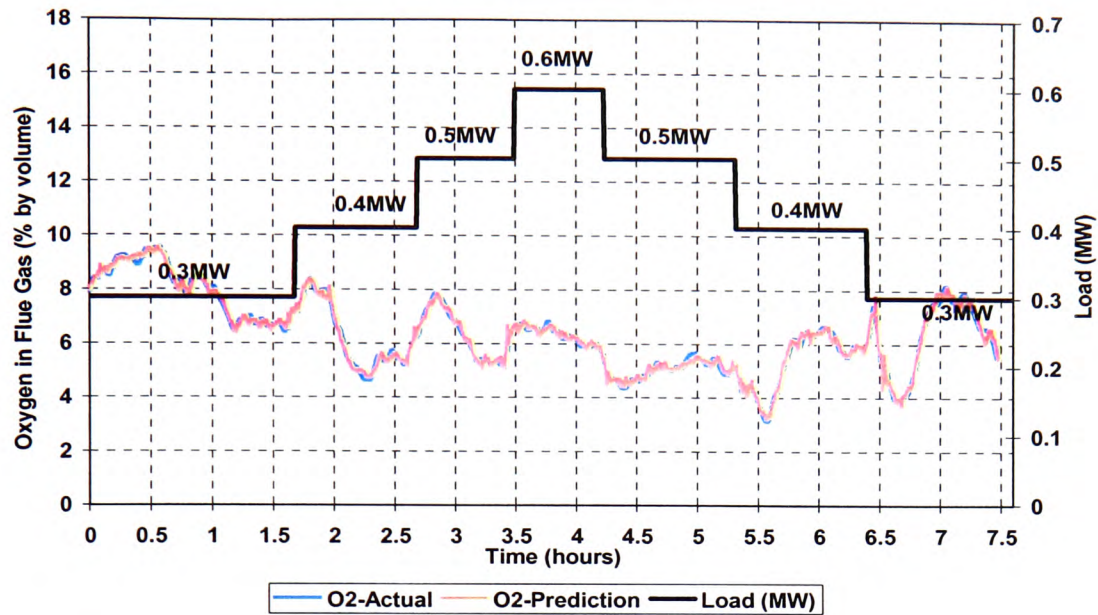


Figure 4.4 Six Step Ahead Predictions by the Pruned Neural Network ARX Model (nnarx) for Oxygen in the Flue Gas following Gradual Load Changes at Near Optimum Air for Dawmill Singles – *Test 4 (Training Model 2)*

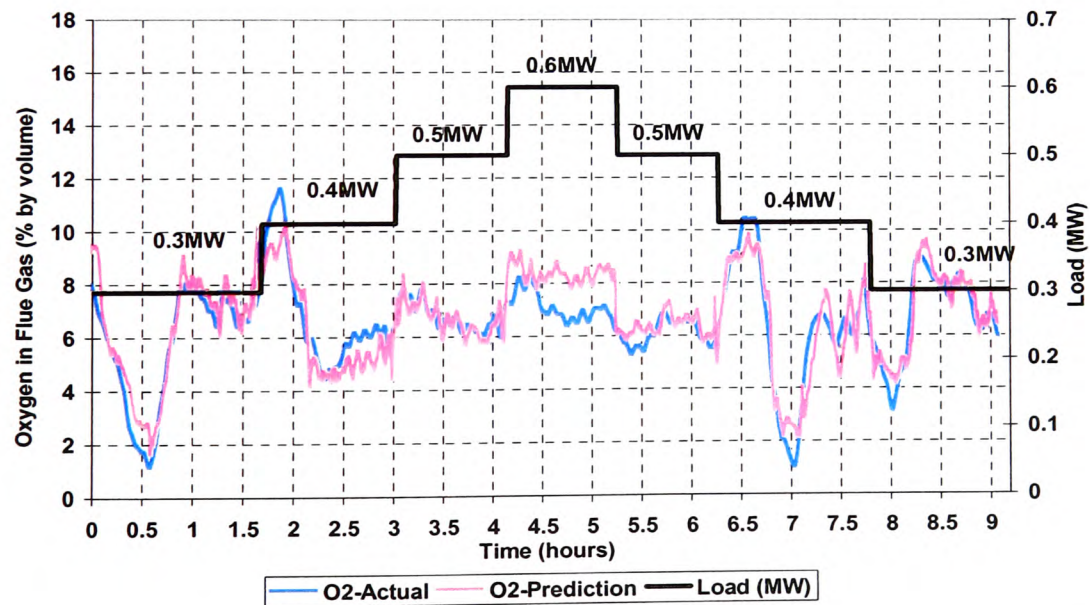


Figure 4.5 Six Step Ahead Simulations of Oxygen in the Flue Gas by *Training Model 2* following Gradual Load Changes at Near Optimum Air for Columbian Smalls – *Test 7 (Validation)*

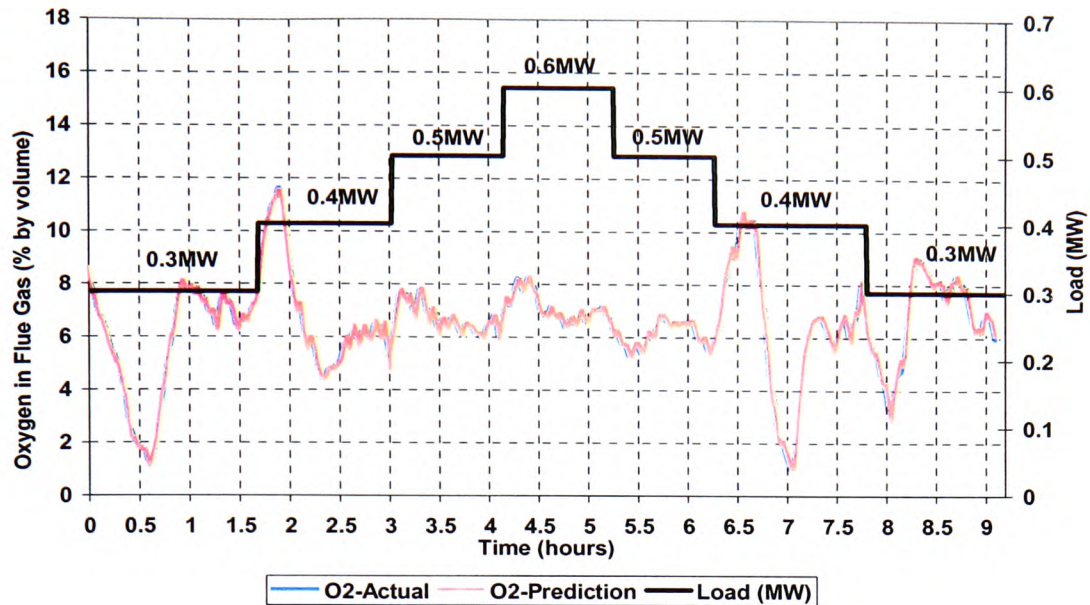


Figure 4.6 Three Step Ahead Predictions by the Pruned Neural Network ARX Model (nnarx) for Oxygen in the Flue Gas following Gradual Load Changes at Near Optimum Air for Columbian Smalls – *Test 7 (Training Model 3)*

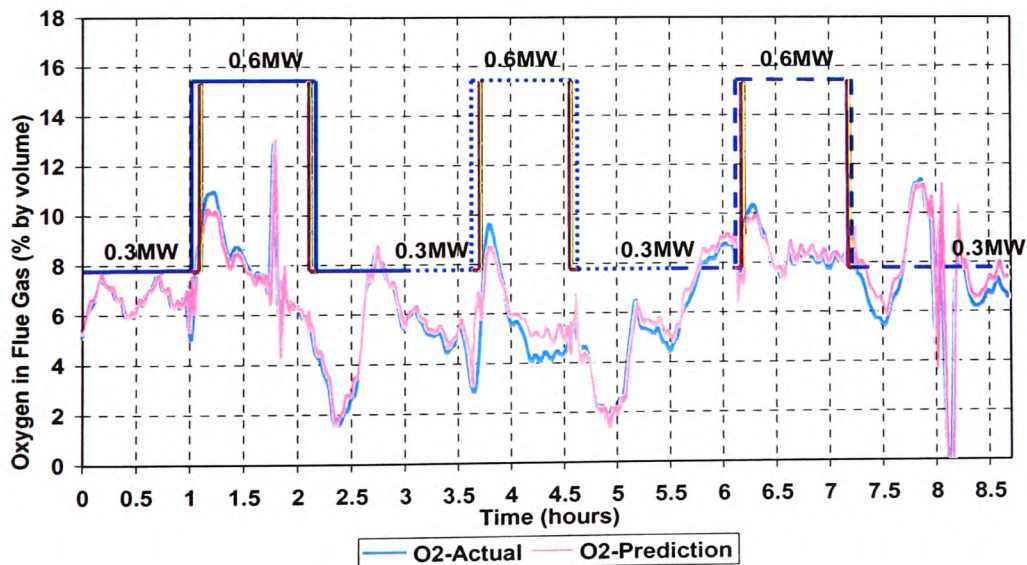


Figure 4.7 Three Step Ahead Simulations of Oxygen in the Flue Gas by *Training Model 3* following Large Load Changes at Optimal and Sub-Optimal Air Settings for Columbian Smalls – *Test 12 (Validation)*

*Discussion of Results* – Based on the regressor vector defined in Section 4.1.1, visual inspection of the three validation data sets clearly indicates that the trained oxygen models were able to deliver predictions of the oxygen concentration in the flue gas into the future. The optimum number of steps ahead into the future for the three different data sets were 3, 6 and 3, which corresponds to 1½ and 3 minutes into future. This means that the neural network based control system would have the maximum of 3 minutes to take action in advance of future problems and control them before they actual happen. However, particular attention must be paid to the second data set in which the validation data was simulated with data obtained whilst burning a different type of coal. In this case, the validation data set collected when using Columbian Smalls (*Test 7*) as a burning coal was simulated using training data that was gathered from burning Dawmill Singles (*Test 4*). Figure 4.5 shows a reasonable correlation between the predicted and actual output results for the entire validation data set by using the configuration of neural model shown in Figure 4.4. Although the graph shows large fluctuations in the entire process, the prediction follows the actual trend quite reasonably (Figure 4.5).

Figures 4.6 and 4.7 show another set of encouraging results. The validation data set was collected following large load changes at near optimum (solid line), lower (small dotted line) and higher (dash line) excess air levels (*Test 12*) and was simulated by the model trained with the data set gathered following gradual load changes at near optimum air settings for Columbian Smalls (*Test 7*). However, good predictions were also achieved and the prediction follows the actual trend fairly well for the entire process following large load changes with staging profile 1 for Dawmill Singles (Figure 4.3). With the predefined regressor vector described earlier in this Section, it can therefore be concluded from these results that the developed non-linear neural network ARX model for the oxygen in the flue gas, has been able to characterise the dynamics of the actual process with reasonable accuracy.

#### 4.1.2 Neural Network ARX Model for Nitrogen Oxides Emissions

This section describes the neural network of ARX structure for nitrogen oxides ( $\text{NO}_x$ ) emission multiple steps into the future. The input parameters for this model were similar to that of the oxygen model but with the inclusion of oxygen concentration as an input parameter to the model. The inclusion of oxygen concentration into the model can be justified by the fact that the fuel and thermal  $\text{NO}_x$  were both greatly influenced by the amount of combustion air available in the combustion zone and also that the oxygen concentration in the flue gas gives an indication of the amount of excess air being provided for the combustion process to take place. Fundamentally, in order to identify the behaviour of the production of  $\text{NO}_x$ , it was evident that the oxygen reading was necessary and plays an important role for the identification of the output variable. Therefore, when it comes to choosing the suitable input parameters for the neural model with the appropriate delays and number of orders to form the corresponding regressor vectors, it is in circumstances like this that an understanding to the process to be modelled is essential.

As with the oxygen model, twelve hidden neurons were chosen from trials and have been found sufficient to generate satisfactory results for the  $\text{NO}_x$  model. Based on the findings from the oxygen model, a delay of four sampling periods and two past values was chosen for the coal feed and a delay of one sampling period and two past values was selected respectively for the airflow and oxygen concentration to predict the  $\text{NO}_x$  emissions. In other words, it should take at least 2 minutes before the nitrogen oxides reading should vary following a change in the coal feed and similarly for the airflow and oxygen concentration. For the last part of the regressor, a delay of one sample period was chosen for the  $\text{NO}_x$  emissions with three past outputs being used. The decision was made based on experience, Noorgard (2000) & Ljung (1998), as experience will to some extent enable the designer to instinctively suggest the orders and delays of the system, even though there is a lack of more precise knowledge. The corresponding regressor vectors were batch fed to the MLP network during training. An illustration of the MLP network structure together with the associated regressor vectors and the ARX structure configuration for predicting the  $\text{NO}_x$  emissions are shown in Figure 4.8 and Table 4.2 respectively.



Table 4.2 ARX Regressor Structure Configuration for Nitrogen Oxides Emission

Variable	Number of Hidden Neurons	Number of Sample Period Delay	Number of Past Inputs	Number of Past Outputs
Rotary Valve Speed (rv)	12	4	2	-
Grate Speed (gs)		4	2	-
Airflows (af) 1,2 ,3 & 4		1	2	-
O <sub>2</sub>		1	2	-
NO <sub>x</sub>		-	-	3

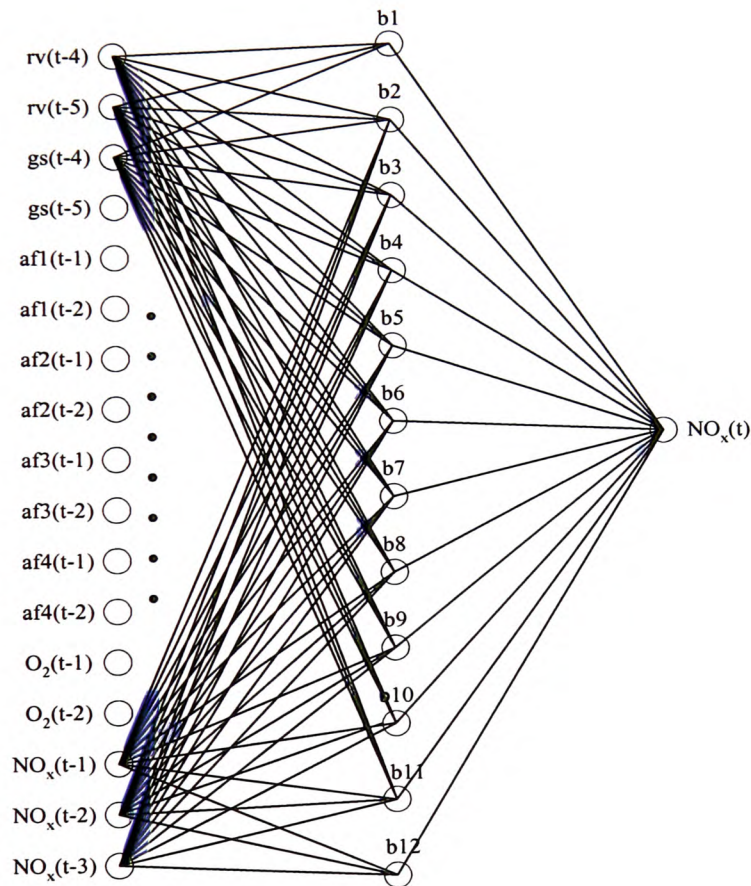


Figure 4.8 Network Structure of ARX Model for Nitrogen Oxides Emission

As with the Oxygen model, experimental results discussed in Section 3.4 and the BCURA B35 data were both used for this exercise. In the training data sets, the results presented will

serve as a benchmark for what the plant operator would call optimum operation of the stoker boiler and would therefore be used to simulate unseen data sets for different air distribution profiles at multiple steps into the future. Figures 4.9 to 4.14 presents the training and validation results for NO<sub>x</sub> emissions multiple time steps into the future.

*Training* – The training data set was first pre-processed by normalising the inputs and targets so that they have means of zero and standard deviations of one using the MATLAB<sup>TM</sup> toolbox function PRESTD. As with the oxygen model, in order to improve the dynamic performance of the neural model, odd number datum points from the data set were used for training and even numbers were used for testing. With the MATLAB<sup>TM</sup> toolbox training function of TRAINBR, which updates the weight and bias values according to a Levenberg-Marquardt optimisation, a function called “stop training” was utilised to stop the training early if the network performance on the testing vectors failed to improve, otherwise the training process stopped when the predefined performance goal was achieved. Finally, the OBS algorithm was employed to prune the network to enhance the model predictions. The optimum trained network for predicting into the future will be presented (Figures 4.9, 4.11 and 4.13).

*Validation* – As with the oxygen model, the neural network model was tested with unseen data for different operating conditions and a different coal type in order to access the capability of this neural network at modelling the combustion process of a stoker-fired boiler. The optimum number of steps into the future simulation will be shown (Figures 4.10, 4.12 and 4.14).

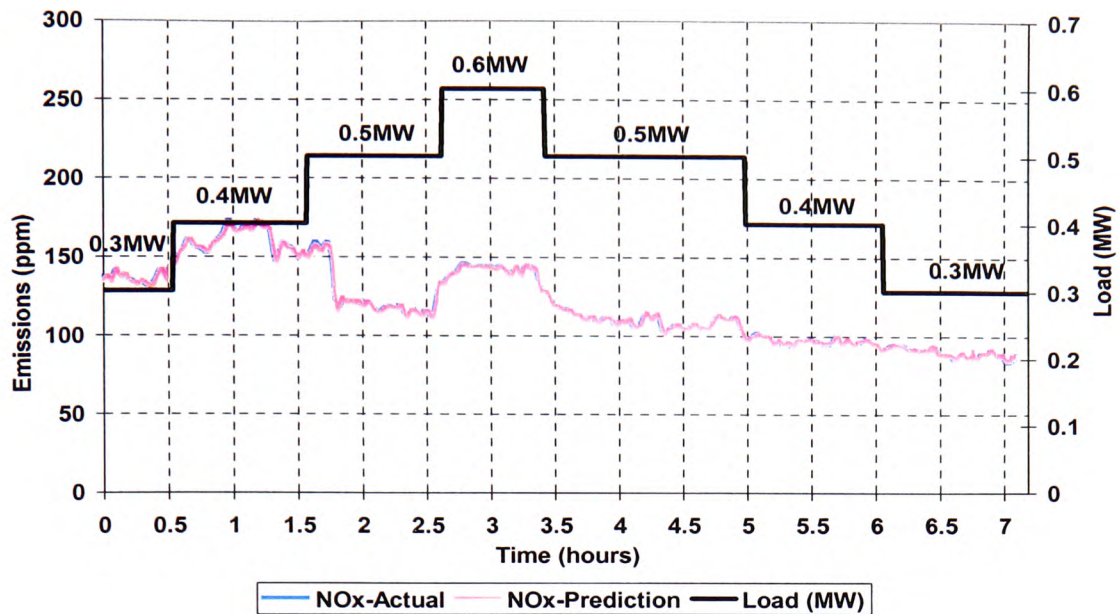


Figure 4.9 Three Step Ahead Predictions by the Pruned Neural Network ARX Model (nnarx) for Nitrogen Oxides Emission following Gradual Load Changes at Near Optimum Air for Dawmill Singles - BCURA B35 Data (*Training Model 4*)

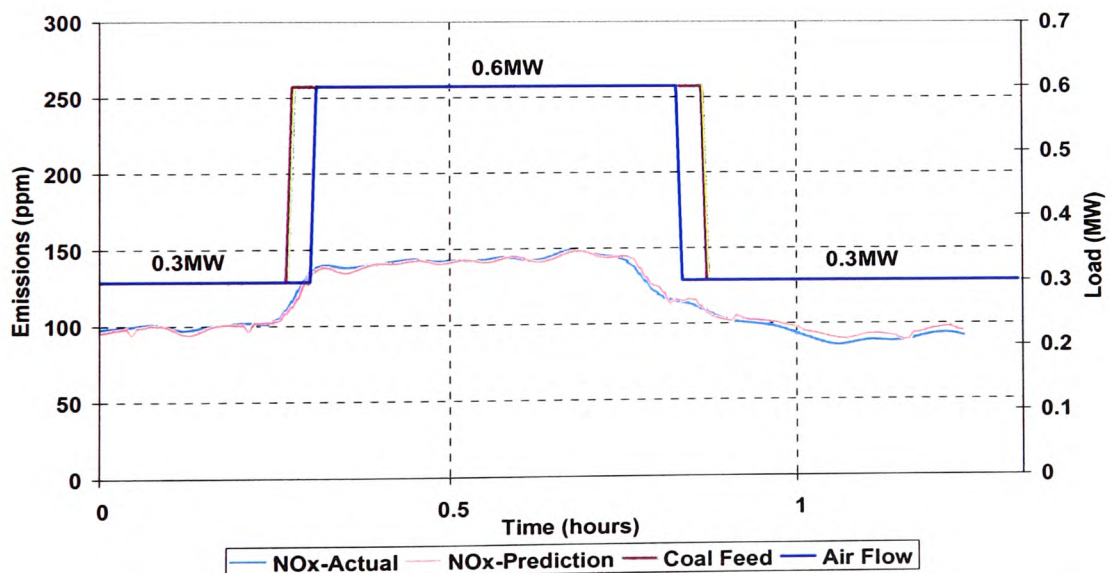


Figure 4.10 Three Step Ahead Simulations of Nitrogen Oxides Emission by *Training Model 4* following Large Load Changes with Staging Profile 1 for Dawmill Singles - BCURA B35 Data (*Validation*)



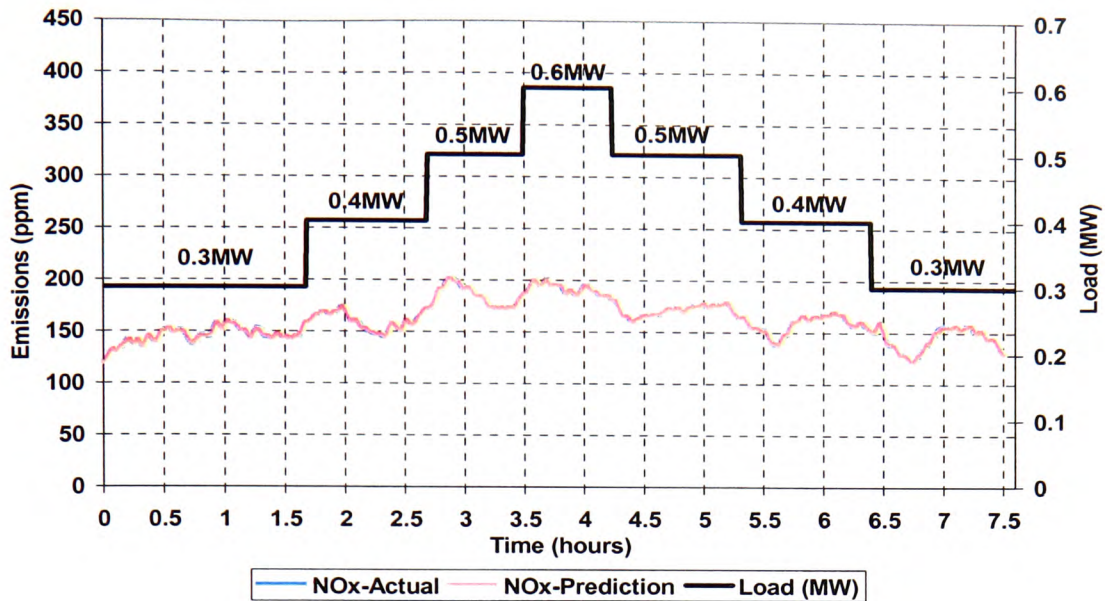


Figure 4.11 Three Step Ahead Predictions by the Pruned Neural Network ARX Model (nnarx) for Nitrogen Oxides Emission following Gradual Load Changes at Near Optimum Air for Dawmill Singles – Test 4 (Training Model 5)

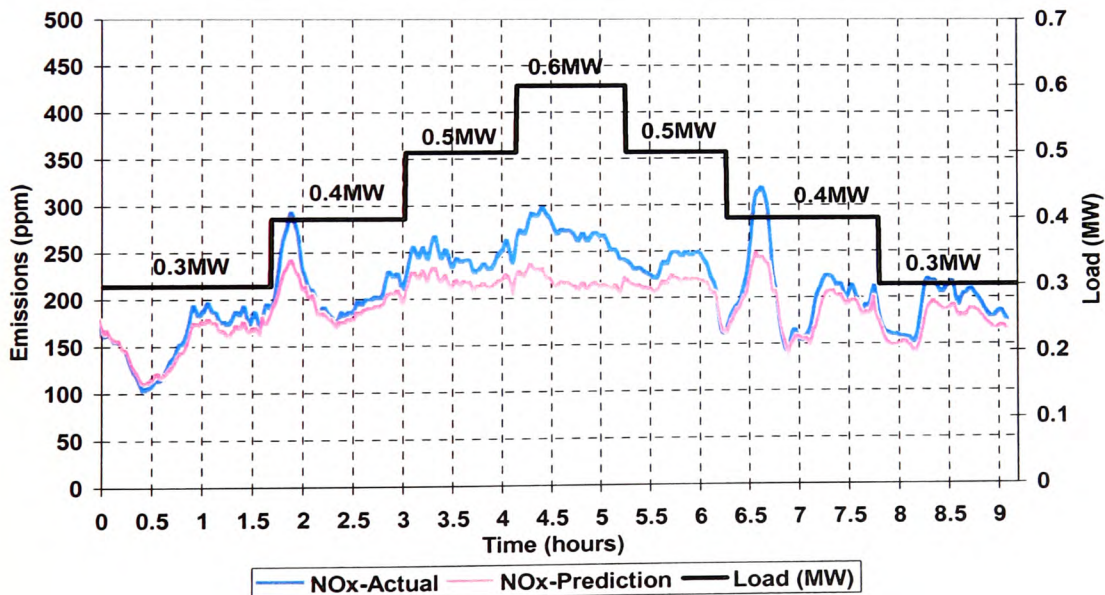


Figure 4.12 Three Step Ahead Simulations of Nitrogen Oxides Emission by Training Model 5 following Gradual Load Changes at Near Optimum Air for Columbian Smalls – Test 7 (Validation)



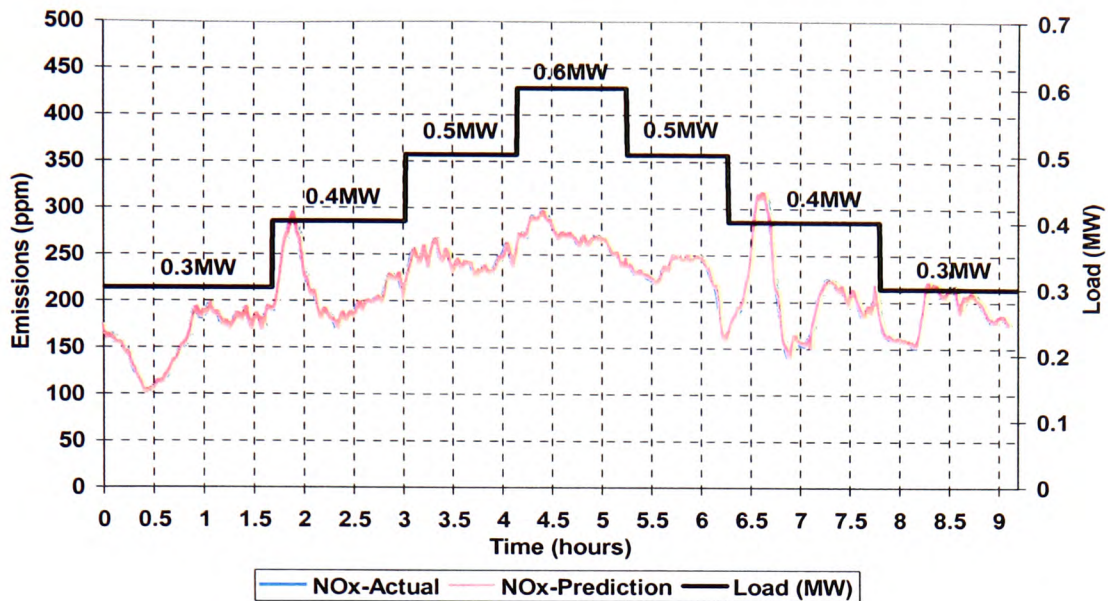


Figure 4.13 Three Step Ahead Predictions by the Pruned Neural Network ARX Model (nnarx) for Nitrogen Oxides Emissions following Gradual Load Changes at Near Optimum Air for Columbian Smalls – *Test 7 (Training Model 6)*

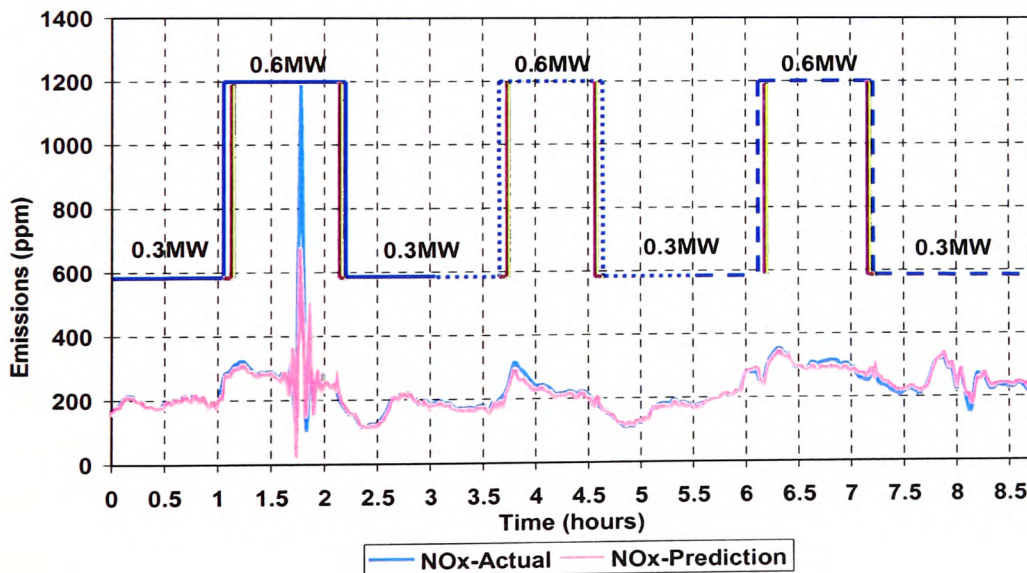


Figure 4.14 Three Step Ahead Simulations of Nitrogen Oxides Emissions by *Training Model 6* following Large Load Changes at Optimal and Sub-Optimal Air Settings for Columbian Smalls – *Test 12 (Validation)*

*Discussion of Results* – The maximum prediction into the future that achieved success was 1½ minutes and this is believed to be the optimum prediction of NO<sub>x</sub> emissions, as shown in Figures 4.10, 4.12 and 4.14 respectively. In other words, the neural network based control system would have at least 1½ minute of advanced warning to undertake a control action before the actual NO<sub>x</sub> changed. An excellent result was achieved when predicting three steps ahead for large load changes at optimal and sub-optimal air settings (Figure 4.14), where a perfect match between the prediction and actual output results was achieved. On the other hand, in contrast to the oxygen model, the validation result for the second data set (Figure 4.12) shows a slightly higher error when burning a different coal type (Figure 4.11). Nevertheless, visual inspection of the plots clearly shows that the prediction follows the actual trend fairly well for the entire validation data set despite the lower prediction accuracy that occurred especially at higher loads. Figure 4.10 demonstrates that the prediction of NO<sub>x</sub> emissions three steps into future were reasonable, despite the validation data being significantly different from the training data. Regardless of the degradation of the prediction for the second data set, the overall results are quite encouraging.

#### 4.1.3 Neural Network ARX Model for Carbon Monoxide Emissions

The input parameters selected for this model were similar to those of NO<sub>x</sub> emissions in the sense that the oxygen concentration was also considered as an input parameter to the model. The same argument (discussed in Section 4.1.2) can be used to justify the inclusion of oxygen concentration for this model in that it provides an obvious indication of the excess air level in the fire bed and hence the overall combustion condition. Therefore, it is the author view that the oxygen reading was important for the identification of the dynamics of the production of carbon monoxide (CO) emission by the neural model. In addition, other input parameters were selected and these included the rotary valve and grate speeds that represent the coal feed rate and the four airflows that constitute the primary airflow. The number of delays and order of the regressor vectors were identical to that of the NO<sub>x</sub> model, in that a delay of four sampling periods overlooking two past values was chosen for the coal feed and a delay of one sampling period also overlooking two past values was selected respectively for the airflow and oxygen concentration. Based on observation, four past outputs with a delay of

one sample period were chosen for the CO emission and the corresponding regressor vectors were then batch fed as inputs to the MLP network during training. It will be worth mentioning that a larger numbers of past inputs and outputs could lower the error goal during training but the added complexity of the model was not justified by the possible improvement in forecasting [Premier *et al.*, 1997]. A MLP network of twelve hidden neurons with a single neuron in the output layer with a linear transfer function was selected as the structure for the ARX model. Figure 4.15 shows the MLP network structure with the associated regressor vectors whilst Table 4.3 outlines the ARX structure configuration for CO emission prediction.

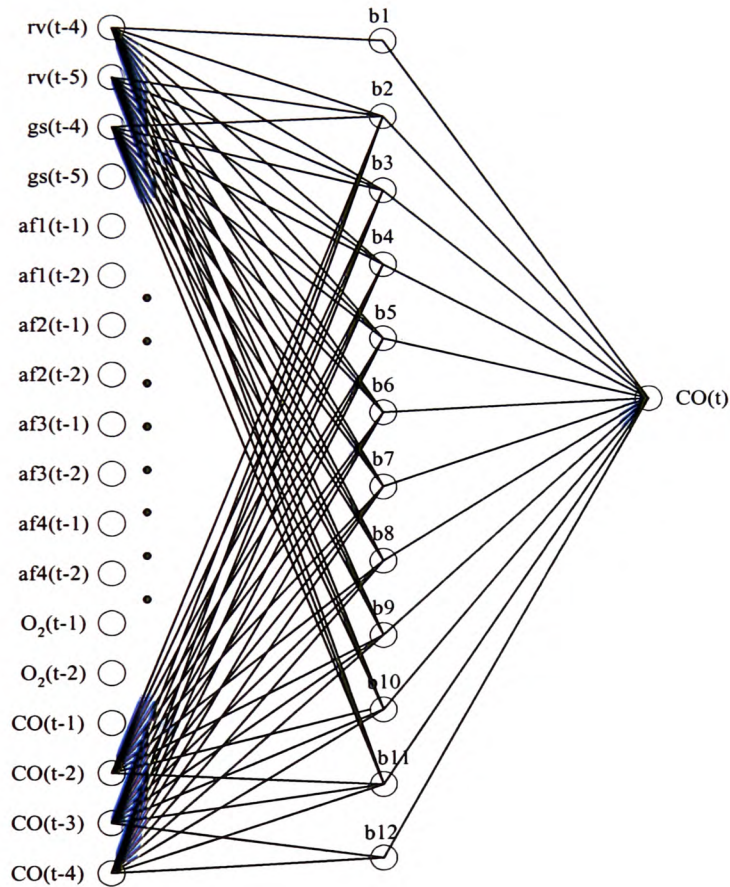


Figure 4.15 Network Structure of ARX Model for Carbon Monoxide Emission

Table 4.3 ARX Regressor Structure Configuration for Carbon Monoxide Emission

Variable	Number of Hidden Neurons	Number of Sample Period Delay	Number of Past Inputs	Number of Past Outputs
Rotary Valve Speed (rv)	12	4	2	-
Grate Speed (gs)		4	2	-
Airflows (af) 1,2 ,3 & 4		1	2	-
O <sub>2</sub>		1	2	-
CO		-	-	4

As for the oxygen and NO<sub>x</sub> modelling, experimental results presented in Section 3.4 and the BCURA B35 data were both used for the training and validation of this CO model. Validation data sets gathered under various operating scenarios were simulated with the training data sets, collected for conditions the operator would call optimum. Figures 4.16 to 4.21 present the prediction of the training and validation data.

*Training* – As with the first two models, the MATLAB<sup>TM</sup> toolbox function PRESTD was used to pre-process the training data set by normalising the inputs and targets so that they had a mean of zero and a standard deviation of one. As for the oxygen and NO<sub>x</sub> models, odd datum points were used for training and even numbers were used for testing to enhance the dynamic performance of the neural model. The training process can either be stopped manually using “stop training” from the TRAINBR training function or wait until the predefined performance goal was reached. The derived network after training was pruned using the OBS algorithm to improve the model’s prediction. The optimum number of steps ahead will be presented for the training data sets in Figures 4.16, 4.18 and 4.20.

*Validation* – The derived neural models were tested with the validation data sets under various operating scenarios and also with different type of coal in order to test the model’s capability at modelling the CO emanating from the combustion. Figures 4.17, 4.19 and 4.21 present the prediction for an optimum number of steps into the future for CO emission.



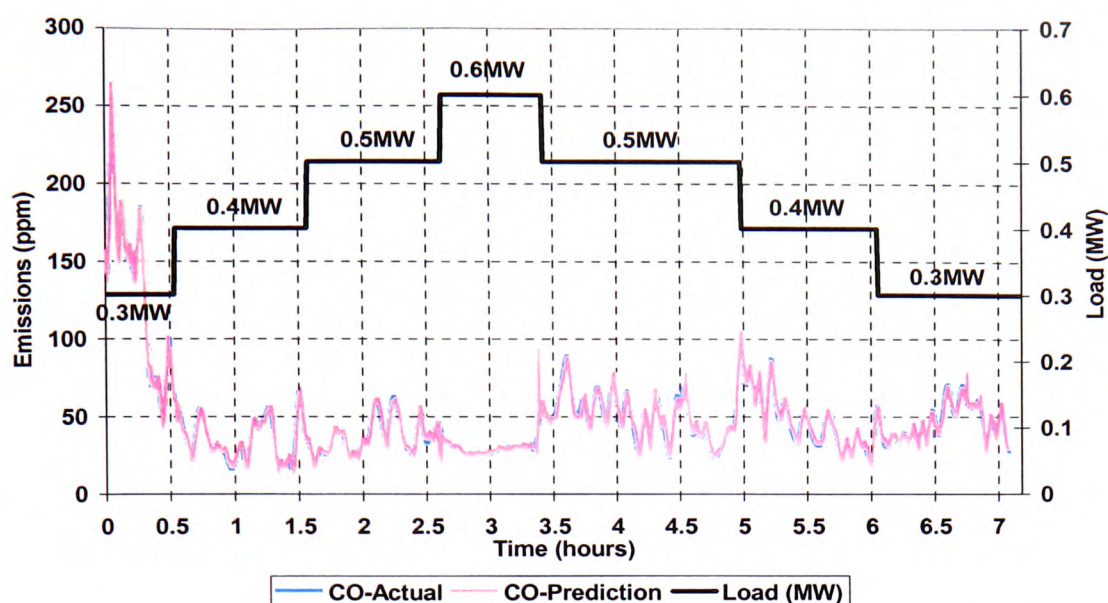


Figure 4.16 Three Step Ahead Predictions by the Pruned Neural Network ARX Model (nnarx) for Carbon Monoxide Emission following Gradual Load Changes at Near Optimum Air for Dawmill Singles - BCURA B35 Data (*Training Model 7*)

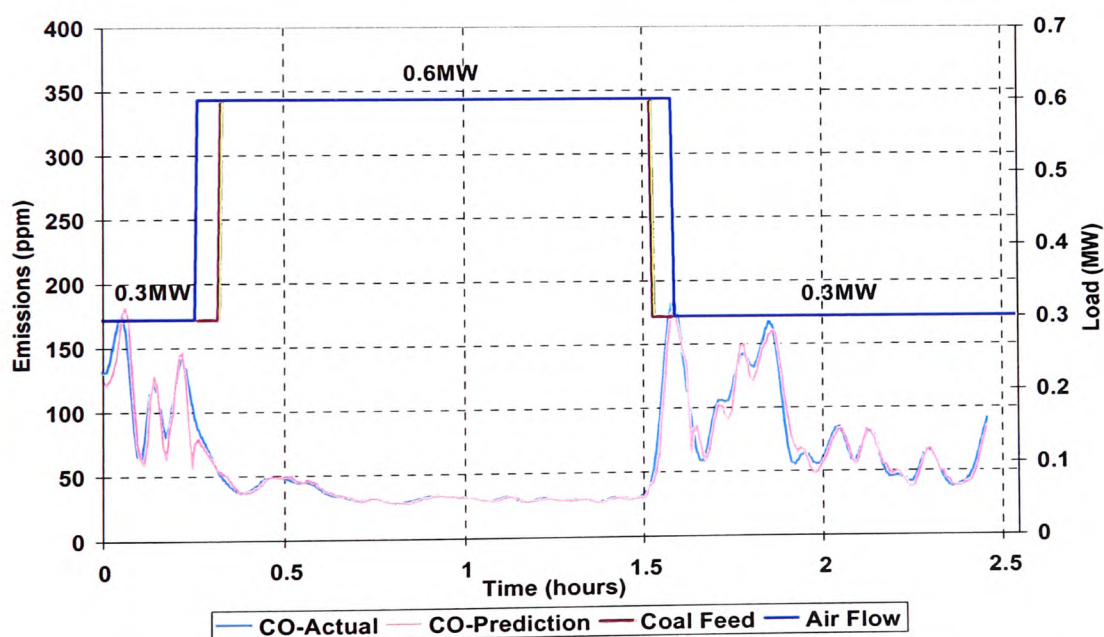


Figure 4.17 Three Step Ahead Simulations of Carbon Monoxide Emission by *Training Model 7* following Large Load Changes with Staging Profile 2<sup>2</sup> for Dawmill Singles - BCURA B35 Data (*Validation*)

<sup>2</sup> Air leads coal on load increase, coal leads air on load decrease

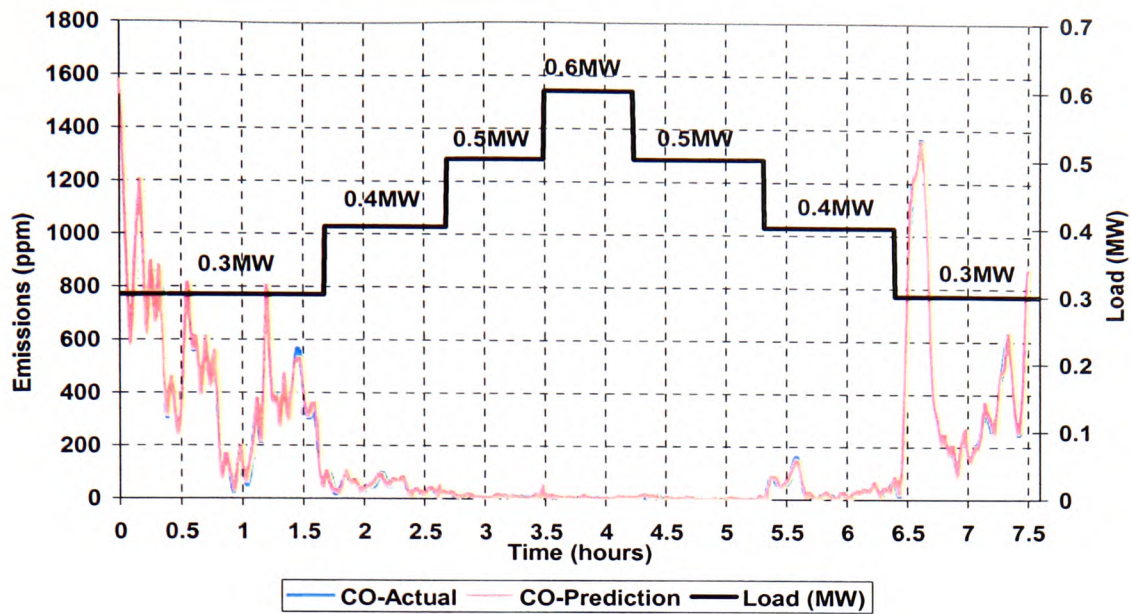


Figure 4.18 Three Step Ahead Predictions by the Pruned Neural Network ARX Model (nnarx) for Carbon Monoxide Emission following Gradual Load Changes at Near Optimum Air for Dawmill Singles – *Test 4 (Training Model 8)*

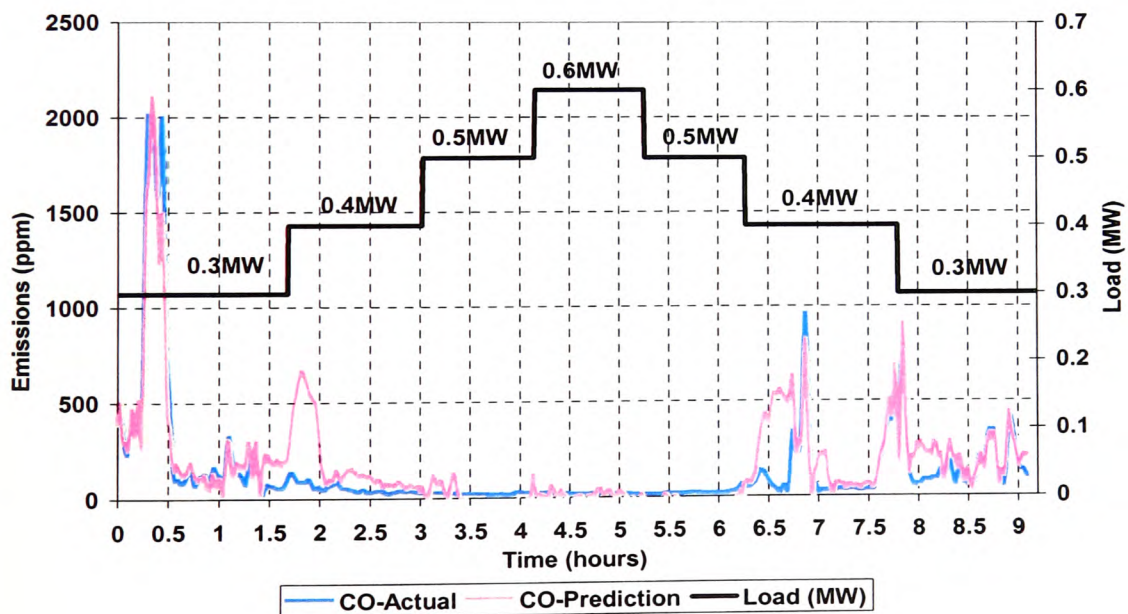


Figure 4.19 Three Step Ahead Simulations of Carbon Monoxide Emission by *Training Model 8* following Gradual Load Changes at Near Optimum Air for Columbian Smalls – *Test 7 (Validation)*



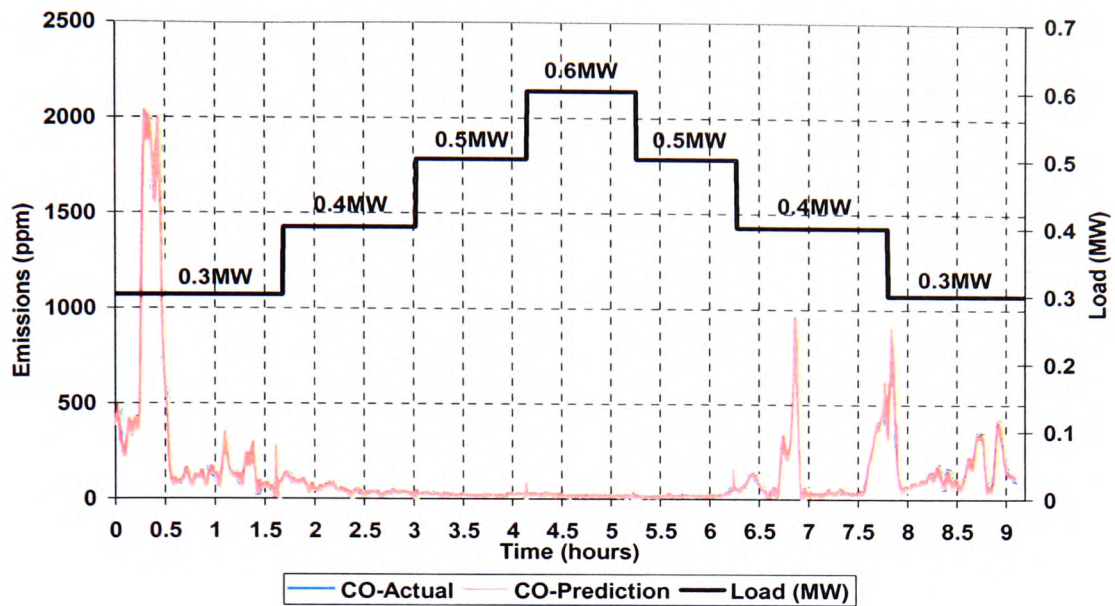


Figure 4.20 Three Step Ahead Predictions by the Pruned Neural Network ARX Model (nnarx) for Carbon Monoxide Emissions following Gradual Load Changes at Near Optimum Air for Columbian Smalls – *Test 7 (Training Model 9)*

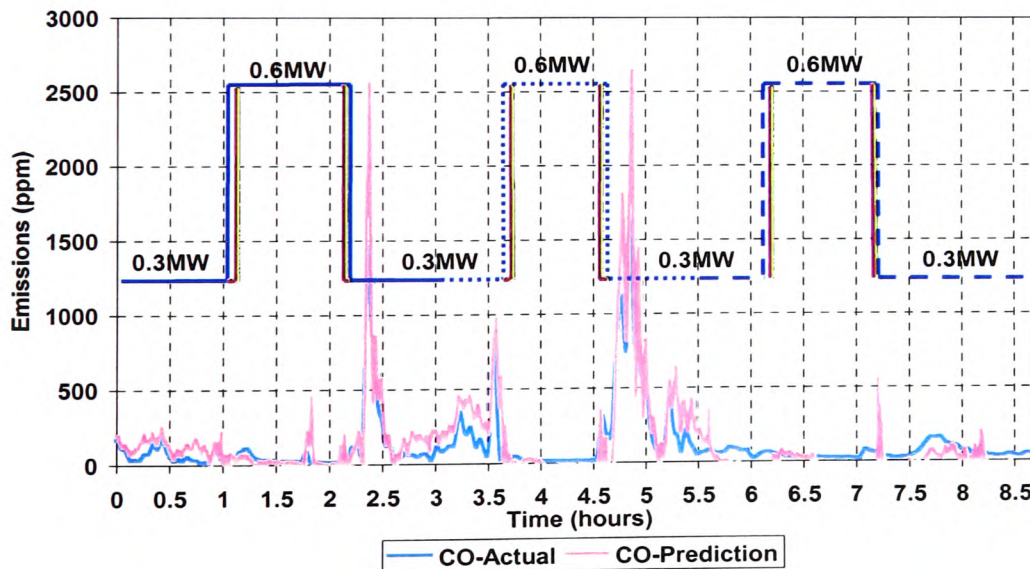


Figure 4.21 Three Step Ahead Simulations of Carbon Monoxide Emissions by *Training Model 9* following Large Load Changes at Optimal and Sub-Optimal Air Settings for Columbian Smalls – *Test 12 (Validation)*

*Discussion of Results* - The optimum prediction into the future for CO emissions for the three different data sets was 3, which corresponds to 1½ minutes (Figure 4.17, 4.19 and 4.21). This time, the best results occurred with the first data set (Figure 4.17) gathered following large load changes with the prediction being in good agreement with the actual results. As for the second and third data sets, reasonable correlation between the target and the predicted values was obtained despite the validation data being significantly different from the training data. Furthermore, the dynamics of the carbon monoxide production was of a considerably higher order when compared to the oxygen and nitrogen oxides data, thus explaining the degradation of the model for CO emission prediction. However, the results shown here demonstrate the reliability of the model for predicting the carbon monoxide emission over a time horizon of 1½ minutes based on the regressor vectors defined in Section 4.1.3.

## 4.2 Summary of Chapter 4

Overall the results are quite encouraging and the use of a neural network to model the gaseous readings of oxygen, NO<sub>x</sub> and CO emanating from a chain grate stoker boiler would prove a useful addition to a control algorithm, helping to reduce the time lag of the process.



## Chapter 5 Plant Description of Industrial Scale Chain Grate Stoker Boiler & Commissioning Test Results

This Chapter describes the main features of one of the three 3.7MW chain grate stoker fired shell boilers located at Her Majesty's Prison (HMP) Garth in Leyland, Lancashire, that used to develop and test the neural network based controller. A series of commissioning tests (i.e. preliminary, detailed and final commissioning tests) were carried out to gather information about the behaviour and response of this boiler by manually altering the firing rate and excess air level over its entire operating range. The gathered information was then used to determine the optimal boiler settings and the data gathered was also used to train the neural networks to predict the oxygen concentration in the flue gas and carbon monoxide emissions as part of a neural network based controller to meet the demand required. The load demand in the case of the industrial stoker was the hot water temperature. However, it will be worth mentioning that the concept and methods used for this test were similar to the earlier work carried out with the 1MW chain grate stoker test facility located at Casella EMC which essentially involved manually operating the boiler over its 6 to 1 operating range under the commissioning engineer's best practise. Finally, commissioning test results will be discussed and conclusions are drawn in the last Section of this Chapter.

### 5.1 Plant Description of 3.7MW Industrial Scale Chain Grate Stoker & Plant Instrumentation

The three 3.7MW chain grate stoker fired shell boilers were situated in a boiler house and each stoker featured a Proctor fire break unit; pneumatic coal feeding system; an effective fire bed area of 1.2m (width of grate) x 3.5m (length of fire bed) which was constructed from grey cast iron links. As with the test facility boiler, the primary combustion air for the industrial stoker was provided via a variable speed forced draught fan motor in order to achieve better air distribution over the entire firing range. The air distribution was controlled

by a damper which was positioned half way along the length of the grate inside the windbox and spread the air into the two sections on the grate. An induced draught fan was fitted to maintain a slight suction in the furnace chamber in order to maintain a suitable pressure drop across the boiler. This feature ensured clean operation of the boiler plant and also to prevent the stoker front from overheating. Hot water was generated at a temperature of 120°C and a pressure of 3 bar was produced by the 3-pass shell boiler. Automatic ash removal and a high efficiency cyclone to arrest grit before the flue gas was discharged to the atmosphere through the stack were other features of the stokers. Each of these coal fired stoker boilers could produce up to 3.7MW of thermal output and possessed a turndown ratio of 6:1. In other words, the lowest operable load was 0.62MW, which corresponded to 16.67% of the Maximum Continuous boiler output Rating (MCR). The overall combustion efficiency of this boiler was claimed to be 80%, a typical figure for the boiler of this type. The main purpose of this 24 hourly manned boiler house is to supply hot water for domestic usage and space heating for approximately 500 inmates in the prison. In order to provide intermittent backup during especially cold weather and also in the summer period when maintenance work was carried out on the coal fired boilers, a natural gas boiler of the same thermal capacity was utilised.

The stoker boiler was fitted with an industrial PID digital control system, namely the Honeywell UDC3000 process controller which regulated the coal feed and airflow rate (so that the desired hot water temperature set point could be achieved) and the whole unit was integrated into an overall energy management system accommodated in a master control room. The process sensor available from the plant was the thermocouple signal measuring the hot water temperature from the outgoing hot water pipe. However, the existing plant conventional PID controller was a single loop process controller with the process variable being the pressurised hot water temperature, which indicated the load demand required. Nevertheless, individual signals to the various actuators i.e. rotary valve, grate and damper motor, and variable speed drives was ratio off the PID controller signal.

For the purpose of collecting information regarding the behaviour and response of the plant, a stand-alone data logging system was developed so that the input variable (firing rate) and

the required process variable (hot water temperature) could automatically be acquired. For firing rate acquisition, the input signal was gathered and passed through a fifth order Butterworth lowpass filter (cut-off frequency of 20Hz) in order to reduce noise before being recorded by the logging system. As for hot water temperature measurement, a K-type thermocouple was used and a conditioning circuit was also necessary in order to amplify the weak signal from the thermocouple through the use of a AD595A integrated circuit chip. The amplification of the weak signal was in the range of  $45\mu\text{V}/^\circ\text{C}$  to the range of  $10\text{mV}/^\circ\text{C}$  (i.e. an output signal of 1219mV from the AD595A corresponded to a temperature reading of  $120^\circ\text{C}$ ). For automatic logging of these analogue signals, a Pentium 3 550MHz PC fitted with the MIO16 Data Acquisition card from National Instruments<sup>TM</sup> also running the related LabVIEW<sup>TM</sup> software was used. The data acquisition sampling period was 30 seconds, which was similar to the sampling rate acquired on the Tactician system of the chain grate stoker test facility at Casella CRE Ltd. The specification and layout of the overall signal interface configuration can be found in the following Chapter where the details of the NNBC development are discussed.

Other measurements taken from these tests included the pollutant emissions ( $\text{CO}$  and  $\text{NO}_x$  normalised to 6% of oxygen), concentration of oxygen in the flue gas and flue gas temperature which was measured by a 'Testo 350' portable flue gas analyser, fitted at the exhaust duct before the cyclone. As with the work on the stoker test facility, the Windows based software 'Testo ComLight' that came with the analyser was used to continuously log the reading to a separate PC with the standard sampling period of 30 seconds. For the experiments conducted on the industrial stoker boiler,  $\text{O}_2$ ,  $\text{CO}$  and  $\text{NO}_x$  measurements have been presented along with other measurements and control variables.

In addition to the data being logged above, for the purpose of the latter two commissioning tests (i.e. detailed and final tests) and also for the final control experiments, two output signals (in volt) generated from the two output channels of the MIO16 Data Acquisition card were employed for the function of manually adjusting the firing rate (coal feed and airflow) in the output voltage range of 0 to 10v (in this case, 2v equates to 16.7% of MCR and 10v corresponds to 100% of MCR).

## 5.2 Commissioning Tests on the 3.7MW Chain Grate Stoker Fired Shell Boiler

The purpose of these experiments was to gather information regarding the behaviour of the industrial scale stoker boiler, in particular the level of excess air at different loads and the corresponding pollutant emissions. The information gathered from these tests was used to determine the optimal boiler setting and the associated data was used to train a neural model for the prediction of future pollutant emissions. In parallel to the previous investigation on the chain grate stoker test facility at Casella CRE, similar methods were implemented in these full-scale tests, which manually varied the working load over the whole operating range of the stoker under the commissioning engineer's best practise. In the following Sub-section, the commissioning tests on the industrial stoker will be organised and discussed in three different stages, namely preliminary, detailed and the final tests. It will be worth stating that the first test was to collect information following the plant response under the influence of the existing PID controller, while the latter two were conducted whilst manually altering the firing rate (coal feed and airflow) at different loads in order to identify the optimal boiler setting. Table 5.1 outlines all the commissioning tests conducted on the industrial stoker boiler whilst Figure 5.1 shows the 3.7MW chain grate stoker fired shell boiler located at HMP Garth.

Table 5.1 Commissioning Tests Conducted on the 3.7MW<sub>th</sub> Chain Grate Stoker Fired Shell  
Boiler

Test No.	Description	Test Condition	Coal Type
13	Preliminary commissioning test following gradual load changes under the influence of PID controller	Operator's best practise	Columbian Smalls
14	Detailed commissioning test whilst manually altering the airflow at different load levels	Optimal boiler setting	Columbian Smalls
15	Repeat of <i>Test 14</i>	Optimal boiler setting	Columbian Smalls
16	Repeat of <i>Test 14</i>	Optimal boiler setting	Columbian Smalls
17	Final commissioning test whilst manually altering the airflow at 30%, 60% & 90% of MCR	Optimal boiler setting	Bean coal
18	Final commissioning test whilst manually altering the airflow at 40% & 70% of MCR	Optimal boiler setting	Bean coal
19	Repeat of <i>Test 18</i>	Optimal boiler setting	Bean coal

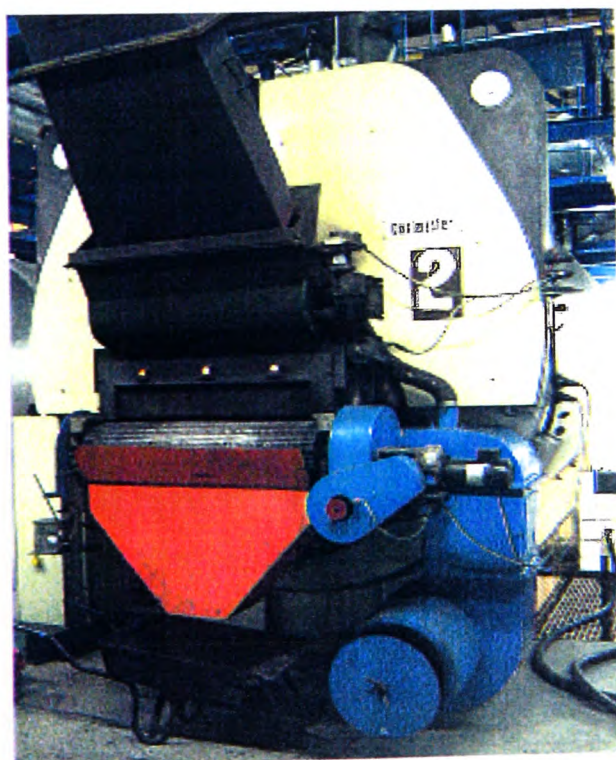


Figure 5.1 The 3.7MW<sub>th</sub> Industrial Scale Stoker located at HMP Garth (Boiler No. 2)

### 5.2.1 Preliminary Commissioning Test

This preliminary commissioning test on “Boiler No. 2” at HMP Garth was conducted within the winter heating seasons so that the full turndown ratio of 6:1 could be achieved. The type of coal burnt in this experiment was a Columbian Smalls grade coal with similar specification to the Columbian type burnt in the earlier test at Casella CRE. The ‘as received basis’ for this coal was as follows: total moisture - 8.4%, ash - 4.6%, Volatile Matter - 34.1% and gross Calorific Value - 29358 kJ/kg. However, the coal analysis for all the other coals can be found in Appendices A and B. The firing rate was defined as a percentage of the MCR of the boiler and was regulated from full turndown at 16.7% MCR to the maximum load of 100% MCR. However, the air:fuel ratio over the operating range was pre-set by the commissioning engineer via the plant PID controller.

Figures 5.2 and 5.3 below show the oxygen concentration in the flue gas, the pollutant emissions, flue gas and hot water temperature data collected from this experiment following gradual load changes at the commissioning engineer’s best practise for Columbian Smalls on the industrial scale stoker boiler. As can be seen in Figure 5.2 (from 16.7% to 50% of MCR), it is quite obvious that this stoker was set up to run at a high excess air level resulting in a high oxygen concentration. The reason for this was to ensure a short fire bed to avoid discharging live fire from the back of the grate hence minimising any operating difficulties at low fire. Furthermore, this relatively high excess air at low to medium fire was also necessary in order to generate sufficient turbulence to promote combustion of the volatile and char and in the mean time provide cooling of the grate.

In contrast, a relatively low excess air level was recorded at higher loads (from 66.7% to 100% of MCR) with the average oxygen level of 10.8% being calculated. On the other hand, the average CO emission for this test is 551ppm (normalised to 6% of oxygen). However, it will be worth mentioning that the hot water temperature at one time exceeded the maximum level of 128°C at full load, triggering the hot water thermostat to cut off the pneumatic coal feeding system and the forced draught fan. The stopped operation of the boiler resulted in a big drop in the flue gas temperature followed by a decreasing hot water temperature (Figure 5.3). The termination of the air supply also resulted in the CO emission rising to over

1500ppm (Figure 5.2). Nevertheless, there was no concern over the level of NO<sub>x</sub> emissions, with an average of 304ppm (normalised to 6% of oxygen) for the entire duration of the experiment.



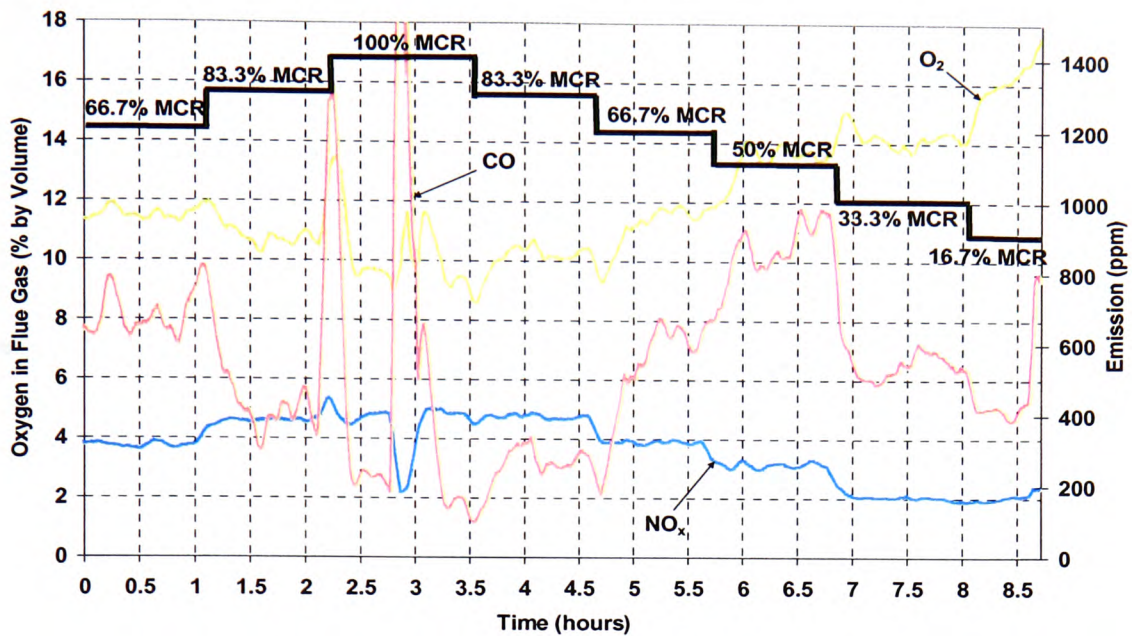


Figure 5.2 NO<sub>x</sub> & CO Emissions and Oxygen Concentration in Exhaust Duct following Gradual Load Changes under Operator's Best Practise for Columbian Smalls on the Industrial Stoker – Test 13

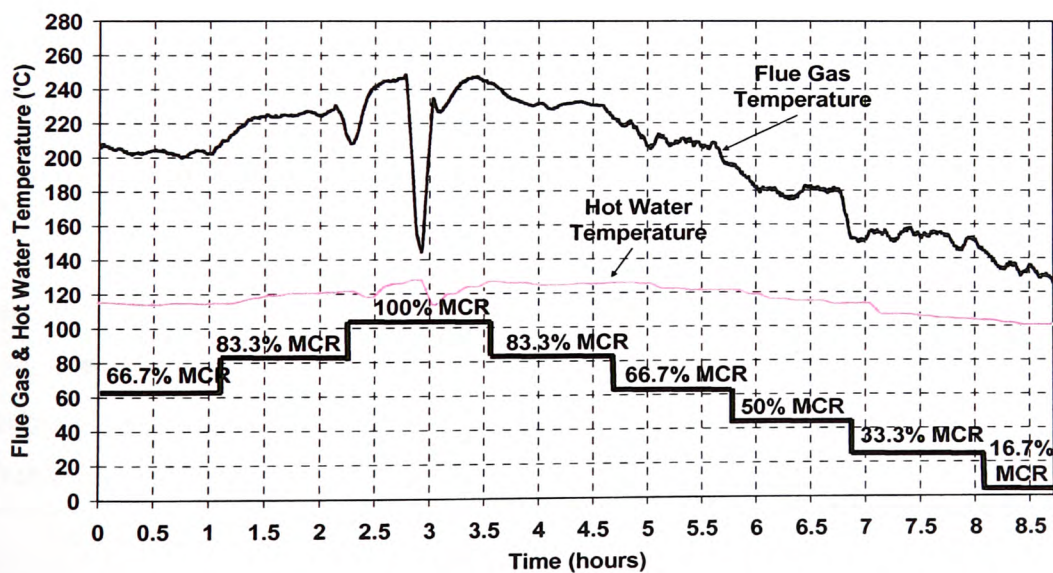


Figure 5.3 Flue Gas & Hot Water Temperature following Gradual Load Changes under Operator's Best Practise for Columbian Smalls on the Industrial Stoker – Test 13



## 5.2.2 Detailed Commissioning Tests

The objective of this experiment was to gather more detailed information about the behaviour of the industrial scale stoker boiler. The method of this test was slightly different to the previous experiment in that it involved manually altering the firing rate and excess air independently. This was felt necessary as the commissioning experiment had highlighted that the excess air was high and therefore the combustion efficiency could be decreased. In addition, it was felt that more information was needed to train the neural network based controller as to the consequences of lowering the excess air too much and the level of excess air that was appropriate.

The coal used for this commissioning test was Columbian Smalls, which was similar to the one used during the preliminary commissioning test. During the experiment, the coal feed and airflow to the plant was manually controlled via the use of the two output signals generated by the MIO16 National Instruments<sup>TM</sup> card, whilst the concentration of the oxygen and CO emission were monitored on-line and the excess air was adjusted from high to low in order to determine the optimal boiler settings. The measurements taken from this experiment were again the pollutant emissions (CO & NO<sub>x</sub> normalised to 6% of oxygen), concentration of oxygen in the flue gas, flue gas and hot water temperature, and firing rate (coal feed and airflow). For the interest of brevity, only the firing rate (coal feed & airflow rate) will be presented along with oxygen concentration and CO emission measurements.

Figures 5.4 to 5.6 show the results obtained from the detailed commissioning tests carried out on “Boiler No. 2” at HMP Garth. As can be seen from these graphs, these tests have covered most of the boiler operating range from full turn down to maximum load. The optimum excess air being determined from the proposed target optimum oxygen band (Table 5.2) together with an acceptable CO level of below 500ppm.

Table 5.2 Target Oxygen Band at Different Range of Firing Rate in Percentage of MCR

Range of Firing Rate in % of MCR	Proposed Target Oxygen Band
(Full Turn Down) 16.67% MCR to 35% MCR	13% to 16%
36% MCR to 50% MCR	11% to 13%
51% MCR to 70% MCR	9% to 11%
71% MCR to 100% MCR	7% to 9%

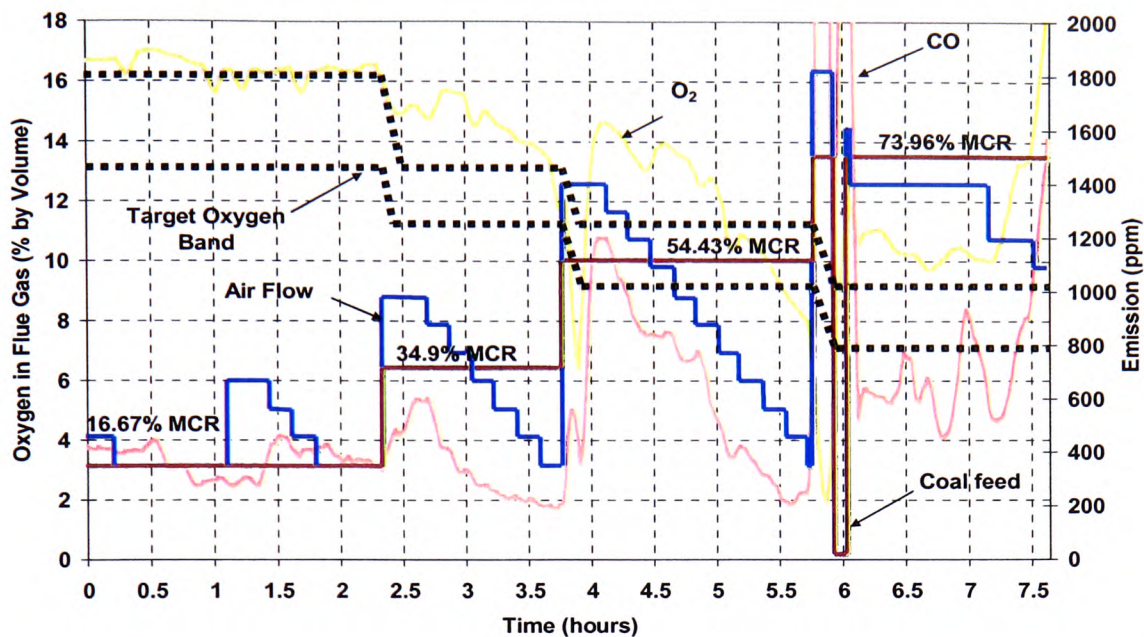


Figure 5.4 CO Emission and Oxygen in Exhaust Duct Whilst Manually Altering the Airflow at Different Load Levels – *Test 14*

Figure 5.4 shows that the majority of the recorded oxygen concentration fell outside the target oxygen band even though the airflow was reduced to a minimum. Perhaps due to a lower demand for hot water when this test was being carried out, the hot water temperature at 73.96% of MCR went beyond the maximum limit of 128°C thus triggering the thermostat to shut down the boiler. This caused an overshoot of CO to more than 2000ppm whilst the oxygen level increased to more than 12%. In addition, the oxygen concentration as well as the CO emission increased to more than 18% and 1600ppm respectively just before the end of the test which probably resulted from insufficient coal being supplied to the stoker (the coal supply ran out). The excess air and CO being high at the same time was contradictory to normal trends but this was perhaps due to the airflow being reduced to 52% of MCR, hence reducing the turbulence and combustion intensity in the bed and causing incomplete mixing between the air and fuel. As a result, the excess air could not properly be used to complete combustion of the coal. In addition, the dynamic behaviour in the fire bed for the boiler of this type was very difficult to capture and identify.

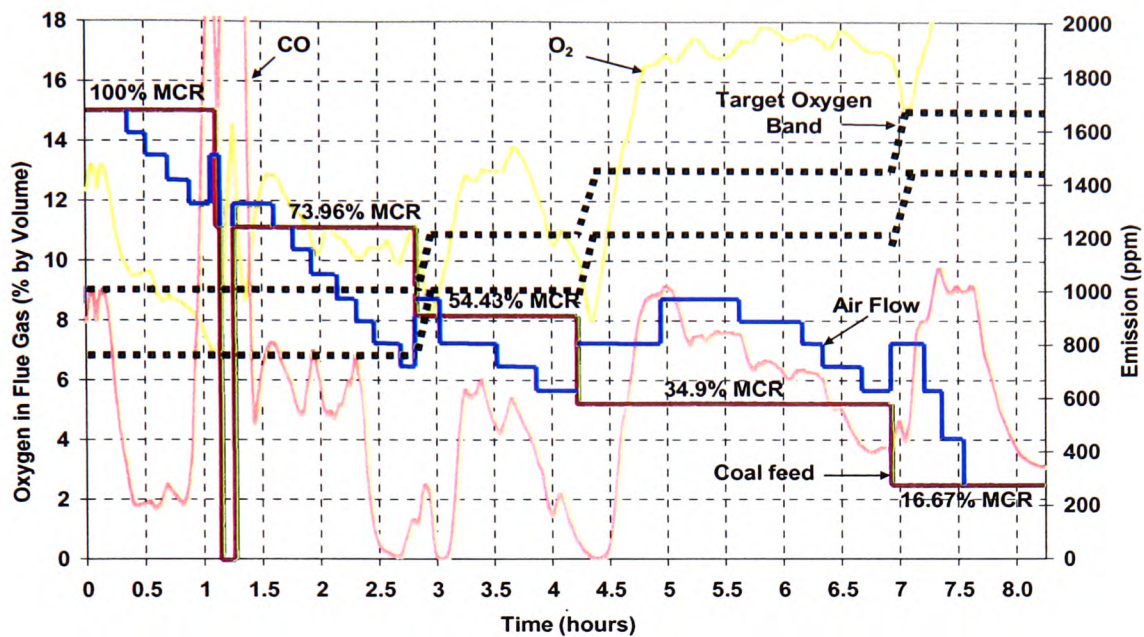


Figure 5.5 CO Emission and Oxygen in Exhaust Duct Whilst Manually Altering the Airflow at Different Load Levels – *Test 15*

As for *Test 15* (Figure 5.5), the airflow adjustment range was reduced so that the identification work for the optimal air:fuel ratio settings could be made easier and quicker. Nevertheless, most of the oxygen levels for this test still fell outside the target oxygen band especially at lower firing rates whilst the corresponding CO emission fluctuated between 0 and 1000ppm. Again, due to low hot water demand, the boiler was automatically turned off as the hot water temperature exceeded the maximum limit of 128°C (approximately after 1 hour, Figure 5.5). In addition, there was air starvation just before the airflow was reduced to its lowest adjustment limit at maximum load (100% of MCR) and this caused the CO emission to increase beyond 2000ppm followed by the overshoot of 4500ppm when the boiler was shut down, correspondingly the oxygen level climbed to 14% in the flue gas. Furthermore, live fire was noticed at the end of 73.96% of MCR (when the airflow was decreased to a minimum adjustment range) which according to Gunn and Horton (1989), even when excess oxygen was present (as shown in Figure 5.5 where the oxygen was around 11% which can be considered high), incompletely burned coal could still be discharged from the grate and under such conditions, a further reduction of air would only further exacerbate the effect.



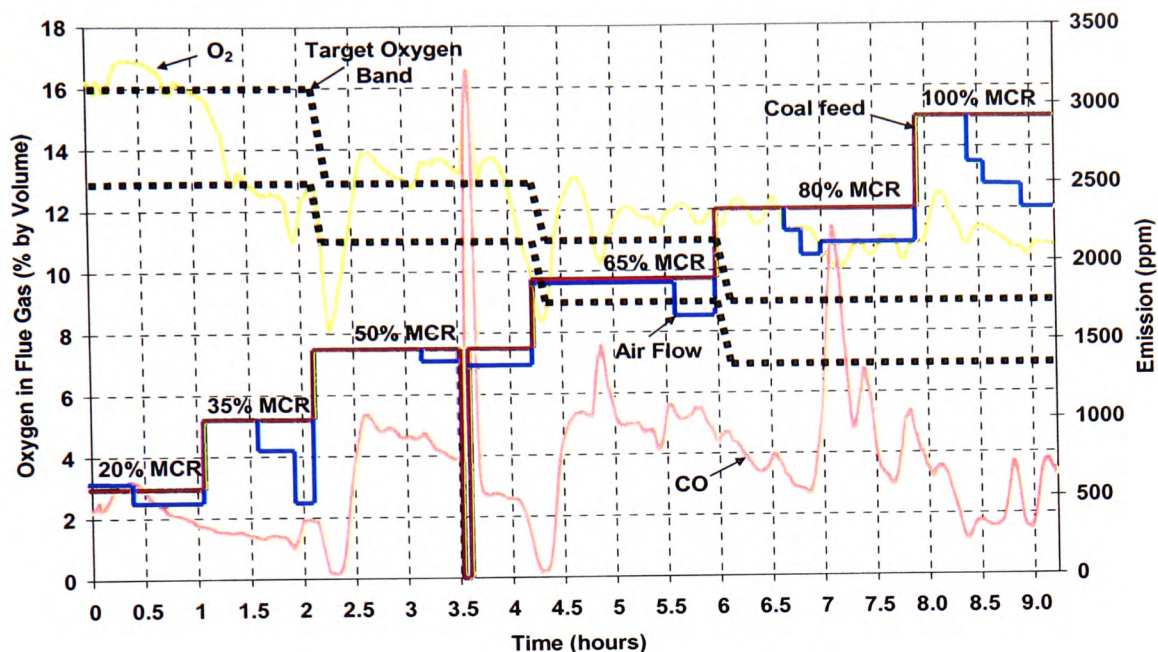


Figure 5.6 CO Emission and Oxygen in Exhaust Duct Whilst Manually Altering the Airflow at Different Load Levels – *Test 16*

The experimental method for *Test 16* (Figure 5.6) made the airflow adjustment range narrower than *Test 15* and in addition, a longer time was allowed for transient boiler behaviour to elapse. Significant improvements can be observed from these adjustments in that most of the oxygen level fell closer to the target oxygen band except at high load due perhaps to the narrower airflow adjustment range. Therefore it is probably valid to assume that most of the oxygen readings fell away from the target oxygen band during *Tests 14* and *15* because not enough time was allowed for steady state conditions to occur. The CO emissions at steady state were also lower as compared to the previous tests. However, it will be worth explaining that the boiler operation was stopped for few minutes when running at 50% of MCR in order to remove slag built up near to the refractory arch. This caused the CO emission to increase beyond 3000ppm and the oxygen level to increase to 16% in the flue gas. By careful observation, there was a drop in the oxygen level at 80% of MCR followed by an obvious overshoot of CO emission to more than 2000ppm. This can probably be explained by the fact that the airflow was decreased below that necessary to complete the combustion of the coal.

Following the detailed commissioning tests carried out to identify the optimal settings of the industrial scale stoker boiler, it has been found that an important reason for the differences between these three days of testing was due to an inconsistency in the coal supply. From visual observation through the inspection porthole located at the rear end of the boiler and also through the storage bunker where the fresh coal was being stored which sat on top of the coal feeding system. It was found that big lumps of coal were dropped from the coal feeder onto the grate from time to time. This could affect stable combustion, as the air supplied to the grate could not be used for proper combustion of the large lumps of coal (i.e. the air supplied from underneath the grate could not penetrate the big lumps of coal and thus left as excess air), the consequence was that excessive air was being supplied to the boiler and resulted in the higher concentration of oxygen being recorded. This was probably the reason why high excess air at higher loads was needed as the possibility of big lumps of coal from the feeder when running at elevated loads was greater as compared to lower loads.

In addition, live fire that was seen at the end of the grate when the air supply was reduced to a minimum in order to bring the oxygen level within the target oxygen band. This was also not a good sign as this would lower the boiler efficiency and also live fire could damage the automatic ash removal system and thus should be avoided. Another point that would be worth making is that the automatic ash removal system operated every 34 minutes for a duration of 4 minutes and caused an 'artificial' drop in the oxygen level (in the range of 1 to 2%) and hence increased the CO emission. Due to these problems it was felt that further commissioning work was required so that an 'ideal' commissioning data set could be obtained to develop the final neural network based system to efficiently control the industrial scale stoker boiler.

### 5.2.3 Final Commissioning Tests

The objective of this final set of commissioning test was to finalise the settings required for the optimum excess air at different load levels. This final test was again conducted on “Boiler No. 2”. The coal used for this commissioning test was a Bean coal (5-22mm), which was different from the coal used for the other tests conducted at HMP Garth. As with the detailed commissioning test, the coal feed and airflow to the plant was manually controlled through the output channels of the National Instruments<sup>TM</sup> card which replaced the existing plant PID controller. In addition, the concentration of oxygen and the CO emissions were monitored on-line and the air supply was adjusted from high to low in order to determine the optimal boiler settings. This should then allow the neural network to learn and mimic the optimal settings and also the corresponding oxygen and CO emission for the final NNBC implementation. It will be worth mentioning that for the interest of final test with the NNBC, the operating ranges at different load levels as considered in the two previous tests were reduced and were mainly concentrated on two firing rates at 40% and 70% of MCR, as these operating ranges covered the two most essential boiler operating levels of low and high load. The following Figures and associated text describes the results obtained from the final commissioning test.

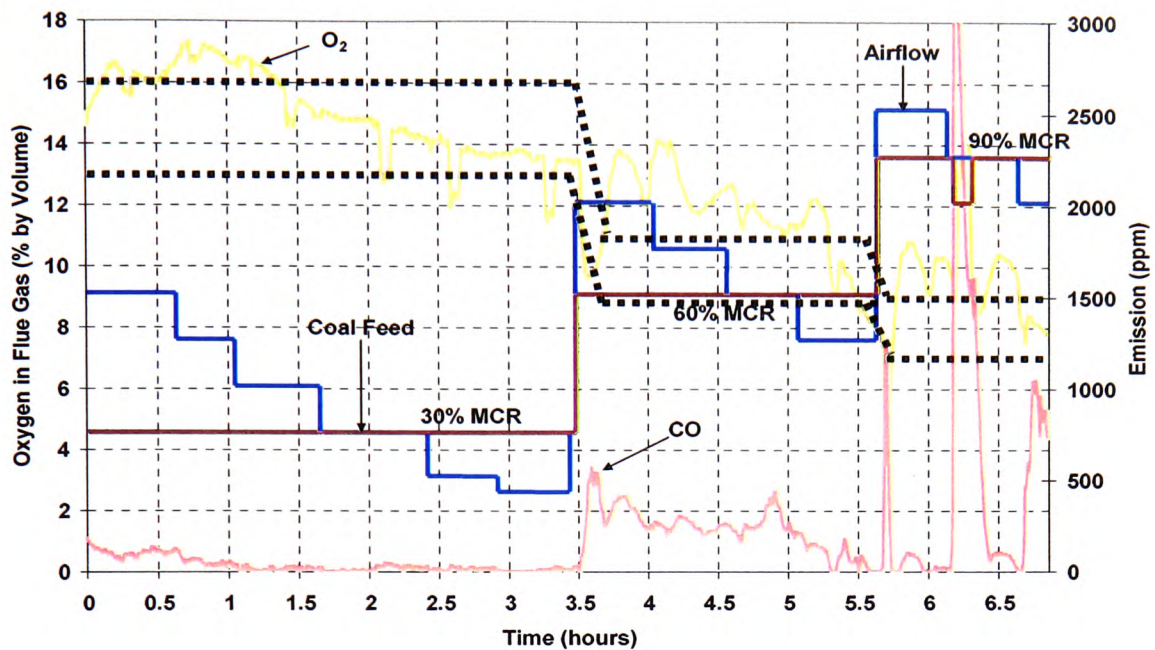


Figure 5.7 CO Emission and Oxygen in Exhaust Duct Whilst Manually Altering the Airflow at 30%, 60% and 90% of MCR – *Test 17*

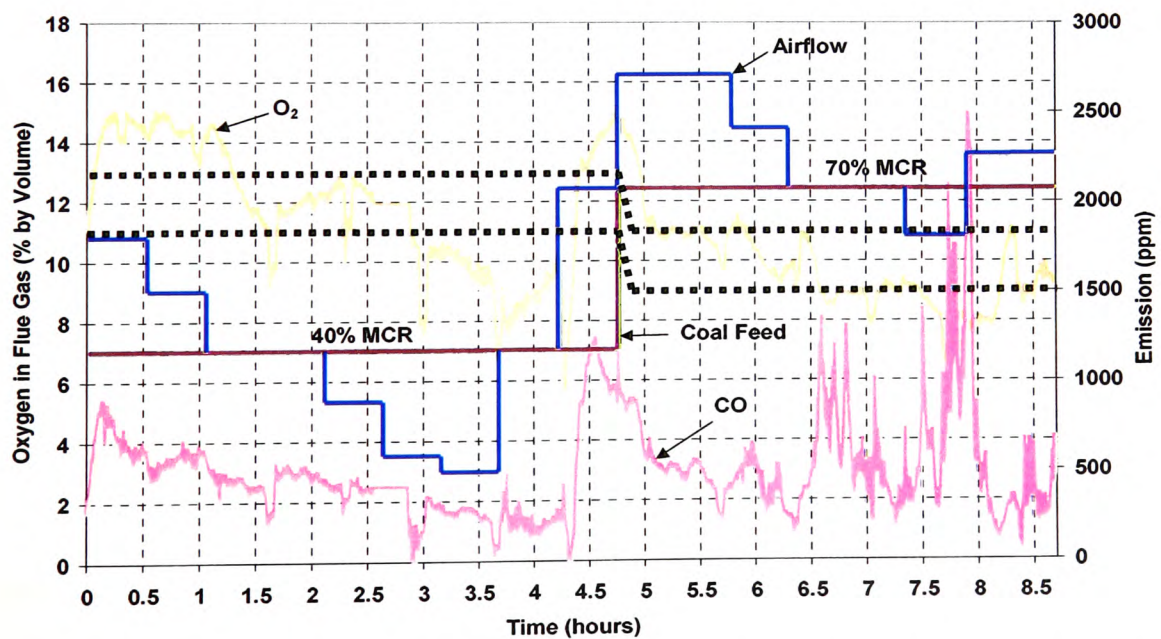


Figure 5.8 CO Emission and Oxygen in Exhaust Duct Whilst Manually Altering the Airflow at 40% and 70% of MCR – *Test 18*



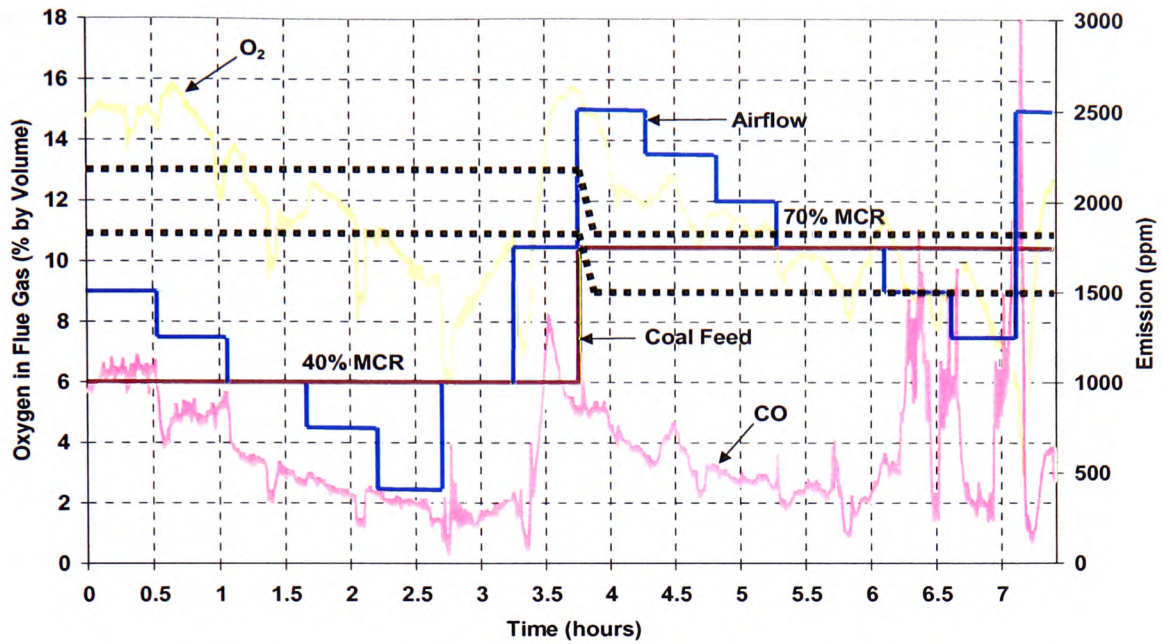


Figure 5.9 CO Emission and Oxygen in Exhaust Duct Whilst Manually Altering the Airflow at 40% and 70% of MCR – *Test 19*

Table 5.3 Final Target Optimum Oxygen Band from Full Turn Down to Maximum Load in Percentage of MCR

Load Indication in % of MCR	Final Target Oxygen Band
16.7% of MCR	13% to 16%
33.3% of MCR	13% to 16%
50.0% of MCR	11% to 13%
66.7% of MCR	9% to 11%
83.3% of MCR	7% to 9%
100% of MCR	7% to 9%

Figures 5.7 to 5.9 show the results obtained following the final commissioning test to finalise the optimum excess air settings required at different load levels. The test operating range for *Tests 18* and *19* (Figures 5.8 and 5.9) was identical except *Test 17* (Figure 5.7) and the aim was to examine the repeatability of these tests following the load change at the indicated



firing rate. As with the previous detailed commissioning test, the airflow for this test was set to a maximum and then gradually decreased to a minimum so that it covered a high to low excess air and the optimum level was determined based on the final target optimum oxygen band (Table 5.3) together with an acceptable CO level of below 500ppm. By careful observation, there were similarities among the three graphs in that significant drops in the oxygen level at even intervals can be noticed which was again due to the automatic ash removing system. However, this issue will be taken into consideration when training the neural model for the final NNBC implementation so that the controller would be able to cope with this disturbance. Nevertheless, most of the oxygen concentrations for these three days of testing were within the target band when the airflow was adjusted to appropriate levels with respect to their firing rate.

Another similarity that can be observed from the graphs was the overshoots of CO when the airflow was brought down to a minimum at higher operating loads. This can also be observed from the excess air level where significant drops in oxygen concentration (except Figure 5.7) can be seen in Figures 5.8 and 5.9 respectively. This was due partly to the ash removal system sucking air from the boiler and also to the low excess air available. The average CO emissions for *Tests 17* and *18* were below 500ppm while the average for *Test 19* was 601ppm. However, this level is still acceptable and it must be stated here that smoking only happened when the CO level exceeded 2000ppm.

### 5.3 Summary

Following the series of commissioning tests conducted at the HMP Garth, it can be concluded that these experiments have successfully gathered information regarding the behaviour and response of the industrial stoker. The objective of these tests was to determine the optimal settings in term of the excess air for a particular load and in the mean time, to improve the overall boiler efficiency and maintain pollutant emissions below future medium term legislation. This knowledge is essential for the purpose of training the NNBC to operate the industrial scale stoker boiler efficiently at different load levels to meet the demand required.

## Chapter 6 Development of the Neural Network Based Controller (NNBC)

This Chapter describes the development of the neural network based controller (NNBC). It involves two distinct areas, namely the fundamental concept of the control strategy, and the overall NNBC development. The basic idea of this NNBC was to provide the minimum airflow required for combustion while maintaining pollutant emissions below future medium term legislation, and in so doing improving the combustion efficiency. The development of the controller included software development in the MATLAB<sup>TM</sup> and LabVIEW<sup>TM</sup> computing environments, which is explained with help of a schematic block diagram in addition to the interface details between the NNBC and the existing plant, including the calibration of the voltage generated by the National Instruments<sup>TM</sup> card to induce a certain percentage firing rate. Moreover, the NNBC development also required careful selection of training data from the final commissioning tests (Section 5.2.3). Upon completion of the development phase, the NNBC was commissioned and its performance evaluated before the final control test on the industrial chain grate stoker fired shell boilers located at HMP Garth in Lancashire.

### 6.1 The Basic Concept of the Control Strategy

This Section provides the elemental concept of the control strategy before discussing the software development where the essential part of the NNBC development is discussed. From the literature review (Chapter 2), it can be seen that the combustion of lump coal on a grate is a complex process and the dynamics of the plant are difficult to ascertain from a conventional control point of view. Therefore, the control strategy implemented here was based on the data collected during the commissioning tests for optimal excess air level settings. The gathered information was used to train artificial neural networks to mimic these settings to ensure stable and efficient combustion whilst minimising pollutant emissions based on future predictions of the combustion gases. The following Sub-Sections review the background of lump coal combustion on chain grates followed by the target areas where heat

losses can be minimised before detailing the control strategy adopted for the optimal operation of the stoker boiler plant.

### 6.1.1 Background

As has already been discussed in Chapter 2, the combustion of lump coal on moving grates is an enormously complex one. There are hundreds of reactions occurring simultaneously involving a large number of chemical species which can generate pollutant emissions if the governing factors are not appropriately controlled. Therefore, it is vital to maintain stable combustion conditions on the bed in order to achieve high efficiency whilst minimising pollutant emissions. This can be achieved by the correct regulation of the coal feed and airflow to meet the load demand. In addition, adequate time must be allowed for a high degree of carbon burn out and also to ensure near complete combustion of the volatile matter. The latter requirement is usually met by providing adequate excess air for better mixing of the reacting substances with oxygen since ultimate stoichiometric conditions are difficult to reach at the appropriate point and also by maintaining an adequate boiler temperature. Additionally, adequate excess air is needed to provide turbulence. It is also equally important for the primary air to meet the requirements of the fuel bed at different loads i.e. the fire bed at full load is longer than at full turn down and higher excess air is required at lower load and vice versa at higher load. However, the excess air must be kept to a minimum to ensure the minimum sensible heat loss in the flue gas whilst maintaining satisfactory combustion, as the sensible heat loss in the flue gas increases with the excess air and the efficiency reduces in proportion to the excess air level.

### 6.1.2 Target Areas where Heat Losses can be Minimised

To optimise and improve the operation of the stoker boiler plant, it is necessary to understand the areas where heat losses are most likely to occur. The major controllable heat losses and hence the target areas for improvements fall into three main areas; heat loss in dry flue gasses, heat loss to carbon monoxide (CO) and heat loss to combustibles in the ash [Good

Practice Guide 30, 1999]. For sensible heat loss in the flue gas, the major influencing factors are the exit flue gas temperature and the excess air level that exists. Therefore, correct combustion is essential in order to minimise the heat loss and these include better fuel preparation and stoking practices and improved control of both the undergrate and the overgrate combustion air. As for heat loss to CO, the level of CO can be kept to a practical minimum if less dark smoke is produced during combustion. Factors that cause the smoke to emerge are insufficient combustion air, inadequate turbulence for air/fuel mixing and/or the ingress of cold air 'freezing' the combustion reaction. However, the heat loss is relatively small if it is measured in terms of the non-conversion of carbon into carbon dioxide but under these circumstances the boiler performance is unfavourably affected by the rapid fouling of heat transfer surfaces. For remedial measures the correct level of excess air must be provided in addition to enhancing turbulence on the fire bed to achieve better air/fuel combination. Finally, typical heat loss to carbon in the ash generally varies from 2 to 3% of efficiency losses and can be exacerbated should combustion air starvation were to prevail [Good Practice Guide 88, 2000]. This is probably caused by; poor air distribution under the grate; inappropriately thick fuel bed and/or uneven fuel distribution resulting from improper stoking practices. Therefore, correct regulation and optimum set-up of the air/fuel ratio is important throughout the entire load range in addition to providing the best stoking practices.

### 6.1.3 The Control Strategy

Based on the target areas where heat losses can be minimised, it is very obvious to state that the first requirement to optimise and improve the operation of the stoker boiler plant would be to provide the plant with the optimum settings of excess air to match the coal feed rates, hence improving the boiler efficiency and reducing the pollutant emissions. Following the commissioning tests carried out on the industrial stoker boiler, the initial near optimum settings of coal feed and airflow have been identified along with the associated oxygen target band at different loads (details of the commissioning results can be found in Section 5.2). Therefore, good and stable combustion conditions will occur if sufficient air is supplied to meet the coal feed. This in turn will maintain carbon monoxide at a minimum for steady state combustion. However, it will be worth pointing out that during both transient and steady state

conditions, it is important to operate the boiler plant as efficiently as possible in order to minimise the possibility of boiler fouling, since most of the heat transfer is by radiation to the combustion chamber walls with the rest being transferred in the reversal chamber and the smoke tube by convection. Furthermore, a smooth change from one state to another is vital to prevent unnecessary losses in unburned carbon and unwanted transient CO emissions.

Once the coal feed and airflow has been brought to the new settings, a so-called 'oxygen trimming' technique which monitored the oxygen concentration in the flue gas followed by adjusting the combustion air in accordance to the fire bed demand can be carried out almost instantly (after each control loop) unless if there was a large load change, when staging of the airflow and coal feed will be needed which according to Gunn (1982) and Chong (1999), the adjustment of air must lead the coal feed on load increase and vice versa on load decrease as a means to ensure good carbon burnout and to provide better transient combustion. These staging sequences can be referred to as 'air leading the coal feed' on load increase and 'coal leading the air feed' on load decrease respectively.

As has already been discussed in the literature, the oxygen trimming technique to ensure the minimum excess air level (hence maximising the efficiency) without negatively disturbing the pollutant emissions has been practically applied on oil and gas fired burners [Gunn and Horton, 1989]. However, due to factors such as longer ignition time, incomplete mixing between air and fuel and hysteresis of lump coal firing on grates could lead to incompletely burned coal if the air is reduced [Gunn and Horton, 1989]. Conversely, this technique has formed an essential part of the current research work for the reason that the oxygen reading with the aid of AI and other complimentary information (CO reading) has enhanced the applicability of this method to reduce the excess air level on lump coal firing on the grates.

Fundamentally, this method used AI techniques to monitor current and past values of the coal feed and airflow, along with the present as well as the past oxygen and CO readings to predict the values of these combustion products into future. The adjustment of the initial air settings (primary air) was dependent on the difference between the predicted oxygen and CO with the pre-set target values. In this case, the target oxygen bands were reliant upon the

optimum range of oxygen concentration in the flue gas at different loads (as obtained from the commissioning tests) and these were 7 to 9% at high fire, 9 to 11% at medium fire, 11 to 13% at intermediate medium fire and 13 to 16% at low fire, and these correspond to excess air levels of 45% to 65%, 65 to 100%, 100 to 150% and 150 to 280% respectively together with an acceptable target limit for CO emission of below 1000ppm (after normalising to 6% of oxygen).

Having addressed the oxygen trimming technique to monitor the amount of excess air level in the fire bed, the next concern would be the impact of the automatic ash removal system on the overall control approach. This system, which operates every 34 minutes for a duration of 4 minutes removes some of the excess air in the boiler resulting in a temporary drop in the oxygen concentration in the flue gas (1 to 2%) in addition to increasing the CO emissions. Under such conditions, the implementation of oxygen trimming under a control loop interval of 3 minutes would increase the excess air (if the oxygen level drops below the target band) to compensate for the perceived insufficient air in the fire bed. However, with the commissioning data gathered to identify the optimum boiler settings, it is believed that the trained neural models would mimic the expert operator's knowledge to cope with the disturbance caused by the automatic ash removal system.

## 6.2 The Development of the Neural Network Based Controller (NNBC)

This Section describes the detailed development of the Neural Network Based Controller (NNBC) in the MATLAB<sup>TM</sup> and LabVIEW<sup>TM</sup> computing environments; the interface configuration between the NNBC and the existing plant interface unit; the calibration settings of coal feed, airflow and K-type thermocouple and finally the selection of the commissioning data for training the neural models. The feed-forward Multi-Layered Perceptron (MLP) network of ARX structure with an error back-propagation learning algorithm has been used. The trained models were subsequently integrated into the overall control strategy to optimise the industrial stoker boiler, as the bench mark of the NNBC was to attain stable combustion

and to achieve the lowest possible level of excess air in order to improve the overall efficiency and in so doing reduce the pollutant emissions. The following Sub-sections deal with the detailed description of the overall control approach as a whole with the help of a schematic block diagram followed by the interface configuration and calibration setting and finally, the selection of the commissioning data for neural network training.

### 6.2.1 The Overall Controller Approach

Figure 6.1 shows a schematic diagram of the neural network based controller (NNBC) for on-line control of the commercial chain grate stoker fired shell boiler located at HMP Garth.

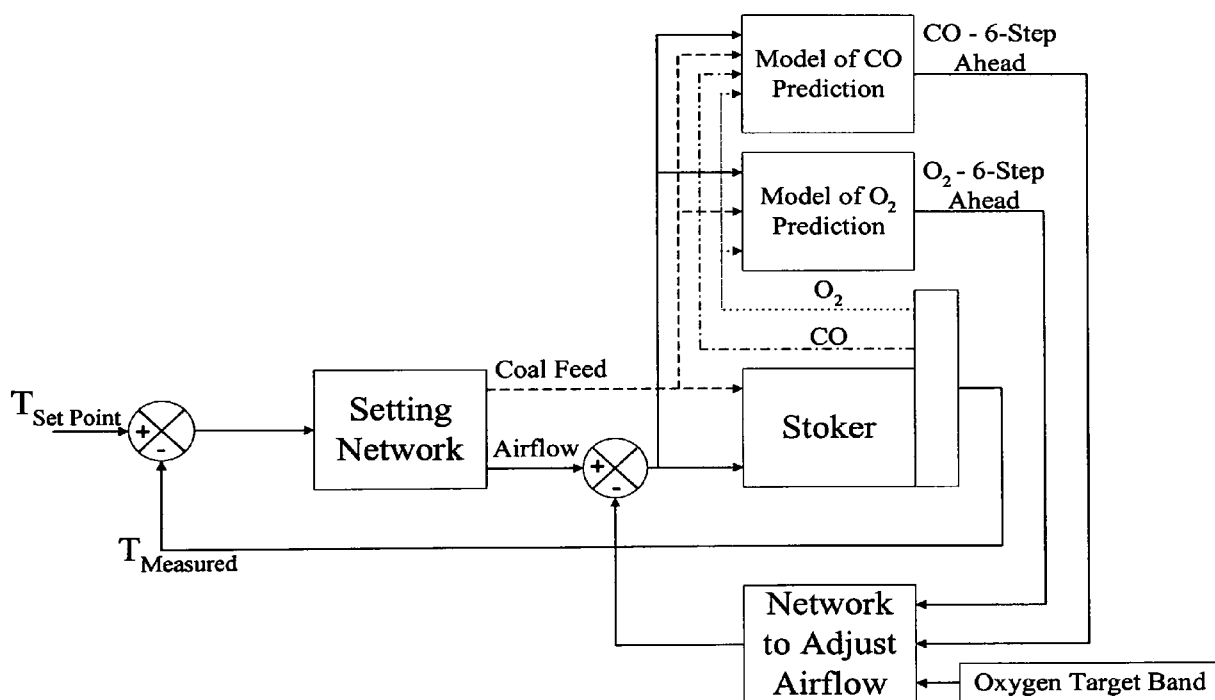


Figure 6.1 Schematic of the Overall NNBC for the Chain Grate Stoker Fired Shell Boiler

Fundamentally, the NNBC identified changes in the load demand (hot water temperature in this case) and through the setting network based on rules that were constructed using information drawn from the commissioning tests, the corresponding optimum settings of coal feed and airflow were delivered to match the load required. Once the coal feed and airflow

were brought to the new settings, the second part of the NNBC was implemented if the load change was small, to fine tune the primary airflow for the purpose of optimising the combustion process on the grate. The so-called oxygen trimming method incorporated with the AI technique was implemented to reduce or increase the primary air in order to make sure that the excess air level fell within the oxygen target band and the CO emissions were within an acceptable limit. Instead of using the actual concentration of oxygen in the flue gas from the flue gas analyser for comparison with the target values, the predicted value that was produced by the neural models at 6-step into future was used to evaluate the error. This error was then fed into the adjusting network for appropriate airflow adjustment to maintain the optimum air/fuel ratio.

For the purpose of the control experiments (the details of which will be discussed in Chapter 7), the description of this diagram can be divided into two different aspects. The first aspect is concerned with the combustion optimisation test whilst the second is the hot water temperature control test. During the first set of control experiments, constant loads of 40%, 60% & 70% of MCR were considered as input parameters to the setting network. The network was then requested to provide the corresponding firing rate with an appropriate air/fuel ratio, meanwhile the present as well as the past values of coal feed and airflow together with the output from the combustion products, in terms of current and previous oxygen and CO readings, were fed as input parameters to the neural models predicting oxygen and CO six steps into the future.

The neural models trained with the commissioning data (Section 5.2.3) were then used to predict future combustion product and pollutant emission and allowing time for remediation before problems actually occurred within a 3-minute time horizon. The estimated oxygen and CO were then fed to the adjusting network for appropriate airflow adjustment to consistently maintain an optimum air/fuel ratio. It will be worth mentioning here that the NNBC was configured so that the network for airflow adjustment would only be activated if the oxygen level fell outside the target band and would take no action within the target band with any action being based on the predicted values. The target oxygen band for this particular coal type was dependent on the firing rate and from the information gathered from the



commissioning test (Section 5.2.3), the target oxygen band shown in Table 5.3 was adopted and used by the adjusting network.

The second part of the control experiment dealt with the water temperature control test. Based on the temperature error, the setting network then provided the coal feed and airflow to the boiler with the optimum air/fuel ratio. When the boiler achieved the set point temperature, as with the combustion optimisation test, combustion air optimisation was undertaken by the neural model to fine tune the excess air level in the fire bed. The NNBC was configured in the MATLAB<sup>TM</sup> computing language together with the suitable communication accessories that enabled the NNBC to interface with the plant interface unit, the details of which is outlined in the following Sub-Section, with the detailed description of the NNBC program being in Appendices D and E.

### 6.2.2 NNBC Signal Interface Configuration

Figure 6.2 shows a schematic diagram of the overall data interface arrangement to gather sensor data and to control the coal feed rate and airflow. It will be worth mentioning here that only one analogue signal was used to control the coal feed rate as the grate speed has been calibrated by the commissioning engineers to match the rotary valve speed to give an appropriate bed height according to the firing rate. A Pentium 3 550MHz PC fitted with a MIO16 National Instruments<sup>TM</sup> data acquisition card running the corresponding LabVIEW<sup>TM</sup> software acquired and sent input and output signals to and from the PC and the plant interface unit (Figure 6.2). For the purpose of communication, a stand-alone signal interface junction box which acted as a “middleman” was developed so that the input variables acquired from the boiler plant and the output signals generated by the National Instruments<sup>TM</sup> card could be correctly interfaced between the PC and the plant. To connect the data acquisition card mounted on the PC with the stand-alone signals interface junction box, a 50-way ribbon cable fitted with polarised sockets at both ends was used to transmit signals to and from the two devices. Then, several co-axial cables were used to convey signals in both directions between the “middleman” and the plant interface unit.

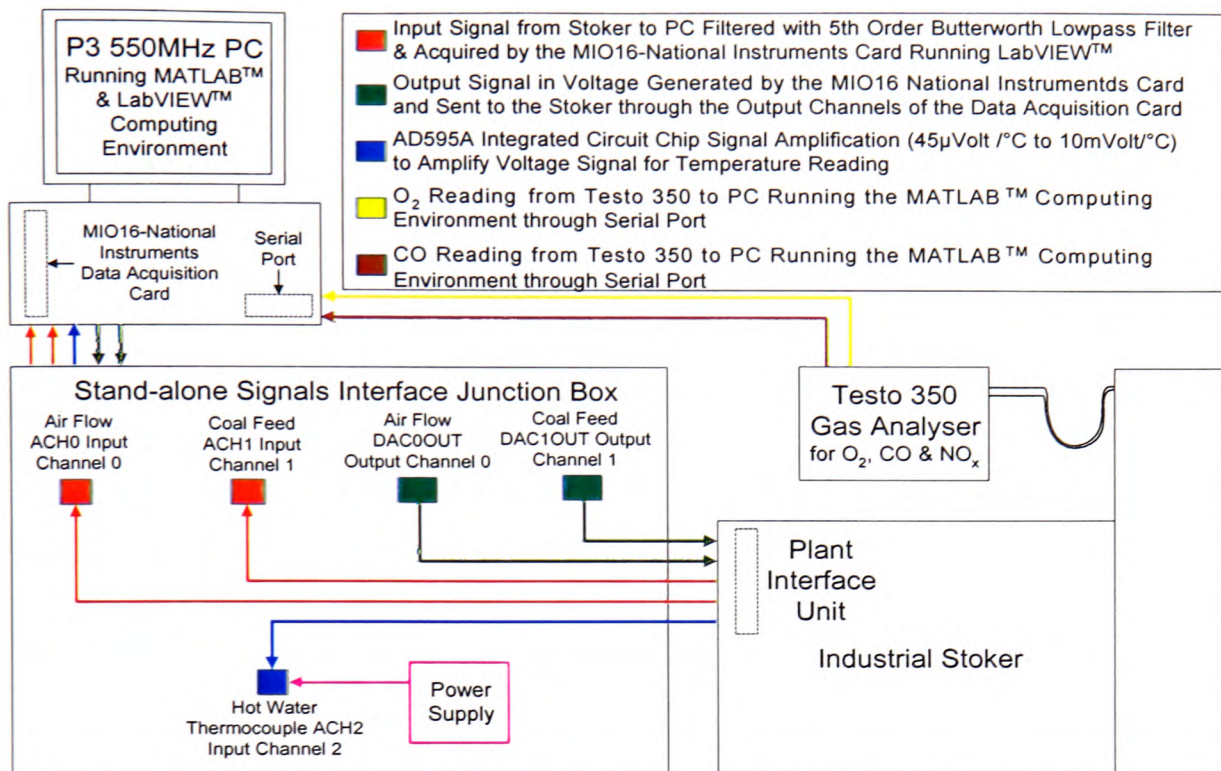


Figure 6.2 Schematic of the Overall Signal Interface Configuration for Part of the NNBC Development

For firing rate acquisition and for noise attenuation, the input analogue voltage signals were filtered by a fifth order Butterworth lowpass filter located inside the junction box before being acquired by the data acquisition card. For hot water temperature measurement, a conditioning circuit was also required for the K-type thermocouple for amplification of the weak signal by an AD595A integrated circuit chip. The sampling period to acquire all the input variables was 30 seconds. The output analogue voltage signals generated by the National Instruments™ card were in the range of 0 to 10V. For the purpose of the control experiment, the output signals were sent to the plant interface unit every 3 minutes, to coincide with cycle time for the generation of a control action.

For flue gas measurement, a Testo 350 portable flue gas analyser was used to measure the oxygen concentration, carbon monoxide and nitrogen oxides. It will be worth pointing out that during the commissioning tests, a separate PC running a Windows based 'Testo

ComLight' software that came with the analyser was used for data logging. For the control experiment, these measurements were acquired by a single PC collecting the data and controlling the stoker. The flue gas measurements were communicated from the Testo 350 to the PC through a serial port interface, with the information being extracted by MATLAB<sup>TM</sup> through the Standard Commands for Programmable Instruments (SCPI) language [MATLAB<sup>TM</sup> External Interfaces, 2000]. The sampling period for the flue gas measurements was 30 seconds so that all acquired data was synchronised. Details of the serial port interface are outlined in the overall NNBC programme and can be found in Appendices D and E.

### 6.2.3 Calibration of the Coal Feed, Airflow and K-Type Thermocouple

This Sub-Section presents the calibration of the coal feed, airflow and thermocouple signals to the corresponding units in percentage of MCR and degree Celsius for use in the NNBC. The output voltage signals generated by the National Instruments<sup>TM</sup> card were calibrated to represent the coal feed and airflow rate as a percentage of MCR, whilst the K-type thermocouple voltage signal was calibrated to a temperature reading in degree Celsius for hot water temperature measurement. The calibration of the coal feed and airflow are shown in Figures 6.3 and 6.4. For the coal feed rate calibration there was a linear relationship between the voltage signal and the resultant firing rate with 2V equating to 16.7% of MCR and 10V equating to 100% of MCR (Figure 6.3). Figure 6.4 shows a non-linear profiler voltage existed for the FD fan speed.

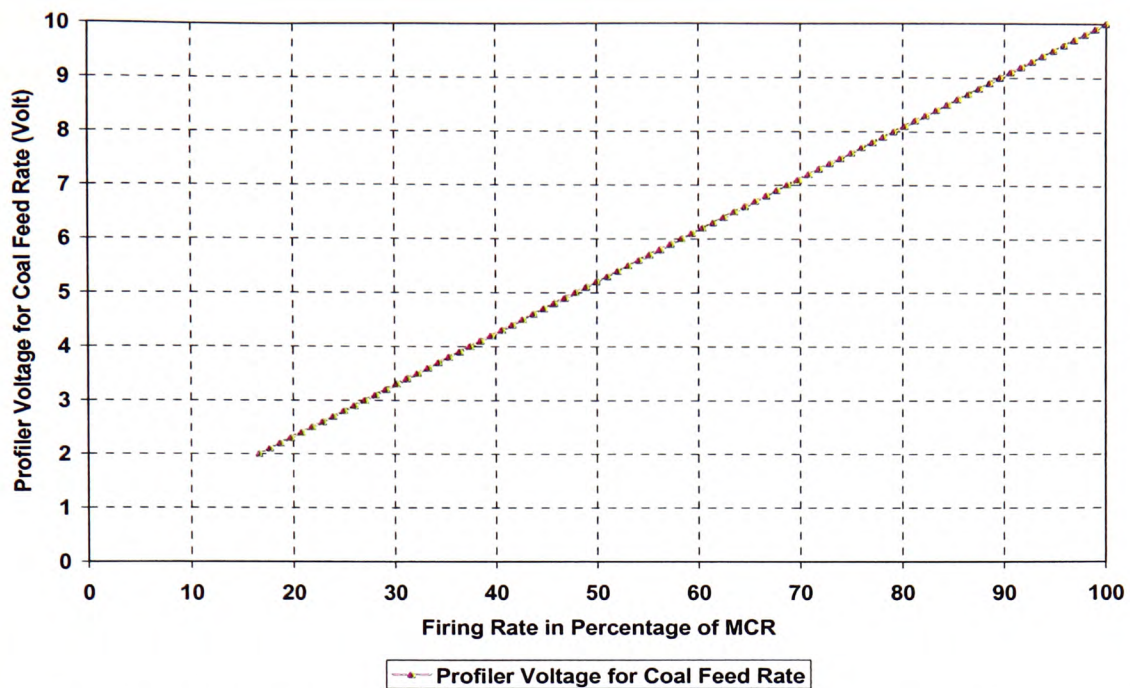


Figure 6.3 Calibration Setting between the Coal Feed Rate (in terms of Percentage of MCR) and the Signal in Voltage for the Boiler Plant in Garth

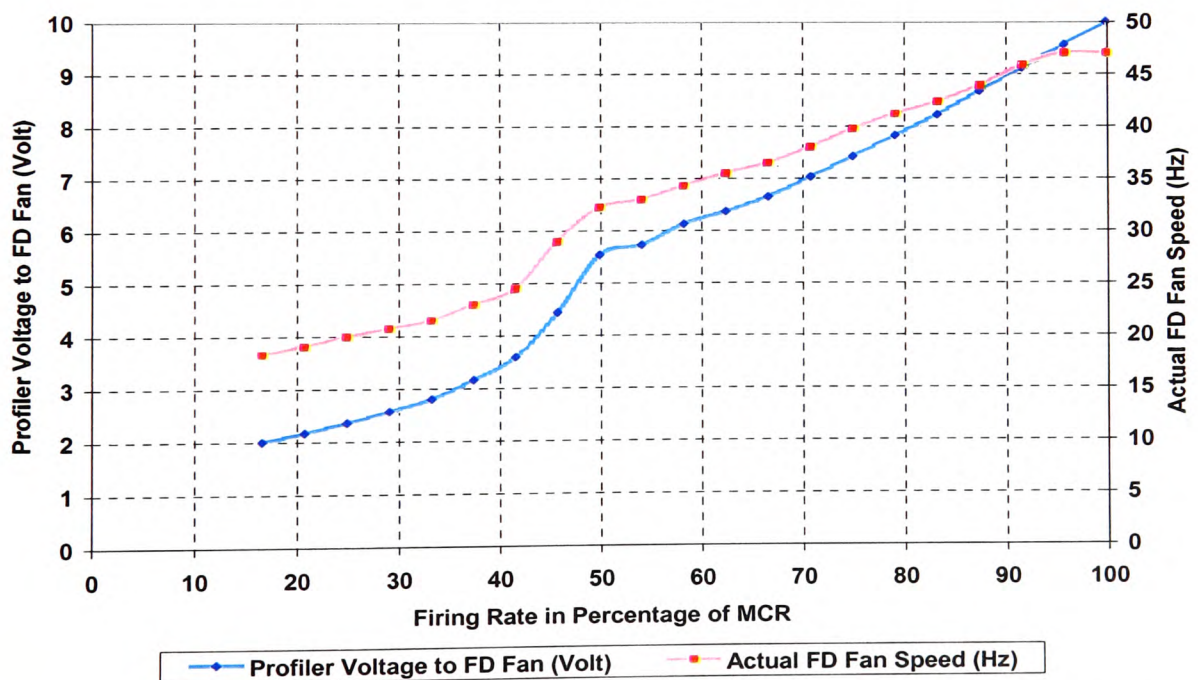


Figure 6.4 Calibration Setting between the Forced Draft Fan Speed (in terms of Percentage of MCR) and the Signal in Voltage for the Boiler Plant in Garth



Figure 6.5 shows the calibration of the K-type thermocouple used to measure the hot water temperature during the control experiment. The K-type thermocouple connected to a screened thermocouple cable was positioned in the outgoing pressurised hot water pipe with the reading being used by the NNBC for comparison with the set point temperature and the corresponding control action. It will be worth stating that in order to allow the NNBC to be able to function, the PC used the Microsoft Excel spreadsheet programme which acted as a Dynamic Data Exchange (DDE) server.

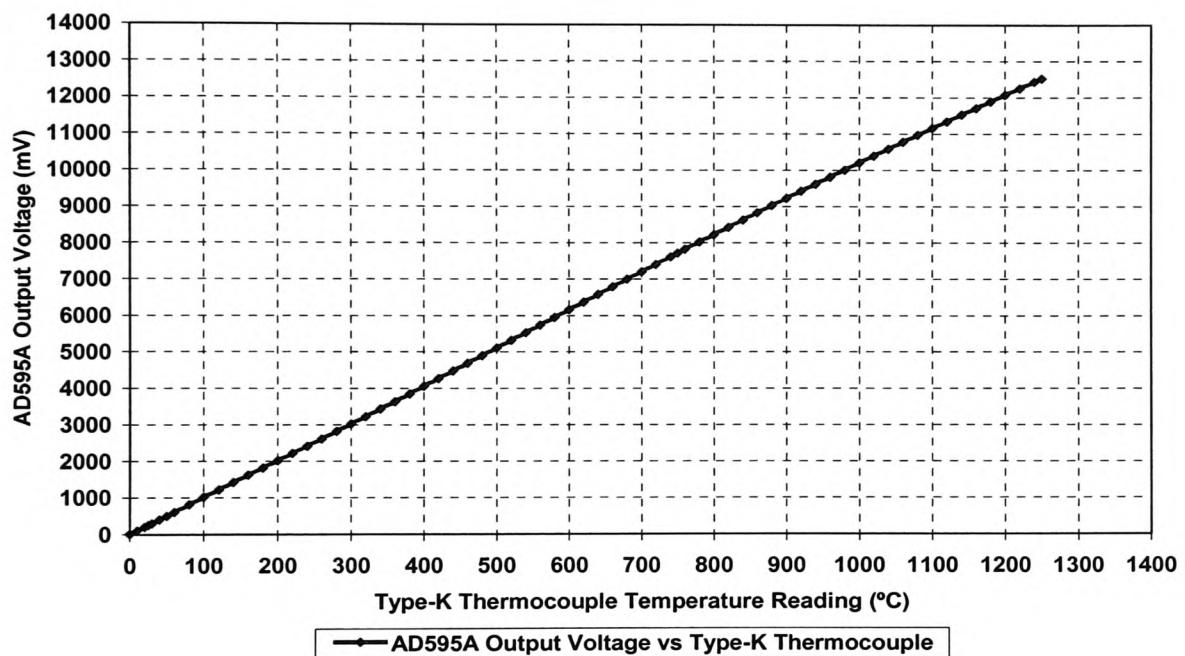


Figure 6.5 Calibration Setting between the Signal Voltage generated by the K-Type Thermocouple and the Temperature Reading in term of Degree Celsius

## 6.2.4 Selection of Training Data

This sub-section discusses the selection of the commissioning data for the training of the NNBC. Following the series of commissioning tests conducted at HMP Garth, useful information about the behaviour and response of the industrial stoker boiler has been gathered. It is important to select an appropriate range of data that covers most of the working conditions to teach the ANNs the optimum settings to ensure a stable and efficient combustion whilst minimising pollutant emissions. The results of training the neural network models will now be presented. The structure of the ARX model employed here was identical to the previous derivation discussed in Section 4.1. However, the training results shown below were only concerned with the combustion optimisation test for the first part of the control experiment, whilst the second part which dealt with the water temperature control test will be treated in the following Chapter.

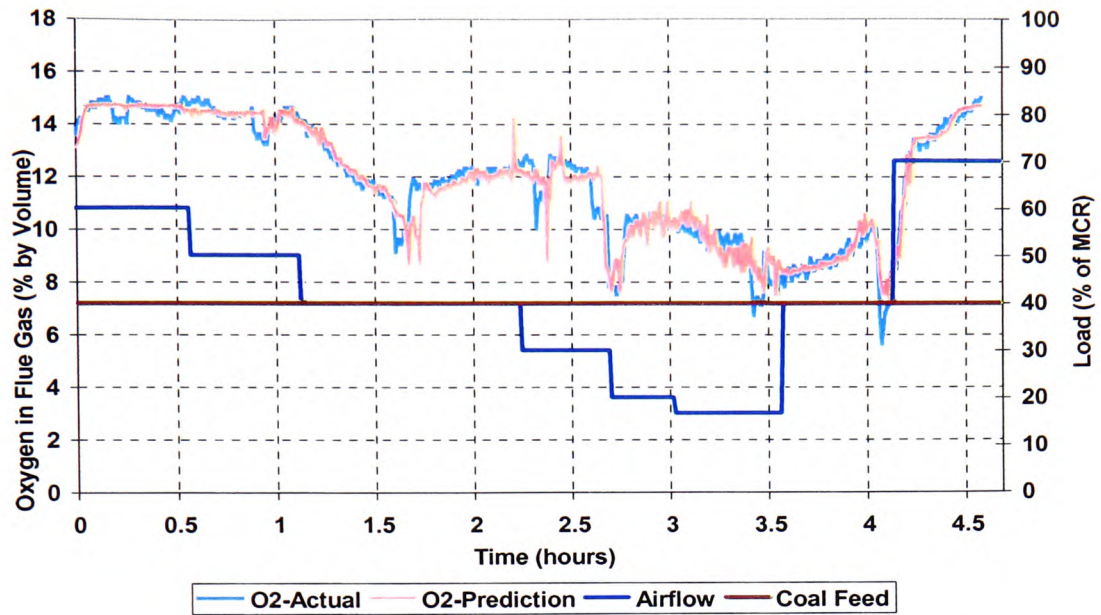


Figure 6.6 Six Steps Ahead Prediction by the ARX Model (nnarx) for  $O_2$  at Constant Load of 40% of MCR Using *Test 18* Data (Odd No. Data Set for Training & Even No. Data Set for Validation - *Training Model 10*)

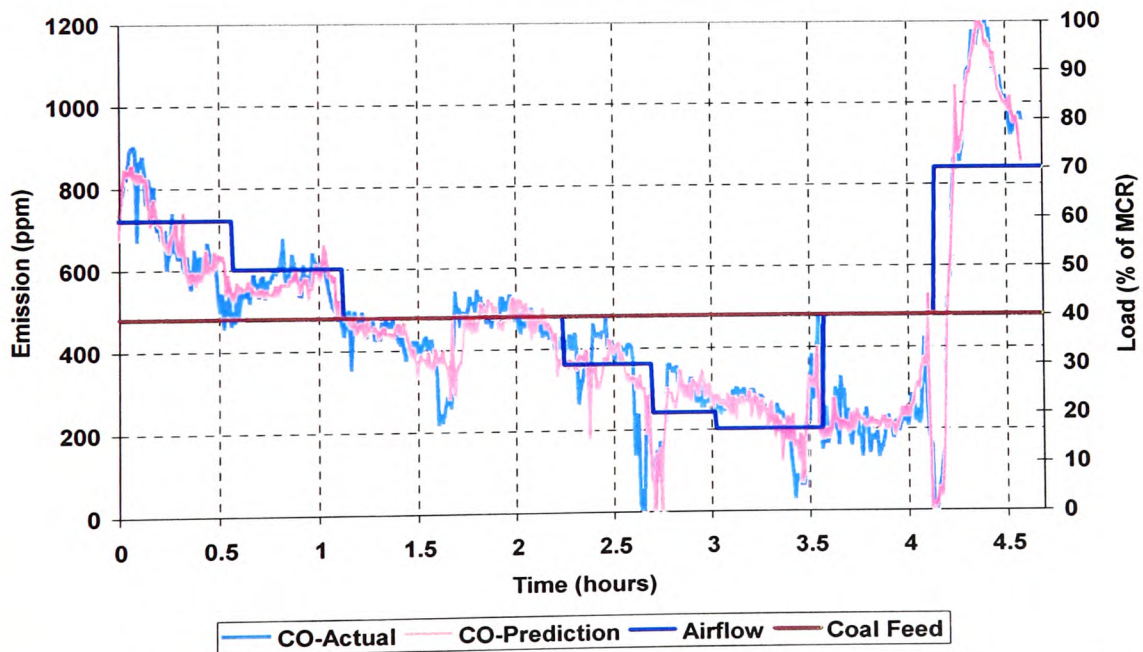


Figure 6.7 Six Steps Ahead Prediction by the ARX Model for CO at Constant Load of 40% of MCR Using *Test 18* Data (1<sup>st</sup> & 3<sup>rd</sup> Quarter Data Set for Training & 2<sup>nd</sup> & 4<sup>th</sup> Quarter Data Set for Validation - *Training Model 11*)

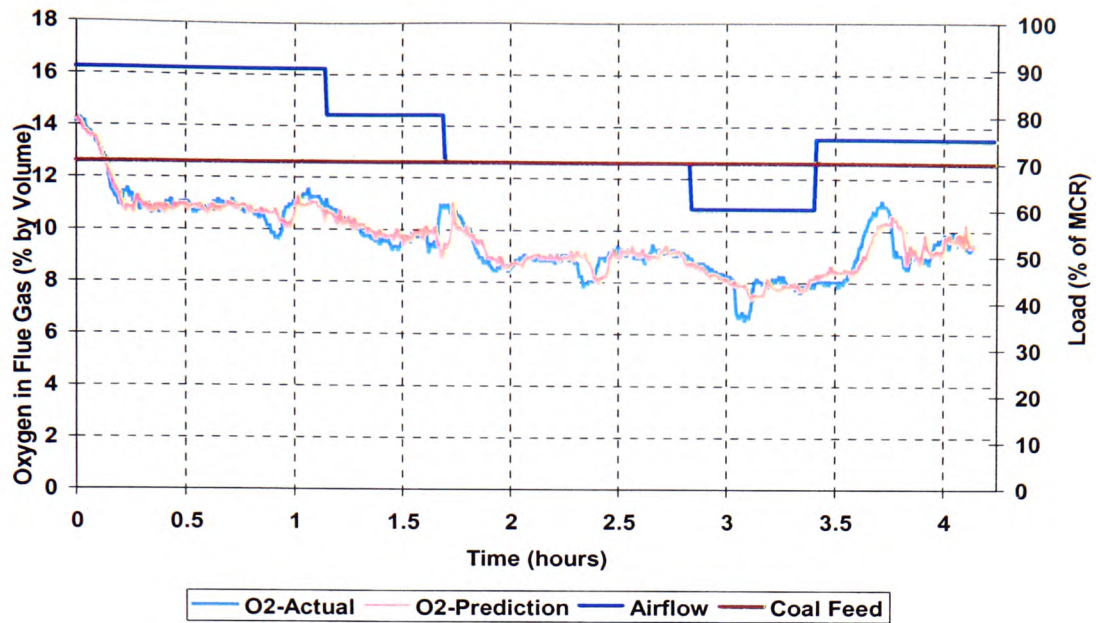


Figure 6.8 Six Steps Ahead Prediction by the ARX Model (nnarx) for  $O_2$  at Constant Load of 70% of MCR Using *Test 18* Data (Odd No. Data Set for Training & Even No. Data Set for Validation - *Training Model 12*)

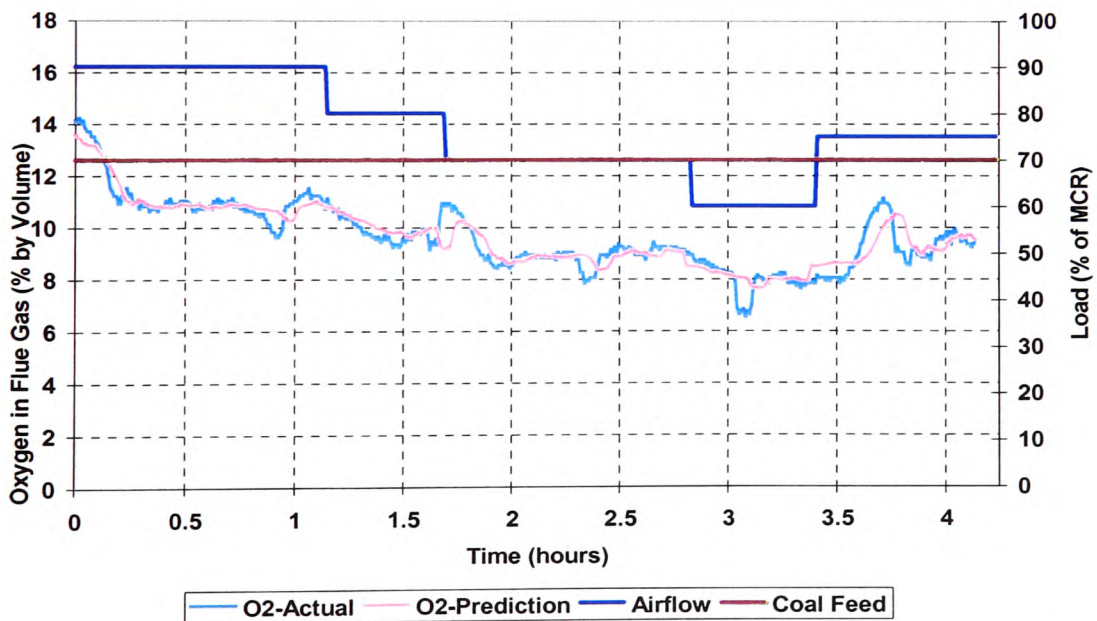


Figure 6.9 Six Steps Ahead Prediction by the ARX Model (nnarx) for  $O_2$  at Constant Load of 70% of MCR Using *Test 18* Data (1<sup>st</sup> & 3<sup>rd</sup> Quarter Data Set for Training & 2<sup>nd</sup> & 4<sup>th</sup> Quarter Data Set for Validation - *Training Model 13*)



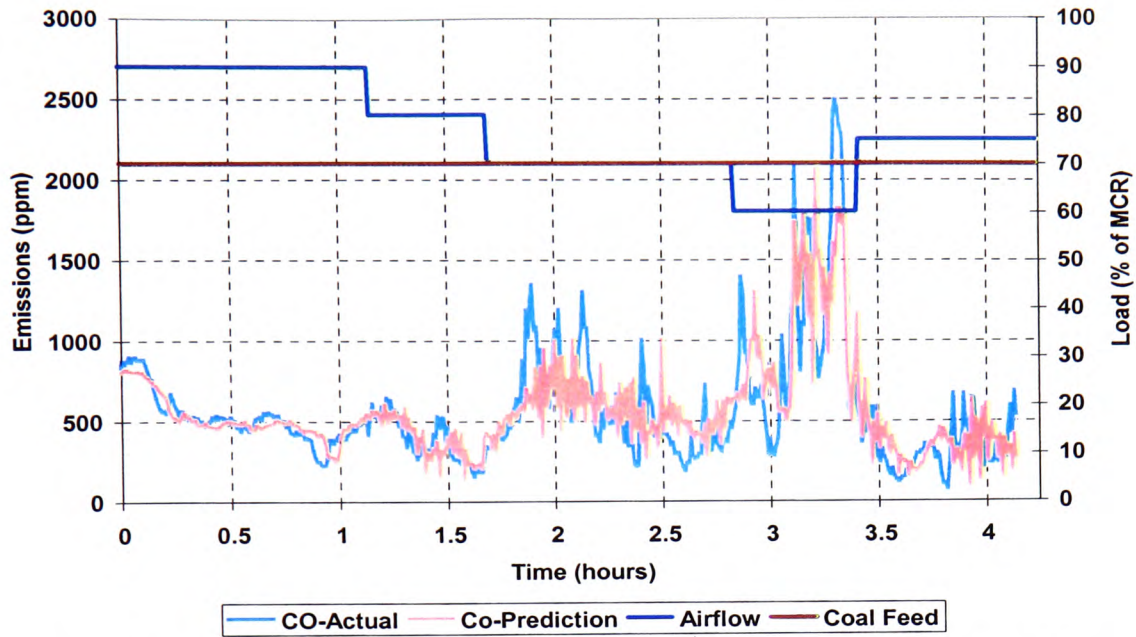


Figure 6.10 Six Steps Ahead Prediction by the ARX Model (nnarx) for CO at Constant Load of 70% of MCR Using *Test 18* Data (Odd No. Data Set for Training & Even No. Data Set for Validation - *Training Model 14*)

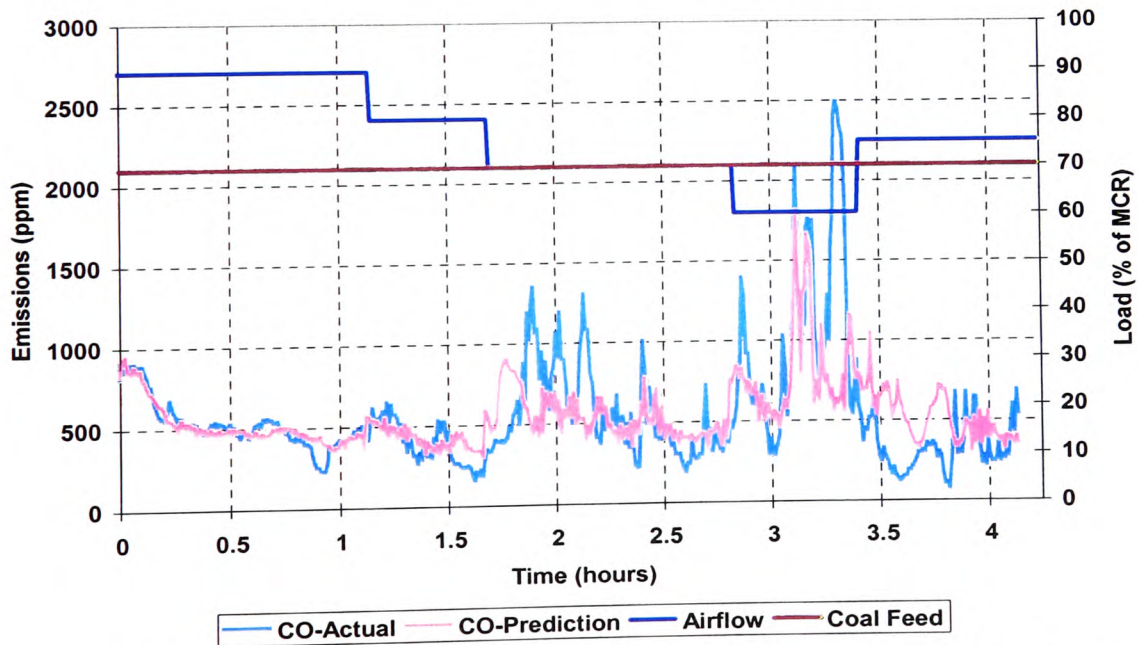


Figure 6.11 Six Steps Ahead Prediction by the ARX Model (nnarx) for CO at Constant Load of 70% of MCR Using *Test 18* Data (1<sup>st</sup> & 3<sup>rd</sup> Quarter Data Set for Training & 2<sup>nd</sup> & 4<sup>th</sup> Quarter Data Set for Validation - *Training Model 15*)

Two different training data arrangements were considered in order to select the best performing neural model. The first arrangement was identical to Chapter 4 where odd number datum points from the data set were used for training and even numbers were used for testing, whilst the second arrangement was organised so that the first and third quarter of the data set were used for training and second and fourth quarter data set were used for testing. However, even though it was found that the derived neural models did result in some dissimilarity, model selection was fairly empirical.

Figures 6.6 to 6.11 show the graphs obtained from the training results using the *Test 18* data (Section 5.2.3). As before, the training data set was initially pre-processed by using the MATLAB<sup>TM</sup> PRESTD function to normalise the inputs and targets so that they have means of zero and standard deviations of one. The TRAINBR training function was used to train the neural model where the weight and bias values were updated according to the Levenberg-Marquardt optimisation algorithm.

Good prediction was achieved with prediction matching the actual trend fairly well for the tests at 40% and 70% of MCR for Bean coal. Visual inspections of these data sets clearly show that the trained neural models were able to deliver predictions six steps into the future for oxygen concentration and CO emissions. In other words, when the neural models were used with gathered unseen data during the control experiment, the NNBC would have three minutes to take a control action.

## 6.3 Conclusion

A neural network based controller (NNBC) system was developed to control the excess air and minimise pollutant emissions using neural networks. The indications from the training data are that the NNBC should be able to predict the future behaviour of the stoker, thereby allowing more time to take remedial action. Such a control system can be used to enhance the efficiency of the chain grate stoker to generate steam/hot water for use in industrial processes and space heating.

## Chapter 7      Commissioning & Testing of the Neural Network Based Controller (NNBC)

This Chapter presents the commissioning and testing of the Neural Network Based Controller (NNBC) on a 3.7MW industrial chain grate stoker fired shell boiler located at HMP Garth. After the commissioning work had determined the different controller parameters in particular the controller gain, the combustion optimisation by the NNBC concentrated on the performance of the NNBC where the plant response under the influence of the NNBC was compared with and without the neural models. Finally the performance of the NNBC is compared with the existing plant PID controller during a hot water temperature control test. For the combustion optimisation test, a constant firing rate at 40% and 70% of MCR was used for validation purposes and a further test at 60% of MCR was also conducted in order to test the ability of the neural network to cope with new conditions. For the water temperature control test, the hot water demand was taken into consideration and the NNBC then adjusted the coal feed and airflow rates to meet the demand required whilst trimming the oxygen concentration. In the following Sections, the controller commissioning results are presented before progressing to discuss the control experiment results that cover the combustion optimisation test and the hot water temperature control test. Table 7.1 outlines all the control experiments conducted on a 3.7MW industrial stoker boiler under the influence of the NNBC and the PID controller.

Table 7.1 Control Experiments Conducted on a 3.7MW<sub>th</sub> Industrial Stoker Boiler under the Influence of the NNBC & the PID Controller

Test No.	Description	Test Condition	Controller Setting	Coal Type
20	Combustion optimisation test at constant load with unsuitable controller settings under NNBC control	40% of MCR	With O <sub>2</sub> & CO neural models	Bean coal
21	Combustion optimisation test at constant load under NNBC control	40% of MCR	With O <sub>2</sub> & CO neural models	Bean coal
22	Combustion optimisation test at constant load under NNBC control	40% of MCR	Without O <sub>2</sub> & CO neural models	Bean coal
23	Combustion optimisation test at constant load under NNBC control (Test Profile 1*)	70% of MCR	With O <sub>2</sub> & CO neural models	Bean coal
24	Combustion optimisation test at constant load under NNBC control (Test Profile 1*)	70% of MCR	Without O <sub>2</sub> & CO neural models	Bean coal
25	Combustion optimisation test at constant load under NNBC control (Test Profile 2*)	70% of MCR	With O <sub>2</sub> & CO neural models	Bean coal
26	Combustion optimisation test at constant load under NNBC control (Test Profile 2*)	70% of MCR	Without O <sub>2</sub> & CO neural models	Bean coal
27	Combustion optimisation test with unseen data at constant load under NNBC control	60% of MCR	With O <sub>2</sub> & CO neural models	Bean coal
28	Hot water temperature set point change under the influence of the NNBC	105°C to 120°C	Without O <sub>2</sub> & CO neural models	Bean coal
29	Hot water temperature set point change under the influence of the NNBC	120°C to 105°C	Without O <sub>2</sub> & CO neural models	Bean coal
30	Tracking hot water temperature set point under the influence of the NNBC	Set point at 120°C	Without O <sub>2</sub> & CO neural models	Bean coal
31	Tracking hot water temperature set point under the influence of the NNBC	Set point at 120°C	With O <sub>2</sub> & CO neural models	Bean coal
32	Tracking hot water temperature set point under the influence of the PID controller	Set point at 120°C	Without O <sub>2</sub> & CO neural models	Bean coal

*\*Note: Test Profile 1 – High initial setting of excess air prior to NNBC tuning.*

*Test Profile 2 – Low initial setting of excess air prior to NNBC tuning.*

## 7.1 Commissioning of the Neural Network Based Controller (NNBC)

After training, the NNBC was commissioned for the industrial stoker located at HMP Garth, with several tests being conducted to determine suitable controller parameters for the

combustion optimisation test at constant load. In the interests of brevity, only one test with a poor set of parameters is presented here along with the successful control experiments that will be discussed in the following Sub-Section.

The gain factor for the airflow adjustment network (Section 6.2.1) was based on the error between the prediction and the actual oxygen and CO against the predefined target values, to establish the quantity of tuning required for the total air supplied to the main combustion zone. The sampling period was the time period between consecutive control actions taken by the NNBC. In this case, a sampling period of 3 minutes was chosen, which was based on the ability of the neural models when performing their prediction task for oxygen and CO predictions at multiple steps into the future. In other words, the ability of the neural models to be able to predict six steps into the future (equivalent to 3-minute) allowed the NNBC to take action one control period ahead, which should improve the response of the controller.

Following the commissioning tests discussed in Section 5.2, empirically the corrective gain factor should be a 7.5% change of the airflow per a 1% change in the oxygen reading, this was used as a starting point for optimisation of different parameters. Table 7.2 outlines the range of the target oxygen band with respect to the percentage change in total air supplied.

Table 7.2 Relationship between the Ranges of Oxygen Readings with respect to the Ranges of Airflow Alterations Required

Ranges of Oxygen Readings (% by Volume)	Ranges of Airflow Alterations Required
9.1 to 10.0 (Higher Excess Air - Less Air Required)	-1 to -7.5% from the Near Optimum
7.0 to 9.0 (Near Optimum Excess Air - No Changes Required)	0%
6.0 to 6.9 (Lower Excess Air - More Air Required)	+1 to +7.5% from the Near Optimum

*Note: Due to the different target oxygen bands at different firing rates, the above relationship only refers to the firing rate from 71% of MCR to maximum load together with the corresponding range of airflow tuning required. Other firing rates (Table 5.2) can follow this correlation accordingly.*

From the relationship stated in Table 7.2, the resolution of the oxygen reading was 0.1%, thus the corrective gain factor was 0.75% of the initial airflow setting per 0.1% difference in the oxygen reading. As a result, an initial gain factor of 15 was intuitively chosen based on the derived value of 7.5% per 1% change in oxygen reading together with the controller sampling period of 3-minute for the following test which from observation has inappropriate controller settings.

### 7.1.1 Stoker Control Using the NNBC with Inappropriate Settings

One control experiment whilst burning Bean coal (coal properties can be found in Appendix B) with unsuitable controller settings is presented here at a constant load of 40% of MCR. At the beginning of this test, the airflow was manually adjusted to a high excess air and the NNBC was then activated to adjust the airflow to an appropriate flow rate to achieve an optimum air fuel ratio with the aim of returning the oxygen concentration to within the target oxygen band. In addition, the NNBC was configured so that the airflow adjustment network would only be activated if the oxygen level fell outside the target. The priority of the control action to tune the airflow was first given to the predicted oxygen reading when it fell outside the target band, followed by the predicted CO emission value if it exceeded the target limit of 1000ppm (normalised to 6% of oxygen). Details of these rules are in the NNBC programme and can be found in Appendix D. For the control experiments, the boiler response is discussed with reference to the oxygen concentration in the flue gas, carbon monoxide (CO) and nitrogen oxides (NO<sub>x</sub>) emissions and variations in the airflow following the tuning effort performed by the NNBC.



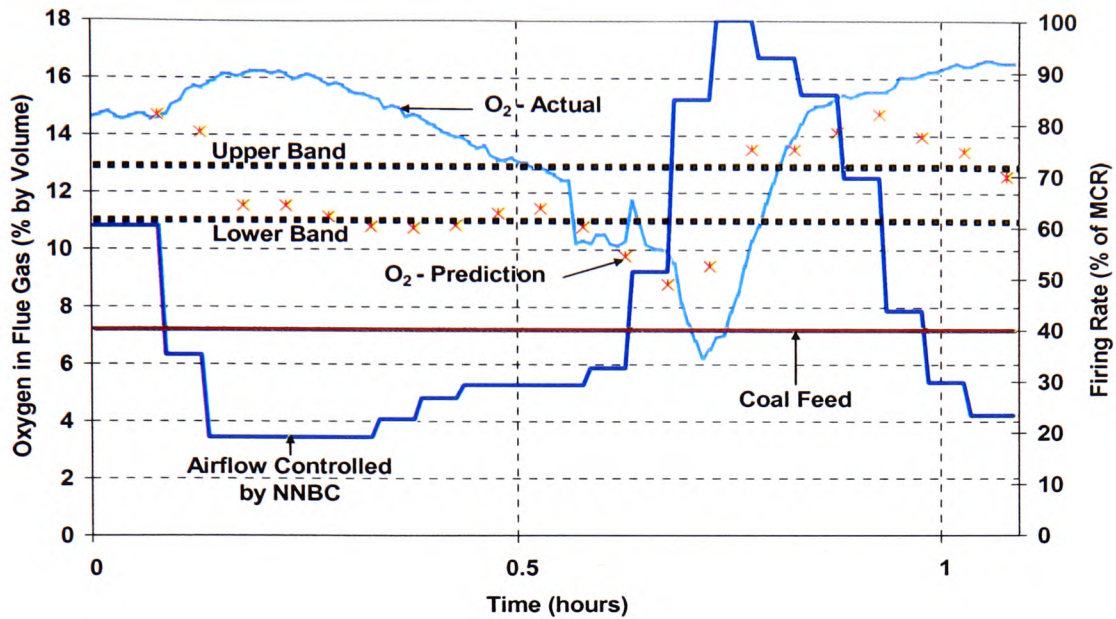


Figure 7.1 Predicted & Actual Oxygen Response to Unsuitable Controller Gain for Combustion Optimisation Test at Constant Load of 40% of MCR – *Test 20*

Figure 7.1 shows the predicted values and the actual oxygen concentration following the combustion optimisation test at a constant load of 40% of MCR with variations in the airflow performed by the NNBC (*Test 20*). The data points shown by red stars (Figure 7.1) indicate the oxygen prediction three minutes into the future. The prediction only started after the first two data points from the beginning of the test which was due to the regressor structure of the NNARX model where five past and current data points were utilised in order to forecast the output value six steps into the future.

Due to the magnitude of the corrective gain factor (15), the decision made by the NNBC was too large even though the control period, of 3 minutes, should have allowed enough time for the boiler to respond to the previous alteration of the airflow. As a result, the oxygen reading shows signs of instability following the poor prediction performed by the oxygen neural model, especially at the beginning of the test. Another possible reason for poor performance was that the data set used for training did not cover such a large variation in airflow. The oxygen concentration follows the large airflow adjustment with the consequence being that only 7% of the total test duration did the oxygen remain inside the target band over the test

duration of 1.1 hours. Even though the prediction was poor, in that the measured oxygen did not coincide with the predicted value, the prediction was inside the target band for a much larger period.

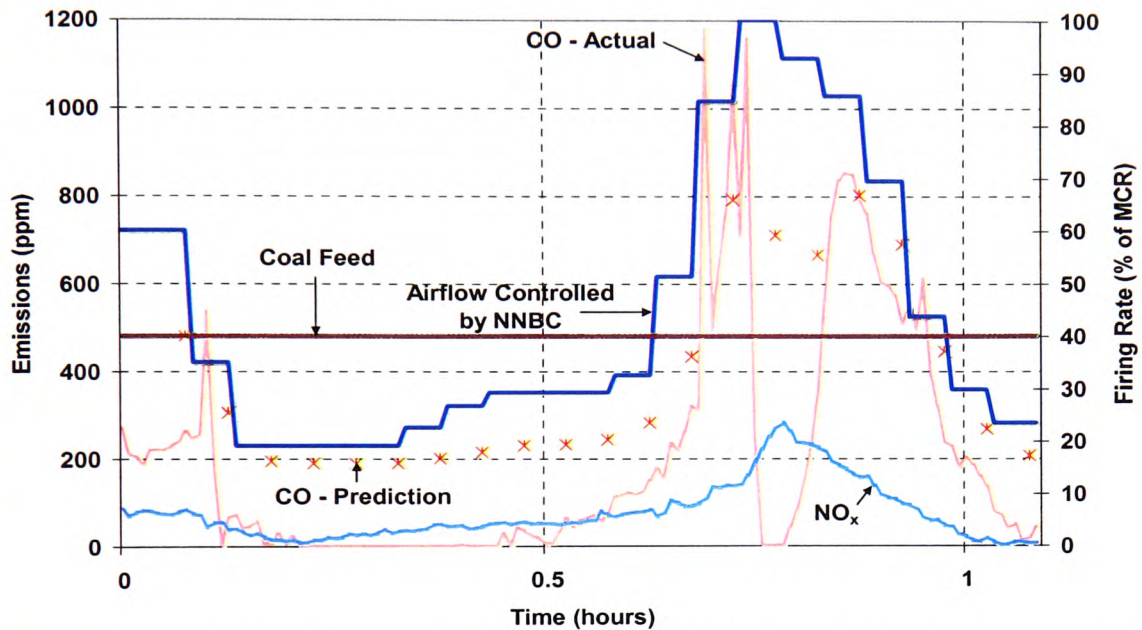


Figure 7.2 Predicted & Actual CO & NO<sub>x</sub> Emissions to Unsuitable Controller Gain for Combustion Optimisation Test at Constant Load of 40% of MCR – Test 20

A similar scenario to that faced by the oxygen neural model was also encountered during the prediction of CO (Figure 7.2). The CO prediction throughout the entire test was acceptable except for maximum airflow where a sudden drop in the recorded CO (at 0.75 hours) was not predicted by the neural network. As the NO<sub>x</sub> emissions are greatly influenced by the amount of combustion air available, the NO<sub>x</sub> emission increase to nearly 300ppm when the airflow was increased to maximum (Figure 7.2).

## 7.2 Testing of the Neural Network Based Controller (NNBC)

Following the controller commissioning tests satisfactory controller parameter settings were found to be 2.5 and 5 respectively. A series of control experiments using these settings were



conducted at the constant loads of 40% and 70% of MCR for validation purposes and a further test at 60% of MCR was also conducted in order to test the ability of the neural network to cope with unseen conditions. In the following Sub-Sections, the combustion controller test results with and without the neural models are discussed and finally the performance of the NNBC is compared with the plant response under conventional PID control during a hot water temperature control test.

### 7.2.1 Combustion Optimisation with the NNBC

Seven control experiments whilst burning Bean coal with suitable controller parameter settings are discussed here for combustion optimisation tests at 40%, 60% and 70% of MCR. The combustion optimisation tests were conducted with and without the O<sub>2</sub> and CO neural models and the results of these are compared and discussed. At the beginning of each test, the airflow was manually adjusted to a higher or lower excess air (depending on the test profile) and the NNBC was activated to adjust the airflow in order to bring the excess air level into the target oxygen band.

#### **Results Obtained at 40% of MCR – Tests 21 & 22**

The results obtained by operating the boiler at a constant load of 40% of MCR with and without the O<sub>2</sub> neural model are shown in Figures 7.3 and 7.4 respectively. The NNBC altered the airflow over a range of 35% to 60% (Figure 7.3) with the O<sub>2</sub> neural model as compared to 25% to almost 90% without the neural model (Figure 7.4). Consequently, the oxygen concentration was inside the target band for 34% of the 2.5-hour test (*Test 21*) as compared to only 16% (*Test 22*) over the 2-hour test. The O<sub>2</sub> model predicted reasonably well, thus narrowing the range of airflow adjustment (*Test 21*). Although the best controller gain was used, the test at 40% of MCR tend to have large fluctuations in the oxygen level; the reason can be partly attributed to the difficulty in controlling stokers at low fire unless the efficiency is sacrificed by allowing the stoker to operate at a higher excess air. The strategy normally adopted by the PID controller in order to minimise the boiler operating problem throughout the entire firing range.

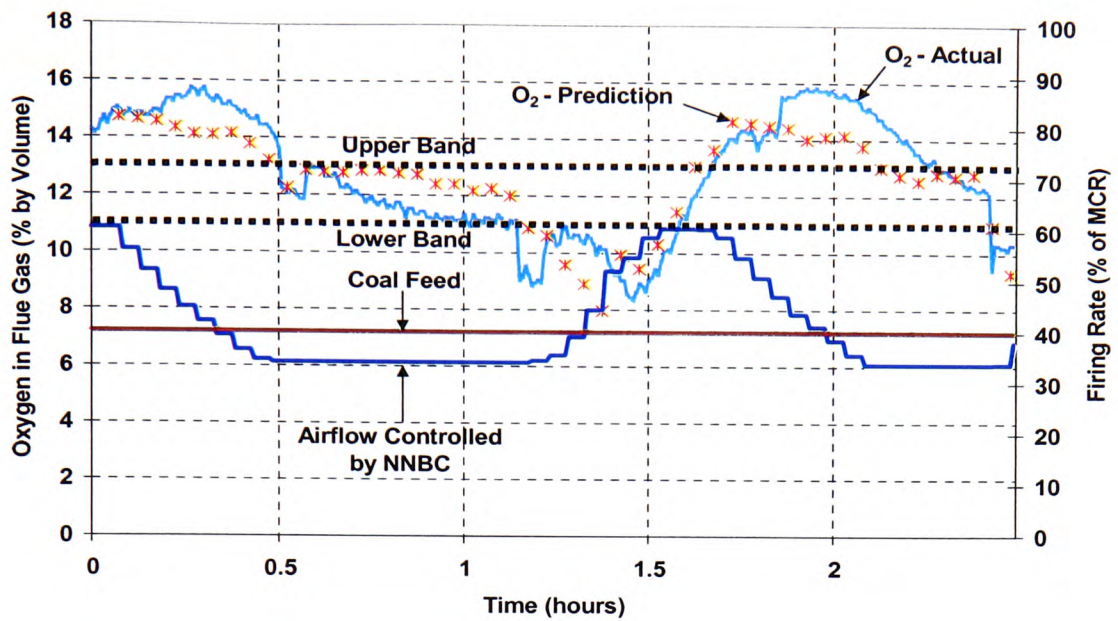


Figure 7.3 Predicted & Actual Oxygen Response following Combustion Optimisation Test at Constant Load of 40% of MCR with O<sub>2</sub> Neural Model Using *Training Model 10 – Test 21*

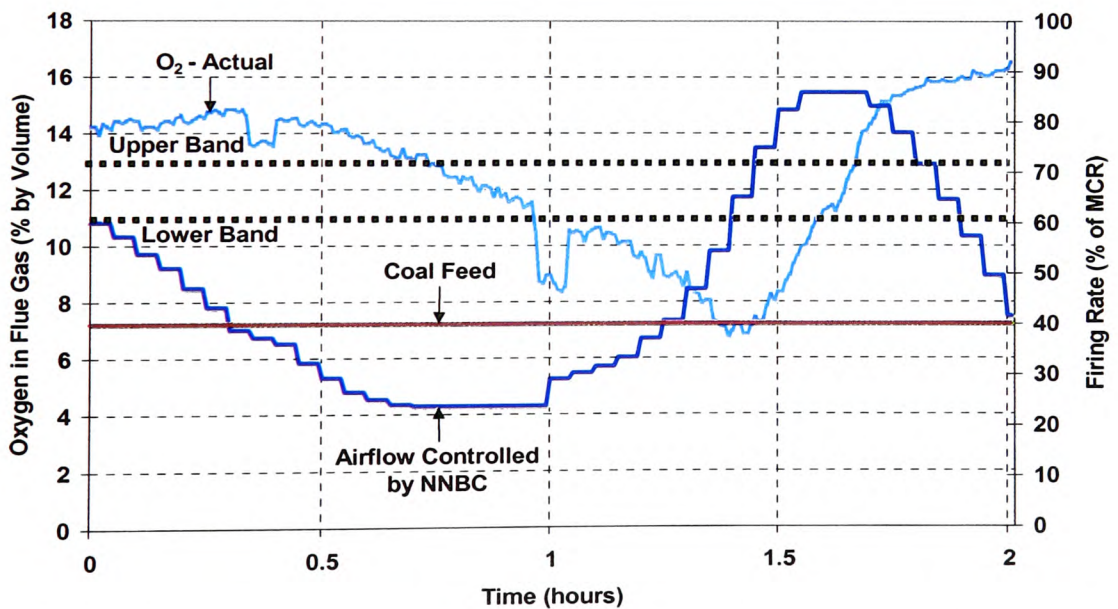


Figure 7.4 Actual Oxygen Response following Combustion Optimisation Test at Constant Load of 40% of MCR without O<sub>2</sub> Neural Model – *Test 22*

Figures 7.5 and 7.6 show the CO and NO<sub>x</sub> emissions recorded during the combustion optimisation test at 40% of MCR integrated with and without the CO neural model. For the test conducted with the CO neural model (Figure 7.5), although the prediction did not coincide with the actual CO for the entire test, the actual CO emissions were well controlled by the NNBC and settled below the target limit of 1000ppm with an average emission of 128ppm (normalised to 6% of oxygen). This was probably due to the model exhibiting the same trends as the recorded CO. The probable reason for the CO neural model predicting higher than the actual CO perhaps results from the data range used during training which was similar to that shown in Figure 7.5. For the results obtained without the CO neural model, an overshoot of CO of more than 1000ppm can be observed in Figure 7.6 although the CO level for the rest of this test was below the limit value with an average emission of 351ppm being recorded.

NO<sub>x</sub> emissions (Figures 7.5) show no concern probably being helped by the natural form of air staging along the fire bed, with an average emission of 161ppm being recorded. Unfortunately, the NO<sub>x</sub> reading was not available for *Test 22* (Figure 7.6) due to failure of flue gas analyser. Although there are no emission restrictions for a boiler of this range, their emission limits will probably have to comply in the future with those of the 20 to 50MW range of coal fired boilers i.e. NO<sub>x</sub> < 245ppm and SO<sub>2</sub> < 700ppm at 6% oxygen for coal fired boilers [IEA Statistics, 1998]. It would appear that the smaller airflow adjustment range, from the use of the neural model generates a more stable combustion process on the bed thus producing more satisfactory combustion.

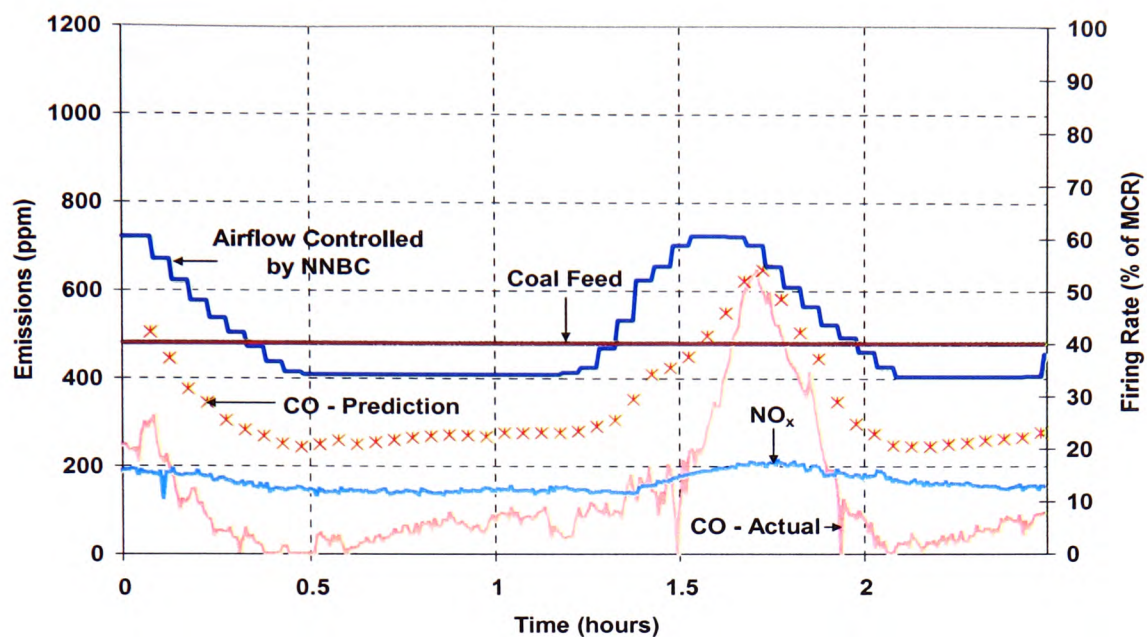


Figure 7.5 Predicted & Actual CO & NO<sub>x</sub> Emissions following Combustion Optimisation Test at Constant Load of 40% of MCR with CO Neural Model Using *Training Model 11 – Test 21*

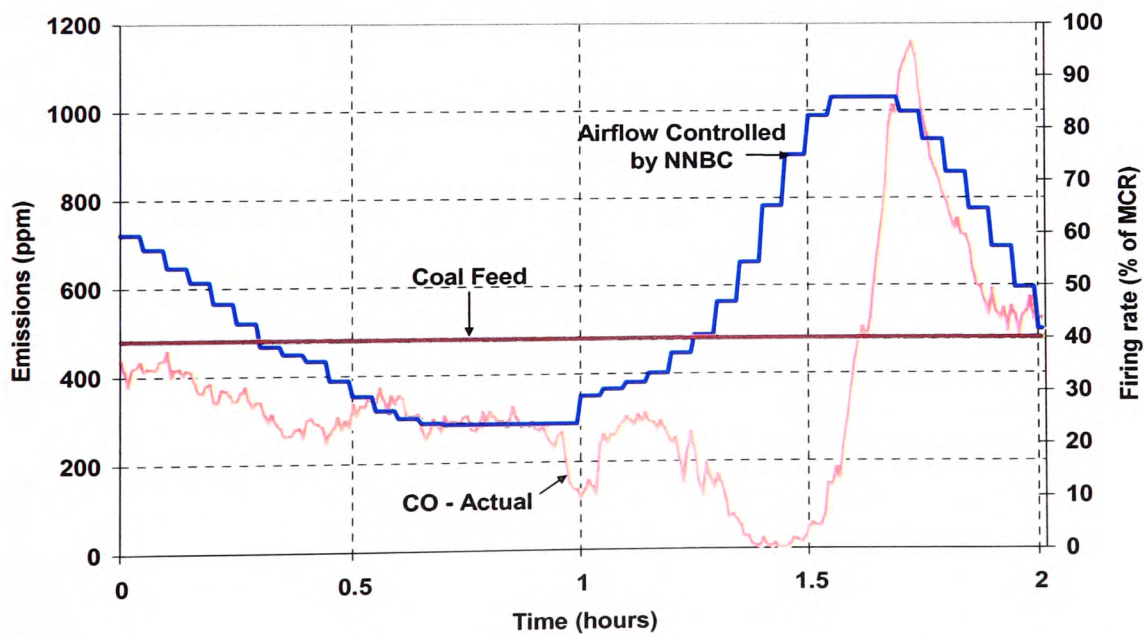


Figure 7.6 Actual CO Emission following Combustion Optimisation Test at Constant Load of 40% of MCR without CO Neural Model – *Test 22*

### **Results Obtained at 70% of MCR (Test Profile 1) – Tests 23 & 24**

Figures 7.7 and 7.8 show the results obtained by operating the boiler at a constant load of 70% of MCR with and without the O<sub>2</sub> neural model. Before progressing further, it must be stated that the tests at 70% of MCR were carried out in two different test profiles (unlike the 40% of MCR tests where only one profile was considered due to the difficulty of operating this stoker at low fire). The first profile (defined as Test Profile 1) was conducted so that the airflow was manually adjusted to a higher excess air and the NNBC was activated to bring the excess air into the oxygen target band, while the second profile (defined as Test Profile 2) was similar except the airflow was initially reduced so the experiment started from a lower excess air.

The tests for the first profile were started with the initial setting of coal feed and airflow being 70% and 100% of MCR respectively. The NNBC with the neural model performed well bringing the oxygen level into the target band of 9% to 11% in addition to performing a smaller magnitude of airflow alteration hence generating more stable combustion on the bed (Figure 7.7). Although the oxygen only lay within the target band for 51% of the total test duration of 2 hours as compared to 87% attained by the NNBC without the neural model, the performance achieved by the NNBC incorporating the O<sub>2</sub> neural model could have been higher if the readings slightly above the target band were taken into account (increasing the upper threshold by 0.1% or 0.2% could increase the 51% to 70% over the 2-hour test). However, according to the prediction made by the neural model, the oxygen readings were inside the target band and hence no oxygen trimming was taken by the NNBC to fine tune the airflow. The effect of the automatic ash removal system can be seen at 40 and 75 minutes (Figure 7.7) and the impact on the performance of the NNBC was negligible. This effect can hardly be seen for *Test 24* as shown in Figure 7.8.



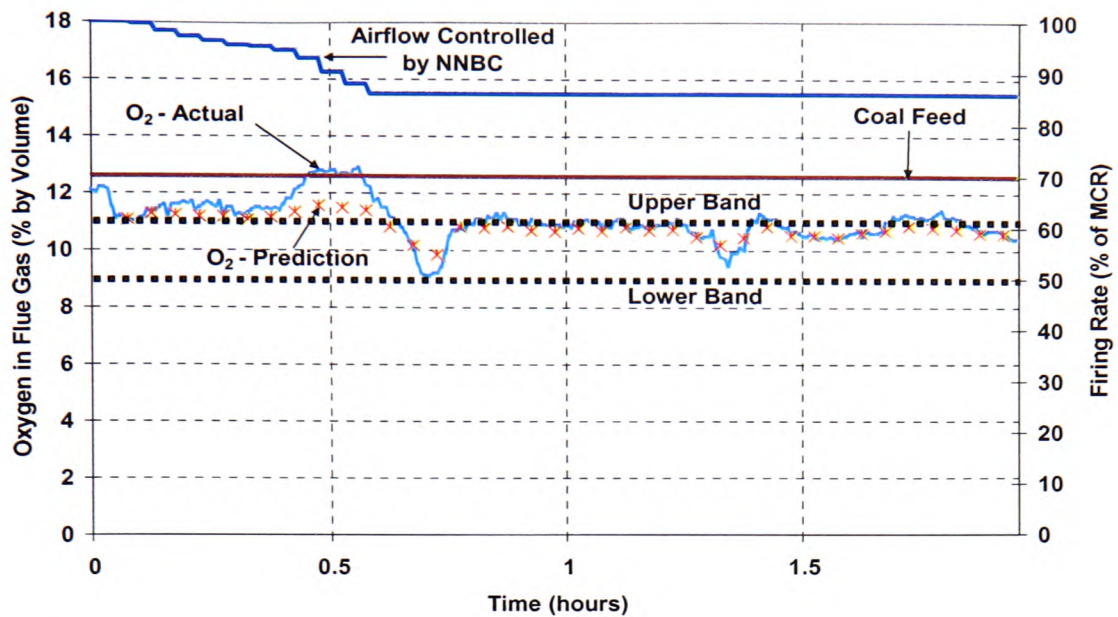


Figure 7.7 Predicted & Actual Oxygen Response following Combustion Optimisation Test at Constant Load of 70% of MCR With O<sub>2</sub> Neural Model Using *Training Model 12* (Test Profile 1) – *Test 23*

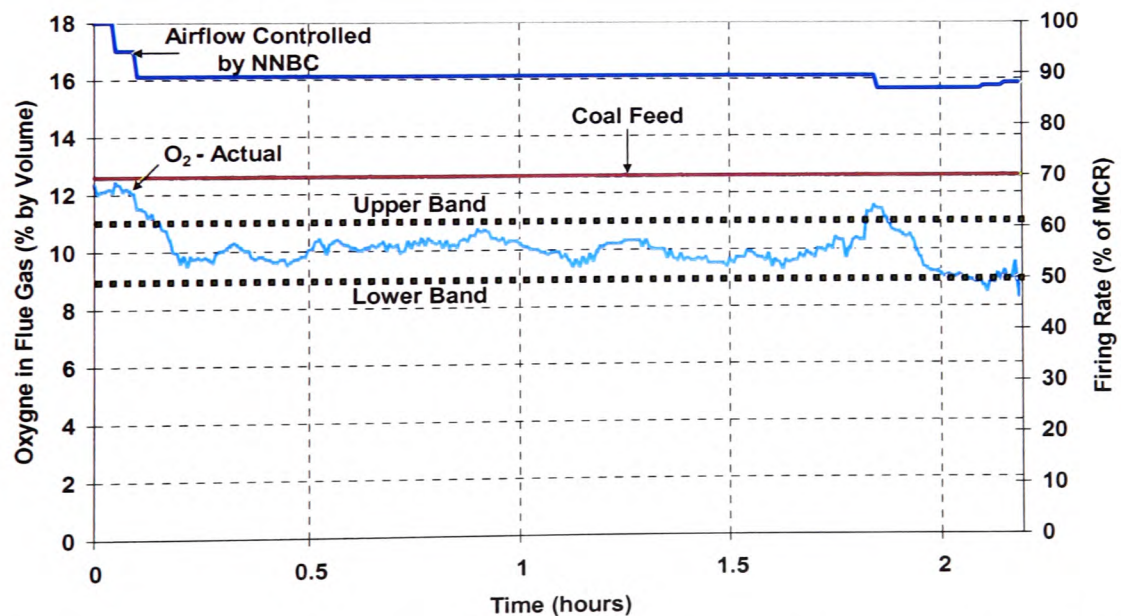


Figure 7.8 Actual Oxygen Response following Combustion Optimisation Test at Constant Load of 70% of MCR without O<sub>2</sub> Neural Model (Test Profile 1) – *Test 24*

The pollutant emission results obtained by operating the boiler with Test Profile 1 at a constant load of 70% of MCR with and without the CO neural model are shown in Figures 7.9 and 7.10. In comparison with *Test 21*, the CO model prediction shown in Figure 7.9 (*Test 23*) was in good agreement with the actual plant response with an average CO emission of 567ppm being recorded over the total test duration of 2 hours. The positive prediction can mainly be attributed to the fact that this experimental data set is relatively similar to that used to train the model (Figure 6.11 of *Test 18*). Therefore, the actual CO was maintained below the target limit of 1000ppm (normalised to 6% of oxygen). The CO emission (Figure 7.10) was also well controlled by the NNBC without the CO neural model (*Test 24*). The NO<sub>x</sub> emission results shown (Figure 7.9) are higher than those obtained at 40% of MCR (Figure 7.10). The mean NO<sub>x</sub> emissions for these tests were 297ppm and 231ppm, which were well below the future legislation limits for coal fired boilers of this range.



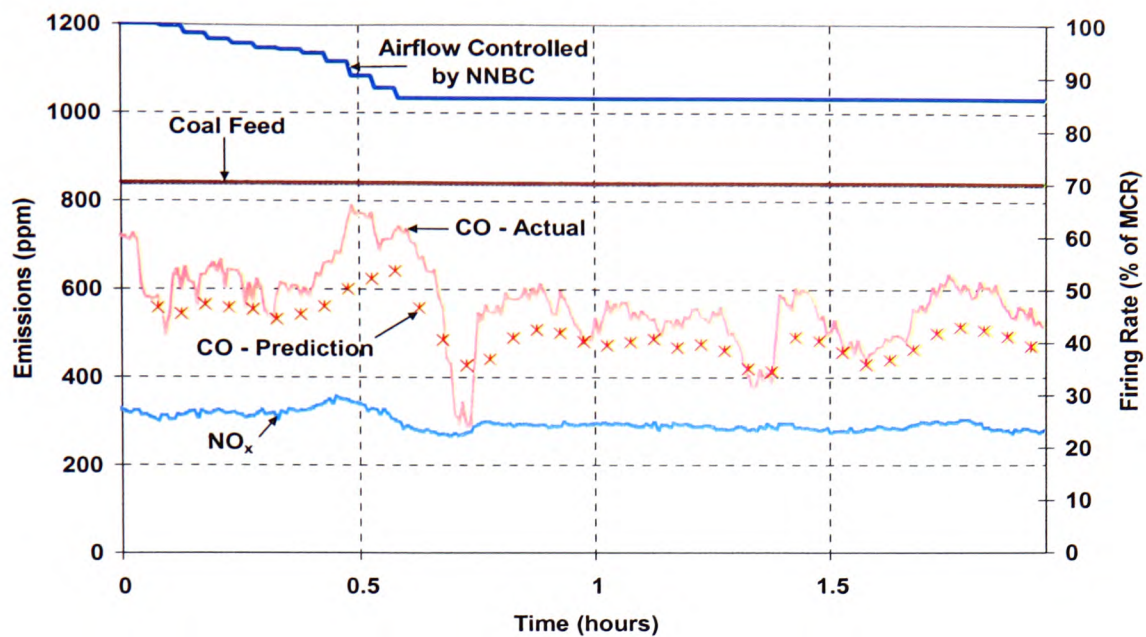


Figure 7.9 Predicted & Actual CO & NO<sub>x</sub> Emissions following Combustion Optimisation Test at Constant Load of 70% of MCR with CO Neural Model Using *Training Model 15* (Test Profile 1) – *Test 23*

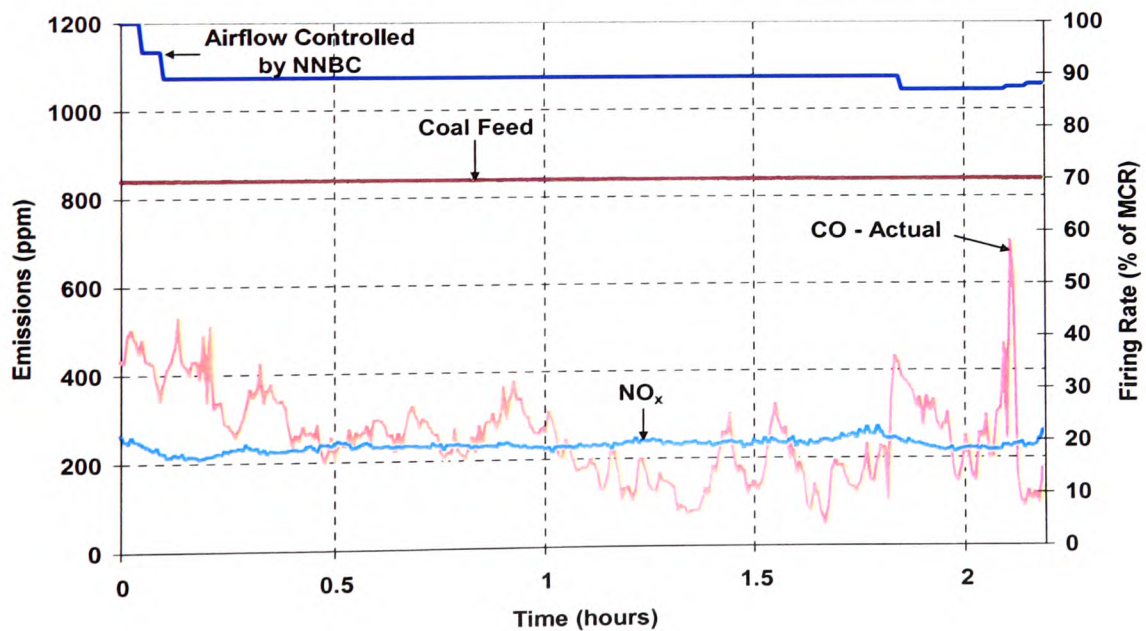


Figure 7.10 Actual CO & NO<sub>x</sub> Emission following Combustion Optimisation Test at Constant Load of 70% of MCR without CO Neural Model (Test Profile 1) – *Test 24*

### **Results Obtained at 70% of MCR (Test Profile 2) – Tests 25 & 26**

The results obtained by operating the boiler under Test Profile 2 at a constant load of 70% of MCR with and without the O<sub>2</sub> neural model are shown respectively in Figures 7.11 and 7.12. The small alteration of the airflow taken by the NNBC with the O<sub>2</sub> neural model resulted in stable combustion on the bed (Figure 7.11). After 20 minutes, the oxygen level was brought into the target band of 9% to 11% from the preliminary low excess air. This result was encouraging, as the NNBC without the neural model took a longer period of time (35 minutes) to reach the target band. Consequently, for 66% of the total test duration did the oxygen concentration lie within the target band (*Test 25*) as compared to only 48% attained by the NNBC without the neural model (*Test 26*).

Another interesting point that will be worth mentioning in *Test 25* is that after 1.5 hours into the experiment, there was a sudden increase in the actual oxygen concentration (perhaps caused by poor coal distribution on the grate due to improper stoking practices giving rise to 'holes' in the bed hence allowing under-grate air to escape) from 10.5% to 12% (Figure 7.11). However, the oxygen concentration predicted by the neural model indicates that the oxygen level increased only slightly above the target band and hence only a small amount of airflow reduction was taken by the NNBC. This decision was proved to be appropriate as the actual oxygen dropped just above the lower band a few minutes later (coincident with the suction caused by the automatic ash removal system) and continued to stay in the middle of the band until the end of the test. This situation could not have been dealt with by the NNBC without the neural model, as there would simply be a decrease of the excess air in proportion to the unexpected rise in the oxygen level. The consequences of a sudden increase or decrease of excess air can result in unstable combustion on the bed with a great possibility of the controller and the process becoming unstable.

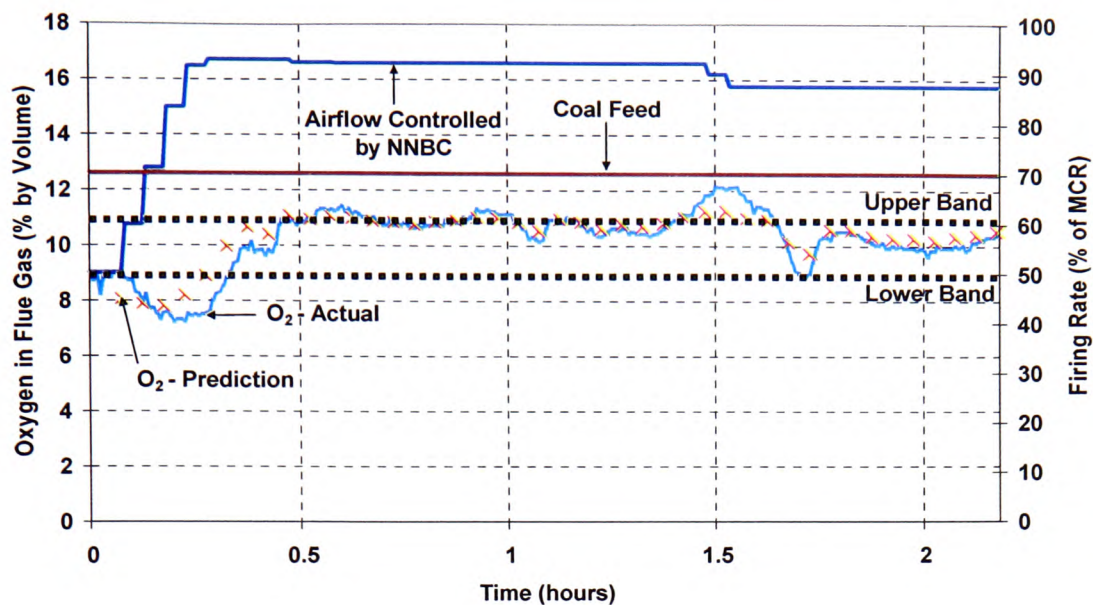


Figure 7.11 Predicted & Actual Oxygen Response following Combustion Optimisation Test at Constant Load of 70% of MCR with O<sub>2</sub> Neural Model Using *Training Model 12* (Test Profile 2) – *Test 25*

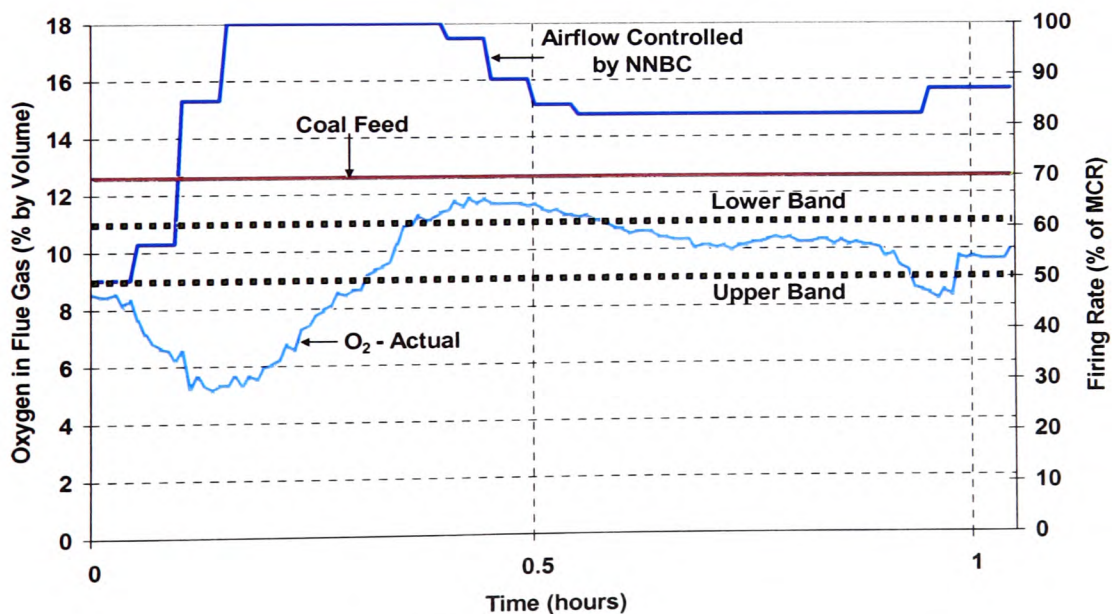


Figure 7.12 Actual Oxygen Response following Combustion Optimisation Test at Constant Load of 70% of MCR without O<sub>2</sub> Neural Model (Test Profile 2) – *Test 26*

The CO and NO<sub>x</sub> emissions attained by operating the boiler under Test Profile 2 at a constant load of 70% of MCR with and without the CO neural model are shown in Figures 7.13 and 7.14 respectively. Although no control action was taken by the NNBC to fine tune the airflow based on the predicted CO emissions (as they were all well below the target limit), the prediction (Figure 7.13) was highly comparable to the actual CO recorded by the flue gas analyser. The average actual CO emission obtained over the test duration of 2.1 hours was 353ppm (*Test 25*). On the other hand, the CO shown in Figure 7.14 (*Test 26*) was also well below the target limit with an average emission of 231ppm being recorded (normalised to 6% oxygen).

As for NO<sub>x</sub> emissions, the production of this derivative of combustion closely followed the firing rate as the emission was mainly dependent on the fuel and the availability of combustion air. This is evident where the NO<sub>x</sub> emission was increased to 300ppm from 200ppm as the airflow was increased from 50 to 90% of MCR (Figure 7.13). However, the resulting NO<sub>x</sub> emissions are perfectly acceptable with an average emission of 270ppm being recorded. The NO<sub>x</sub> reading in Figure 7.14 was not available as *Test 26* was carried out the same day as *Test 22* (failure of flue gas analyser). Although no NO<sub>x</sub> reading was available, the firing rate and the amount of combustion air supplied as illustrated in Figure 7.14 should have kept the average emission below 300ppm.



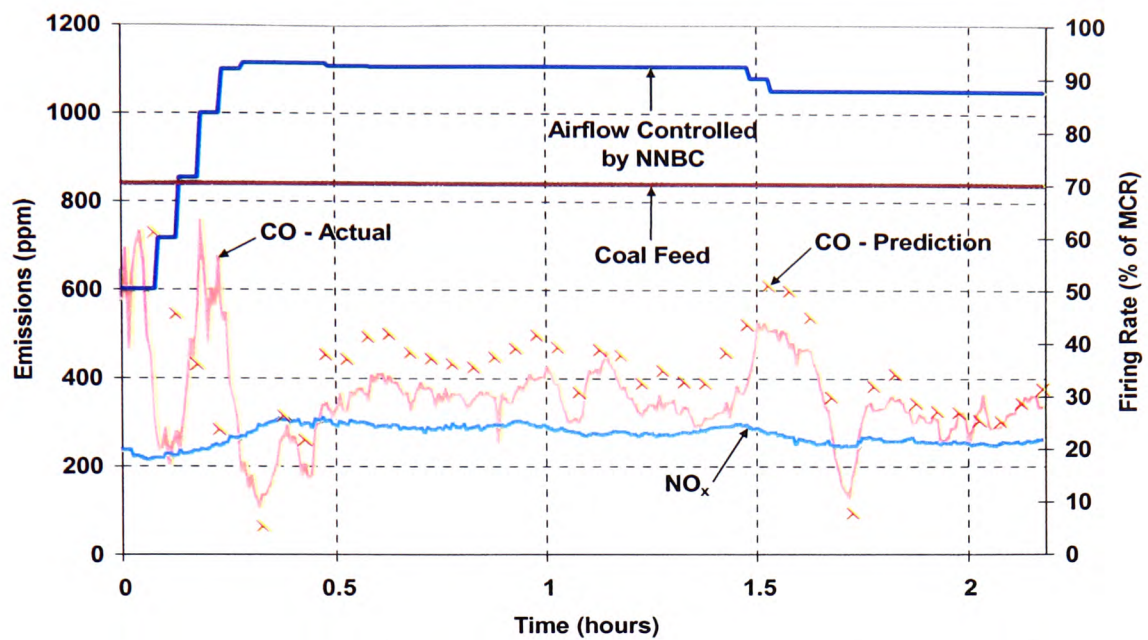


Figure 7.13 Predicted & Actual CO & NO<sub>x</sub> Emissions following Combustion Optimisation Test at Constant Load of 70% of MCR with CO Neural Model Using *Training Model 14* (Test Profile 2) – *Test 25*

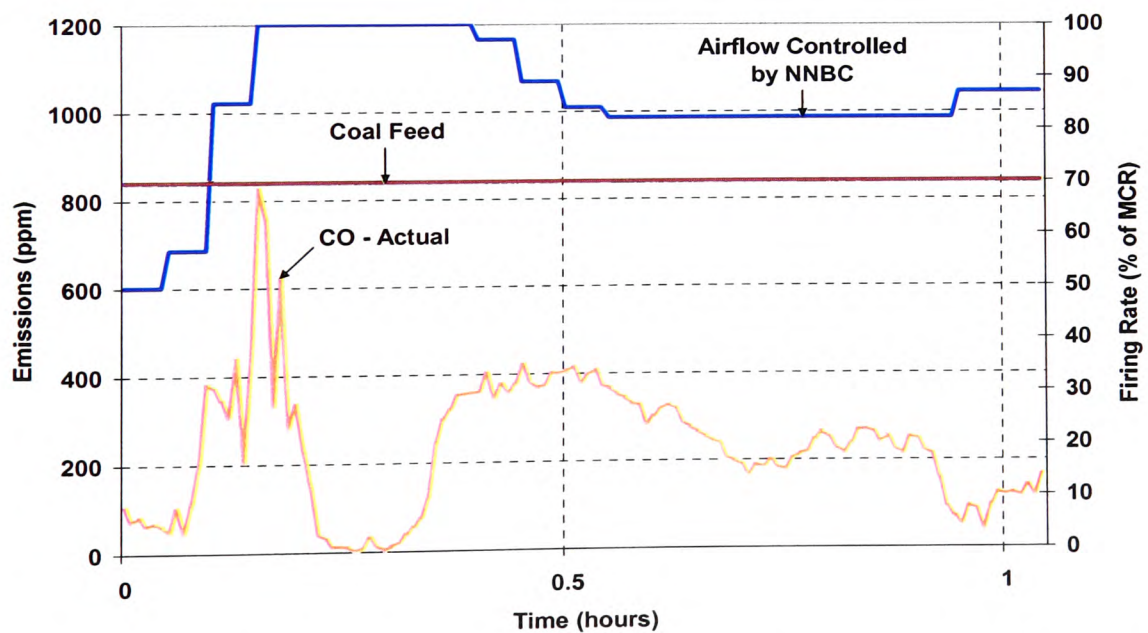


Figure 7.14 Actual CO Emission following Combustion Optimisation Test at Constant Load of 70% of MCR without CO Neural Model (Test Profile 2) – *Test 26*

### **Results Obtained at a Constant Load of 60% of MCR – Test 27**

In order to impose a stiffer test on the performance of the neural models, *Test 27* was conducted at a constant load of 60% of MCR (Figures 7.15 and 7.16). *Training Model 13* and *Training Model 15* obtained from the training of “*Test 18 Data*” at a constant load of 70% of MCR was used to predict the O<sub>2</sub> and CO. As can be seen in Figure 7.15, this validation test was started at a high excess air with the initial settings of the coal feed and airflow being 60% and 90% of MCR. From observation, the O<sub>2</sub> neural model has performed very well, bringing the oxygen level into the target band of 9 to 11% within 20 minutes. In addition, the prediction made by the O<sub>2</sub> neural model compared to the actual results is very good. As for the magnitude of airflow alteration, smaller adjustments were once again imposed by the NNBC when using the O<sub>2</sub> neural model to fine tune the excess air. This lead to the oxygen concentration remaining in the target band for 52% of the time of the test. The reason the actual oxygen was not reduced was because the predictions made by the O<sub>2</sub> neural model were within the target band and therefore, no action was taken by the NNBC to trim the oxygen.

Figure 7.16 shows the results obtained following the combustion optimisation test at a constant load of 60% of MCR for CO and NO<sub>x</sub>. Although the prediction in the first half was not in good agreement with the actual one, the second half was very close to the actual reading taken by the flue gas analyser. However, the control action (smaller magnitude of airflow adjustment and appropriate air fuel ratio) imposed by the NNBC integrated with the CO neural model maintained the overall CO emission below the target limit of 1000ppm (normalised to 6% oxygen). The NO<sub>x</sub> emissions possess no cause for concern with a mean of 266ppm being recorded.

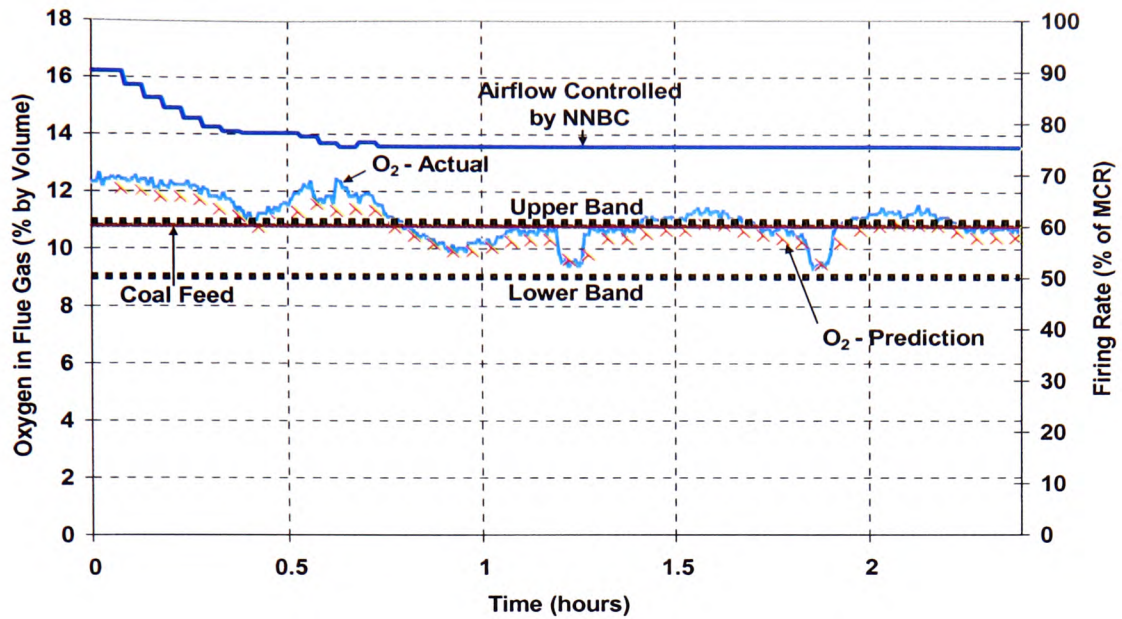


Figure 7.15 Predicted & Actual Oxygen Response following Combustion Optimisation Test with Unseen Data at Constant Load of 60% of MCR with O<sub>2</sub> Neural Model Using *Training Model 13 – Test 27*

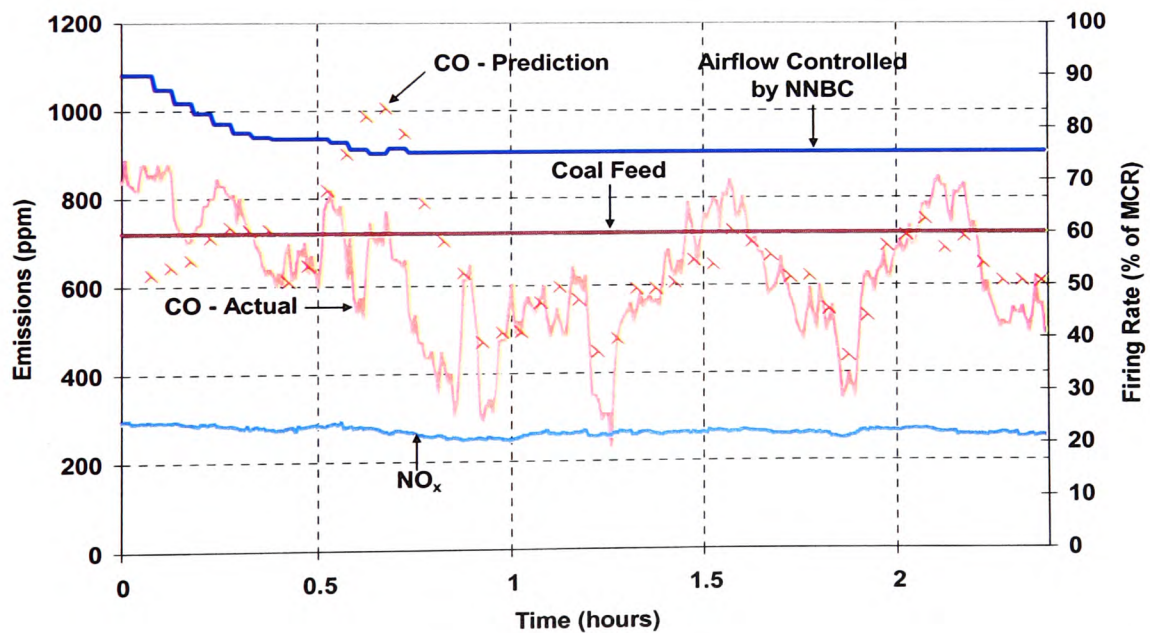


Figure 7.16 Predicted & Actual CO & NO<sub>x</sub> Emissions following Combustion Optimisation Test with Unseen Data at Constant Load of 60% of MCR with CO Neural Model Using *Training Model 15 – Test 27*



### 7.2.2 Hot Water Temperature Control Experiments with the NNBC

The objective of these control experiments was to test the performance of the developed NNBC on the 3.7MW industrial stoker boiler located at HMP Garth, and to compare the results obtained with the existing plant PID control system. The load demand in this case was the hot water temperature, and in addition to tracking the water temperature set point, the NNBC also trimmed the oxygen based on the target oxygen band derived during the final commissioning test (Section 5.2) that summarised in Table 7.3. As a result, there were two parameters which the NNBC needed to control, the primary control loop tracked the process parameter set point while the secondary control loop trimmed the oxygen. Details of the NNBC programme for hot water temperature control experiments can be found in Appendix E.

Table 7.3 Oxygen Target Band at Different Range of Firing Rate in Percentage of MCR

Range of Firing Rate in % of MCR	Final Target Optimum Oxygen Band
$16.67\% \leq \text{MCR} \leq 35\%$	13% to 16%
$36\% \leq \text{MCR} \leq 50\%$	11% to 13%
$51\% \leq \text{MCR} \leq 70\%$	9% to 11%
$71\% \leq \text{MCR} \leq 100\%$	7% to 9%

Five hot water temperature control tests are discussed here whilst burning Bean coal. The experiments include the plant response under NNBC control following a temperature set point change from 105°C to 120°C and vice versa and also the plant response under NNBC control with and without the O<sub>2</sub> and CO neural models whilst tracking the hot water temperature set point of 120°C. The later test was also conducted under conventional PID control and the results are discussed. As with earlier discussion, the plant response under the influence of the NNBC and the conventional PID controller are discussed with reference to the oxygen concentration in the flue gas, CO and NO<sub>x</sub> emissions.

### **Plant Response Under NNBC Control following a Temperature Set Point Change from 105°C to 120°C – Test 28**

Figures 7.17 and 7.18 show the response of the plant under NNBC control to the set point change from 105°C to 120°C. Upon detection of the error between the actual temperature and the desired set point, the NNBC ramped up the firing rate to full load in two consecutive steps and took 26 minutes to reach the set point temperature at the desired 120°C. The corresponding oxygen concentration was on average 6%, which was 1% lower than the associated target band of 7 to 9%. As a result, the coal feed and airflow trends start deviating 54 minutes into the experiment as the NNBC attempts to bring the oxygen level into the target band at steady state. However, a few minutes later there was a little overshoot in hot water temperature 1 hour into the experiment which resulted in priority being given to the firing loop (Figure 7.17). As a result, the coal feed and airflow were decreased in three consecutive steps to maintain the hot water temperature set point. This lower firing rate brought the hot water to the desired 120°C and also leads to the oxygen level being maintained within the target band. The effect of the automatic ash removal system was quite obvious in this experiment, and can be observed at 10, 50, 87 and 126 minutes into the experiment although the impact on the performance of the NNBC was insignificant (Figure 7.17).

With a steady adjustment of the firing rate taken by the NNBC, the pollutant emissions also demonstrated a stable pattern (Figure 7.18). The corresponding CO emission in this experiment was well below the target limit of 1000ppm (normalised to 6% of oxygen) with peak of up to 600ppm. In addition, the emission of NO<sub>x</sub> was well below future legislative limits for coal fired boilers of this range with average emissions of 266ppm being recorded.

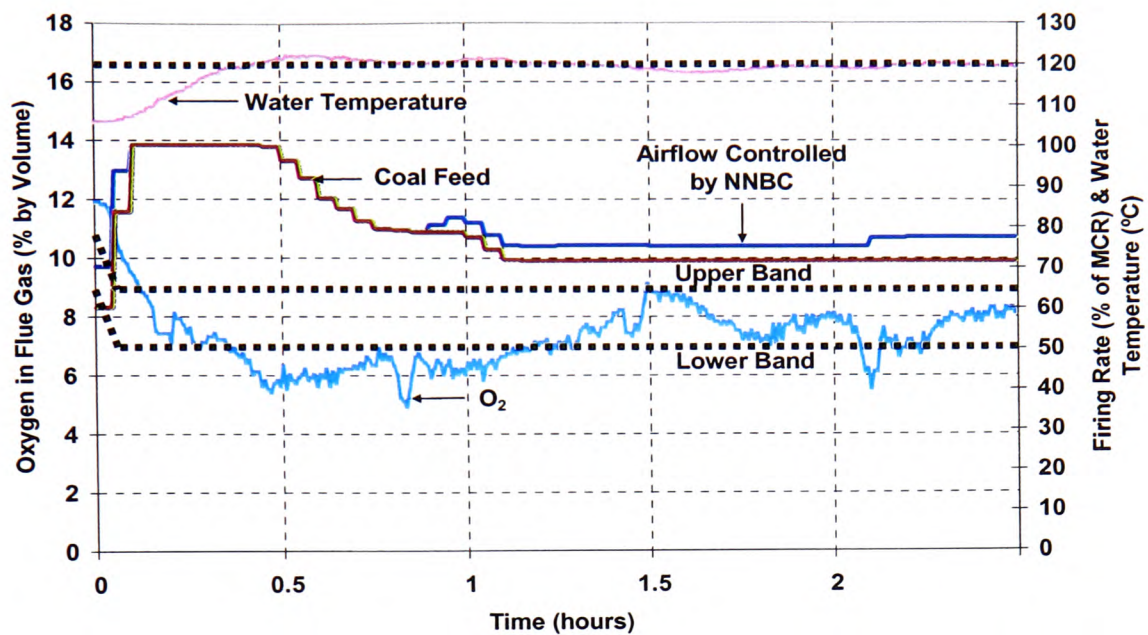


Figure 7.17 Water Temperature & Oxygen Concentration under NNBC Mode following A Step Change in the Hot Water Temperature from 105°C to 120°C – Test 28

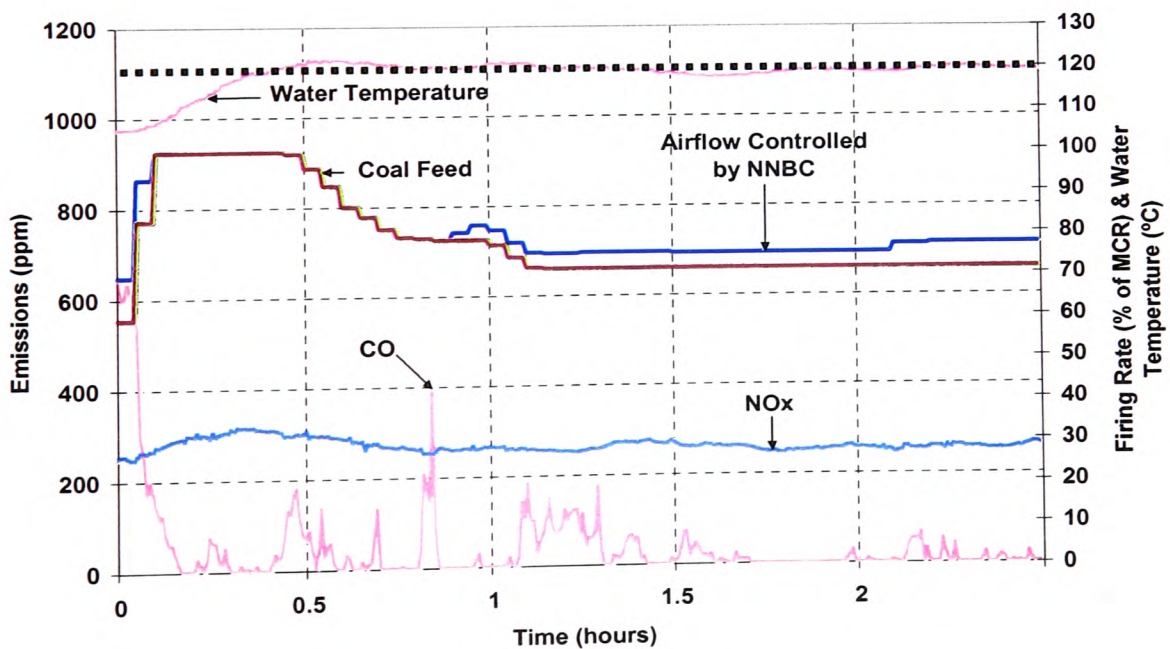


Figure 7.18 Pollutant Emissions under NNBC Mode following A Step Change in the Hot Water Temperature from 105°C to 120°C – Test 28

### **Plant Response Under NNBC Control following a Temperature Set Point Change from 120°C to 105°C – *Test 29***

The set point change in this experiment was from 120°C to 105°C and the response of the plant under the influence of the NNBC is shown in Figures 7.19 and 7.20. For this test, the firing rate was ramped down to full turndown in two steps as the NNBC detected the error between the actual temperature and the desired set point. The time taken for the water temperature to decrease from 120°C to 105°C was 15 minutes. However, an undershoot of 6°C in the water temperature can be seen in Figure 7.19 before the firing rate was gradually brought up in order to compensate for the temperature variation. The corresponding oxygen concentration in the first half was well within the desired green band even though the target band depends on the firing rate. However, an overshoot of the oxygen (from 10% to almost 13%) followed by a 5°C drop in the water temperature to 100°C occurred just before 2 hours into the experiment. This could have occurred because of an increased demand for hot water or as a result of poor coal distribution due to inappropriate stoking practices giving rise to 'holes' in the bed (less coal was being fed onto the grate) therefore allowing under-grate air to escape thus reducing the boiler efficiency. The consequence of the small divergence in the hot water temperature (5°C) from the set point of 105°C resulted in instability in the controller output. This situation could have been dealt with by the NNBC with the oxygen neural model as the model prediction, that is partly based on the given firing rate (recorded before the condition deteriorated) should have predicted a relatively reasonable oxygen level thus avoiding the unnecessary control action caused by the disturbance in the bed and the consequent oscillation in the controller output.

The CO emission throughout the entire test was acceptable except for intermittent peaks at turndown (Figure 7.20 at 0.1 and 2.7 hours into the experiment resulting from the fuel bed being built up from high fire and insufficient combustion air) with an overall average emission of 412ppm being recorded. On the other hand, the NO<sub>x</sub> emission in this experiment was lower than those shown in Figure 7.18 (*Test 28*). However, the NO<sub>x</sub> emission showed no cause for concern with average emission of 226ppm being taken by the flue gas analyser.

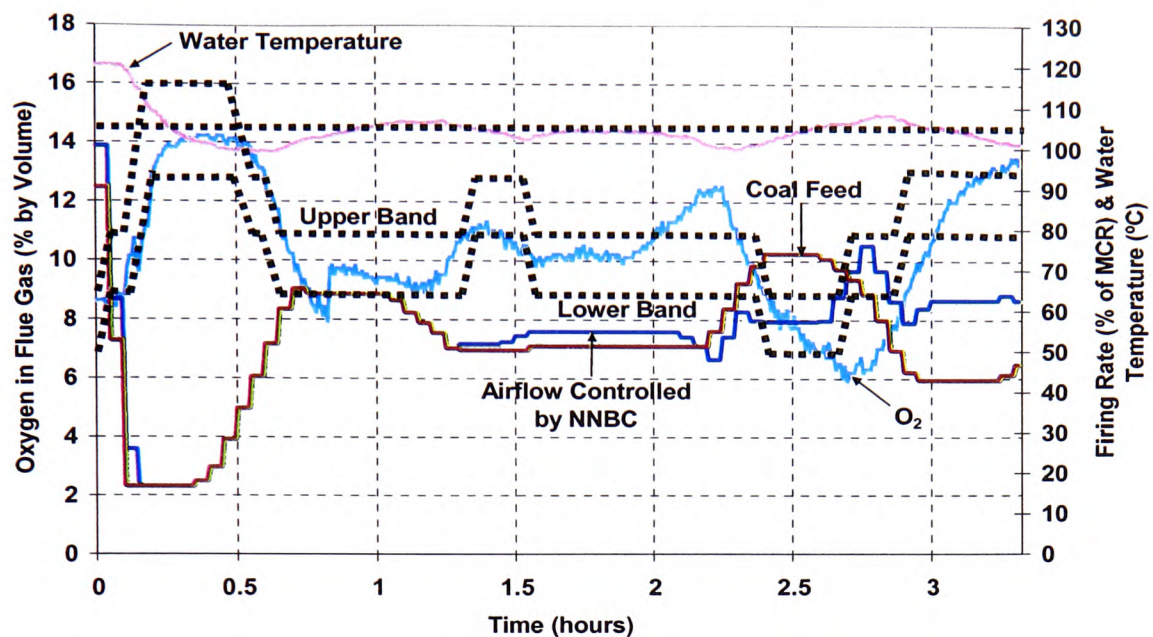


Figure 7.19 Water Temperature & Oxygen Concentration under NNBC Mode following A Step Change in the Hot Water Temperature from 120°C to 105°C – Test 29

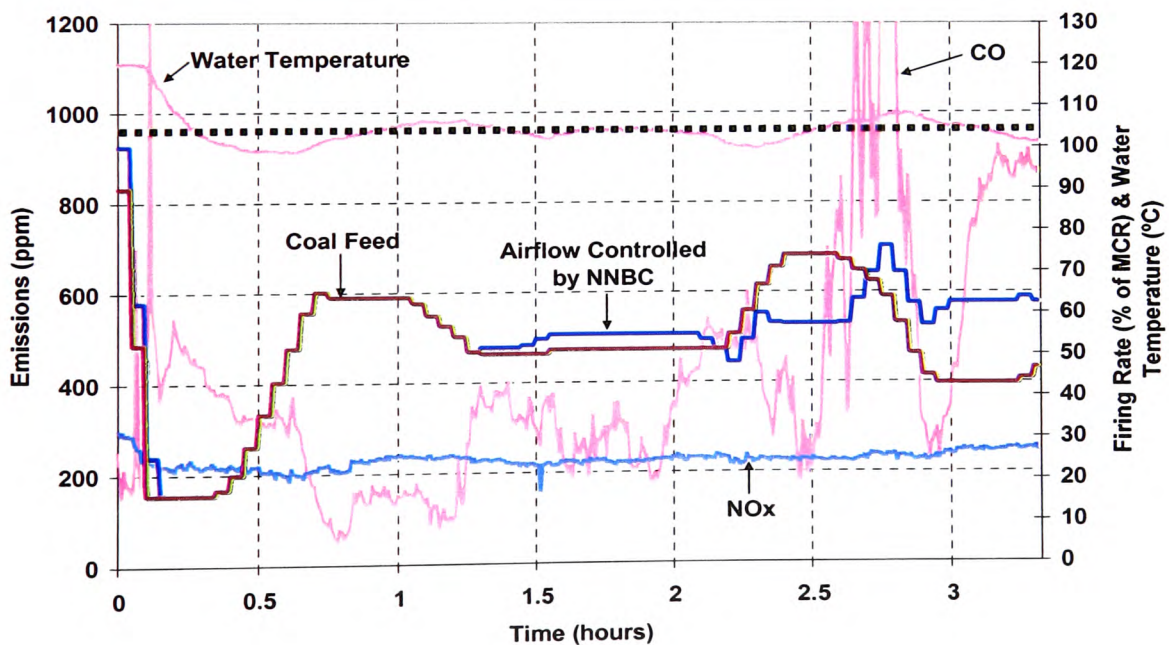


Figure 7.20 Pollutant Emissions under NNBC Mode following A Step Change in the Hot Water Temperature from 120°C to 105°C – Test 29



### **Plant Response Under NNBC Control Tracking a Hot Water Temperature Set Point at 120°C – Test 30**

Instead of changing the process variable from one set point to another, the NNBC was set the task of maintaining the hot water at a set point (*Test 30*). Figures 7.21 and 7.22 show the plant response under the influence of the NNBC whilst keeping the hot water temperature at 120°C. As can be seen in Figure 7.21, the coal feed and airflow were gradually brought down at the beginning of the test by the NNBC in an attempt to maintain the water temperature at 120°C. However, the NNBC tended to alter the load more frequently and this led to fluctuations in the oxygen level within and slightly outside the target band. The effect of the automatic ash removal system is clearly visible in this experiment as indicated by significant drops in the oxygen concentration at equal intervals over the 4-hour test. The overshoots of the oxygen at 1.5 and 3.25 hours into the experiment followed by slight drops in the water temperature perhaps occurred due to uneven coal distribution. Although the oxygen level tends to fluctuate between the 7 and 9% levels, and sometimes lies outside this range, for 81% of the total test the oxygen concentration was inside the desired green band. The CO emission in this case oscillates between 100 to 400ppm with an overall average emission of 220ppm and occasional peaks at turndown of up to 1000ppm. As for NO<sub>x</sub> emission, similar trends to those of Figures 7.18 and 7.20 (*Tests 28 and 29*) can be observed from Figure 7.22 with average emission of 262ppm being recorded.

Figures 7.23 and 7.24 show the training results for the O<sub>2</sub> and CO neural models that were not covered in Chapter 6 under the Selection of Training Data. In order to test the performance of the NNBC integrated with the neural models whilst maintaining the hot water at a set point temperature, data collected from *Test 30* as shown in Figures 7.21 and 7.22 were used to train the O<sub>2</sub> and CO neural models six-step into the future. These neural models were then incorporated into the NNBC for online simulation during the hot water temperature control test that will be covered and discussed in the following section.

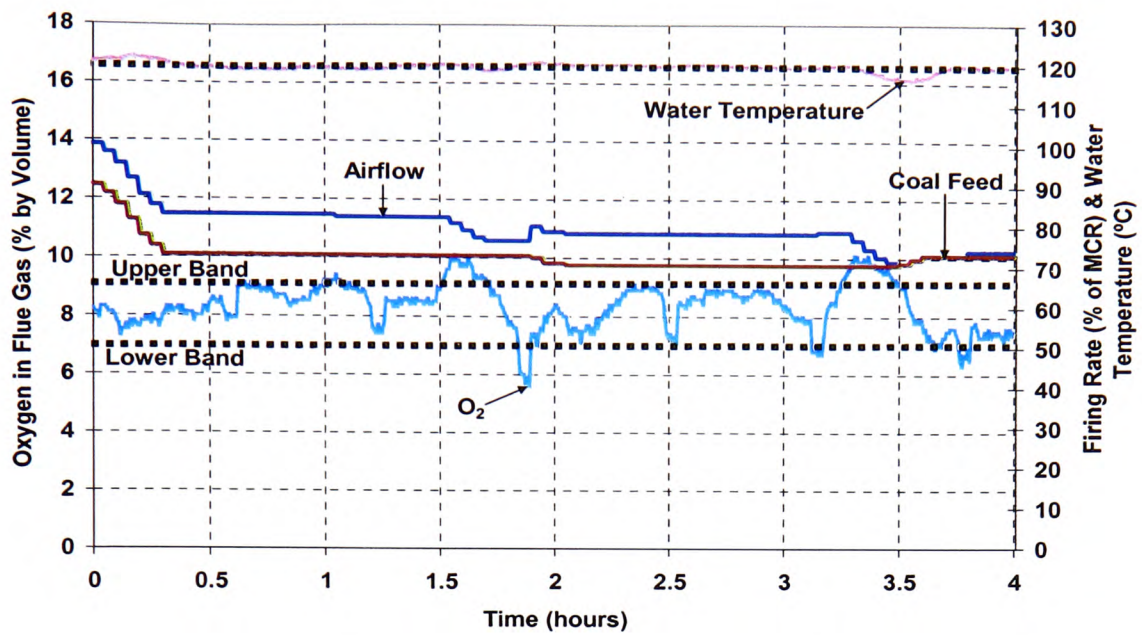


Figure 7.21 Water Temperature & Oxygen Concentration under NNBC Mode While Tracking Hot Water Temperature Set Point at 120°C – Test 30

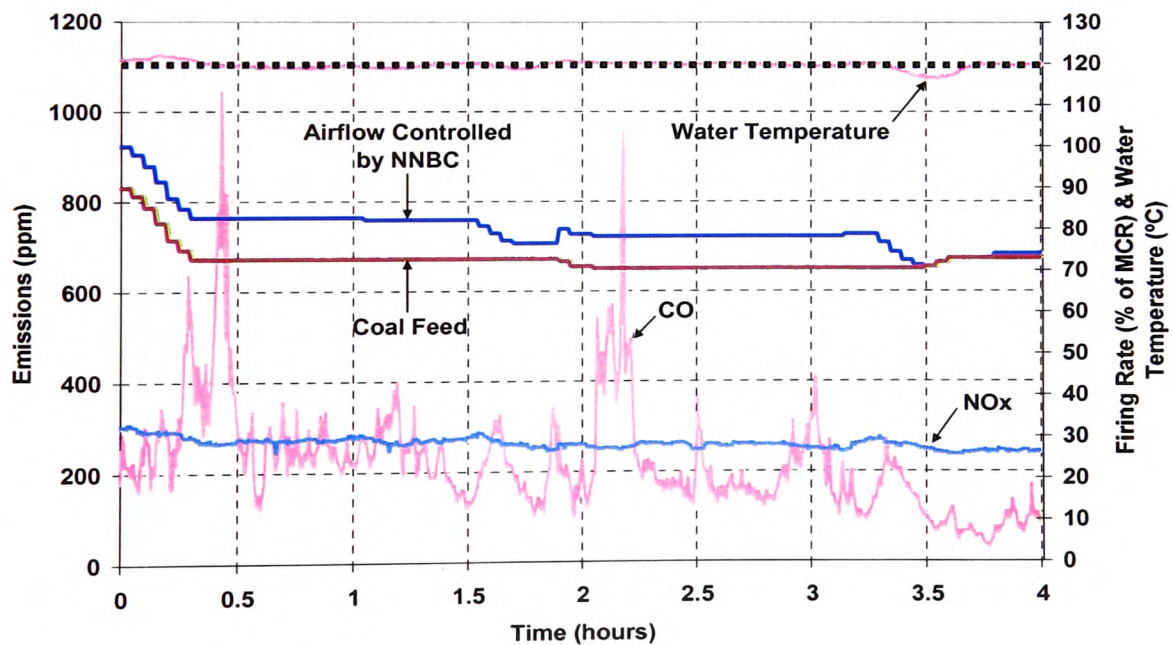


Figure 7.22 Pollutant Emissions under NNBC Mode While Tracking Hot Water Temperature Set Point at 120°C – Test 30



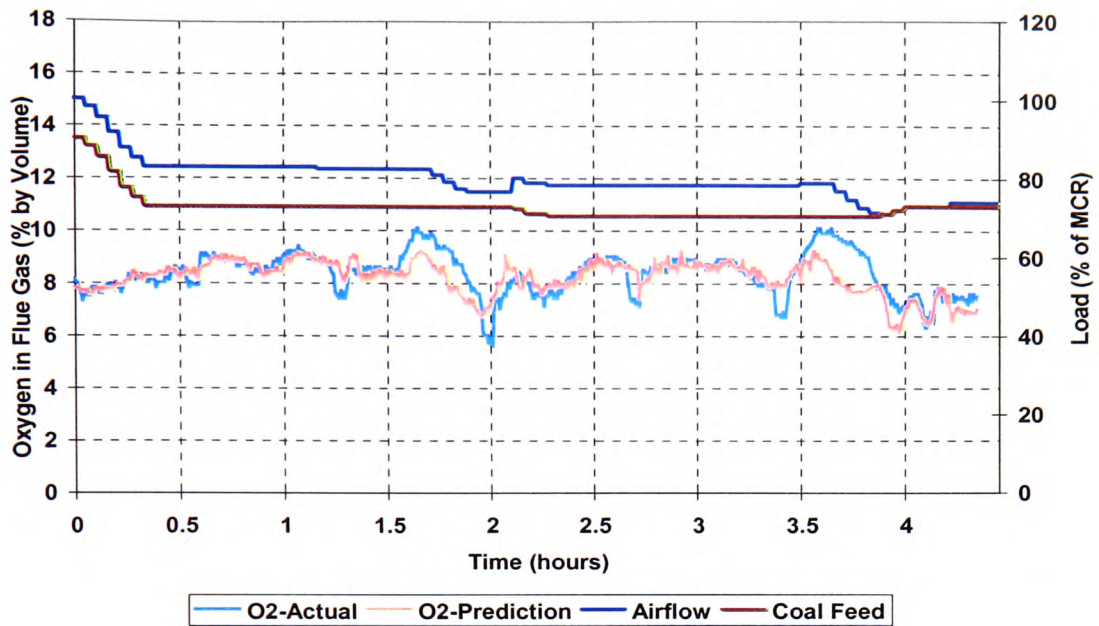


Figure 7.23 Six Steps Ahead Prediction by the ARX Model (nnarx) for Oxygen in the Flue Gas While Tracking Hot Water Temperature at 120°C Using *Test 30* Data (1<sup>st</sup> & 3<sup>rd</sup> Quarter Data Set for Training & 2<sup>nd</sup> & 4<sup>th</sup> Quarter Data Set for Validation - *Training Model 16*)

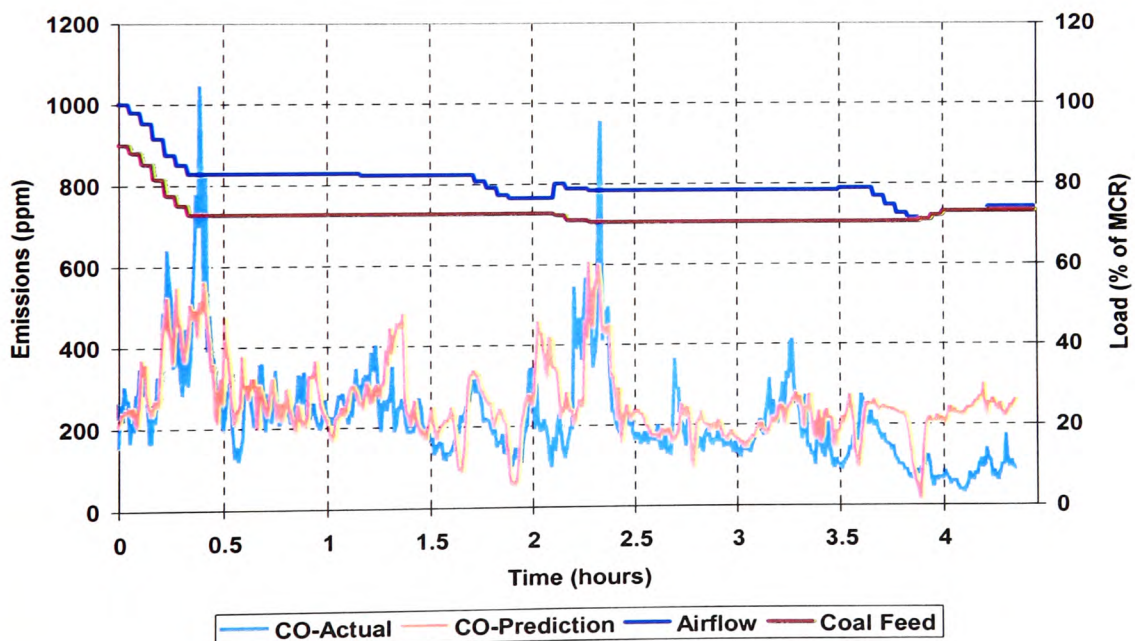


Figure 7.24 Six Steps Ahead Prediction by the ARX Model (nnarx) for CO Emission While Tracking Hot Water Temperature at 120°C Using *Test 30* Data (1<sup>st</sup> & 3<sup>rd</sup> Quarter Data Set for Training & 2<sup>nd</sup> & 4<sup>th</sup> Quarter Data Set for Validation - *Training Model 17*)

### **Plant Response Under NNBC Control with O<sub>2</sub> and CO Neural Models, Whilst Tracking a Hot Water Temperature Set Point of 120°C – Test 31**

Figures 7.25 and 7.26 show the results obtained from the response of the plant under the influence of the NNBC with the O<sub>2</sub> and CO neural models whilst keeping the hot water at a set point temperature of 120°C (*Test 31*). As shown in Figure 7.25, the model of O<sub>2</sub> has performed reasonably well to maintain the actual oxygen inside the target band whilst keeping the water temperature at the desired 120°C. An overshoot of the oxygen occurred at 0.75 hours (an increase in the excess air from 9% to 11%) exceeding the upper target, followed by a slight drop in the water temperature which was probably caused by a disturbance in the fuel bed. However, no action was taken by the NNBC as the oxygen concentration predicted by the O<sub>2</sub> neural model was within the target band. This control decision was justified by the fall in the actual oxygen back into the target band and the recovery of the water temperature to its initial set point a few minutes later. If the airflow had have been altered in order to decrease the excess air, the control of the boiler could have been jeopardised. Furthermore, the inevitable interruptions caused by the automatic ash removing system were noticeable at equal intervals but the impact on the performance of the NNBC was insignificant. By observation, most of the actual and predicted oxygen readings lay slightly outside or on the upper limit of the target band. Consequently, for only 65% of the total test did the actual oxygen concentration lie inside the target band. This percentage figure could have been increased to 83% if the oxygen readings which were 0.1% or 0.2% above the upper limit band were taken into account.

Although the prediction performed by the CO neural model was less comparable to the actual one than the O<sub>2</sub> model, the actual CO emission in this case was well controlled by the NNBC and remained below the target limit of 1000ppm (normalised to 6% of oxygen). An average emission of 243ppm and occasional peaks of up to 1300ppm were recorded for the test (Figure 7.26). As for NO<sub>x</sub> emission, it shows no cause for concern with average emission of 283ppm being recorded.

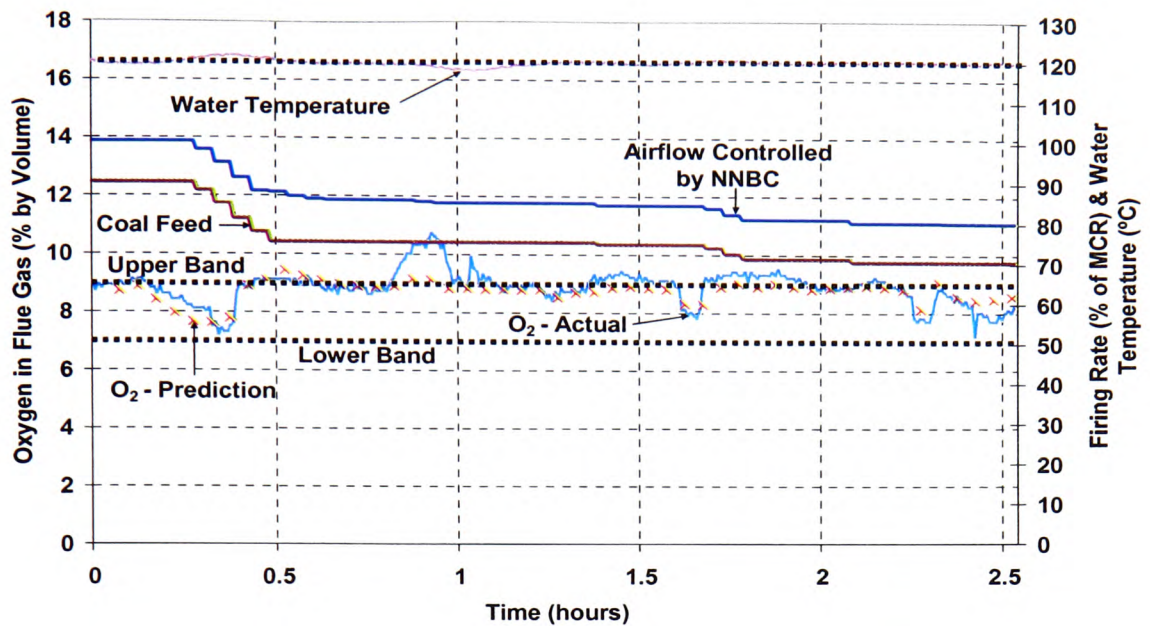


Figure 7.25 Water Temperature & Oxygen Concentration under NNBC Integrated with O<sub>2</sub> Neural Model Mode While Tracking Hot Water Temperature Set Point at 120°C – Test 31

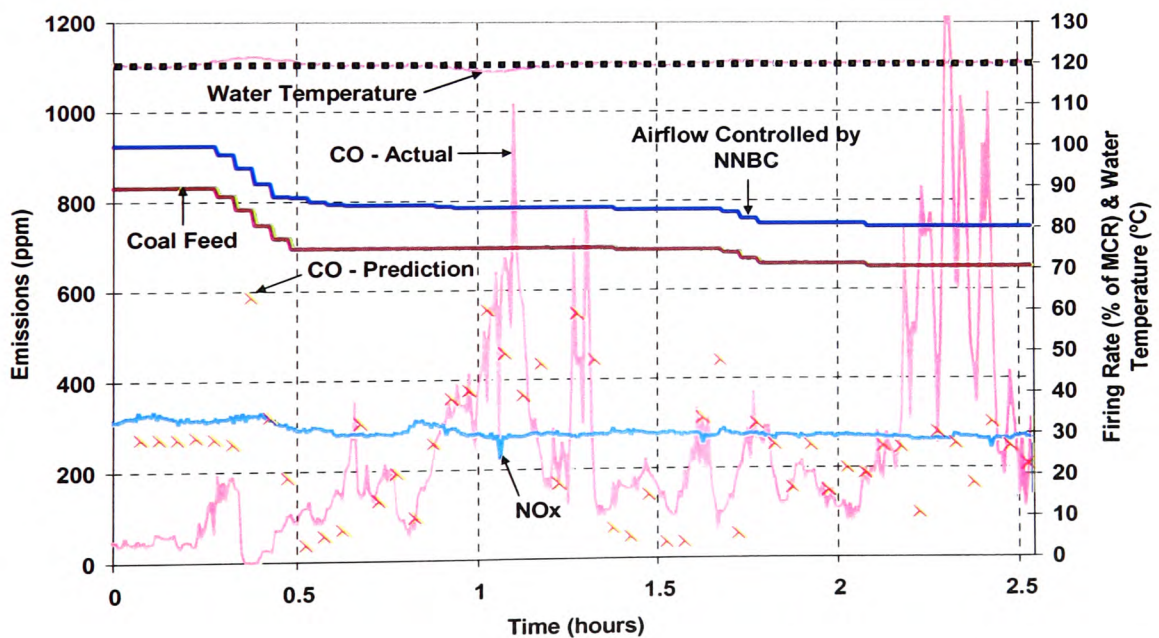


Figure 7.26 Pollutant Emissions under NNBC Integrated with CO Neural Model Mode While Tracking Hot Water Temperature Set Point at 120°C – Test 31

### **Plant Response Under the PID Controller Whilst Tracking a Hot Water Temperature Set Point of 120°C – Test 32**

Figures 7.27 and 7.28 show the results obtained whilst maintaining the hot water temperature at a set point of 120°C by the existing plant PID controller (*Test 32*). It can clearly be seen that the PID controller tended to alter the firing rate much more frequently than the NNBC controller. Furthermore, the load variation imposed by the PID controller was greater than the NNBC (full load to 60% of MCR as compared to full load to above 70% by the NNBC) in an attempt to maintain the hot water temperature at 120°C. The corresponding oxygen concentration possesses a similar sinusoidal pattern to the firing rate but in the opposite direction as would be expected. It would also appear that the boiler was tending to oscillate just before the end of the test. As a result, for only 46% of the test did the oxygen readings lie inside the target band. Although the oxygen trimming system was not available as the PID controller was a single loop process controller, the pattern of oscillations in the controller output and the oxygen concentration (especially at the end of the test) resembles that of critical stability with a great possibility of becoming unstable.

Figure 7.28 shows the CO level in the flue gas for *Test 32*. The overall CO emission in this case was acceptable although there was a peak of 2000ppm when the firing rate change became greater. As with the previous tests under the influenced of NNBC (*Tests 30 & 31*), the emission of NO<sub>x</sub> possesses no cause for concern with average emission of 264ppm being recorded.



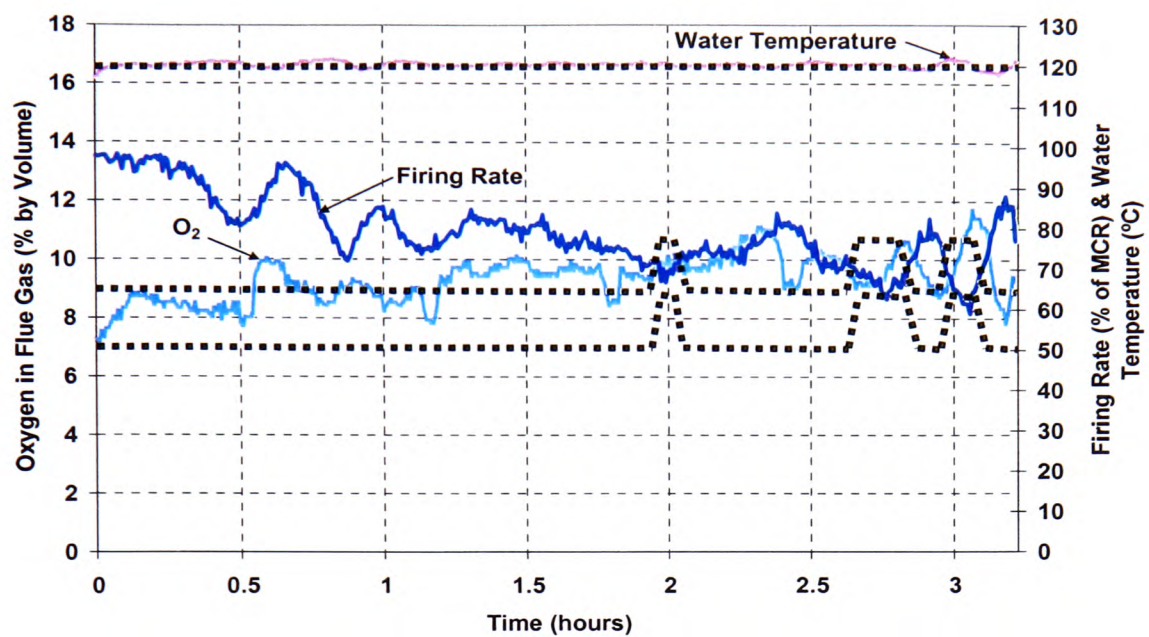


Figure 7.27 Water Temperature & Oxygen Concentration under Plant PID Controller While Tracking Hot Water Temperature Set Point at 120°C – *Test 32*

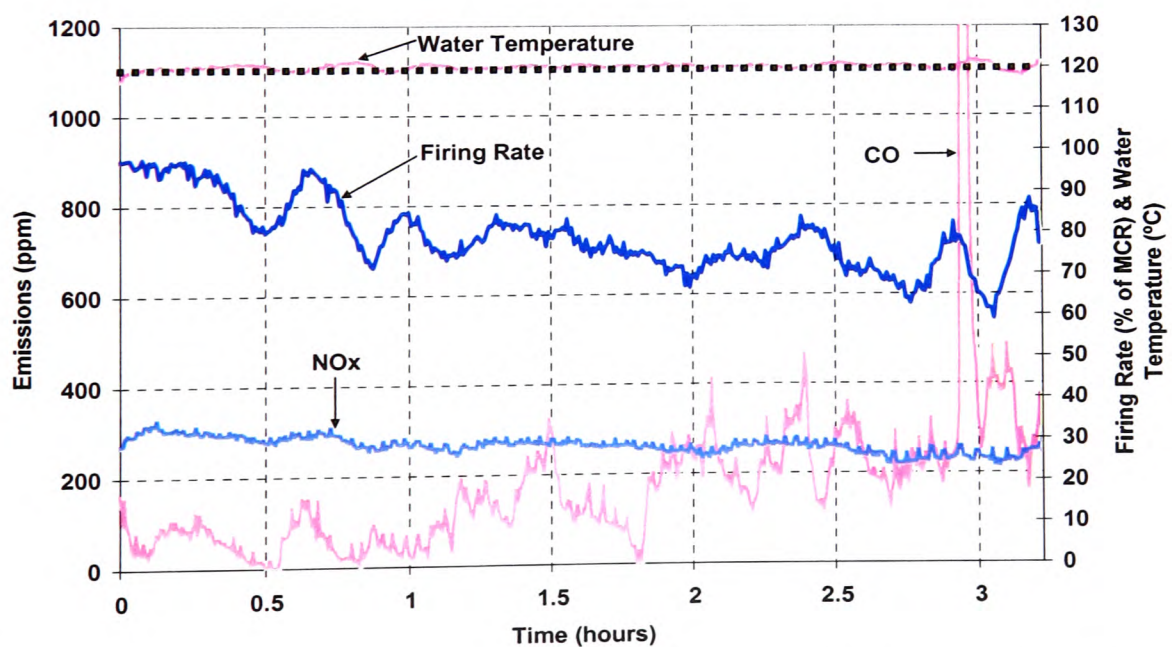


Figure 7.28 Pollutant Emissions under Plant PID Controller While Tracking Hot Water Temperature Set Point at 120°C – *Test 32*

### 7.3 Summary of Chapter 7

Overall, it can be concluded that the control experiments for combustion optimisation and hot water temperature control have been successfully carried out. For the combustion optimisation test, the NNBC with the O<sub>2</sub> and CO neural models was able to bring the initial high or low excess air and the corresponding oxygen into the pre-defined oxygen target band. This was even true when the boiler was operated with totally unseen data at 60% of MCR (*Test 27*). In addition, the NNBC was able to operate the industrial scale stoker boiler to meet the demand required in a more stable manner than the plant PID controller, in addition to trimming the oxygen level. In other words, the NNBC was able to deliver the load required with less fluctuation than the plant PID controller with a lower excess air, hence minimising the sensible heat loss from the boiler therefore improving the overall boiler efficiency. In so doing the NNBC managed to maintain the pollutant emissions below probable future legislation limits.

## Chapter 8 Conclusions & Further Recommendation

Although the use of renewable energy like bio-fuels to replace coal as a primary source of energy has been growing rapidly worldwide over the past few years, there is still a strong indication that coal will remain a major source of energy for power generation as well as for industrial and domestic applications for some time, due in part to higher prices and inconsistency of supply of bio-fuel. Moreover, with the volatility of crude oil prices and the inevitable decline in the supply, the importance of coal to sustain global economic progress and improve the standard of living cannot be under estimated. However, with the introduction of stringent environmental legislation on emission limits from industrial coal-fired plant, focus has been placed on efficiency and environmental improvements through changes in operating practice and cleaner ways in which coal can be utilised for heat generation.

### 8.1 Identification of Combustion Derivatives Using Black Box Models

The complex non-linear lump coal combustion process on the chain grate stoker in addition to the practical difficulties involved in manipulating various parameters in controlling such a process justifies the use of ANNs for this research project. In this study, training and testing of a comprehensive neural network ARX model to predict the combustion process and pollutant formations were accomplished. It must be stressed that these models were developed and tested using data extracted from the experiment conducted on the pilot-scale 0.7MW chain grate stoker test facility. In this case, a novel prediction at six steps into the future of the combustion derivatives ( $O_2$ ,  $NO_x$  and  $CO$ ) emanating from the stoker test facility has been investigated rather than one step ahead prediction as previously considered in BCURA B35. This is particularly useful for complex time-varying systems (i.e. coal combustion on chain grate stoker) where the prediction horizon has to be expanded so that the essential dynamics of the process can be covered, reducing the effect of any time-delay. From the literature review, it was suggested that a prediction of just two minutes would



enable a control system to act on future problems (combustion process and gaseous products) before they occurred, thereby ensuring more stable boiler operation thus improving thermal efficiency and maintaining pollutant emissions below future limits. Upon completion of model training and validation with the gathered data, results showed that the developed models delivered an accurate prediction over a time horizon of three minutes. Despite some poorer results obtained during the prediction process, the overall results are encouraging enough to make use of a neural network to predict the  $O_2$ , CO and  $NO_x$ . The suitability of the ARX structure in modelling the combustion process and pollutant emissions into future is further substantiated with its implementation into the NNBC system to control the 3.7MW stoker boiler plant.

## 8.2 Application of the Neural Network Based Controller to an Industrial Stoker Boiler

Following the encouraging results obtained during the combustion modelling on the 0.7MW test facility, the non-linear ARX models neural networks were integrated within a carefully devised control strategy, which was based on the experience and decision making process of an expert human operator. This was written in the MATLAB<sup>TM</sup> and LaBVIEW<sup>TM</sup> computing environments. The novel NNBC strategy utilised the data collected during the commissioning tests for optimal excess air level settings and the gathered information was used to train ANNs to imitate these settings to ensure stable and efficient combustion whilst minimising pollutant emissions based on future predictions of the combustion derivatives. For combustion optimisation test, the NNBC with and without the neural models was tested at constant loads of 40% and 70% of MCR. Test results showed that the NNBC with the  $O_2$  and CO neural models performed in a better manner than the one without the neural models when bringing the sub-optimum excess air level into the pre-defined target band. This was particularly obvious with the stable trend of airflow adjustment taken by the NNBC with the neural models together with the ability to avoid disturbances caused by the automatic ash removal system and poor stoking practices. In addition, the performance was also encouraging when tested with totally unseen data at a firing rate of 60% of MCR.

In addition to the combustion optimisation test, the NNBC was able to operate the 3.7MW industrial stoker boiler during a temperature set point change from 105°C to 120°C and vice versa, and the NNBC with and without the neural models were also able to maintain the hot water temperature at a set point of 120°C. This test was also studied under a conventional PID controller. By comparing the test results attained under the influence of these three control strategies, the performance of the NNBC would appear to be superior to the PID controller when tracking the hot water temperature set point. As a result, a 0.5 to 1% improvement in thermal efficiency as estimated from the percentage loss in the dry flue gas using the Siegert formula based partly on the thermal efficiency evaluating method described in BS 845, was exhibited by the NNBC. Furthermore, most of the predicted oxygen concentrations lay at the top of the target band (9% of oxygen level) as the NNBC was configured so that the airflow adjustment network would only take action if the oxygen fell outside the target band (Figure 7.25). In other words, the airflow adjustment rule could have been configured to narrow the 'no' action band limit so that the control action would reduce the oxygen level to 8% which would have been an improvement of 1.3% a significant improvement over the PID controller. In addition, the instability in the PID controller output (in particular the oscillations in the firing rate and the oxygen concentration just before the end of the test, Figure 7.27), a further 0.5% of thermal efficiency improvement could be obtained.

With respect to the results obtained from the NNBC, the oxygen level achieved by the NNBC controller with the O<sub>2</sub> and CO models was more stable than the one without the neural models. This was mainly due to the aptitude of the novel NNBC incorporated with the neural models avoiding unnecessary changes in load and excess air caused by temporary disturbances in the boiler operating mechanisms. The stable oxygen level controlled by the NNBC with the O<sub>2</sub> and CO models would thus further enhance the applicability of limiting the 'no' action band limit. As for the plant PID controller, the load change imposed on the stoker was greater with a consequence that for only 46% of the total test did the oxygen readings lie inside the target band as compared to 65% and 81% for the NNBC with and without the neural models over the total test duration of 2.5 and 4 hours, respectively. However, it will be worth mentioning again that the percentage figure for the neural model

controller could have been higher if the actual oxygen readings which were slightly above the upper limit were taken into account. Finally, it can be concluded that the developed NNBC has been able to operate the industrial scale stoker boiler in delivering the demand required with less fluctuation than the plant PID controller whilst consistently keeping the excess air level to a minimum, hence minimising the sensible heat loss from the boiler and therefore improving the overall thermal efficiency. In so doing, the NNBC managed to maintain the pollutant emissions within probable future legislation limits that will be imposed by the European Commission.

### 8.3 Recommendation for Further Work

Throughout the entire course of this research project, it is the author's conviction that the implementation of AI techniques using ANNs to model the complex non-linear lump coal combustion on chain grate stoker can be further researched. The use of ANNs is particularly necessary so as to offer the stoker boiler plant better reliability and assurance to the industrial user when it is left functioning in a fully automatic mode. By taking advantage of ANNs which are able to learn should help to make the stoker boiler more attractive and competitive with other appliances in the market place. One approach to this is to develop a NNBC which can automatically cope with a variety of coal types. This is thought to be essential as the commissioning work for burning different types of coal is time consuming and labour intensive. This approach can be achieved by developing a setting network which includes different types of coal properties together with the load demand required as inputs parameters to the network. Basically, the function of this setting network would be to provide the initial 'near optimum' settings of coal feed and airflow for the desired load and for the given coal properties. The input variables to this setting network would be the ultimate coal analysis data (calorific value, carbon, hydrogen, nitrogen and oxygen) together with the demand required (i.e. error between the hot water temperature and hot water temperature set-point) while the outputs would be the three input parameters to the stoker boiler plant (rotary valve speed, grate speed and airflow). As with all empirical work, data would have to be gathered from carefully designed experiments in order to generate reliable information for neural network training and validation. Figure 8.1 below shows a proposed schematic of the setting

network architecture while Figure 8.2 shows the inclusion of coal properties as input parameters to the setting network encoding into the overall NNBC system for the chain grate stoker boiler.

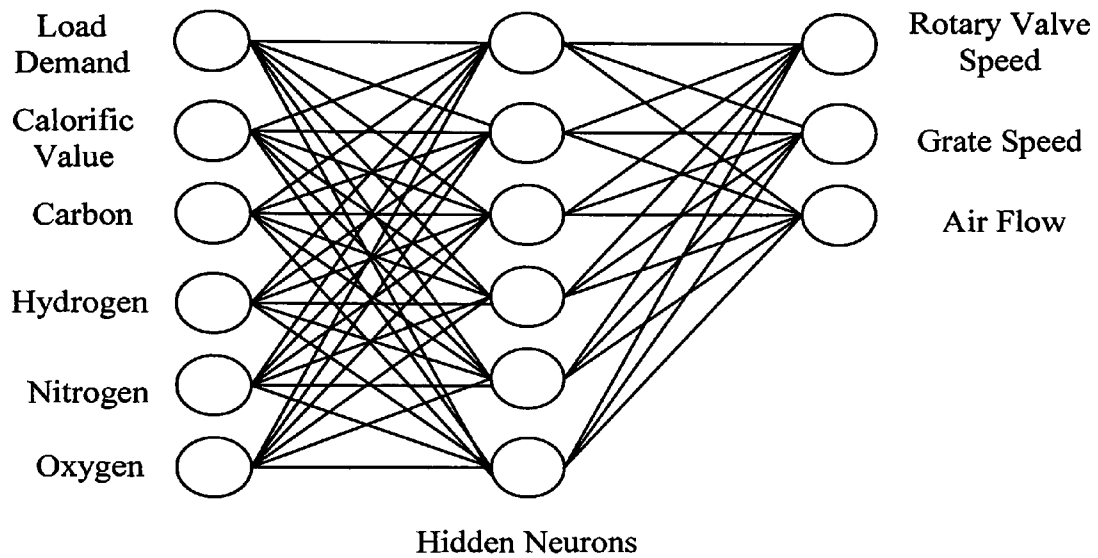


Figure 8.1 Propose Setting Network Architecture

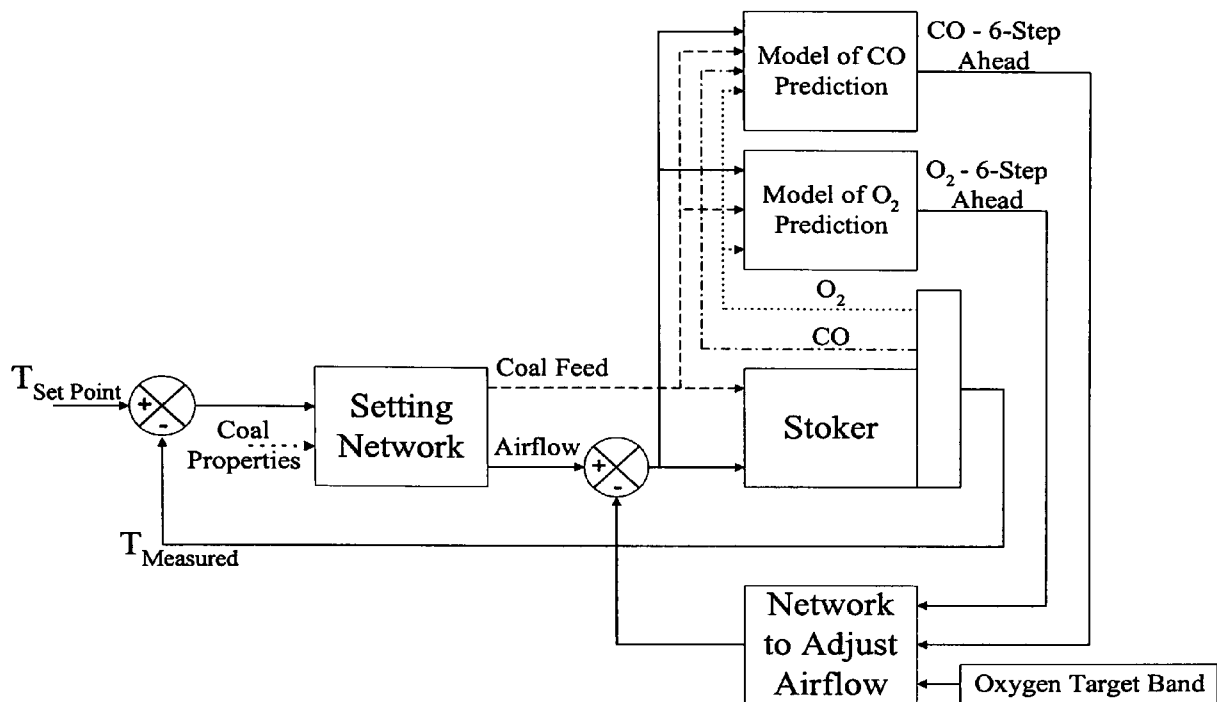


Figure 8.2 The Inclusion of Coal Properties as Input Parameters to the Setting Network  
Encoding into the Overall NNBC System Strategy

Perhaps one of the areas that might be worth investigating would be to include a CCD video camera to view combustion conditions on the fuel bed. With the use of the CCD video camera together with the Image Acquisition Devices (available from the National Instruments<sup>TM</sup>), any 'holes' in the bed (as a result of improper stoking practices) could be captured and pre-processed using the MATLAB<sup>TM</sup> Image Processing Toolbox. With this toolbox, the binary version of the image can be created and can be used for statistics computation of objects in the image [MATLAB<sup>TM</sup> Image Processing Toolbox, 2003]. The detection of any 'holes' in the bed would probably trigger an alarm for a plant operator to take appropriate action if the condition persists. This could offer the prospective user better reliability and assurance when the stoker boiler plant is left on automatic operation by the influence of the NNBC.

As a result of the future emission legislation, other areas that might be worth investigating include the burning of unprepared biomass (i.e. wood chips, short rotation coppice etc) with prepared biomass (i.e. wood pellets) or coal as support fuels which aims to reduce carbon emissions. AI techniques such as fuzzy logic and neural networks could probably be used to develop an “intelligent” software-based operating strategy to ensure the optimum conditions for the combustion of these mixtures and the amount of support fuel that might be required.

## References

- Baines, G. (1999) Neural Networks for Boiler Emission Prediction. *IEEE Instrumentation and Measurement Technology Conference*, **1**, 435-439.
- Bakal, B., Adali, T., Fakory, R., Komo, D., Sönmez, M.K. and Tsaoi, C.O. (1995) Neural Network Simulation of Real Time Core Neutronic Model. *In Proceedings of the Society for Computer Simulation's Simulation Multiconference*, **27(3)**, 160-165.
- Bauer, F.W., Mancini, R.A. and Kimiecik, D. (1991) Mathematical Modelling Development and Application for Evaluation of Fuels on Chain Grate Stoker Boilers. *International Power Generation Conference*, 1-6.
- Berger, D., Landau, M.V., Herskowitz, M. and Boger, Z. (1996) Deep Hydrodesulphurisation of Atmospheric Gas Oil: Effects of Operating Conditions and Modelling by Artificial Neural Network Techniques. *Fuel*, **75(7)**, 907-911.
- Billings, S.A., Jamaluddin, H.B. and Chen, S. (1992) Properties of Neural Networks with Applications to Modelling Non-Linear Dynamical Systems. *Int. J. Control*, **55(1)**, 193-224.
- Booth, R.C. and Roland, W.B. (1998) Neural Network Based Combustion Optimisation Reduces NO<sub>x</sub> Emissions while Simultaneously Improving Thermal Efficiency. *The Proceeding of the American Power Conference*, **2**, 667-672.
- CARNOT On-line Case Study (2000) Chain Grate Stoker with Firebreak at Nottingham City Hospital. *CARNOT Online Case Study: Industrial, Commercial and Domestic Use of Coal*.
- CARNOT On-line Case Study (2000) Post-Combustion Emission Control Technologies. *CARNOT Programme of DG Tren (EC) Energy and Transport*.



- Chen, S. and Billings, S.A. (1990) Non-Linear System Identification using Neural Networks. *International Journal of Control*, **51**(6), 1191-1214.
- Chong, Z.S. (1999) *The Monitoring and Control of Stoker-Fired Boiler Plant By Neural Networks*. Doctoral Dissertation, The University of Glamorgan, South Wales, UK.
- Chong, Z.S., Wilcox, S.J. and Ward, J. (2000) Neural Network Models of the Combustion Derivatives Emanating from A Chain Grate Stoker Fired Boiler Plant. *IEE Seminar on Advanced Sensors and Instrumentation Systems for Combustion Processes*, 6/1-6/4.
- Chong, Z.S., Wilcox, S.J. and Ward, J. (2001) Prediction of Gaseous Emissions from a Chain Grate Stoker Boiler using Neural Networks of ARX Structure. *IEE Proceeding of Science and Measurement Technology*, **148**(3), 95-102.
- Clarke, A.G. and Williams, A. (1992) The Formation and Control of NO<sub>x</sub> Emission. *Chemistry and Industry*, **24**, 917-920.
- Cooke, M.J. and Pragnell, R.J. (1989) Technology to Meet Proposed Environmental Standards. *Proceedings of the First European Fine Coal Conference*, 23-25.
- Demuth, H. and Beale, M. (1998) *Neural Network Toolbox Manual for Use With MATLAB<sup>TM</sup>*. The MathWorks Inc., USA.
- DTI Case Study 004 (1998) *Industrial Boiler Control*. DTI Cleaner Coal Technology Programme.
- DTI Capability Brochures CB001 (2002) *Coal-Fired Industrial Boilers*. DTI Cleaner Coal Technology Programme.

- Dudek, S.A. and Wessel, R.A. (1999) Three-Dimensional Numerical Modelling of Stoker Fired Power Boilers. *Proceedings of the ASME Heat Transfer Division*, **364**(2), 413-423.
- Eki, Y., Hirasawa, K., Nakamura, M. and Oouchi, K. (1997) New Method of Off-Line Adjustment of Feed-Forward Control for Fossil-Fired Plant Main Control System. *Electrical Engineering in Japan*, **119**(1), 55-61.
- Eki, Y., Hirasawa, K. and Nomura, M. (1999) Comparison Between Various Control Methods for Thermal Power Plant Main Control System. *Electrical Engineering in Japan*, **128**(3), 72-81.
- Evans, J.T., Gomm, J.B., Williams, D. and Lisboa, P.J.G. (1994) Implementation and Performance Evaluation of an On-Line Neural Network Control Scheme. *IEE Control Conference*, 629-633.
- Giammar, R.D., Hopper, D.R., Webb, P.R. and Radhakrishnan, E. (1979) Evaluation of Emissions and Control Technology for Industrial Stoker Boilers. *Proceedings of the 3<sup>rd</sup> Stationary Source Combustion Symposium*, **1**, 3-35.
- Good Practise Guide 30 (1999) *Energy Efficient Operation of Industrial Boiler Plant*. Energy Efficiency Office: Best Practise Programme.
- Good Practice Guide 88 (2000) *Energy Efficient Use of Boilers Using Chain Grate Stokers*. Energy Efficiency Office: Best Practice Programme.
- Grainger, L. and Gibson, J. (1981) *Coal Utilisation: Technology, Economics & Policy*. Graham and Trotman Limited.
- Gunn, D.C. and Horton, R. (1989) *Industrial Boilers*. Longman Scientific & Technical.

- Gutmark, E., Parr, T.P., Hanson-Parr, D.M. and Schadow, K.C. (1990) Use of Chemiluminescence and Neural Networks in Active Combustion Control. *Proceedings of the 23<sup>rd</sup> International Symposium on Combustion: The Combustion Institute*, **23**, 1101-1106.
- Hadvig, S. (1989) Advanced Air Control for Combustion on Travelling Grates. *Proceedings of the Applied Energy Research Conference*, 207-220.
- Harris, M., Rivett, W.L. and Thurlow, G.G. (1962) Some Experiments and Developments Towards Improved Coal and Ash Handling for Small Boiler Plant. *Journal of the Institute of Fuel*, **35**, 523-531.
- Hobbs, M.L., Radulovic, P.T. and Smoot, L.D. (1993) Combustion and Gasification of Coals in Fixed-Beds. *Progress in Energy and Combustion Science*, **19**, 505-586.
- Hunt, K.J., Sbarbaro, D., Zbikowski, R. and Gawthrop, P.J. (1992) Neural Networks for Control Systems – A Survey. *International Federation of Automatic Control*, **28**(6), 1083-1112.
- IEA Statistics (1998) *Coal Information*. International Energy Agency.
- Jain, A.K., Mao, J.C. and Mohiuddin, K.M. (1996) Artificial Neural Networks: A Tutorial. *Computer*, **29**(3), 31-44.
- Jensen, R.R., Karki, S. and Salehfar, H. (2004) Artificial Neural Network-Based Estimation of Mercury Speciation in Combustion Flue Gases. *Fuel Processing Technology*, **85**, 451-462.
- Kasparian, V. and Batur, C. (1998) Model Reference Based Neural Network Adaptive Controller. *ISA Transactions*, **37**(1), 21-39.

- Kay, J. (1994) Monitoring – Equipment and Methods. *Boilers*, 6-10.
- Livingston, W.R., Chakraborty, R.K. and Birch, M.C. (1995) The Control of NO<sub>x</sub> Emissions from Stoker Fired Boilers. *Proceedings of the 2<sup>nd</sup> Combustion and Emissions Control Conference*, 273-283.
- Ljung, L. (2000) *System Identification Toolbox Manual for Use with MATLAB<sup>TM</sup>*. The MathWorks Inc., USA.
- Lu, S. (1997) Towards Intelligent Systems for Boiler Design. *Journal of Power and Energy*, **211**(5), 399-409.
- MATLAB<sup>TM</sup> External Interfaces*, (2000) The MathWorks Inc., USA.
- MATLAB<sup>TM</sup> Image Processing Toolbox*, (2003) The Math Works Inc., USA.
- McHale, A.P. (1988) Business Opportunities in Boiler Control Systems. *Energy World: Electronic Energy Management*, **156**, 7-9.
- Munakata, T. (1998) *Fundamentals of the New Artificial Intelligence: Beyond traditional Paradigms*. Graduate Texts in Computer Science. Springer-Verlag New York, Inc.
- Narendra, K.S. and Parthasarathy, K. (1990) Identification and Control of Dynamical Systems Using Neural Networks. *IEEE Transactions on Neural Networks*, **1**(1), 4-27.
- Neuffer, D., MacConnell, P.F., Patrick, M.A. and Owens, D.H. (1996) A Two-Dimensional Heterogeneous Model for the Control of a Chain Grate Stoker. *IEE Colloquium on Physical Modelling as a Basis for Control*. Digest No. 96/042, IEE, London, 5/1-5/7.

- Neuffer, D., MacConnell, P.F., Patrick, M.A. and Owens, D.H. (1998) Plant Trials of a Rule Based Control System for Coal Combustion. *International Conference on Control*, **455**, 497-502.
- Nguyen, D.H. and Widrow, B. (1991) Neural Networks for Self-Learning Control Systems. *International Journal of Control*, **54**(6), 1439-1451.
- Noorgard, M. (2000) *Neural Network Based System Identification Toolbox Manual: For Use with MATLAB<sup>TM</sup>*. Technical Report 00-E-891, Department of Automation, Technical University of Denmark.
- Parlos, A.G., Rais, O.T. and Atiya, A.F. (1999) Multi-Step-Ahead Prediction Using Dynamic Recurrent Neural Networks. *Proceedings of the International Joint Conference on Neural Networks*, 349-352.
- PowerClean (2003) Fossil Fuel Power Generation in the European Research Area. *R, D&D Thematic Network*.
- Prasad, G., Swidenbank, E. and Hogg, B.W. (1996) A Multivariable Predictive Control Strategy for Economical Fossil Power Plant Operation. *UKACC International Conference on Control*, 1444-1449.
- Prasad, G., Swidenbank, E. and Hogg, B.W. (1998) A Neural Net Model-based Multivariable Long-range Predictive Control Strategy Applied in Thermal Power Plant Control. *IEEE Transactions on Energy Conversion*, **13**(2), 176-182.
- Premier, G.C., Dinsdale, R., Guwy, A.J., Hawkes, F.R., Hawkes, DL. and Wilcox, S.J. (1997) Simple Black Box Models Predicting Potential Control Parameters during Disturbances to a Fluidised Bed Anaerobic Reactor. *Water Science and Technology*, **36**(6-7), 229-237.

- Premier, G.C., Dinsdale, R., Guwy, A.J., Hawkes, F.R., Hawkes, DL. and Wilcox, S.J. (1999) A Comparison of the Ability of Black Box and Neural Network Models of ARX Structure to Represent a Fluidised Bed Anaerobic Digestion Process. *Water Research*, **33**(4), 1027-1037.
- Prizzi, J. J. (1985) A Low Cost Option for Controlling Particulate Emissions from Chain Grate Stoker Fired Boilers. *Proceedings of the 76<sup>th</sup> Annual Conference of the International District Heating Association*, **76**, 207-218.
- Proctor, J. (2000) *Solid Fuel Solutions*. Company Brochure.
- Reifman, J. and Feldman, E.E. (1997) Neural Networks for Control of NO<sub>x</sub> Emissions in Fossil Plants. *Proceeding of the Society for Computer Simulation*, 64-69.
- Reifman, J. and Feldman, E.E. (1998) Identification and Control of NO<sub>x</sub> Emissions Using Neural Networks. *Journal of the Air & Waste Management Association*, **48**, 408-417.
- Reifman, J., Feldman, E.E. and Wei, T.Y.C. (2000) An Intelligent Emissions Control for Fuel Lean Gas Reburn in Coal-Fired Power Plants. *Journal of the Air & Waste Management Association*, **50**, 240-251.
- Reinschmidt, K.F. and Ling, B. (1994) Neural Networks for Plant Simulation and Control. *Proceedings of American Power Conference*, 796-801.
- Reinschmidt, K.F. and Ling, B. (1994) Neural Networks with Multiple-State Neurons for Nitrogen Oxide (NO<sub>x</sub>) Emissions Modelling and Advisory Control. *Proceedings of the IEEE International Conference on Neural Networks*, **6**, 3834-3839.
- Ribeiro, B., Dourado, A. and Costa, E. (1993) A Neural Network Based Control of a Simulated Industrial Lime Kiln. *Proceedings of the International Joint Conference on Neural Networks*, **2**(2), 2037-2040.

- Robson, B.T., Johnstone, C.D. and Crowther, M. (1988) Fully Automatic Unmanned Solid and Multi-Fuel Shell Boilers. *IMechE Seminar on the Continuing Role of Steam*, 7-17.
- Rolfe, T. J. K. (1961) Distribution of Primary Air in Chain Grate Stokers. *Journal of the Institute of Fuel*, **34**, 481-493.
- Rumelhart, D.E. and McClelland, J.L. (1986) *Parallel Distributed Processing*. MIT Press, Vols. 1 and 2.
- Rumelhart, D., Hinton, G. & Williams, R. (1986) Learning Internal Representations by Error Propagation. In *Parallel Distributed Processing*. MIT Press, Cambridge, MA.
- Saha, P.K., Shoib, M. and Kamruzzaman, J. (1998) Diagonal Recurrent Neural Network Based Integrated Control System of an Industrial Boiler. *Proceedings of IEEE TENCON' 98*, **1**, 200-203.
- Saha, P.K., Shoib, M. and Kamruzzaman, J. (1998) Development of a Neural Network Based Integrated Control System of 120 ton/h Capacity Boiler. *Computer & Electrical Engineering*, **24**, 423-440.
- Singer, J.G. and Owens, K.R. (1966) Combustion, Fossil Power Systems: A Reference Book on Fuel Burning. 4<sup>th</sup> Edition. Combustion Engineering (Volume 1), 13-16-13-26.
- Smoot, L.D. and Hill, S.C. (1983) Critical Requirements in Combustion Research. *Progress in Energy and Combustion Science*, **9**, 77-103.
- Smoot, L.D. (1984) Modelling of Coal Combustion Process. *Journal of the Progress in Energy and Combustion Science*, **10**, 229-272.
- Starley, G.P., Bradshaw, F.W., Carrel, C.S. and Pershing, D.W. (1985) The Influence of Bed-Region Stoichiometry on Nitric Oxide Formation in Fixed-Bed Coal Combustion. *Combustion and Flame*, **59**, 197-211.



- Tan, Y.H. and Keyser, R.D. (1994) Adaptive PID Control with Neural Network Based Predictor. *IEE Control Conference*, 1490-1494.
- Tan, Y.H. and Cauwenberghe, A.V. (1999) Neural Network Based D-Step Ahead Predictors for Nonlinear Systems with Time Delay. *Engineering Applications of Artificial Intelligence*, **12**, 21-35.
- Teruel, E., Cortés, C., Díez, L.I. and Arauzo, I. (2005) Monitoring and Prediction of Fouling in Coal-Fired Utility Boilers Using Neural Networks. *Chemical Engineering Science*, **60**, 5039-5052.
- Thurlow, G.G. (1962) The Mechanisation and Automatic Control of Coal Fired Shell Boilers: A Summary of Work Carried Out by the BCURA. *Journal of the Institute of Fuel*, **35**, 516-522.
- Venkatasubramanian, V. and Chan, K. (1989) A Neural Network Methodology for Process Fault Diagnosis. *Journal of the American Institute of Chemical Engineers*, **35**(12), 1993-2002.
- Warwick, K., Irwin, G.W. and Hunt, K.J. (1992) *Neural Network for Control and Systems*. IEE Control Engineering Series 46. Peter Peregrinus Ltd.
- Yao, H.M., Vulthaluru, H.B., Tade, M.O. and Djukanovic, D. (2005) Artificial Neural Network-Based Prediction of Hydrogen Content of Coal in Power Station Boilers. *Fuel*, **84**, 1535-1542.
- Zhou, H., Cen, K.F. and Fan J.R. (2004) Modelling and Optimisation of the NO<sub>x</sub> Emission Characteristics of a Tangentially Fired Boiler with Artificial Neural Networks. *Energy*, **29**, 167-183

## Appendix A – Fuel Specification for Experiments on the Stoker Test Facility

Casella CRE Ltd  
Stoke Orchard,  
Cheltenham,  
Gloucestershire  
GL52 4RZ

Proximate and Ultimate Analysis / Coal Type	Analysing Condition	Dawmill Washed Smalls	Dawmill Washed Singles	Columbian Smalls
Proximate Analysis:				
Moisture	% AR	10.0	9.1	8.4
Ash	% AR	4.8	4.6	4.6
Volatile Matter	% AR	34.3	36.2	34.1
	% DAF	-	-	39.2
Fixed Carbon	% AR	50.9	50.1	52.9
Gross Calorific Value	kJ/kg AR	28306	28712	29358
	kJ/kg DAF	31450	31583	33740
Ultimate analysis:				
Carbon	% AR	69.0	70.54	71.48
Hydrogen	% AR	4.78	4.77	4.60
Nitrogen	% AR	1.1	1.23	1.36
Oxygen	% AR	8.6	7.33	9.0
Sulphur	% AR	1.62	1.56	0.54
Chlorine	% AR	-	-	0.05
BS swell number		0.5	0.5	1.0
Gray King Coke		B	B	B

*Legend: AR – As Received*

*DAF – Dry-Ash Free*

Size Analysis / Coal Type	Dawmill Washed Smalls	Dawmill Washed Singles	Columbian Smalls
Size fraction (mm)	% by Weight	% by Weight	% by Weight
+ 50.0	0	0	-
50.0 – 37.5	0	2.2	-
37.5 – 31.5	0	3.6	-
31.5 – 28.0	0	7.6	-
28.0 – 25.0	0	16.3	-
25.0 – 19.0	0	30.4	-
19.0 – 16.0	1.5	23.2	-
16.0 – 12.5	53.8	13.5	-
12.5 – 3.15	28.9	1.3	-
3.15 – 1.0	11.3	0.8	-
1.0 – 0.5	1.3	1.1	-
- 0.5	3.2	0	-

## Appendix B – Fuel Specification for Experiments on the Industrial Stoker Plant

James Proctor Ltd.  
PO Box 19  
Cow Lane  
Burnley  
Lancashire BB11 1NN

Proximate and Ultimate Analysis / Coal Type	Analysing Condition	Beans (5-22mm)
Proximate Analysis:		
Moisture	% AR	10.6
Ash	% AR	7.2
Volatile Matter	% AR	31.8
Fixed Carbon	% AR	50.4
Net Calorific Value	kJ/kg AR	26478
Gross Calorific Value	kJ/kg DAF	33666
Ultimate analysis:		
Carbon	% AR	-
Hydrogen	% AR	-
Nitrogen	% AR	-
Oxygen	% AR	-
Sulphur	% AR	0.64
Chlorine	% AR	0.01
BS swell number	-	-
Gray King Coke	-	-

*Legend: AR – As Received  
DAF – Dry-Ash Free*

## Appendix C – Grate Ash Analysis for Experiments on the Stoker Test Facility

Casella CRE Ltd  
Stoke Orchard,  
Cheltenham,  
Gloucestershire  
GL52 4RZ

Coal Type	Rating (KW)	Excess Air Setting	Ash Content (%)	Loss on Ignition (%)
Dawmill Smalls	600-500	Low Excess Air	80.8	7.4
Dawmill Smalls	600	High Excess Air	80.9	7.5
Dawmill Singles	500-600	Optimum Excess Air	60.2	34.8
Dawmill Singles	600	Low Excess Air	71.3	24.9
Dawmill Singles	600	High Excess Air	80.6	14.7
Columbian Smalls	600	Optimum Excess Air	43.1	55.7
Columbian Smalls	500-600	High Excess Air	29.0	70.2

# Appendix D - The NNBC Programme in MATLAB™

## File for the Industrial Stoker Plant - Combustion Optimisation Test

%Neural Network Based Controller (NNBC) for Combustion Optimisation Test at  
%Constant Loads of 40%, 60% & 70% of MCR for Industrial Stoker Plant Located in  
%Garth, Lancashire in Collaboration with James Proctor Ltd. & HMP Garth

% [7 March 2003].

%Please note:

%\*\*\*\*\*

%First of all, LabVIEW will acquire signals from the Plant to Excel through the National  
%Instruments Data Acquisition Card (DAQ MIO-16) via Channel 2 to Channel 5. The  
%distribution of these channels are as follows:

%From Boiler Plant to LabVIEW and then to Excel:

%\*\*\*\*\*

%Channel 2 (ACH2) - Hot Water Temperature (°C)

%Channel 3 (ACH3) - Arch Temperature (°C)

%Channel 4 (ACH4) - Oxygen Concentration (%) (From our own developed sensor)

%Channel 5 (ACH5) - CO Emissions (ppm) (From our own developed sensor)

%From LabVIEW to MATLAB Via Excel Using Dynamic Data Exchange (DDE):

%\*\*\*\*\*

%Secondly, MATLAB will acquire data from Excel through DDE (Dynamic Data  
%Exchange) for airflow (since this value is being changed in Excel and the input value is  
%similar to the original output value which is sent through the output channel of the DAQ  
%via LabVIEW back to the plant).

%Thirdly, MATLAB will also acquire data directly from the Testo Analyser through the  
%PC's serial port interface (COM1) and the acquire data are as follows:

%From Testo Analyser:

%\*\*\*\*\*

%O2 (% by Volume)

%CO (ppm)

%NOx (ppm)

%SO2 (ppm)

%CO2 (%)

%Flue Gas Temperature (°C)

```

%From LabVIEW back to Boiler Plant:
%*****
%Channel 0 (DAC 0 OUT) - Airflow Rate (2 to 10 volts, 16.67%MCR to 100%MCR)
%It will be worth stating that MATLAB would only use data of Airflow (in Excel) and O2 &
%CO from Testo analyser for control action.
%However, Channel 2, 3, 4, 5, and NOx, SO2, CO2 & Flue Gas Temperature would be
%stored in 'dat' & Excel files for future reference. After MATLAB gone through the entire
%'FOR' loop, it will send the parameter that need to be changed (i.e. airflow rate) back to
%Excel via DDE. Finally, LabVIEW will acquire these data from Excel and send the signal
%in voltage back to the boiler plant via Channel 0 (OUT):

%Important Note: Parameters need to be changed before you run this M-file:
%*****
% In MATLAB:
%*****
% 1. Change parameters in the oxygen & carbon monoxide tuning loop.
% 2. Change all the file names to an appropriate date.

% In LabVIEW:
%*****
% 1. Change the 'dat' file name to an appropriate date.

% Parameters for the oxygen tuning loop:
%*****
%You will need to set the target depending on the firing rate. i.e. You will need to establish
%the load before setting for every 1% difference in oxygen.
% firerate>=16.67 & firerate<=35, O2_sethigh=16; O2_setlow=13; end;
% firerate>=36 & firerate<=50, O2_sethigh=13; O2_setlow=11; end;
% firerate>=51 & firerate<=70, O2_sethigh=11; O2_setlow=9; end;
% firerate>=71 & firerate<=100, O2_sethigh=9; O2_setlow=7; end;
% firerate>=50, K_O2=6; end;    % Air setting for every 1% difference in O2 if % of MCR
%>= 50%.
% firerate<50, K_O2=15; end;    % Air setting for every 1% difference in O2 if % of MCR
%< 50%.

% Parameters for the CO tuning loop:
%*****
CO_sethigh=1000;    % High limit of CO emission in ppm after normalised to 6% of O2.

% Parameters for the plotting functions - defining empty matrices:
%*****
figure(5);
oxygen=[]; oxygen_sim=[]; highO2=[]; lowO2=[];    % Oxygen concentration reading.
carbon_monoxide=[]; carbon_monoxide_sim=[]; highCO=[];    % CO emissions reading.
coal=[];    % Coal feed.
air=[];    % Air feed.

```



```

%Establish Link with Testo Gas Analyser via Serial Port Interface:
%*****
s=serial('COM1');
set(s,'BaudRate',4800);
s.InputBufferSize=10000000;
fopen(s)
m=1;    %Sampling time for Control Interval
Q=6;    %Control Interval

%Predefined spaces for Vectors to be stored:
%*****
Total_Data=[];
Model_Data=[];
Sim_Data=[];
Sim_Ave=[];
Ave_Data=[];

%_____ Start of FOR Loop _____%

for k=1:100000;    %Dummy cycle
    start_time=clock;    % Recording the initial loop time.

    %Requesting data directly from Testo through serial port interface COM1:
    %*****
    %Please note: fprintf and fscanf must be in pair

    tt=round(start_time(1,4:6));
    T=tt;
    T1=T(1,1);
    T2=T(1,2);
    T3=T(1,3);
    Time=strcat(num2str(T1),':',num2str(T2),':',num2str(T3));

    range1=strcat('r',num2str(k+1),'c1');
    mat2xls('d:\MiddleMan1.xls:sheet2',k,range1);

    range2=strcat('r',num2str(k+1),'c2');
    mat2xls('d:\MiddleMan1.xls:sheet2',date,range2);

    range3=strcat('r',num2str(k+1),'c3');
    mat2xls('d:\MiddleMan1.xls:sheet2',Time,range3);

    airflow=xls2mat('d:\MiddleMan1.xls:sheet1','r15c1');
    range4=strcat('r',num2str(k+1),'c4');
    mat2xls('d:\MiddleMan1.xls:sheet2',airflow,range4);

```

```

coalfeed=xls2mat('d:\MiddleMan1.xls:sheet1','r15c2');
range5=strcat('r',num2str(k+1),'c5');
mat2xls('d:\MiddleMan1.xls:sheet2',coalfeed,range5);

hotwater=xls2mat('d:\MiddleMan1.xls:sheet1','r15c5');
range6=strcat('r',num2str(k+1),'c6');
mat2xls('d:\MiddleMan1.xls:sheet2',hotwater,range6);

%Get reading from Testo:
%*****
% Please note again: fprintf and fscanf must be in pair

fprintf(s,'JB');
Flue_Gas=fscanf(s);

fprintf(s,'JC');
O2=fscanf(s);

fprintf(s,'JE');
CO2=fscanf(s);

fprintf(s,'JI');
CO=fscanf(s);

fprintf(s,'JJ');
NOx=fscanf(s);

fprintf(s,'JL');
SO2=fscanf(s);

%Convert string to numeric (i.e. str2num)
%or Convert string to double (i.e. str2double)

O2=str2num(O2(1:5));
range7=strcat('r',num2str(k+1),'c7');
mat2xls('d:\MiddleMan1.xls:sheet1',O2,'r15c3');
mat2xls('d:\MiddleMan1.xls:sheet2',O2,range7);

CO=str2num(CO(1:5));
range8=strcat('r',num2str(k+1),'c9');
mat2xls('d:\MiddleMan1.xls:sheet2',CO,range8);

CO_Nor=((20.9-6)/(20.9-O2))*CO;
range9=strcat('r',num2str(k+1),'c8');
mat2xls('d:\MiddleMan1.xls:sheet1',CO_Nor,'r15c4');
mat2xls('d:\MiddleMan1.xls:sheet2',CO_Nor,range9);

```

```

NOx=str2num(NOx(1:5));
range10=strcat('r',num2str(k+1),'c10');
mat2xls('d:\MiddleMan1.xls:sheet2',NOx,range10);

SO2=str2num(SO2(1:5));
range11=strcat('r',num2str(k+1),'c11');
mat2xls('d:\MiddleMan1.xls:sheet2',SO2,range11);

CO2=str2num(CO2(1:4));
range12=strcat('r',num2str(k+1),'c12');
mat2xls('d:\MiddleMan1.xls:sheet2',CO2,range12);

Flue_Gas=str2num(Flue_Gas(1:5));
range13=strcat('r',num2str(k+1),'c13');
mat2xls('d:\MiddleMan1.xls:sheet2',Flue_Gas,range13);

Total_Data=[Total_Data; start_time(1,4:6) hotwater CO NOx SO2 CO2];
Model_Data=[Model_Data; airflow coalfeed O2 CO_Nor];

% _____ %

% Model of Future Prediction:
%*****
% The model prediction for O2 & CO "6" steps into future (3 minutes) to predict future
%emission problems and to allow time for remediation before it actually happens for
%Combustion Optimisation Test at constant load (i.e. 40%, 60% & 70% of MCR).

if k>=5;

%O2 Simulation:
%*****
%load trained network
load O2403Model2b70.mat %variables: net,na,nb,nk,meanp,stdp,meant,stdt

%Normalise Data (0 mean and 1 std):
%*****
O2_Model=[trastd(Model_Data(k-4:k,1:2)',meanp,stdp)'trastd(Model_Data(k-4:k,3)',
    meant,stdt)'];
%[b,a]=butter(5,0.008/(1/30));
%O2_Modelf=filtfilt(b,a,O2_Model);
R_O2 = size(O2_Model,1)+1;
O2_ip=[O2_Model(R_O2-1,1);O2_Model(R_O2-2,1);O2_Model(R_O2-4,2);
    O2_Model(R_O2-5,2); O2_Model(R_O2-1,3);O2_Model(R_O2-2,3);
    O2_Model(R_O2-3,3)];

```

```

%Simulate Network:
%*****
inpt=O2_ip;
%target=poststd(tregn,meant,stdt);
Yn=sim(net,inpt);           %network prediction
Y=poststd(Yn,meant,stdt);   %transform Yn to original unit
Y_O2=Y';
Sim_O2=Y_O2;

%_____ End of O2 Simulation _____%

%CO Simulation:
%*****
%load trained network
load CO403Model2b70.mat    %variables: net,na,nb,nk,meanp,stdp,meant,stdt

%Normalise Data (0 mean and 1 std):
%*****
CO_Model=[trastd(Model_Data(k-4:k,1:3)',meanp,stdp)'trastd(Model_Data(k-4:k,4)',
               meant,stdt)'];
%[b,a]=butter(5,0.008/(1/30));
%CO_Model=filtfilt(b,a,CO_Model);
R_CO = size(CO_Model,1)+1;
CO_ip=[CO_Model(R_CO-1,1);CO_Model(R_CO-2,1);CO_Model(R_CO-4,2);
        CO_Model(R_CO-5,2);CO_Model(R_CO-1,3);CO_Model(R_CO-2,3);
        CO_Model(R_CO-3,3);CO_Model(R_CO-1,4);CO_Model(R_CO-2,4);
        CO_Model(R_CO-3,4);CO_Model(R_CO-4,4)];

%Simulate Network:
%*****
inpt=CO_ip;
Yn=sim(net,inpt);           %network prediction
Y=poststd(Yn,meant,stdt);   %transform Yn to original unit
Y_CO=Y';
Sim_CO=Y_CO;

%_____ End of CO Simulation _____%

Sim_Data=[Sim_Data; Sim_O2 Sim_CO];
Sim_Ave=Sim_Data;

range14=strcat('r',num2str(k+1),'c14');
mat2xls('d:\MiddleMan1.xls:sheet2',Sim_O2,range14);

range15=strcat('r',num2str(k+1),'c15');
mat2xls('d:\MiddleMan1.xls:sheet2',Sim_CO,range15);

```

```

end

%_____ Averaging _____%

x=size(Sim_Ave);
x=x(1,1);

if x==m*Q
y=x-(Q-4);

Point_O2=Sim_Ave(y:x,1);
Point_CO=Sim_Ave(y:x,2);

%Averaging:
%*****
Ave_O2=mean(Point_O2);
range16=strcat('r',num2str(k+1),'c16');
mat2xls('d:\MiddleMan1.xls:sheet1',Ave_O2,'r16c3');
mat2xls('d:\MiddleMan1.xls:sheet2',Ave_O2,range16);

Ave_CO=mean(Point_CO);
range17=strcat('r',num2str(k+1),'c17');
mat2xls('d:\MiddleMan1.xls:sheet1',Ave_CO,'r16c4');
mat2xls('d:\MiddleMan1.xls:sheet2',Ave_CO,range17);

Ave_Data=[Ave_Data; k Ave_O2 Ave_CO];

%_____ Start of Combustion Optimisation Action _____%

% Setting of the target oxygen band depending on the firing rate:
%*****
% Please Note: coalfeed is the firing rate and in this case, the firing rate is constant
%i.e. 40%, 60% or 70% of MCR.

firerate=round(coalfeed);
newcoalfeed=round(coalfeed);
mat2xls('d:\MiddleMan1.xls:sheet1',newcoalfeed,'r24c2');

%Since coalfeed is the firing rate and it ranges from 0 to 100%, therefore we use the
%newcoalfeed to determine the target oxygen band at different firing rate.

if firerate>=16.67 & firerate<=35, O2_sethigh=16; O2_setlow=13; end;
if firerate>=36 & firerate<=50, O2_sethigh=13; O2_setlow=11; end;
if firerate>=51 & firerate<=70, O2_sethigh=11; O2_setlow=9; end;
if firerate>=71 & firerate<=100, O2_sethigh=9; O2_setlow=7; end;
if firerate>=50, K_O2=2.5; end;

```

```

if firerate<50, K_O2=5; end;

% _____ %

% Oxygen tuning loop:
%*****

if Ave_O2>O2_sethigh & Ave_CO<CO_sethigh, O2_error=O2_sethigh-Ave_O2;
% Note the -ve sign.
    U_O2=K_O2*O2_error;    % Reduction on the air.
    newairflow=U_O2+airflow;
    disp('less air required');
    disp('ATTENTION!OXYGEN TUNING LOOP - airflow.sp. is =');
    disp(newairflow);
    mat2xls('d:\MiddleMan1.xls:sheet1',newairflow,'r24c1');

elseif Ave_O2>O2_sethigh & Ave_CO>CO_sethigh, O2_error=Ave_O2-O2_sethigh;
%Note the +ve sign.
    U_O2=K_O2*O2_error;    % Increase on the air.
    newairflow=U_O2+airflow;
    disp('more air required');
    disp('ATTENTION!CARBON MONOXIDE TUNING LOOP - airflow.sp. is =');
    disp(newairflow);
    mat2xls('d:\MiddleMan1.xls:sheet1',newairflow,'r24c1');

elseif Ave_O2<O2_sethigh & Ave_CO>CO_sethigh, O2_error=O2_sethigh-Ave_O2;
%Note the +ve sign.
    U_O2=K_O2*O2_error;    % Increase on the air.
    newairflow=U_O2+airflow;
    disp('more air required');
    disp('ATTENTION!CARBON MONOXIDE TUNING LOOP - airflow.sp. is =');
    disp(newairflow);
    mat2xls('d:\MiddleMan1.xls:sheet1',newairflow,'r24c1');

elseif Ave_O2<O2_setlow & Ave_CO<CO_sethigh, O2_error=O2_setlow-Ave_O2;
%Note the +ve sign.
    U_O2=K_O2*O2_error;    % Increase on the air.
    newairflow=U_O2+airflow;
    disp('more air required');
    disp('ATTENTION!OXYGEN TUNING LOOP - airflow.sp. is =');
    disp(newairflow);
    mat2xls('d:\MiddleMan1.xls:sheet1',newairflow,'r24c1');

elseif Ave_O2<O2_setlow & Ave_CO>CO_sethigh, O2_error=O2_setlow-Ave_O2;
%Note the +ve sign.
    U_O2=K_O2*O2_error;    % Increase on the air.

```

```

newairflow=U_O2+airflow;
disp('more air required');
disp('ATTENTION!OXYGEN & CARBON MONOXIDE TUNING LOOP -
airflow.sp. is =');
disp(newairflow);
mat2xls('d:\MiddleMan1.xls:sheet1',newairflow,'r24c1');

elseif Ave_O2>O2_setlow & Ave_CO>CO_sethigh, O2_error=Ave_O2-O2_setlow;
%Note the +ve sign.
    U_O2=K_O2*O2_error;    % Increase on the air.
    newairflow=U_O2+airflow;
    disp('more air required');
    disp('ATTENTION!CARBON MONOXIDE TUNING LOOP - airflow.sp. is =');
    disp(newairflow);
    mat2xls('d:\MiddleMan1.xls:sheet1',newairflow,'r24c1');

elseif Ave_O2>=O2_setlow & Ave_O2<=O2_sethigh & Ave_CO<=CO_sethigh;
    U_O2=0; newairflow=airflow;    %Note no air adjustment.
    disp('OPTIMUM AIR');
    end;

%_____

% Logging of Auxillary Information:
%*****

% Plotting Functions – Temp, Oxygen & Coal/Air/Firing Rate Vs Time:
%*****
oxygen=[oxygen O2]; highO2=[highO2 O2_sethigh]; lowO2=[lowO2 O2_setlow];
oxygen_sim=[oxygen_sim Sim_O2];
carbon_monoxide=[carbon_monoxide CO]; highCO=[highCO CO_sethigh];
carbon_monoxide_sim=[carbon_monoxide_sim Sim_CO];
coal=[coal newcoalfeed]; air=[air newairflow];

% Plotting the Oxygen Concentration:
%*****
    subplot(5,1,1)
    plot(1:m,oxygen,'b',1:m,highO2,'y--',1:m,lowO2,'g--');
    grid on;
    %text(6,5,'Lower O2 Limit = 6%'); text(6,7,'Upper O2 Limit = 8%');
    ylabel('% of O2 Vol');
    %xlabel('Elapsed Time in Multiple of 3 Minutes');
    title('OXYGEN CONCENTRATION WITH TIME');

% Plotting the Simulated Oxygen Concentration:
%*****

```



```

subplot(5,1,2)
plot(1:m,oxygen_sim,'r',1:m,highO2,'y--',1:m,lowO2,'g--');
grid on;
%text(6,5,'Lower O2 Limit = 6%'); text(6,7,'Upper O2 Limit = 8%');
ylabel('% of O2 Vol');
%xlabel('Elapsed Time in Multiple of 3 Minutes');
title('SIMULATED OXYGEN CONCENTRATION WITH TIME');

%Plotting the CO emissions:
%*****
subplot(5,1,3)
plot(1:m,carbon_monoxide,'b',1:m,highCO,'y--');
grid on;
%text(6,5,'Upper CO Limit = 600ppm');
ylabel('CO Emissions (ppm)');
%xlabel('Elapsed Time in Multiple of 3 Minutes');
title('CO EMISSIONS WITH TIME');

% Plotting the Simulated CO emissions:
%*****
subplot(5,1,4)
plot(1:m,carbon_monoxide_sim,'r',1:m,highCO,'y--');
grid on;
%text(6,5,'Upper CO Limit = 600ppm');
ylabel('CO Emissions (ppm)');
%xlabel('Elapsed Time in Multiple of 3 Minutes');
title('SIMULATED CO EMISSIONS WITH TIME');

% Plotting the coal/air/firing rate:
%*****
subplot(5,1,5)
plot(1:m,coal,'b:',1:m,air,'r:');
grid on;
text(3,5,'coal feed rate=blue'); text(3,25,'airflow rate=red');
ylabel('Airflow & Coal Feed Rate in %MCR');
xlabel('Elapsed Time in Multiple of 3 Minutes');
title('AIRFLOW & COAL FEED RATE WITH TIME');
m=m+1;

% _____ %

end
while etime(clock,start_time)<30, end; % Data Acquisition loop is 30 seconds interval.
disp('next FOR loop!!'); % Simulation loop is also 30 seconds interval.
end % End for the FOR loop. % Control loop is 3 minutes interval.

% _____ End of FOR Loop _____ %

```

# Appendix E - The NNBC Programme in MATLAB™

## File for the Industrial Stoker Plant – Hot Water Temperature Control Test

%Neural Network Based Controller (NNBC) for Hot Water Temperature Control Test for  
%Industrial Stoker Plant Located in Garth, Lancashire in Collaboration with James Proctor  
%Ltd. & HMP Garth

% [14 March 2003].

%Please note:

%\*\*\*\*\*

%First of all, LabVIEW will acquire signals from the Plant to Excel through the National  
%Instruments Data Acquisition Card (DAQ MIO-16) via Channel 0 to Channel 5. The  
%distribution of these channels are as follows:

%From Boiler Plant to LabVIEW and then to Excel:

%\*\*\*\*\*

%Channel 2 (ACH2) - Hot Water Temperature ('C)

%Channel 3 (ACH3) - Arch Temperature ('C)

%Channel 4 (ACH4) - Oxygen Concentration (%) (From our own developed sensor)

%Channel 5 (ACH5) - CO Emissions (ppm) (From our own developed sensor)

%From LabVIEW to MATLAB Via Excel Using Dynamic Data Exchange (DDE):

%\*\*\*\*\*

%Secondly, MATLAB will acquire data from Excel through DDE (Dynamic Data  
%Exchange) for coal feed & airflow (since these values are being changed in Excel and the  
%input values are similar to the original output values which are sent through the output  
%channels of the DAQ via LabVIEW back to the plant).

%Thirdly, MATLAB will also acquire data directly from the Testo Analyser through a  
%PC's serial port interface (COM1) and the acquire data are as follows:

%From Testo Analyser:

%\*\*\*\*\*

%O2 (% by Volume)

%CO (ppm)

%NOx (ppm)

%SO2 (ppm)

%CO2 (%)

%Flue Gas Temperature ('C)

%From LabVIEW back to Boiler Plant:

%\*\*\*\*\*

%Channel 0 (DAC 0 OUT) - Airflow Rate (2 to 10 volts, 16.67%MCR to 100%MCR)

%Channel 1 (DAC 1 OUT) - Coal Feed Rate (2 to 10 volts, 16.67%MCR to 100%MCR)

%It will be worth stating that MATLAB would only use data of hot water temperature  
%(Channel 2), Airflow & Coal Feed (in Excel) and O2 & CO from Testo analyser for  
%control action.

%However, Channel 2, 3, 4, 5, and NOx, SO2, CO2 & Flue Gas Temperature would be  
%stored in 'dat' & Excel files for future reference. After MATLAB gone through the entire  
%'FOR' loop, it will send the parameters that need to be changed (i.e. airflow & coal feed)  
%back to Excel via DDE. Finally, LabVIEW will acquire these data from Excel and send the  
%signal in voltage back to the boiler plant via Channel 0 & 1 (OUT):

%Important Note: Parameters need to be changed before you run this M-file:

%\*\*\*\*\*

% In MATLAB:

%\*\*\*\*\*

% 1. Change parameters in the oxygen & carbon monoxide tuning loop.

% 2. Change all the file names to an appropriate date.

% In LabVIEW:

%\*\*\*\*\*

% 1. Change the 'dat' file name to an appropriate date.

% Parameters for the firing loop:

%\*\*\*\*\*

sethigh=120; % High limit of hot water temperature.

setlow=117; % Low limit of hot water temperature.

% Parameters for the oxygen tuning loop:

%\*\*\*\*\*

%You will need to set the target depending on the firing rate. i.e. You will need to establish  
%the load before setting for every 1% difference in oxygen.

% firerate>=16.67 & firerate<=35, O2\_sethigh=16; O2\_setlow=13; end;

% firerate>=36 & firerate<=50, O2\_sethigh=13; O2\_setlow=11; end;

% firerate>=51 & firerate<=70, O2\_sethigh=11; O2\_setlow=9; end;

% firerate>=71 & firerate<=100, O2\_sethigh=9; O2\_setlow=7; end;

% firerate>=50, K\_O2=6; end; % Air setting for every 1% difference in O2 if % of MCR  
%>= 50%.

% firerate<50, K\_O2=15; end; % Air setting for every 1% difference in O2 if % of MCR  
%< 50%.

% Parameters for the CO tuning loop:

%\*\*\*\*\*

CO\_sethigh=1000; % High limit of CO emission in ppm after normalised to 6% of O2.

```

% Parameters for the plotting functions - defining empty matrices:
%*****
figure(6);
hwtemp=[]; hightemp=[]; lowtemp=[];      % pv = hot water temp.
oxygen=[]; oxygen_sim=[]; highO2=[]; lowO2=[];      % Oxygen concentration reading.
carbon_monoxide=[]; carbon_monoxide_sim=[]; highCO=[];      % CO emissions reading.
coal=[];      % Coal feed.
air=[];      % Air feed.

%Establish link with Testo Gas Analyser via Serial Port Interface:
%*****
s=serial('COM1');
set(s,'BaudRate',4800);
s.InputBufferSize=10000000;
fopen(s)

m=1;      %Sampling time for Control Interval
Q=6;      %Control Interval

%Predefined spaces for Vectors to be stored:
%*****
Total_Data=[];
Model_Data=[];
Sim_Data=[];
Sim_Ave=[];
Ave_Data=[];

%_____ Start of FOR Loop _____%

for k=1:100000;      %Dummy cycle
    start_time=clock;      % Recording the initial loop time.

    %Requesting data directly from Testo through serial port interface COM1:
    %*****
    %Please note: fprintf and fscanf must be in pair

    tt=round(start_time(1,4:6));
    T=tt;
    T1=T(1,1);
    T2=T(1,2);
    T3=T(1,3);
    Time=strcat(num2str(T1),',',num2str(T2),',',num2str(T3));

    range1=strcat('r',num2str(k+1),'c1');
    mat2xls('d:\MiddleMan8.xls:sheet2',k,range1);

```

```

range2=strcat('r',num2str(k+1),'c2');
mat2xls('d:\MiddleMan8.xls:sheet2',date,range2);

range3=strcat('r',num2str(k+1),'c3');
mat2xls('d:\MiddleMan8.xls:sheet2',Time,range3);

airflow=xls2mat('d:\MiddleMan8.xls:sheet1','r15c1');
range4=strcat('r',num2str(k+1),'c4');
mat2xls('d:\MiddleMan8.xls:sheet2',airflow,range4);

coalfeed=xls2mat('d:\MiddleMan8.xls:sheet1','r15c2');
range5=strcat('r',num2str(k+1),'c5');
mat2xls('d:\MiddleMan8.xls:sheet2',coalfeed,range5);

hotwater=xls2mat('d:\MiddleMan8.xls:sheet1','r16c5');
range6=strcat('r',num2str(k+1),'c6');
mat2xls('d:\MiddleMan8.xls:sheet2',hotwater,range6);

%Get reading from Testo:
%*****
%Please note again: fprintf and fscanf must be in pair

fprintf(s,'JB');
Flue_Gas=fscanf(s);

fprintf(s,'JC');
O2=fscanf(s);

fprintf(s,'JE');
CO2=fscanf(s);

fprintf(s,'JI');
CO=fscanf(s);

fprintf(s,'JJ');
NOx=fscanf(s);

fprintf(s,'JL');
SO2=fscanf(s);

%Convert string to numeric (i.e. str2num)
%or Convert string to double (i.e. str2double)

O2=str2num(O2(1:5));
range7=strcat('r',num2str(k+1),'c7');
mat2xls('d:\MiddleMan8.xls:sheet1',O2,'r15c3');

```

```

mat2xls('d:\MiddleMan8.xls:sheet2',O2,range7);

CO=str2num(CO(1:5));
range8=strcat('r',num2str(k+1),'c9');
mat2xls('d:\MiddleMan8.xls:sheet2',CO,range8);

CO_Nor=((20.9-6)/(20.9-O2))*CO;
range9=strcat('r',num2str(k+1),'c8');
mat2xls('d:\MiddleMan8.xls:sheet1',CO_Nor,'r15c4');
mat2xls('d:\MiddleMan8.xls:sheet2',CO_Nor,range9);

```

```

NOx=str2num(NOx(1:5));
range10=strcat('r',num2str(k+1),'c10');
mat2xls('d:\MiddleMan8.xls:sheet2',NOx,range10);

```

```

SO2=str2num(SO2(1:5));
range11=strcat('r',num2str(k+1),'c11');
mat2xls('d:\MiddleMan8.xls:sheet2',SO2,range11);

```

```

CO2=str2num(CO2(1:4));
range12=strcat('r',num2str(k+1),'c12');
mat2xls('d:\MiddleMan8.xls:sheet2',CO2,range12);

```

```

Flue_Gas=str2num(Flue_Gas(1:5));
range13=strcat('r',num2str(k+1),'c13');
mat2xls('d:\MiddleMan8.xls:sheet2',Flue_Gas,range13);

```

```

Total_Data=[Total_Data; start_time(1,4:6) hotwater CO NOx SO2 CO2];
Model_Data=[Model_Data; airflow coalfeed O2 CO_Nor];

```

```

%_____ %

```

```

% Model of Future Prediction:

```

```

%*****

```

```

%The model prediction for O2 & CO "6" steps into future (3 minutes) to predict future
%emission problems and to allow time for remediation before it actually happens for
%Hot Water Temperature Control Test.

```

```

if k>=5;

```

```

%O2 Simulation:

```

```

%*****

```

```

%load trained network

```

```

load O21203Model2b.mat %variables: net,na,nb,nk,meanp,stdp,meant,stdt

```

```

%Normalise Data (0 mean and 1 std):
%*****
O2_Model=[trastd(Model_Data(k-4:k,1:2)',meanp,stdp)'trastd(Model_Data(k-4:k,3)',
            meant,stdt)'];
%[b,a]=butter(5,0.008/(1/30));
%O2_Modelf=filtfilt(b,a,O2_Model);
R_O2 = size(O2_Model,1)+1;
O2_ip=[O2_Model(R_O2-1,1);O2_Model(R_O2-2,1);O2_Model(R_O2-4,2);
        O2_Model(R_O2-5,2);O2_Model(R_O2-1,3);O2_Model(R_O2-2,3);
        O2_Model(R_O2-3,3)];

%Simulate Network:
%*****
inpt=O2_ip;
%target=poststd(tregn,meant,stdt);
Yn=sim(net,inpt);           %network prediction
Y=poststd(Yn,meant,stdt);   %transform Yn to original unit
Y_O2=Y';
Sim_O2=Y_O2;

%_____ End of O2 Simulation _____%

%CO Simulation:
%*****
%load trained network
load CO1203Model2b.mat    %variables: net,na,nb,nk,meanp,stdp,meant,stdt

%Normalise Data (0 mean and 1 std):
%*****
CO_Model=[trastd(Model_Data(k-4:k,1:3)',meanp,stdp)'trastd(Model_Data(k-4:k,4)',
            meant,stdt)'];
%[b,a]=butter(5,0.008/(1/30));
%CO_Modelf=filtfilt(b,a,CO_Model);
R_CO = size(CO_Model,1)+1;
CO_ip=[CO_Model(R_CO-1,1);CO_Model(R_CO-2,1);CO_Model(R_CO-4,2);
        CO_Model(R_CO-5,2);CO_Model(R_CO-1,3);...CO_Model(R_CO-2,3);
        CO_Model(R_CO-3,3);CO_Model(R_CO-1,4);CO_Model(R_CO-2,4);
        CO_Model(R_CO-3,4);CO_Model(R_CO-4,4)];

%Simulate Network:
%*****
inpt=CO_ip;;
Yn=sim(net,inpt);           %network prediction
Y=poststd(Yn,meant,stdt);   %transform Yn to original unit
Y_CO=Y';
Sim_CO=Y_CO;

```



% \_\_\_\_\_ End of CO Simulation \_\_\_\_\_ %

```
Sim_Data=[Sim_Data; Sim_O2 Sim_CO];
Sim_Ave=Sim_Data;
```

```
range14=strcat('r',num2str(k+1),'c14');
mat2xls('d:\MiddleMan8.xls:sheet2',Sim_O2,range14);
```

```
range15=strcat('r',num2str(k+1),'c15');
mat2xls('d:\MiddleMan8.xls:sheet2',Sim_CO,range15);
```

```
end
```

% \_\_\_\_\_ Averaging \_\_\_\_\_ %

```
x=size(Sim_Ave);
x=x(1,1);
```

```
if x==m*Q
y=x-(Q-4);
```

```
Point_O2=Sim_Ave(y:x,1);
Point_CO=Sim_Ave(y:x,2);
```

```
%Averaging:
%*****
```

```
Ave_O2=mean(Point_O2);
range16=strcat('r',num2str(k+1),'c16');
mat2xls('d:\MiddleMan8.xls:sheet1',Ave_O2,'r16c3');
mat2xls('d:\MiddleMan8.xls:sheet2',Ave_O2,range16);
```

```
Ave_CO=mean(Point_CO);
range17=strcat('r',num2str(k+1),'c17');
mat2xls('d:\MiddleMan8.xls:sheet1',Ave_CO,'r16c4');
mat2xls('d:\MiddleMan8.xls:sheet2',Ave_CO,range17);
```

```
Ave_Data=[Ave_Data; k Ave_O2 Ave_CO];
```

% \_\_\_\_\_ Start of Control Action \_\_\_\_\_ %

```
% Rules for firing loop Control:
% *****
```

```
if hotwater>sethigh, hwerror=hotwater-sethigh; end;
if hotwater<setlow, hwerror=setlow-hotwater; end;
if hotwater>=setlow & hotwater<=sethigh, hwerror=0; end;
```

```

if hwerror>10, K_fr=2.5; end;    %10% MCR increment or decrement per 'C difference
if hwerror>=5 & hwerror<=10, K_fr=5; end;    %5% MCR increment or decrement per
                                                %'C difference
if hwerror<5, K_fr=2.5; end;    %2.5% MCR increment or decrement
                                %per 'C difference

```

```

% Calculating error between process variable (PV) & set points & controller effort – U:
%*****

```

```

    if hotwater>sethigh, hwerror=sethigh-hotwater;
        U_fr=K_fr*hwerror; % -ve value, i.e. DECREASE on the firing rate.
    end;
    if hotwater<setlow, hwerror=setlow-hotwater;
        U_fr=K_fr*hwerror; % +ve value, i.e. INCREASE on the firing rate.
    end;
    if hotwater>=setlow & hotwater<=sethigh, hwerror=0;
        U_fr=0; % Firing rate achieving set point.
    disp('Boiler Load Providing Desired PV Set Point');
    end;

```

```

%_____ %

```

```

% Firing rate control loop:
%*****

```

```

% Calculating the new coal feed and airflow required.

```

```

newairflow=U_fr+airflow;
disp('ATTENTION!airflow.sp. is ='); disp(newairflow);
mat2xls('d:\MiddleMan8.xls:sheet1',newairflow,'r24c1');

```

```

newcoalfeed=U_fr+coalfeed;
disp('ATTENTION!coalfeed.sp. is ='); disp(newcoalfeed);
mat2xls('d:\MiddleMan8.xls:sheet1',newcoalfeed,'r24c2');

```

```

if newcoalfeed<coalfeed;
    disp('Load Decrease');
elseif newcoalfeed>coalfeed;
    disp('Load Increase');
else newcoalfeed=coalfeed;
    disp('Load Maintain');
end;

```

```

%_____ Start of Oxygen Trimming Loop _____ %

```

```

% Setting of the target oxygen band depending on the firing rate:
%*****

```

```

% Please Note: Coalfeed is the firing rate and in this case, the firing rate is changing

```

```

%from time to time in order to cope with the hot water demand.
firerate=round(newcoalfeed);

%Since Coalfeed is the firing rate and it ranges from 0 to 100%, therefore we use the
%newcoalfeed to determine the target oxygen band at different firing rate.

if firerate>=16.67 & firerate<=35, O2_sethigh=16; O2_setlow=13; end;
if firerate>=36 & firerate<=50, O2_sethigh=13; O2_setlow=11; end;
if firerate>=51 & firerate<=70, O2_sethigh=11; O2_setlow=9; end;
if firerate>=71 & firerate<=100, O2_sethigh=9; O2_setlow=7; end;
if firerate>=50, K_O2=2.5; end;
if firerate<50, K_O2=2.5; end;

%_____

if abs(U_fr)<3;
disp('Air Tuning Loop Due to Small Load Change');

% Oxygen tuning loop:
%*****
if Ave_O2>O2_sethigh & Ave_CO<CO_sethigh, O2_error=O2_sethigh-Ave_O2;
% Note the -ve sign.
    U_O2=K_O2*O2_error;    % Reduction on the air.
    newairflow=U_O2+airflow;
    disp('less air required');
    disp('ATTENTION!OXYGEN TUNING LOOP - airflow.sp. is =');
    disp(newairflow);
    mat2xls('d:\MiddleMan8.xls:sheet1',newairflow,'r24c1');

elseif Ave_O2>O2_sethigh & Ave_CO>CO_sethigh, O2_error=Ave_O2-O2_sethigh;
%Note the +ve sign.
    U_O2=K_O2*O2_error;    % Increase on the air.
    newairflow=U_O2+airflow;
    disp('more air required');
    disp('ATTENTION!CARBON MONOXIDE TUNING LOOP - airflow.sp. is =');
    disp(newairflow);
    mat2xls('d:\MiddleMan8.xls:sheet1',newairflow,'r24c1');

elseif Ave_O2<O2_sethigh & Ave_CO>CO_sethigh, O2_error=O2_sethigh-Ave_O2;
%Note the +ve sign.
    U_O2=K_O2*O2_error;    % Increase on the air.
    newairflow=U_O2+airflow;
    disp('more air required');
    disp('ATTENTION!CARBON MONOXIDE TUNING LOOP - airflow.sp. is =');
    disp(newairflow);
    mat2xls('d:\MiddleMan8.xls:sheet1',newairflow,'r24c1');

```

```
elseif Ave_O2<O2_setlow & Ave_CO<CO_sethigh, O2_error=O2_setlow-Ave_O2;
%Note the +ve sign.
```

```
    U_O2=K_O2*O2_error;    % Increase on the air.
    newairflow=U_O2+airflow;
    disp('more air required');
    disp('ATTENTION!OXYGEN TUNING LOOP - airflow.sp. is =');
    disp(newairflow);
    mat2xls('d:\MiddleMan8.xls:sheet1',newairflow,'r24c1');
```

```
elseif Ave_O2<O2_setlow & Ave_CO>CO_sethigh, O2_error=O2_setlow-Ave_O2;
%Note the +ve sign.
```

```
    U_O2=K_O2*O2_error;    % Increase on the air.
    newairflow=U_O2+airflow;
    disp('more air required');
    disp('ATTENTION!OXYGEN & CARBON MONOXIDE TUNING LOOP -
    airflow.sp. is =');
    disp(newairflow);
    mat2xls('d:\MiddleMan8.xls:sheet1',newairflow,'r24c1');
```

```
elseif Ave_O2>O2_setlow & Ave_CO>CO_sethigh, O2_error=Ave_O2-O2_setlow;
%Note the +ve sign.
```

```
    U_O2=K_O2*O2_error;    % Increase on the air.
    newairflow=U_O2+airflow;
    disp('more air required');
    disp('ATTENTION!CARBON MONOXIDE TUNING LOOP - airflow.sp. is =');
    disp(newairflow);
    mat2xls('d:\MiddleMan8.xls:sheet1',newairflow,'r24c1');
```

```
elseif Ave_O2>=O2_setlow & Ave_O2<=O2_sethigh & Ave_CO<=CO_sethigh;
    U_O2=0; newairflow=airflow;    %Note no air adjustment.
    disp('OPTIMUM AIR with boiler load achieving set point');
    end;
```

```
else abs(U_fr)>=3;
end;
```

```
%_____ End of Oxygen Trimming Loop _____%
```

```
% Logging of Auxillary Information:
%*****
```

```
% Plotting Functions - Temp, Oxygen & Coal/Air/Firing Rate Vs Time:
%*****
hwtemp=[hwtemp hotwater]; hightemp=[hightemp sethigh]; lowtemp=[lowtemp setlow];
oxygen=[oxygen O2]; highO2=[highO2 O2_sethigh]; lowO2=[lowO2 O2_setlow];
oxygen_sim=[oxygen_sim Sim_O2];
```

```
carbon_monoxide=[carbon_monoxide CO_Nor]; highCO=[highCO CO_sethigh];
carbon_monoxide_sim=[carbon_monoxide_sim Sim_CO];
coal=[coal newcoalfeed]; air=[air newairflow];
```

```
% Plotting the coal/air/firing rate:
```

```
%*****
```

```
    subplot(3,2,1)
    plot(1:m,coal,'b:',1:m,air,'r:');
    %grid on;
    text(3,5,'coal feed rate = blue'); text(3,25,'airflow rate = red');
    ylabel('Airflow & Coal Feed Rate in MCR%');
    xlabel('Elapsed Time in Multiple of 3 Minutes');
    title('AIRFLOW & COAL FEED RATE WITH TIME');
```

```
% Plotting the hot water temp:
```

```
%*****
```

```
    subplot(3,2,2)
    plot(1:m,hwtemp,'b',1:m,hightemp,'y--',1:m,lowtemp,'g--');
    %grid on;
    %text(1,(fr_setlow-2),'Lower temp limit = 115');
    %text(1,(fr_sethigh-2),'Upper temp limit = 120');
    ylabel('Temp in Deg C');
    %xlabel('Elapsed Time in Multiple of 3 Minutes');
    title('HOT WATER TEMPERATURE WITH TIME');
```

```
% Plotting the flue gas oxygen content:
```

```
%*****
```

```
    subplot(3,2,3)
    plot(1:m,oxygen,'b',1:m,highO2,'y--',1:m,lowO2,'g--');
    %grid on;
    %text(6,5,'Lower O2 Limit = 6%');
    %text(6,7,'Upper O2 Limit = 8%');
    ylabel('% of O2 Vol');
    %xlabel('Elapsed Time in Multiple of 3 Minutes');
    title('EXCESS AIR LEVEL WITH TIME');
```

```
% Plotting the CO emissions:
```

```
%*****
```

```
    subplot(3,2,4)
    plot(1:m,carbon_monoxide,'b',1:m,highCO,'y--');
    %grid on;
    %text(6,5,'Upper CO Limit = 1000ppm');
    ylabel('CO Emissions (ppm)');
    %xlabel('Elapsed Time in Multiple of 3 Minutes');
    title('CO EMISSIONS WITH TIME');
```

```

% Plotting the Simulated Oxygen Concentration:
%*****
    subplot(3,2,5)
    plot(1:m,oxygen_sim,'r:',1:m,highO2,'y--',1:m,lowO2,'g--');
    grid on;
    %text(6,5,'Lower O2 Limit = 6%'); text(6,7,'Upper O2 Limit = 8%');
    ylabel('% of O2 Vol');
    %xlabel('Elasped Time in Multiple of 3 Minutes');
    title('SIMULATED OXYGEN CONCENTRATION WITH TIME');

% Plotting the Simulated CO emissions:
%*****
    subplot(3,2,6)
    plot(1:m,carbon_monoxide_sim,'r:',1:m,highCO,'y--');
    grid on;
    %text(6,5,'Upper CO Limit = 600ppm');
    ylabel('CO Emissions (ppm)');
    %xlabel('Elasped Time in Multiple of 3 Minutes');
    title('SIMULATED CO EMISSIONS WITH TIME');
    m=m+1;

%_____ %

end
while etime(clock,start_time)<30, end;    % Data Acquisition loop is 30 seconds interval.
disp('next FOR loop!!');                % Simulation loop is also 30 seconds interval.
end    %End for the FOR loop.            % Control loop is 3 minutes interval

%_____ End of FOR Loop _____ %

```